HIRDLS

High Resolution Dynamics Limb Sounder
Earth Observing System (EOS)
Data Description and Quality
Version 7 (V7)
(HIRDLS Version 7.00.00)
June, 2013

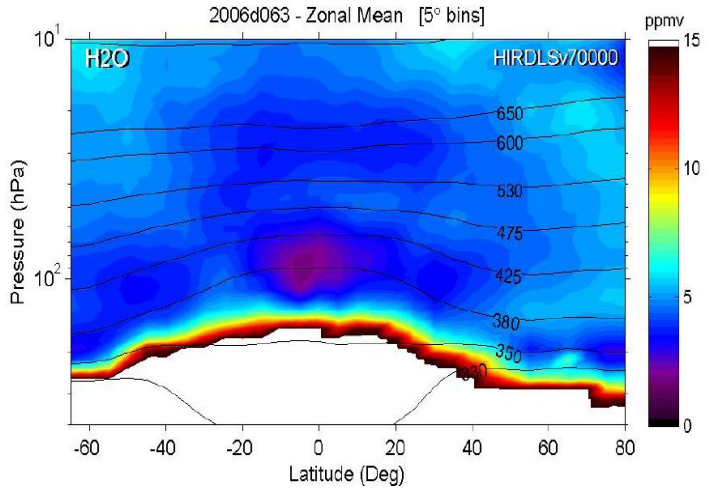

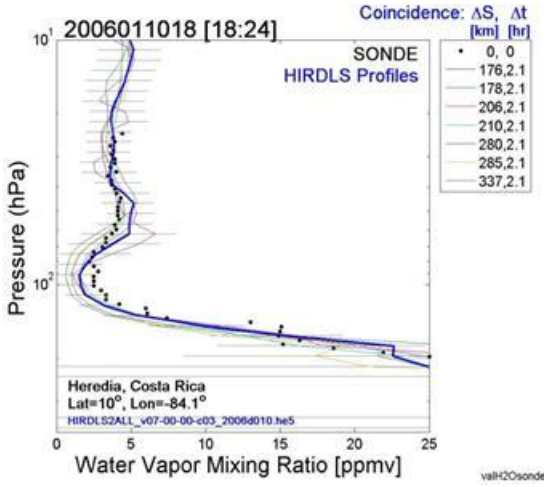

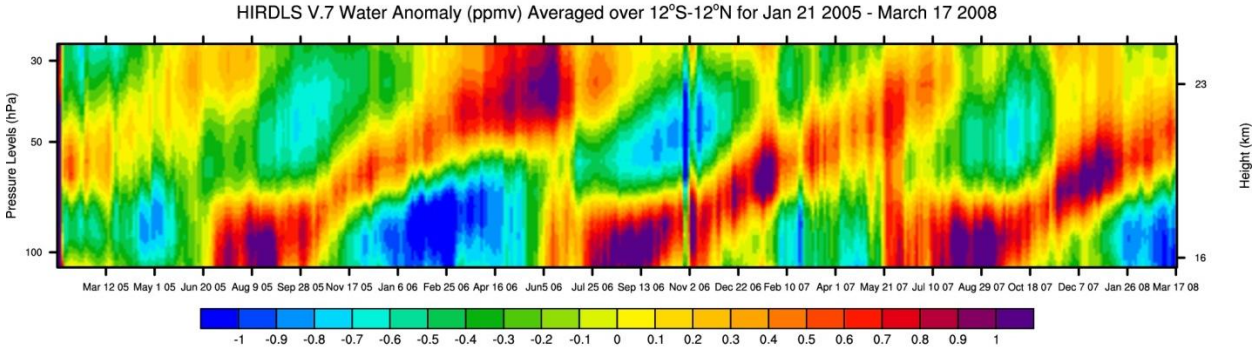

Oxford University
Department of Atmospheric
Oceanic & Planetary Physics
Oxford, UK

University of Colorado
Center for Limb
Atmospheric Sounding
Boulder, Colorado, USA

National Center for
Atmospheric Research
Boulder, Colorado
USA

Cover Page:

Three views of HIRDLS V7 water vapor.
Upper left- zonal mean cross-section of water vapor mixing ratio for March 4, 2006 (day 63). Thin black lines show isentropic surfaces.

Upper right- Cryogenic Frostpoint Hygrometer (CFH) sonde measurement of water vapor profile at Heredia, Costa Rica, on January 10, 2006 (black dots), with closest HIRDLS profile (thick blue line). Closest was 172 km distant, and 2.1 hours different. Next 6 closest profiles are shown by thinner lines.

Bottom- Water vapor"tape recorder" signal over length of HIRDLS mission. The departure from the mission time mean is plotted. Alternate high and low values show the imprint of the tropical tropopause temperature on the water vapor mixing ratio of the upwelling air in the tropics.

Contributors to this assessment:

John Gille, US PI, Univ. of CO/NCAR

Charles Cavanaugh, NCAR
Vince Dean, NCAR
Svetlana Karol, NCAR
Douglas Kinnison, NCAR
Bruno Nardi, NCAR
Lesley Smith, NCAR
Alison Waterfall, Rutherford Appleton Lab

Lesley Gray, UK PI, Oxford University
(until 30 September 2011)

Michael Coffey, NCAR
Chris Halvorson, NCAR
Rashid Khosravi, NCAR
Steve Massie, NCAR
Maria Belmonte Rivas, NCAR
Brendan Torpy, CU
Corwin Wright, NCAR

Acknowledgement:

This research was carried out at the University of Colorado, Boulder and the National Center for Atmospheric Research (NCAR) under a contract (NAS5-97046) with the National Aeronautics and Space Administration (NASA) and, until 30 September 2011, with the University of Oxford and Rutherford Appleton Laboratory with funding from the Natural Environment Research Council (NERC).

I.0 Information That Every HIRDLS Data User Needs to Know

The High Resolution Dynamics Limb Sounder (HIRDLS) instrument was launched on the Aura satellite in August, 2004. It is a 21 channel limb-scanning infrared radiometer that acquired about 5600 vertical scans across the atmospheric limb each day, from which vertical profiles of temperature, ozone, nitric acid, CFC11, CFC12, H2O, N2O, NO2, N2O5, ClONO2 plus cloud and aerosol extinction data are retrieved.

These data are unique in having a vertical resolution of ~ 1 km, and frequently the ability to sound down into the upper troposphere. Geographically the data extend from 63°S to 80°N with 1 degree spacing, and cover the period from 29 January 2005 to 17 March 2008, with very few gaps.

Some critical parameters describing the version 7 (V7) data are briefly summarized in Table I-I (page 7). Any potential user should read the relevant sections for more complete information.

I.1 Acquiring & Reading HIRDLS Data

HIRDLS data are available from several worldwide data repositories. In the United States, HIRDLS data can be downloaded from the Goddard Earth Sciences Data and Information Services Center (GES DISC) (http://disc.sci.gsfc.nasa.gov/data-holdings). HIRDLS data are also available in the United Kingdom and Europe from the British Atmospheric Data Centre (BADC) (http://badc.nerc.ac.uk/browse/badc/hirdls). In both institutions, several versions of HIRDLS data are available and care should be taken to make sure that V7 data is requested.

HIRDLS data are stored in the HDF-EOS5 format in the HDF-EOS Aura File Format Guidelines (http://www.eos.ucar.edu/hirdls/HDFEOS_Aura_File_Format_Guidelines.pdf). These data files can be read via C/C++ or Fortran using either the HDF-EOS5 or HDF5 library. A HIRDLS developed IDL routine "get_aura" is also available upon request for those users who wish to use IDL to access the HIRDLS Level 2 (L2) data.

Users should obtain the pre-compiled HDF5 library for their operating system, if possible. Otherwise, source code is also available (see http://hdf.ncsa.uiuc.edu). These are prerequisite in order to compile the HDF-EOS5 library (see http://www.hdfeos.org/). Both libraries are needed to fully access the Aura HIRDLS data files. For additional help contact the GES DISC at help-disc@listserv.gsfc.nasa.gov or telephone 301-614-5224.

Level 2 Data Products

Each HIRDLS Level 2 file contains one day's worth of data for the L2 (profile) products listed in Table 1. The HIRDLS data are a set of values of temperature or mixing ratio on a

set of 24 pressure levels per decade of pressure, uniformly distributed in log pressure (see Section 5.). The recommended pressure ranges for V7 are shown in Table 1. For users who require only a subset of the HIRDLS species, the GES DISC has the ability to subset data before distributing them to users. Contact the DISC directly for more information on this service.

Individual HIRDLS data values for a product are stored in fields labeled with the species name (see Table 1 for the exact names). The estimated precision of each data point is a corresponding field named *Species*Precision (for instance, Temperature and TemperaturePrecision). Two additional fields for each species, *Species*NormChiSq and *Species*Quality, are both filled with missing for V7. CloudTopPressure does not have Precision, NormChiSq or Quality fields. For V7 data, the fields for products other than those listed in Table 1 are filled with missing values (-999.0) since the radiance correction algorithms for these products are not mature yet.

There are two time fields in the HIRDLS Level 2 data file, Time and SecondsInDay. Time is stored in TAI time (seconds since the epoch of 00.00 UTC 1-1-1993). This time includes leap seconds and can cause problems with simplistic conversions. For this reason, HIRDLS is also storing SecondsInDay which is seconds since midnight of the data day. Leap seconds do not pose a problem when using this field. Note that the first data point may be negative which indicates a time stamp before midnight. This is the case for scans that span a day boundary.

Level 3 Data Products

As of V6, HIRDLS released new level 3 (L3) data products. V7 will release L3 versions of all released L2 products. These will be created by applying a Kalman filter mapping algorithm similar to that described by Remsberg et al. [1990]. The algorithm inputs L2 retrieval results for a 1° latitude band for the length of the mission, and creates daily estimates of the zonal mean plus amplitudes and phases of the first seven zonal waves using both forward and backward passes through the data (see Section 4.5). The means plus coefficients for a latitude may then be used to calculate values at any longitude. The algorithm also provides values for the precision, which is the root-mean square of the differences between the estimated fields and the input data. For the gridded data provided here results are generated every 1° of longitude, to create a 1° x 1° grid. The L3 data will be released later, with an addition to this document. This may also be found at http://www.eos.ucar.edu/hirdls/data.

I.2 Data That Should Be Used With Caution

Level 2 Data Products

Data points for which most of the information comes from the *a priori* have their precision fields set negative, and the user should decide whether data are suitable for scientific studies.

See Khosravi et al., [2009a,b]; http://www.agu.org/journals/jd/jd0920/2009JD011937/ for details on quantitative *a priori* contributions to the errors. In addition, one may consult the document "Description of HIRDLS Predicted Precision Data", available from the web page http://www.eos.ucar.edu/hirdls/data for details on negative precision.

HIRDLS data processing makes use of some Microwave Limb Sounder (MLS) data for contaminants. Because of the lack of full days of MLS data for 29 March-4 April (days 88-94) 2006, HIRDLS processing used data from NCAR's Whole Atmosphere Community Climate Model (WACCM), driven by the GEOS5 meteorological data. These data are denoted by version v07-00-10, but are included as part of the V7 time series. Although no anomalies in these data have been noticed, users should be aware of this.

I.3 Known Problems

A few cloud tops are not detected, resulting in retrievals at low altitudes of cloud-contaminated radiances. This can result in retrieved temperatures being too warm, and positive or negative spikes in species retrievals.

HIRDLS scans across the limb in both directions, from space to Earth (down-scan) followed by a scan from Earth to space (up-scan). The two scan directions interact differently with the material blocking the optical train (Section 2.2), so different corrections for the blockage are used for the two scan directions. Every effort is made to make the two sets of results agree. While not expected, there may be some residual differences between up and down scans. Critical features in the data should be checked to ensure they appear in scans in both directions. Scan direction of a profile can be easily determined by examining the value of its ScanUpFlag in the HIRDLS2 file: 0 for down scan, 1 for up scan.

The ozone data show a slightly greater ozone amount on the ascending (day) segments of the orbit than on the descending (night) segment. The reason for this is not known. It is believed to be an artifact, and not a real effect.

Data from the period 3 January – 17 March 2008, when the chopper frequency was erratic, are provided, but the user should check them before using them. HIRDLS stopped acquiring data after 17 March 2008 when the chopper stalled.

From 4-18 December 2007, there were problems with the spacecraft data system, resulting in some corrupted data products. Subsequently the input data were reconstructed by the NASA ground data system, and reprocessed in the HIRDLS Science Investigator Led Processing System (SIPS). We are not aware of any resulting undetected problems at this time, but users should scrutinize these data carefully.

Table 1 below briefly summarizes the useful vertical range, estimated accuracy, and the HIRDLS team contact for each product in this version. The vertical range and accuracy entries generally simplify complex variations, and the listed references, or the web page http://www.eos.ucar.edu/hirdls/, should be consulted before any use of the data.

Table I-1: Information concerning V7 HIRDLS standard L2 products

Product	Field Name	Useful Range	Estimated Accuracy	Contact Name	Contact Email
Temperature	Temperature	1000 –0.01 hPa*	± 1 K p>10 hPa ± 2 K .1<p<10 hPa	John Gille	gille@ucar.edu
O_3	O3	422 – 0.1 hPa	† 1-10% 10 - >50%, tropical UTLS	Bruno Nardi	nardi@ucar.edu
HNO_3	HNO3	215 – 5.1 hPa	† 3% to 15%	Bruno Nardi	nardi@ucar.edu
CFC11	CFC11	316 – 17.8 hPa	†5-15%, 316-30hPa 10 - >50%, p<30hPa	Bruno Nardi	nardi@ucar.edu
CFC 12	CFC12	316 – 8.3 hPa	†3-10%, 316-70hPa 10 - >50%, p<70hPa	Bruno Nardi	nardi@ucar.edu
H_2O	Water	200 – 10 hPa	10% 80-10 hPa	John Gille	gille@ucar.edu
N_2O	N_2O	100 – 5.1 hPa Use zonal mean Data**	+/- 10%** ** See sec. 5.6	Rashid Khosravi	Rashid@ucar.edu
NO_2	NO_2	287 – 0.1 hPa	20 - 30%	Lesley Smith	lsmith@ucar.edu
N_2O_5	N_2O_5	82.5 – 1.0 hPa	30 - 50%	Lesley Smith	lsmith@ucar.edu
$ClONO_2$	ClONO2	100 – 1.0 hPa	30%	Lesley Smith	lsmith@ucar.edu
Cloud top pressure	CloudTopPressure	422 - 10 hPa	± 20%	Steven Massie	massie@ucar.edum
12.1 and 8.3 Micron Extinction	12.1 Micron Extinction, 8.3 MicronExtinction	215 – 20 hPa	Extinction positive bias is 2 x 10^{-5} km^{-1}	Steven Massie	massie@ucar.edu
GPH	GPH	1000 – 0.01 hPa*	2%	Lesley Smith	lsmith@ucar.edu
HDF5, HDF-EOS5	Library Installation		NA	GSFC DAAC	Help-disc@listserv.gsfc.nasa.gov
HDF-EOS5	Reading HIRDLS Data		NA	Vince Dean	vdean@ucar.edu

* *A priori* >383 hPa

† Varies with latitude and altitude.

Note that the following references refer to the V3 data, but the descriptions of the data and the methods of evaluation are still applicable. In addition, one may consult the web page http://www.eos.ucar.edu/hirdls/ for more recent information.

Gille et al., [2008], The High Resolution Dynamics Limb Sounder (HIRDLS): Experiment Overview, Results and Validation of Initial Temperature Data, *Journal of Geophysical Research*; doi:10.1029/2007JD008824.

Khosravi, R., et al., [2009a]; Overview and characterization of retrievals of temperature, pressure, and atmospheric constituents from the High Resolution Dynamics Limb Sounder (HIRDLS) measurements, J. Geophys. Res., 114, D20304, doi:10.1029/2009JD011937.

Khosravi, R., et al., [2009b]; Correction to ''Overview and characterizati7/17/2011on of retrievals of temperature, pressure, and atmospheric constituents from High Resolution Dynamics Limb Sounder (HIRDLS) measurements,'' J. Geophys. Res., 114, D23399, doi:10.1029/2009JD013507.

Kinnison et al., [2008], Global Observations of HNO3 from the High Resolution Dynamics Limb Sounder (HIRDLS) – First Results, *Journal of Geophysical Research*; doi:10.1029/2007JD008814.

Massie et al., [2007], Validation of HIRDLS Observations PSC's and Subvisible Cirrus, *Journal of Geophysical Research*; doi:10.1029/2007JD008788.

Nardi et al., [2008], Validation of HIRDLS Ozone Measurements, *Journal of Geophysical Research*; doi:10.1029/2007JD008837.

-End of Information That Every HIRDLS Data User Needs to Know -

Table of Contents

1.0 Overview

1.1 Introduction

As the following sections describe, the entrance aperture of the High Resolution Dynamics Limb Sounder (HIRDLS) was largely obscured by a piece of plastic material that came loose during launch. This resulted in a partial blocking of the signal from the atmosphere, and the addition of extraneous signals from the plastic blockage material. Because of the position of the blockage, coverage of Antarctica and the higher longitudinal resolution expected are precluded, although latitudinal resolution has been increased, and vertical resolution maintained.

The HIRDLS team has worked since the discovery of this anomaly to understand the nature of the blockage, and to develop four major correction algorithms and a final adjustment to make the resulting radiances as close as possible to those originally expected. Corrections for some channels, and therefore the products retrieved from them, are more advanced than for others. This document provides a description of the fifth fully-released version of data for the entire mission, which includes retrieved temperature, ozone, nitric acid, chlorofluorocarbons (CFC) 11 and 12, H_2O, N_2O, day and night profiles of the diurnally varying species NO_2, N_2O_5, and $ClONO_2$, geopotential height, and aerosol extinction, as well as cloud top pressure.

Major work to continue to improve the radiances, and the resulting retrievals has now come to an end, so this is likely to be the final version of HIRDLS data, except for some possible incremental improvements.

Previous versions of these data have proven to be scientifically valuable. Some of the known problems with the data are described below, but these are almost surely not the only ones.

The information needed by a HIRDLS data user is presented in Section I (Information That Every HIRDLS Data User Needs to Know) at the front of this document. We strongly suggest that anyone wishing to work with the data contact the HIRDLS team. In the first instance, this should be the Principal Investigator (PI).

A programmatic note should be added. The experiment was developed, calibrated and operated in orbit as a harmonious collaboration between groups at the University of Colorado and NCAR on the U.S. side and at Oxford University on the U.K. side. The Oxford participation came to an end when funding from NERC ended on 30 September 2011. Following the death of John Barnett, the original UK P.I., Lesley Gray became the U.K. P.I. The U.S. team is profoundly grateful for having had the opportunity to share this adventure with the Oxford group.

John Gille
HIRDLSP.I.
gille@ucar.edu

2.0 The HIRDLS Experiment

2.1 The Experiment as Designed

HIRDLS is an infrared limb-scanning radiometer designed to sound the upper troposphere, stratosphere, and mesosphere to determine temperature; the mixing ratios of O_3, H_2O, CH_4, N_2O, NO_2, HNO_3, N_2O_5, CFC11, CFC12, $ClONO_2$, Geopotential Height (GPH), and aerosols; and the locations of polar stratospheric clouds and cloud tops. The goals were to provide sounding observations with horizontal and vertical resolution superior to that previously obtained; to observe the lower stratosphere with improved sensitivity and accuracy; and to improve understanding of atmospheric processes through data analysis, diagnostics, and use of two- and three-dimensional models.

HIRDLS performs limb scans in the vertical, measuring infrared emissions in 21 channels ranging from 6.12 to 17.76 μm. Although the retrieval operates somewhat differently, functionally the retrieval uses measurements of the emitted radiance by CO_2 in four channels. With knowledge of the known (and increasing) mixing ratio of CO_2 transmittances in the the 4 channels are calculated. Inversion of the equation of radiative transfer leads to determination of the vertical distribution of the Planck black body function, from which the temperature is derived as a function of pressure. This temperature profile is used to calculate the Planck function profile for the trace gas channels. The measured radiance and the Planck function profile are then used to determine the transmittance of each trace species and its mixing ratio distribution.

The overall measurement goals of HIRDLS were to observe the global distributions of temperature, the 10 trace species and particulates from the upper troposphere into the mesosphere at high vertical and horizontal resolution. Observations of the lower stratosphere are improved through the use of special narrow and more transparent spectral channels.

2.2 The Launch-induced Anomaly

2.2.1 History and Present Status

HIRDLS was launched on the EOS Aura spacecraft on 15 July 2004. All steps in the initial activation were nominal until the initialization of the scanner on 30 July 2004 indicated more drag than anticipated, and a subsequent health test of the scan mechanism indicated that the damping of the elevation mechanism was ~ 20% greater than on the ground. After the cooler was turned on and the detectors reached their operating temperature (~61 K), initial scans showed radiances much larger and more uniform than atmospheric radiances, except for a region of lower signals at the most negative azimuths. The HIRDLS team immediately identified this as indicating a probable blockage of a large part of the optical aperture.

Tests confirmed that the blockage emits a large, nearly uniform radiance, and covers all of the aperture except a small region 47° from the orbital plane on the side away from the sun.

A number of scan mirror and door maneuvers were conducted in an attempt to dislodge the obstruction, now believed to be a piece of plastic film that was installed to maintain the cleanliness of the optics. None of these maneuvers was successful in improving HIRDLS' view of Earth's atmosphere.

However, these studies and subsequent operations of the instrument have shown that, except for the blockage, HIRDLS performed extremely well as a stable, accurate and low noise radiometer. These qualities have allowed the HIRDLS team to develop methods for extracting the atmospheric radiance from the unwanted blockage radiance and to retrieve all but one of the desired species. Some are better than others as this document describes. These data allow HIRDLS to meet most of the original science objectives.

Data are presented from 29 January 2005 until 17 March 2008, although occasional periods are missing when various non-science scans were run for test purposes. There are some data between 21 and 28 January 2005, but the instrument had not yet settled into a stable state, and the data are of substandard quality. Data from the period 3 January – 17 March 2008, when the chopper frequency was erratic, are provided, but the user should be careful in using them. HIRDLS stopped acquiring data after 17 March 2008 when the chopper stalled. Efforts to restore it to operation have been unsuccessful.

2.2.2 Impact of Loss of Azimuth Scan Capability

In its present configuration, HIRDLS can view past the blockage only at the extreme anti-sun edge of the aperture. Vertical scans are made at a single azimuth angle of 47° line of sight (LOS) from the orbital plane, on the side away from the sun. (This differs from the original design, in which HIRDLS would have made vertical scans at several azimuth angles, providing orbit-to-orbit coverage with a spacing of ~ 400-500 km in latitude and longitude.) The inability to make vertical scans at a range of azimuths is a definite loss in data gathering, but not a major loss of scientific capability for many of the mission goals. Some of the effects of the present observing characteristics are:

Changes in coverage

The single-azimuth coverage is plotted in Figure 2.1, which shows that coverage only extends to 63.4°S, thus missing all of Antarctica and the S. Polar cap. In the Northern Hemisphere (N.H.) it reaches 80° N. In mid-latitudes of the N. Hemisphere, the descending orbit views nearly the same orbit just before 1a.m. as the ascending orbit at 3:00pm, 9 orbits or 15 hours later, as shown by the measurement times displayed in Figure 2.2

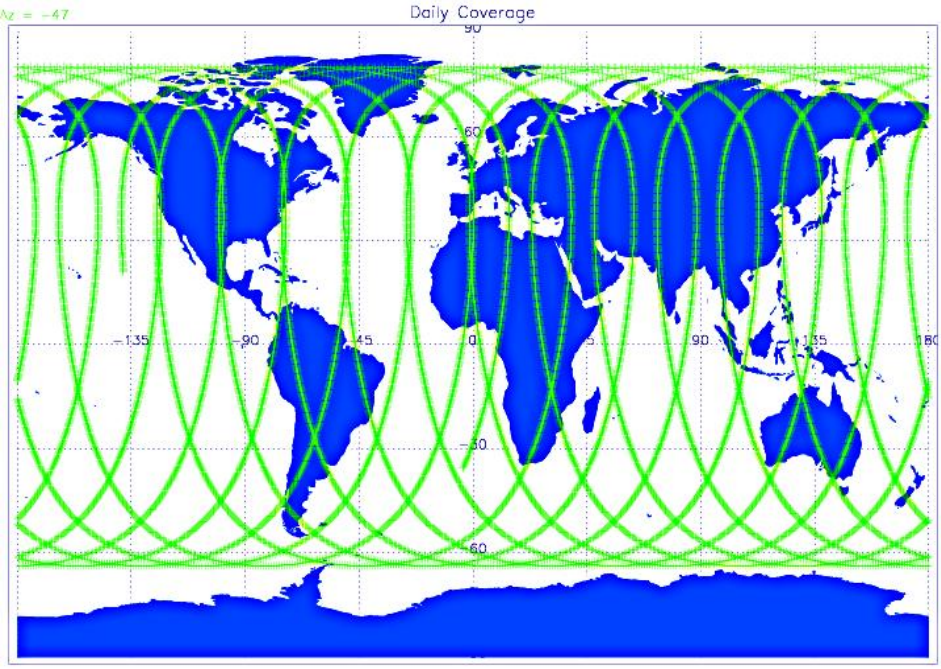

Figure 2.1 HIRDLS Single Day Coverage

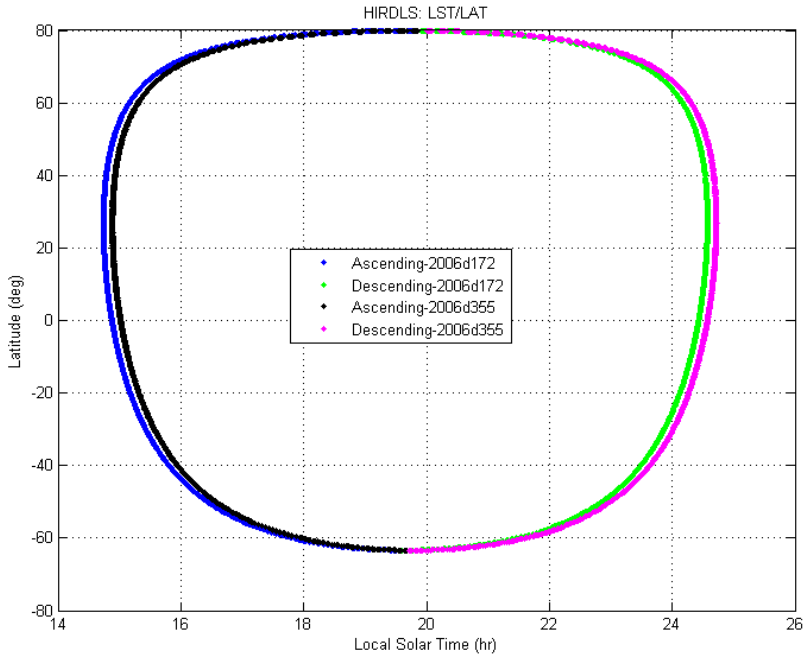

Figure 2.2 Local time of HIRDLS observations for the solstices, as a function of observing latitude

Inability to View the Same Air Mass as MLS, TES or OMI Within 15 Minutes

The HIRDLS scan track is compared with the MLS scan track in Figure 2.3. HIRDLS views nearly the same volume as MLS at night (descending part of orbit, left side of figure), but one orbit earlier. Thus HIRDLS views the same volume 84 minutes earlier than MLS (one

orbit, or 99 minutes, minus the 15 minutes that separate MLS views ahead of the S/C and HIRDLS measurements behind the S/C). In the daytime (ascending part of orbit, right side of plot), HIRDLS observations fall 17° to the east of the MLS track in the same orbit, or 8° to the west of the MLS track in the previous orbit. Especially in the daytime, this difference impacts making comparisons, the planning of correlative measurements, and the opportunities to do combined science. However, comparisons and science can easily be done at night where desired.

A corollary feature is that, in the daytime, HIRDLS and MLS combined observe more longitude at a given latitude, which will improve the spatial resolution. At night, together they look at the same volume 84 minutes apart, increasing the temporal resolution.

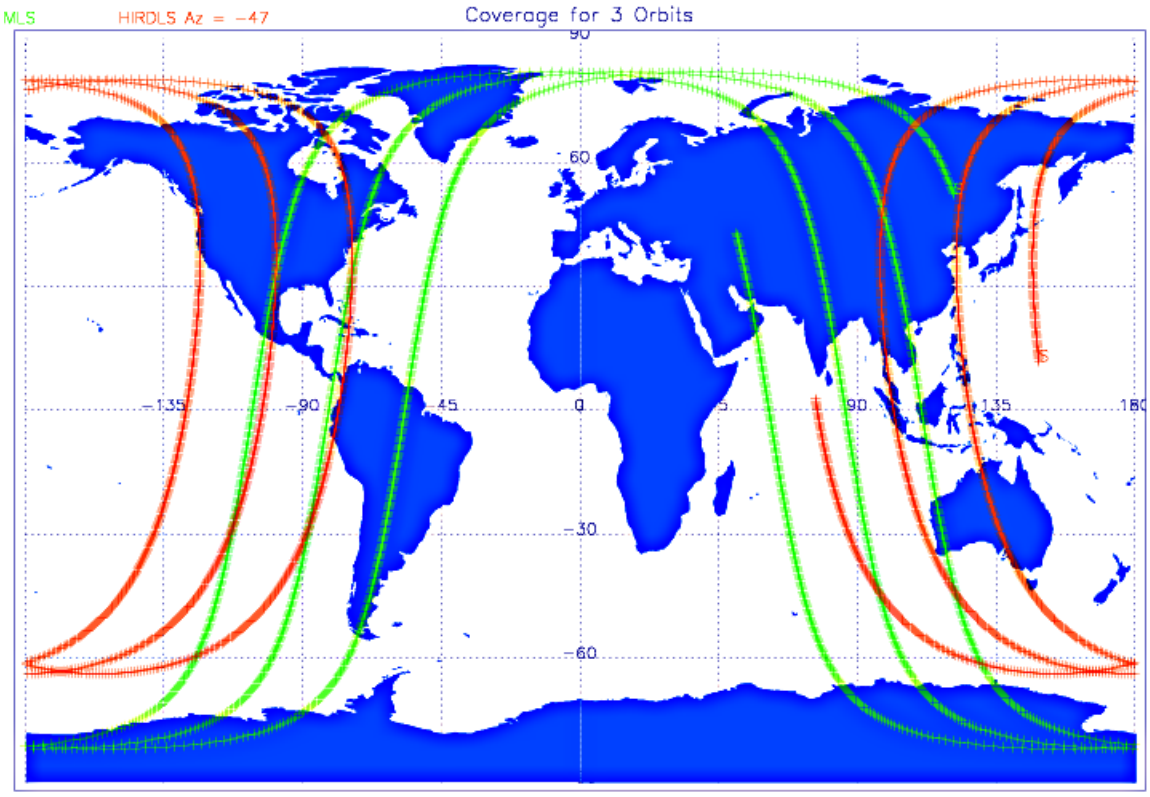

Figure 2.3. Comparison of 3 orbits of HIRDLS (red) measurement locations to MLS (green). HIRDLS is measuring the atmosphere at one azimuth angle (i.e., -47° from the orbit plane). The day and night portion of the orbits are on the right and left side of the figure respectively. During the day part of the orbit, HIRDLS is trailing MLS by one orbit (99-minutes). During the night part of the orbit, the spatial coincidence is much better, although HIRDLS leads MLS by one orbit.

Some compensating effects

With the azimuthal limitation, the profiles will have closer latitudinal separation (corresponding to ~100 km along track spacing), facilitating gravity wave studies. Transects through tropospheric intrusions into the lower stratosphere and tropopause folds are improved by continuous views at one azimuth.

Since HIRDLS views a long way off the orbital track, as seen above, it measures at a different local time than MLS, the Tropospheric Emission Spectrometer (TES) and the Ozone Monitoring Instrument (OMI), which are all flying on Aura. At the northern and southern extremes it means that HIRDLS will get data at a significantly different local time from the other instruments, which could help constrain data assimilation models.

3.0 Revised Operational Scan Patterns –

The limited angle at which HIRDLS can see the atmosphere necessitated a revision to previously planned scan patterns. Scans of the atmosphere are done in the region in which the view of the atmosphere is the clearest, at -23.5° azimuth shaft angle, or -47° LOS from the orbital plane (on the side away from the sun).

Science Scan Modes

Scan Table (ST) 30 (21 January 2005-28 April 2005). This initial scan used a more rapid vertical scan speed, which generated larger amplitude spurious oscillations in the signals. Because of the difficulty in completely removing these, data from this period are not as good as later data obtained with the other scan tables. This scan also made vertical scans at a LOS azimuth angle of -44.8°, which were found to be inferior to those at -47°.

Scan Table 13: (28 April 2005 - 24 April 2006). Upper and lower limits of scans vary around the orbit, following Earth's oblateness. This was discovered to cause different types of oscillations to be seen in the signals, complicating attempts to remove these artifacts.

Scan Table 16: (26 October 2005, 1 & 2 November 2005, 21 & 22 February 2006, 16 April 2006). Same vertical scan speed as ST 22 & 23, but with greater space-ward and Earth-ward limits. Similar scan pattern as ST 30, with vertical scans at LOS azimuth angles of -44.8 and -47.0.

Scan Table 22: (25 April 2006 to 3 May 2006) Similar to ST 23, but with lower space-ward limit on the scans.

Scan Table 23: (Used after 4 May 2006) It makes slower vertical scans; 27 pairs of vertical up and down scans of ~ 15.5 seconds duration each, followed by a 1-2 second space view before the next 27 scan pairs. To facilitate removal of the oscillations, the space-ward and earth-ward limits of the scans are at fixed elevation scan angles.

4.0 Processing HIRDLS Data –

The modified science scans described in Section 3 and the need to account for blockage of the scene and radiance from the blockage require substantial modifications to the operational data processing. A diagram of the flow of data in the HIRDLS processing is shown in Figure 4.1.

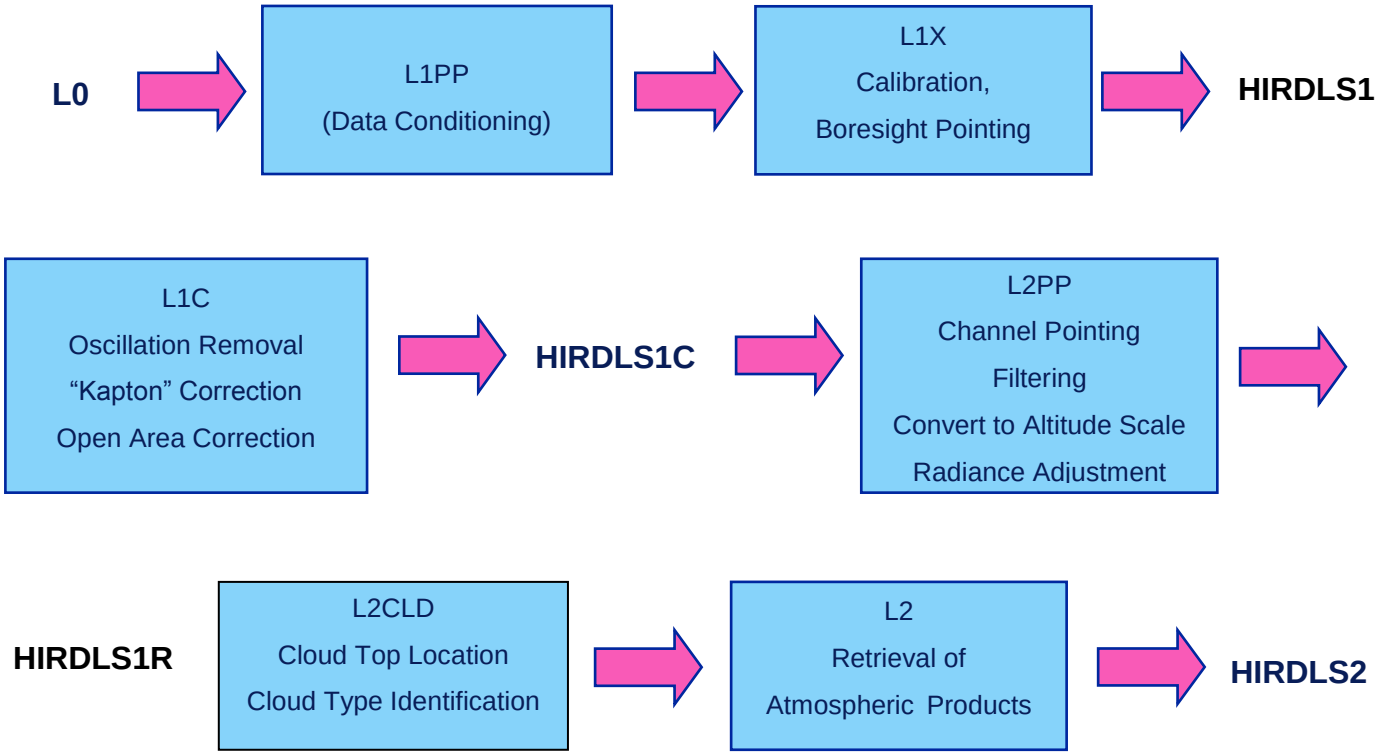

Figure 4.1 HIRDLS Processing Flow Through L2

4.1 L0-1 Processor (L1PP, L1X, L1C)

In the L0-1 suite of processors, the Level 1 Pre-processor (L1PP) corrects an occasional problem with the time in Level 0 (L0) data (raw data counts) while Level 1 Excellorator (L1X) carries out the modified calibration and geolocation. The data resulting from these data operations are released as HIRDLS1 The Level 1 Corrector (L1C) applies the 3 main correction algorithms to remove the effect of the blockage that are outlined in Gille et al., [2008], and some recent work described in Gille et al., [2010]. These data are released as HIRDLS1C. Overall, the L0-1 processor creates a time series of calibrated radiances blocked into profiles as well as housekeeping data necessary to the further data processing.

4.2 L2 Pre-processor (L2PP)

The L2PP process takes the time series of radiance profiles from L1, separates it into individual geolocated vertical scans, determines the vertical registration in altitude, and performs low-pass filtering to condition the radiances for retrieval by the L1-2 software. These data are released as HIRDLS1R, the team's best estimate of the radiances that would have been measured if the blockage were not present.

4.3 L2 Cloud Detection (L2CLD)

The L2CLD routine screens for clouds based on detection of radiance perturbations from the average clear sky case in channels 6 and 12. Cloud tops are located and identified.

4.4 L1-2 Processor (L2)

The L2 step accepts the conditioned radiance data from the L2CLD, and performs the retrievals through a series of iterations. This code is designed to be flexible in handling combinations of radiance channels to retrieve the HIRDLS target species in a user-defined sequence. One of the major features is the use of ancillary data from the Goddard Earth Observing System Model (GEOS-5), produced by NASA's Global Modeling and Assimilation Office (GEOS-5) to determine temperature gradients along the line of sight, which are incorporated to yield an improved retrieval. This processor is described in detail in the L1-2 Algorithm Theoretical Basis Document (ATBD) available on the web at http://www.eos.ucar.edu/hirdls/docs/atbds.shtml. GEOS-5 version 5.01 data were used through January 2, 2008, after which version 5.1 data were used.

A major enhancement to HIRDLS L2 for version 7 processing is a new method of treating aerosol extinction, which in previous versions had been fixed to SAGE-II data mapped to the spectral passband of each channel. In v7, aerosol extinction in channel 6, which is centered at 12.1 microns and is the clearest HIRDLS aerosol channel, is retrieved simultaneously in each product block except temperature and ozone (deemed better using the previous method). During the iteration process, the retrieved channel 6 extinction is mapped by a spectral model to the passband (s) of the channel (s) involved in retrieving the trace gase (s) in a given retrieval block. The mapped extinctions are then passed to the forward model for calculation of radiances. The new method has removed to a large extent the "hot spots" in CFC11 and CFC12 in the tropical UTLS, the noise in the upper altitude ranges of these products as well as in HNO_3, and has resulted in smoother retrievals.

4.5 L2-3 Processor (L3)

The L3 processor is a Kalman filter used as a sequential estimator that combines weighted data from a single profile with a weighted estimate based on the previous data, as described by Rodgers [1977, 2000], Kohri [1981], and Remsberg et al. [1990]. In this process each data point is used to update estimates of the zonal mean and coefficients of the sine and cosine coefficients of the first 7 zonal waves (15 values, equivalent to the mean

plus amplitudes and phases of the first 7 zonal waves). This is done for each pressure level and zonal band going both forward and backward in time, and the results are combined, thus ensuring smooth time evolution. Values are output at one time of day, resulting in daily values of the estimated quantities every 1° in latitude. This produces an optimal estimate of the state of the system in this representation. In general the final estimated field will not go through the input points, but will have an rms difference from them, termed the precision, approximately equal to the precision of the single profile observations. The output data includes this rms value, as well as the values from each of the diagonal elements of the covariance matrix that give the predicted variance of each of the estimated quantities. The output data also includes the number of points that went into producing the estimate for that day. Since the Kalman estimator produces estimates even in the absence of data, a negative number of points indicates the number of days without data since (or until) a day with data.

For gridded data, the coefficients are used to calculate values every 1° in longitude, creating a 1° x 1° grid. V7 L3 products will be described in a later addition to this Data Description and Quality Document, and in http://www.eos.ucar.edu/hirdls/data/.

5.0 HIRDLS Standard Products

Comments common to all products:

Vertical Range

The radiance measured by limb viewing instruments generally decreases as altitude increases, since there are fewer emitting molecules along the path through the atmosphere. The level where the signal to noise ratio (S/N) becomes of order 1 generally sets the approximate upper limit of useful retrievals. Gases with smaller mixing ratios at all levels, will in general have lower top altitudes.

For those gases whose distribution has a layer structure in the stratosphere, the fall to low mixing ratios at and below the layer peak may also lead to low S/N, and no useful retrievals at low altitudes. For species with mixing ratios that fall with altitude, the lower boundary will be reached either when a cloud intercepts the ray path from the tangent point to the detector, or where the channels become optically thick, so that no radiance reaches the detector from the geometric tangent level.

Vertical Resolution

The vertical resolution is shown by the full-width at half-maximum (FWHM) of the averaging kernels. These are presented for the different products in paired panels, with the averaging kernels on the left, and the FWHM on the right. Typically these are very close to 1 km over the range of interest.

The left panel also shows the sum of the averaging kernel values at a given tangent altitude. Values ≈ 1 indicate that all of the information is coming from the measured radiances, with little effect of the *a priori* values. Because of the low noise of the HIRDLS measurements, this is usually the case over the ranges of interest.

HIRDLS Pressure Levels

HIRDLS data are provided on 24 levels per decade of pressure, uniformly distributed in the logarithm of pressure, resulting in spacing that is consistent with the vertical resolution. The levels in a typical decade, 1 to 10 hPa, are listed in Table 5.1.

Table 5.1: HIRDLS Pressure Levels for the Decade of Pressure 1 – 10 hPa

HIRDLS pressures in other decades are these values multiplied by powers of 10.

1.	
1.10069	3.481
1.212	3.831
1.334	4.217
1.4677	4.642
1.616	5.109
1.778	5.623
1.957	6.190
2.154	6.813
2.371	7.499
2.610	8.254
2.873	9.085
3.162	10.00

Precision

There are 2 measures of precision of the HIRDLS products. The L2 retrieval, which uses the Rodgers Maximum A-Posteriori Likelihood method [Rodgers, 2000], calculates an expected uncertainty of the retrievals based on the uncertainties of the input parameters (Khosravi et al., [2009a, b]), http://www.agu.org/journals/jd/jd0920/2009JD011937/.
These are referred to here as the predicted uncertainties.

As described in section 1.3, the predicted precision values are flagged as negative when most of the information in the retrieval comes from the *a priori*. Details regarding negative precision and an example of how to assess the *a priori's* contribution to the retrievals are given in Khosravi et al., [2009a,b].

We also estimate the precision from the variability of the retrieved products; this is referred to as the empirical or observed precision. These values are derived from an analysis of the variability in a set of multiple consecutive adjacent scans. The precision is estimated as the standard deviation of 10 consecutive profiles taken in a ~2.5 minute window over about 1000 km, roughly equivalent to 10 degrees latitude. The set of values at each pressure level is de-trended with a linear least squares fit in order to remove effects introduced by a mean gradient with latitude. The data for a day have been evaluated and averaged over 20° latitude bands. The standard deviation may still include some level of geophysical variability and is therefore an upper limit to the precision. To minimize the effects of geophysical variation we taken the mean of the 10 smallest values in the band, and compared them to the mean of all scans. As expected, these are very similar in summer conditions, when there is less meteorological variability. In these sections we present values in tropical and mid-latitude bands for the equinox or summer periods, respectively. In these conditions the results for all cases are very close to the best 10 cases, indicating we have minimized the effects of geophysical variability. The actual precision of the measurements is then very close to the standard deviation given here.

Accuracy

Because of the aperture blockage, it is not possible to do a first principles estimate of accuracy by the propagation of calibration and instrument characterization errors. We have taken the approach of comparing the HIRDLS products with results from conventional methods, or well-validated satellite data sets. These are the results presented here.

5.1 Temperature

Species:	Temperature
Data Field Name:	Temperature
Useful Range:	1000* – 0.004 hPa **A priori* for pressures >383 hPa
Vertical Resolution:	1 Km
Contact:	John Gille
Email:	gille@ucar.edu
Validation paper (V3):	Gille, J., et al., [2008], High Resolution Dynamics Limb Sounder: Experiment overview, recovery, and validation of initial temperature data, J. Geophys. Res., 113, D16S43, doi:10.1029/2007JD008824.

General Comments:

HIRDLS Temperatures have high (1 km) vertical resolution, as shown by the comparison with COSMIC, and the widths of the averaging kernels. In the stratosphere the precision is independent of latitude and season, and varies from 0.5K in the upper troposphere to about 1K at the stratopause, above which it grows to 3-8K, depending on latitude and season. Temperatures are 0.5 K cooler than sondes and the ECMWF analysis in the stratosphere, save for a positive bias of ~ 1K at the tropical tropopause. HIRDLS temperatures are 1-2 K cooler than SABER and MLS temperatures at the stratopause, and up to 3 K cooler that SABER up to 90 km, where they become too cold.

Resolution:

The vertical resolution is determined from the full-width at half maximum of the averaging kernels. These are shown for each altitude level by the green lines in the left panel of Figure 5.1.1. The blue line in the right panel shows the half-widths explicitly, indicating the vertical resolution is ~1 km from 13-60 km.

The red line in the left panel indicates the fraction of the information that comes from the HIRDLS measurements; values of 1 mean that there is negligible influence from the *a priori*.

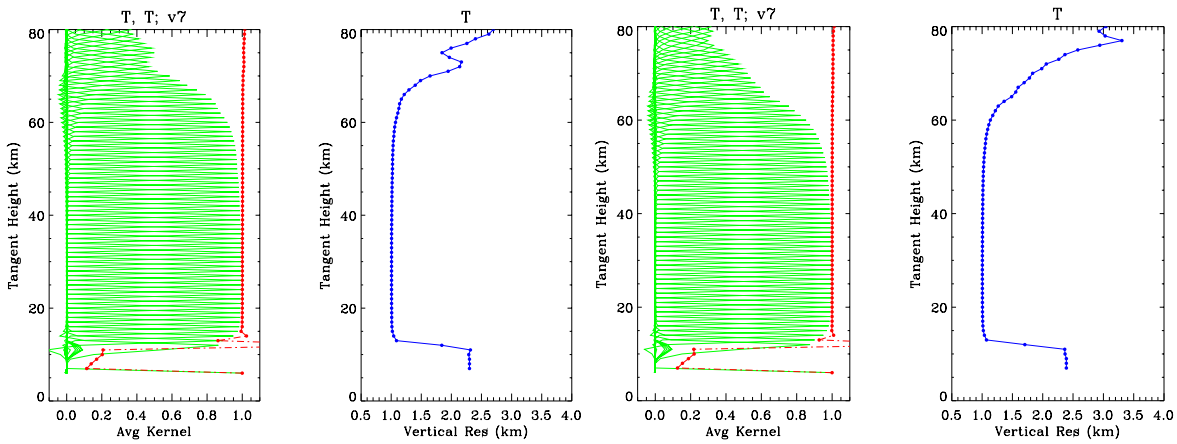

Figure 5.1.1. Averaging kernels for temperature (green lines), and vertical resolution (blue lines) as functions of altitude for HIRDLS temperature profiles. Left, January 15 at 3°N; right, 45°N. Cloud top at 8 km.

The averaging kernels were calculated for 15 January at 3°N (left) and 45°N (right) with a cloud top altitude of 8 km. The rapid drop of the averaging kernel maxima, increase in the half widths, and increase in the fraction of information at altitudes below about 12 km results from relaxation to the *a priori*. This is the GEOS5 temperature for the day for which the data are retrieved. Thus, the retrieval relaxes seamlessly to temperatures that are accurate in the lower atmosphere. Since the GEOS5 resolution is ~1 km in this altitude range, the resolution of the combined retrieval is not degraded. Under clear conditions HIRDLS profiles do not extend below 383 hPa.

The vertical broadening and reduced peaks of the averaging kernels above 60 km are a result of the reduced signal, and thus reduced signal to noise ratio (S/N), at these levels.

Another indication of the resolution comes from comparison with the results from the radio-occultation temperature profiles obtained by the FORMOSAT-3/COSMIC constellation of 6 GPS receivers launched on 14 April 2006 [Gille et al., 2008; Barnett et al., 2008]. These enable temperatures up to the mid-stratosphere to be retrieved with vertical resolution of about 1 km (C. Rocken, private communication). With 1000-3000 such temperature profiles being measured per day at quasi-random locations, a number of coincidences within 0.75° great circle distance and 500 sec can be found with which to undertake comparisons of the two data types, including the fine vertical structure which tends to vary on a short time scale. In this study, each COSMIC profile was paired with the 1 or 2 HIRDLS profiles that fit the criteria for closeness in space and time. If there were 2, the HIRDLS profiles were averaged together. Where there were COSMIC profiles very close together in space and time, a HIRDLS profile might be used more than once in different comparisons. In addition, the GEOS-5 data were included as an indication of the absence of short vertical scales in the operational meteorological analyses.

For this evaluation, data from 11 July 2006 to 31 October 2007 were used. To isolate the small scales, a parabolic fit was subtracted from all 3 types of profiles over the range 2.2-5.7 scale heights, and the residual profiles then apodized. (The pressure scale height is ln 1013/p, so this corresponds to a range of 112-3.4 hPa. Since the scale height is approximately 7 km, this corresponds to an altitude range of ~24 km).

When the apodized profiles are Fourier transformed, the spectra, plotted as amplitudes vs spatial frequency, are as shown in Figure 5.1.2 (from Barnett et al., 2008). Here all 1217 COSMIC profiles are included, irrespective of difference of viewing directions between HIRDLS and COSMIC. As expected, the spectra all have their largest amplitudes at the lowest frequencies. The COSMIC and HIRDLS spectra are very similar for frequencies up to 12 cycles per 24 km, or a 2 km wavelength, and beyond, although the amplitudes become quite small. Clearly these small-scale motions are not contained in the GEOS-5 analyses.

This establishes that HIRDLS is capable of resolving vertical variations in the atmosphere with scales down to ~2 km wavelengths, or 1 km features.

This is consistent with the results obtained by Wright et al., [2011].

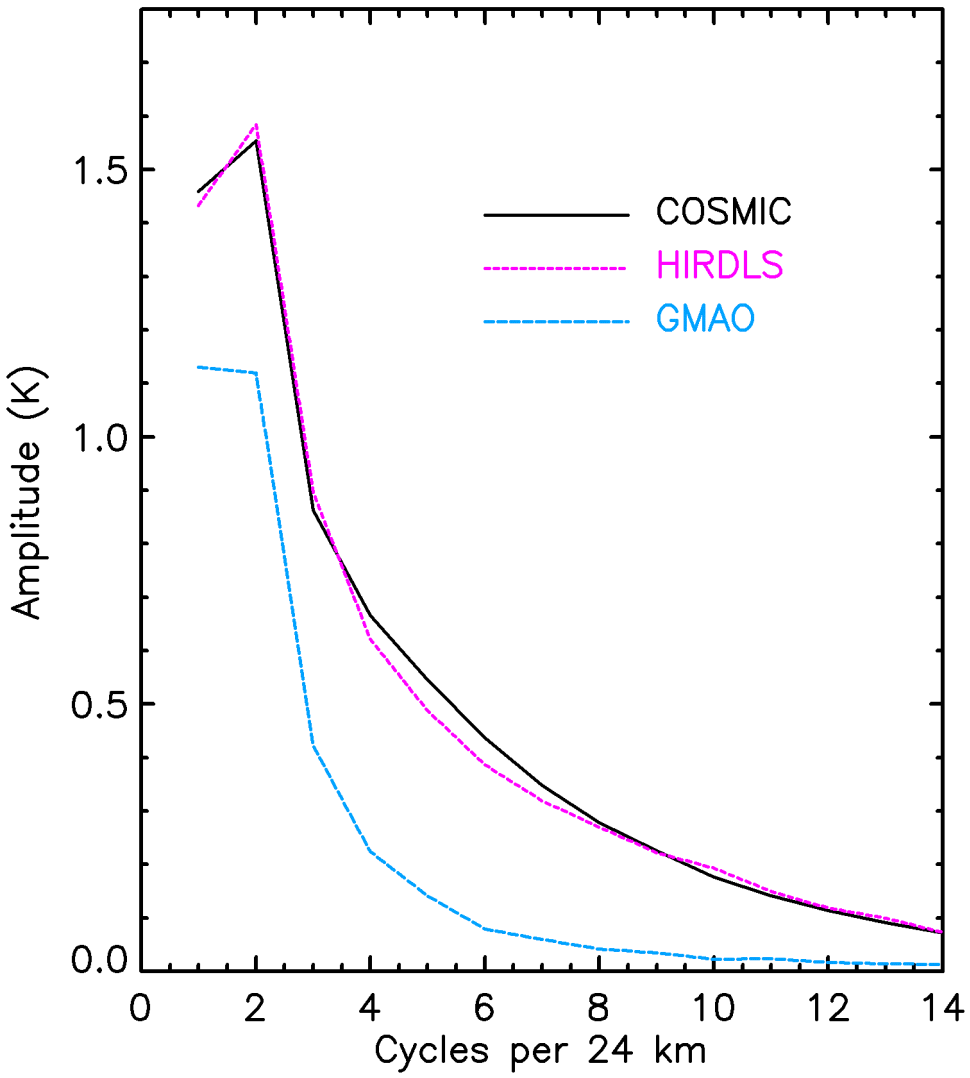

Figure 5.1.2. Comparison of amplitudes versus small scale wavelengths among HIRDLS, COSMIC and GEOS-5. HIRDLS and COSMIC recover vertical scales down to and beyond 12 cycles per 24 km, or 2 km wavelengths.

Precision

The precision of the temperature data was calculated as described in Section 5.0. Results for different latitude bends and seasons are displayed in Figure 5.1.3. Below cloud tops the retrieval precision is that of the GEOS-5 data, taken to be 2K, essentially that of the *a priori* data there. From pressures of 300 hPa to 0.3 hPa the observed (empirical and) predicted values are usually in good agreement. The variations with latitude and season are fairly small in the upper troposphere, stratosphere and lower mesosphere, with values ~0.4-0.5K at 100 hPa, increasing to 1K at 1 hPa.. Precision increases rapidly in the mesosphere, and appears to be larger in the Northern Hemisphere, especially in summer. As noted above, the empirical method of estimating the precision may necessarily include some atmospheric variability, so is an upper limit to HIRDLS retrieval precision. This may contribute to some of the increase with altitude where the effect of small-scale wave motions, especially gravity waves, may be included.

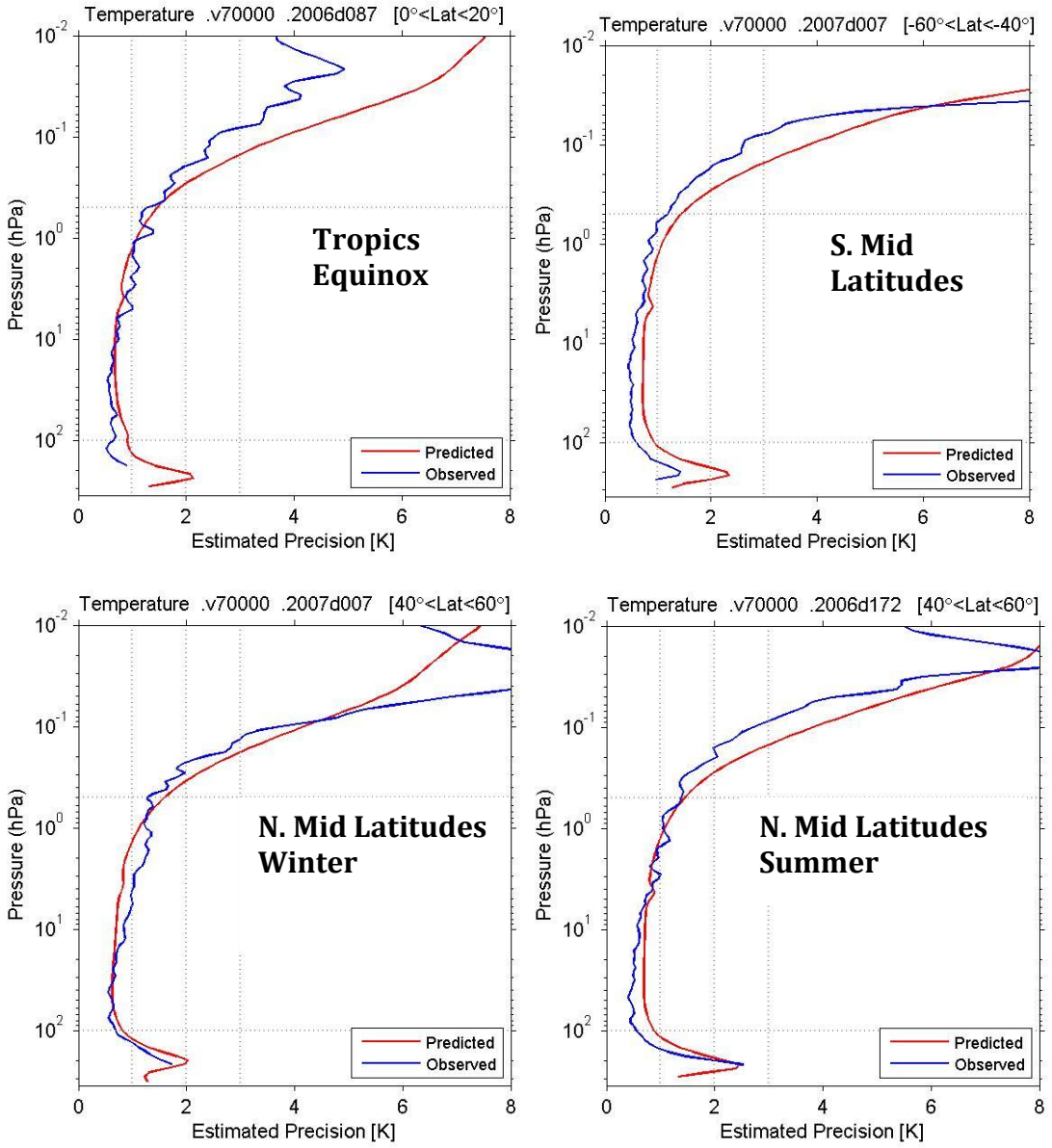

Figure 5.1.3. Estimated empirical (observed) precision of HIRDLS V7 temperature retrievals (blue lines), compared with precision predicted by the retrieval algorithm (red lines). Upper row-tropics at equinox (left), Southern mid-latitudes in Southern summer; Lower row- Northern mid-latitudes in winter (left) and summer (right).

Certainly above 0.1 hPa reduced S/N plays a major role, and relaxation to the *a priori* keeps the precision from being even larger.

Accuracy (Biases)

HIRDLS temperatures have been compared to several data sets in an effort to determine the extent and magnitude of any biases. The results shown here update results of comparisons described by Gille et al., [2008] for V3. An important set of profile comparisons up to about 30 km is between radiosondes and nearby HIRDLS temperatures.

Figure 5.1.4 shows comparisons between high-resolution radiosonde profiles and 2 nearby HIRDLS retrievals at St. Helena and at Gibraltar. The differences in space and time are given. Points to note, in addition to the good agreement, are the way the HIRDLS retrievals follow the small-scale vertical structure in the radiosonde data, as discussed above. Note in particular that one of the Gilbraltar retrievals follows the sharp kink at the lower tropopause exactly, and both follow the double tropopause structure.

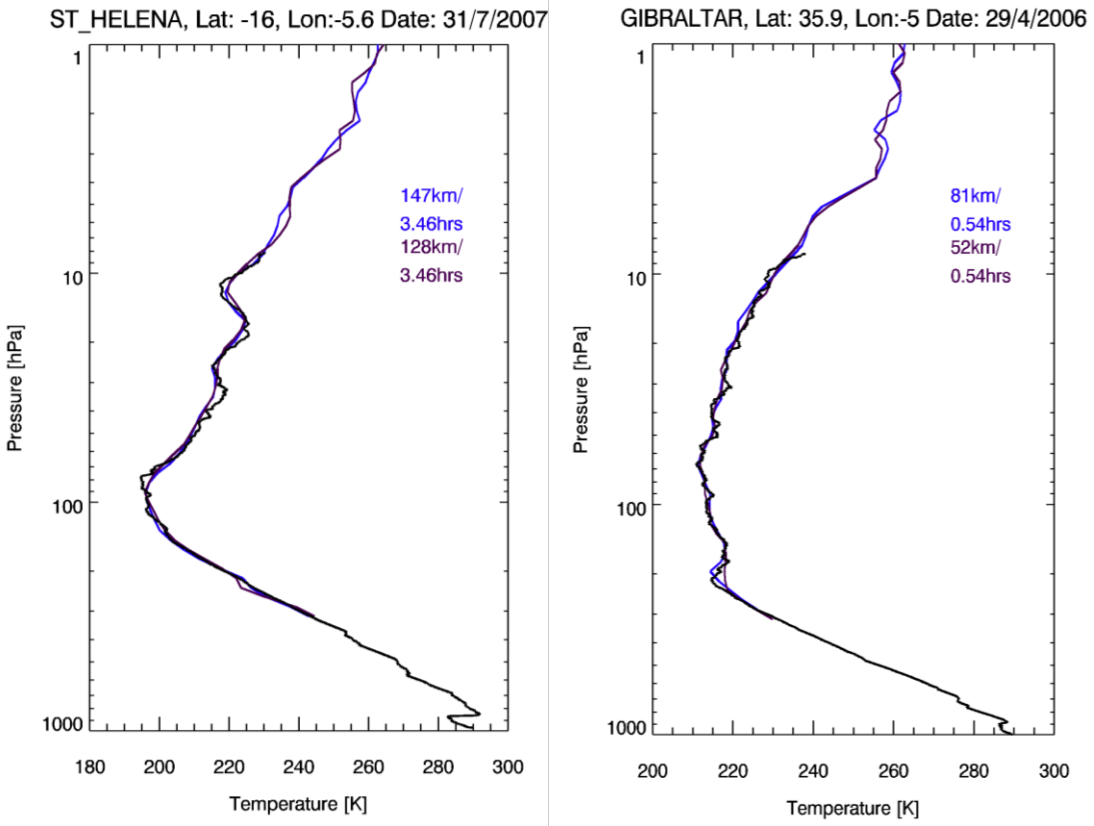

Figure 5.1.4. Temperature comparisons between radiosonde profiles at St. Helena (left) and Gibraltar. Black lines are high-resolution radiosondes, blue and magenta are two nearby HIRDLS retrievals. Differences in distances and times are given.

Statistics of such comparisons at St. Helena, a tropical site (-15.9° latitude), and Gibraltar, a mid-latitude site (36.2°) are displayed in Figure 5.1.5. The green line indicates the mean difference HIRDLS minus sondes, the blue lines show the standard deviation (s.d.) of the differences, while the red dotted lines are ± the predicted precision value calculated in the retrieval code. The mean differences show that in mid-latitudes HIRDLS is within 0.5K of the sondes over the range from ~300 hPa to 10 hPa. The tropical retrieval is similar above 200 hPa, with the exception of a region at the tropical tropopause that is 1K high. This latter effect may be due to the uncorrected effects of stratospheric aerosols. Otherwise, it is believed that most of the differences come from differences in time and space between the radiosondes and the HIRDLS profiles, as well as possible effects of gradients along the HIRDLS line of sight, which are not completely corrected. Differences in vertical resolution may also enter, although HIRDLS is sensitive to temperature variations with wavelengths as small as 2 km as pointed out above and in Gille et al., [2008].

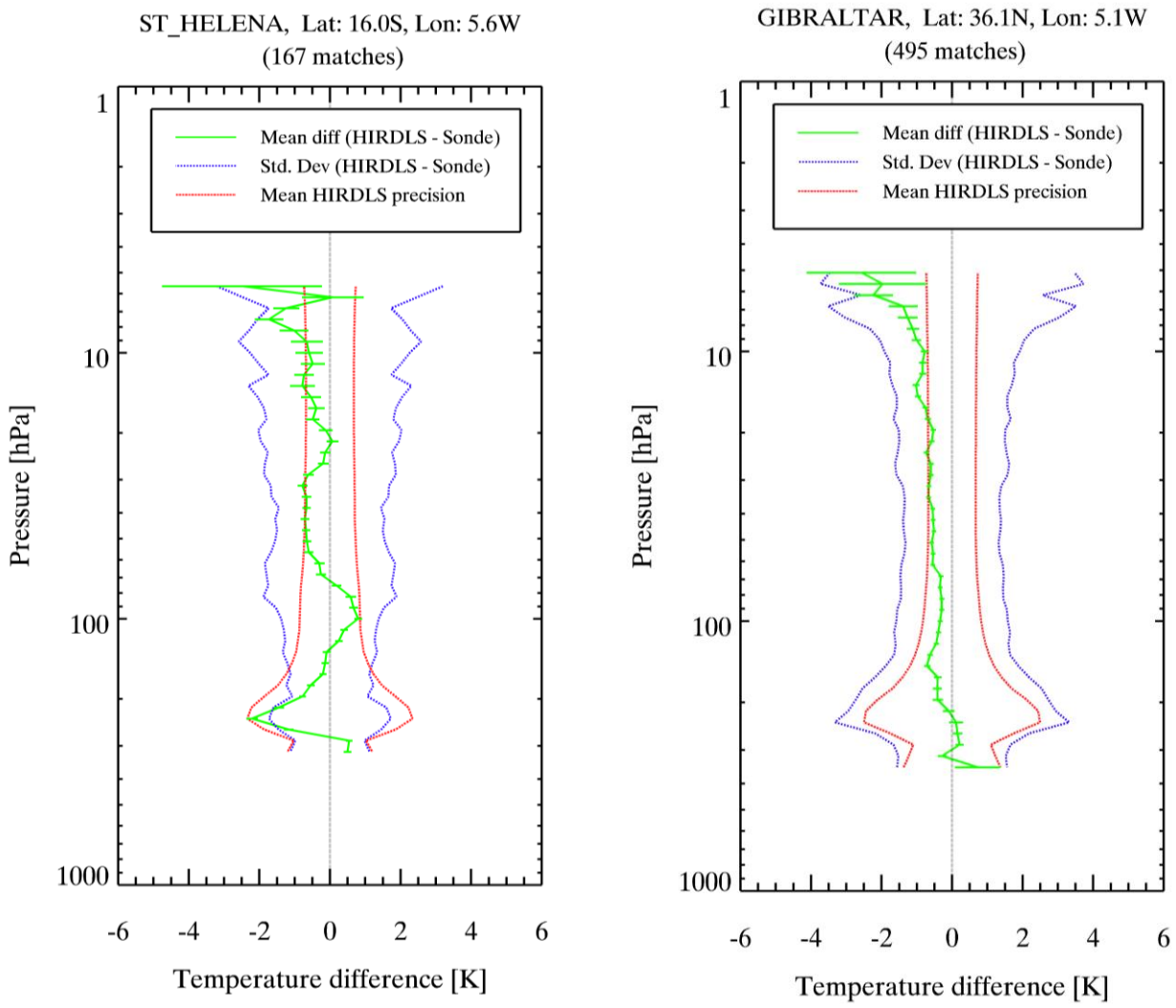

Figure 5.1.5. Statistics of HIRDLS minus sonde differences for Gibraltar. Green line shows mean differences, while blue line shows the standard deviation of the differences. The red lines indicate the predicted precision of the temperatures, which in this region are very close to the empirical precisions.

Comparisons with lidar data allow extending the assessment into the mesosphere. An example of such a comparison with the lidar at Mauna Loa is shown in Figure 5.1.6. This again shows the retrieval following the sharp tropopause and stratopause, and tracking the temperature up to 0.01 hPa (~80 km).

Statistics for comparisons between HIRDLS temperatures and the lidar for Table Mountain, California, are shown in Figure 5.1.7. HIRDLS temperatures are within 2K of the lidar temperatures up to 1 hPa, then remain ~ 5K cooler up to 0.01 hPa. Similar statistics are obtained at Mauna Loa.

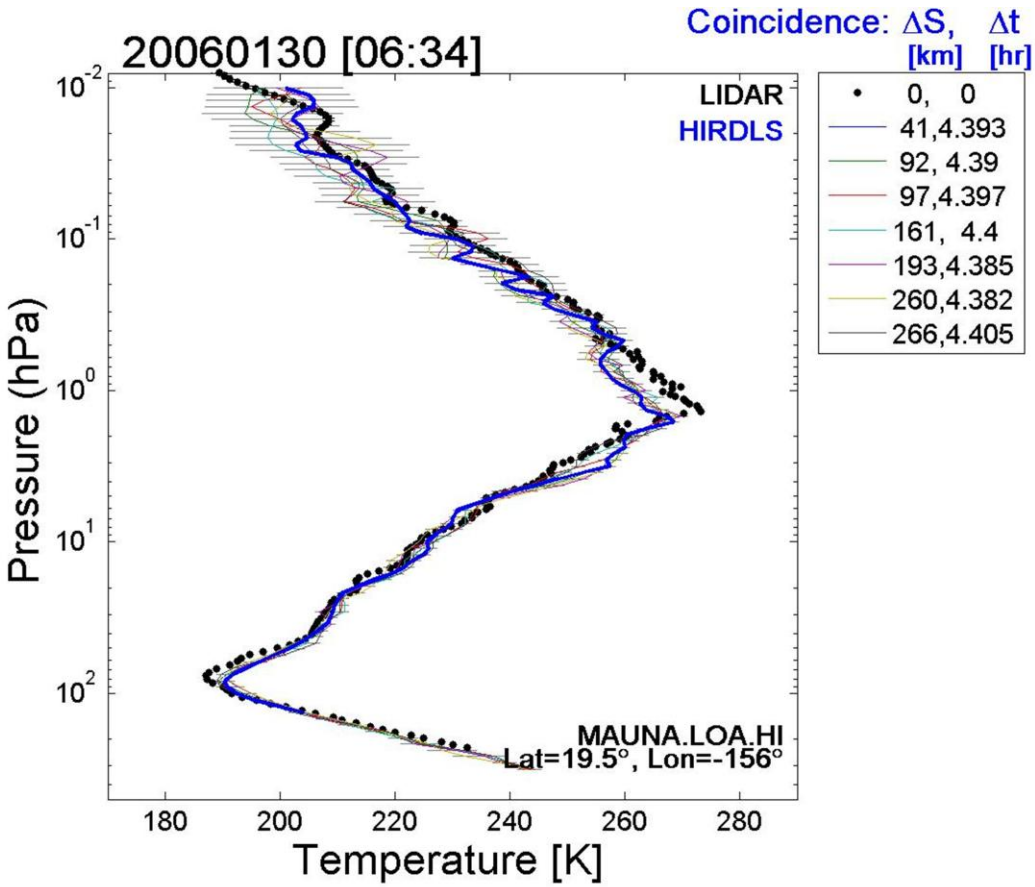

Figure 5.1.6. Comparison between lidar temperature measurement at Manua Loa, Hawaii on 30 January 2006 (black dots) with the closest HIRDLS V6 retrieval, where the closest (41 km distant, 4.4 hours different in time) (solid blue line) and 6 other nearby retrievals (thin lines.) [To be updated]

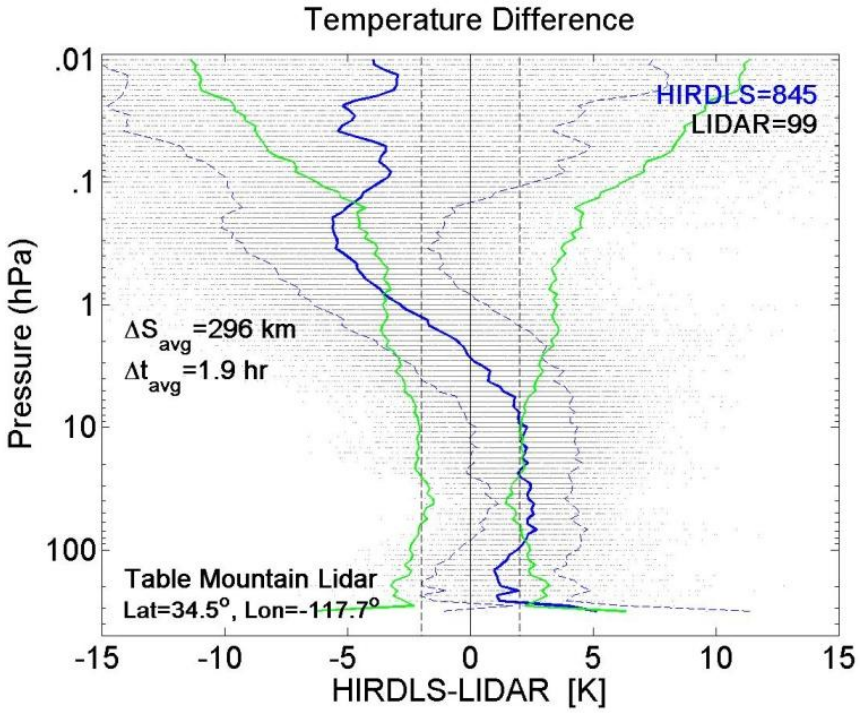

Figure 5.1.7. Statistics of HIRDLS V6 minus lidar temperatures for 99 lidar profiles and 845 closely coincident HIRDLS retrievals. The vertical dashed lines indicate ± 2K, the horizontal lines indicate the standard deviation of the differences, and the green lines indicate the random error predicted by the retrieval algorithm. [To be updated].

To investigate possible latitudinal or seasonal biases, comparisons are next shown with global data such as those obtained from other validated satellite instruments or operational assimilated data sets. A set of such comparisons is presented in Figure 5.1.8, which compares latitude-altitude cross-sections of HIRDLS minus other data differences for November 2007.

Comparison with data from the Sounding the Atmosphere by Broadband Emission Radiometry (SABER) evaluated by Remsberg et al., [2008] shown in the top panel does not indicate large latitudinal variations, except possible at high southern latitudes. This supports a small warm region at the tropical tropopause, but indicates cooler temperatures in the stratosphere, good agreement around the stratopause, and cooler temperatures by a few degrees in the mesosphere.

A comparison between HIRDLS and the European Centre for Medium-range Weather Forecasting (ECMWF) ERA-Interim assimilated data [Dee et al., 2011] over the HIRDLS latitude range for November 2007 is shown in the middle panel of Figure 5.1.8. From this we see that HIRDLS V7 temperatures are within 1K of ECMWF temperatures from 400 to ~3 hPa, becoming lower above that level. Again, there is little latitudinal structure, but again an indication that HIRDLS may be warm at the tropical tropopause. (The ERA-Interim data for this study are from the Research Data Archive (RDA) which is maintained by the Computational and Information Systems Laboratory (CISL) at the National Center

for Atmospheric Research (NCAR). NCAR is sponsored by the National Science Foundation (NSF). The original data are available from the RDA (http://dss.ucar.edu) in dataset number ds627.0.)

Finally, the lower panel shows HIRDLS minus Microwave Limb Sounder (MLS) version 3.3 temperatures, indicating agreement within 1-2 degrees in the stratosphere, but with HIRDLS cooler in the upper mesosphere. The earlier V2.2 has been validated by Schwartz et. al., [2008], while the Data User's Guide for V3.3 may be found at http://mls.jpl.nasa.gov/data/datadocs.php There is no indication of latitudinal variation, but there is a small scale vertical banding not apparent in the other comparisons.

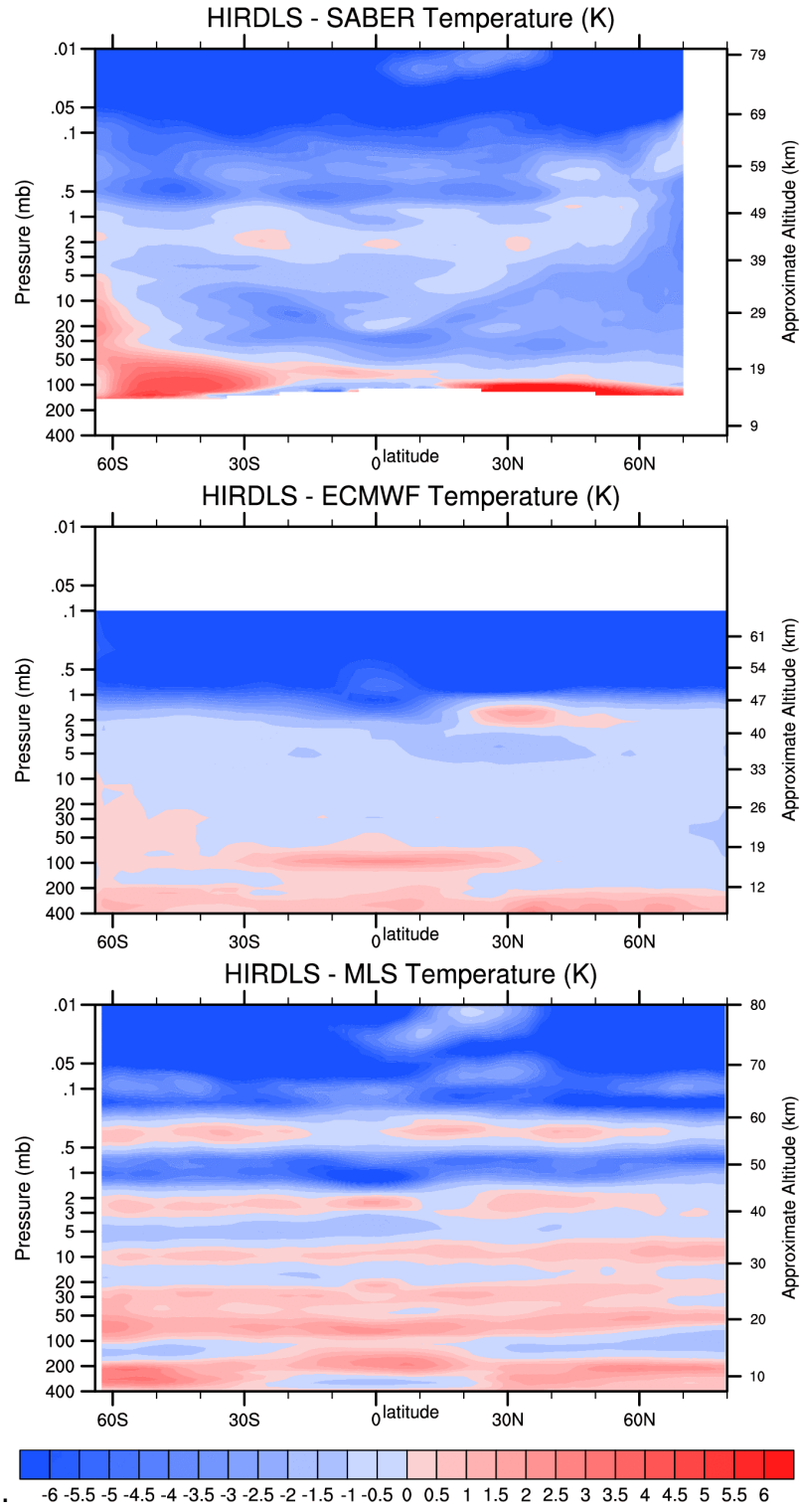

Figure 5.1.8. Monthly mean difference cross-sections, HIRDLS minus SABER (top panel), HIRDLS minus ECMWF ERA-Interim (center panel) and HIRDLS minus MLS (bottom panel).

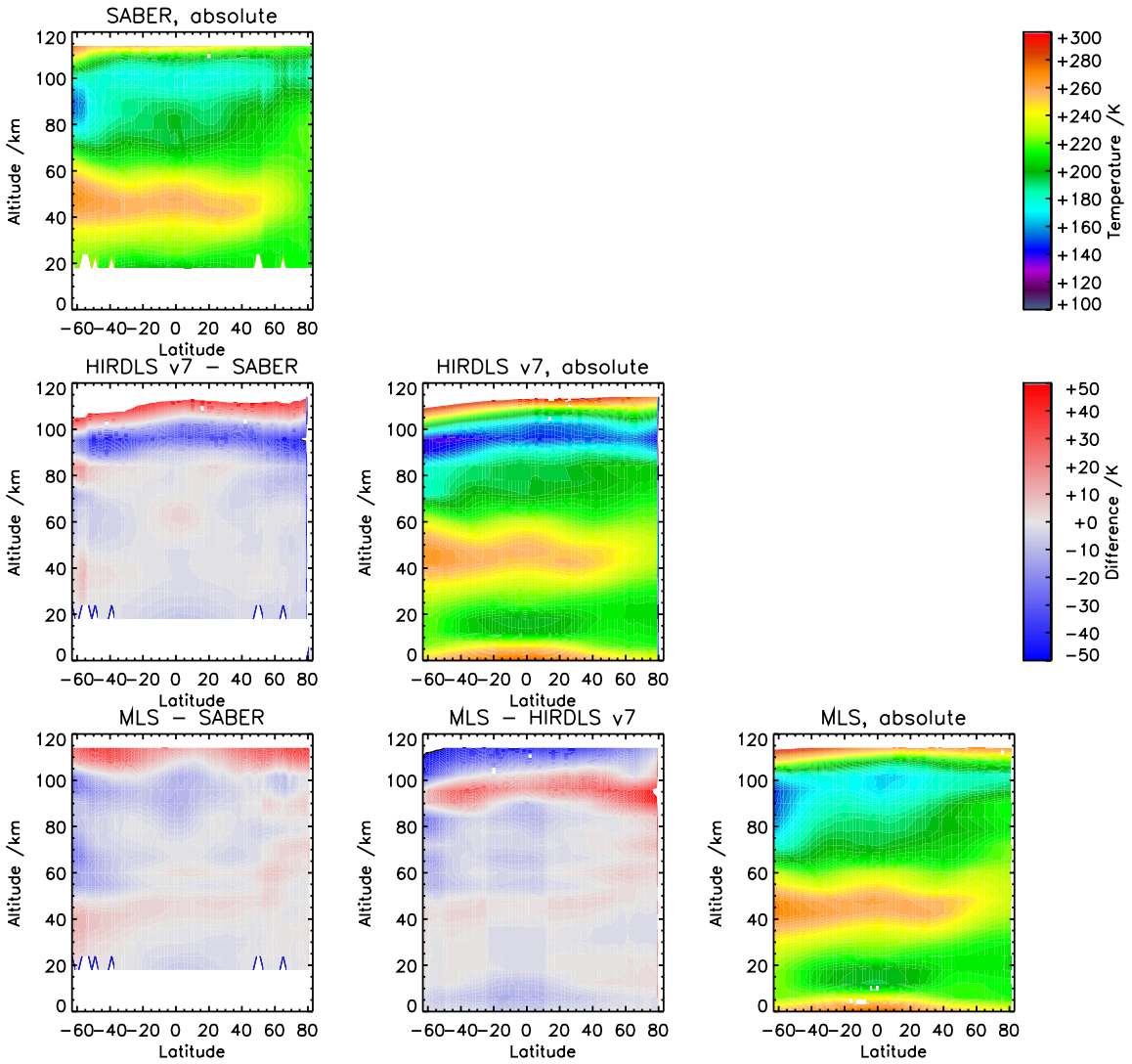

Fig. 5.1.9 SABER, HIRDLS and MLS temperatures and differences up to 100 km, averaged over the HIRDLS mission. HIRDLS agrees with SABER and MLS up close to 86 km (0.004 hPa).

Another comparison is shown in Fig. 5.1.9, indicating that V7 temperatures are close to SABER and MLS up to about 86 km, or 0.004 hPa, a few km higher than the previous V6 data.

Summary

The HIRDLS temperatures have 1 km vertical resolution, a precision between ≤ 0.5K (lower stratosphere) to > 3K (mesopause) and are accurate to ≤ 1K from the 300-400 hPa to 1 hPa, becoming cooler above that level. In the mesosphere HIRDLS temperatures are cooler than lidar temperatures and other global data from SABER, MLS, and ECMWF ERA-Interim, but they show the same temporal and spatial variations seen in other observations.

5.2 Ozone (O_3)

Name of Product: O3 (ozone)
Useful Range: 422 hPa - 0.1hPa
Vertical Resolution: 1 km
Contact: Bruno Nardi
Email: nardi@ucar.edu
Validation Paper: Nardi, B., et al. (2008), Initial validation of ozone measurements from the High Resolution Dynamics Limb Sounder, *J. Geophys. Res.*, 113, D16S36, doi:10.1029/2007JD008837.

General Comments

HIRDLS V7 ozone has a bias within 10% of most other data sources and often less than 5%. There remains a high bias in the tropical UTLS region, possibly related indirectly to the presence of aerosols there. There persists a small day-night asymmetry in the ozone magnitude, with higher values in daytime (ascending orbital node), though at a diminished level compared to V6. About 30% of the profiles extend down to 422 hPa and about 60% extend to 250 hPa maintaining positive precision (not dominated by *a-priori* information); comparisons with ozonesondes indicate that these are also useful. The precision outside of the tropics is estimated at 2-5% between 0.5-70 hPa, and <20% out to 0.2 hPa and to 200 hPa. In the tropics it is somewhat worse than this below 50 hPa, in large part due to the low ozone values there.

Vertical Resolution

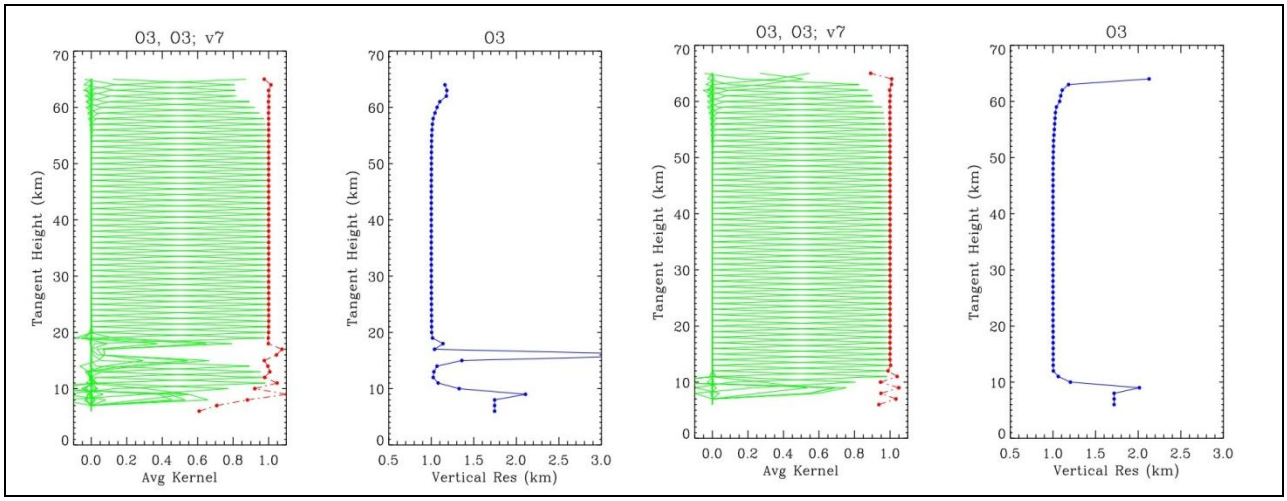

Figure 5.2.1. Shown for low latitudes (first plot) and mid-latitudes (third plot) are the averaging kernels for HIRDLS ozone (green), and the integrated area under each kernel (red). Integrated area values of unity indicate that all information for that vertical step comes fully from measurements and not the *a priori*. The second and fourth plots represent the ozone vertical resolution (blue) as a function of altitude for the respective latitude region, as derived from the FWHM of each kernel.

The vertical resolution is given most directly by the averaging kernels shown in figure 5.2.1. The resolution is 1km between 12-62 km, roughly 200-0.2 hPa. The resolution decreases to about 2 km at 10 km (~260 hPa) and earthward, and at 62 km (0.2 hPa) and spaceward. A note on the kernels in the tropical UTLS: the broader kernels between 15-20 km are indicative of the fact that there is a sharp reduction in ozone to low values at those altitudes.

Comparisons of HIRDLS ozone with ozonesondes profiles taken during the NH mid- and high latitude winter and spring, where ozone lamina are widespread in the upper troposphere lower stratosphere (UTLS) region, show clearly that HIRDLS resolves the fine vertical scales of these features, (see figure 5.2.2). This is confirmed statistically by calculating the altitude-dependent HIRDLS-sonde ozone bias for all comparison cases, and comparing it with the bias using only those cases where strong laminae were present. If the presence of thin ozone laminae with high vertical gradients posed a greater difficulty for HIRDLS to resolve, then either the mean difference (bias), or the standard deviation of the differences would have larger values for the laminae-only case in the region of the profile where those laminae are present; and this is not the case as seen in figure 5.2.3. In fact, the bias is somewhat smaller for the lamina-only case, near ~150 hPa, so it can be inferred that the ozone lamina are resolved with similar accuracy compared to the more gradually-varying ozone profiles.

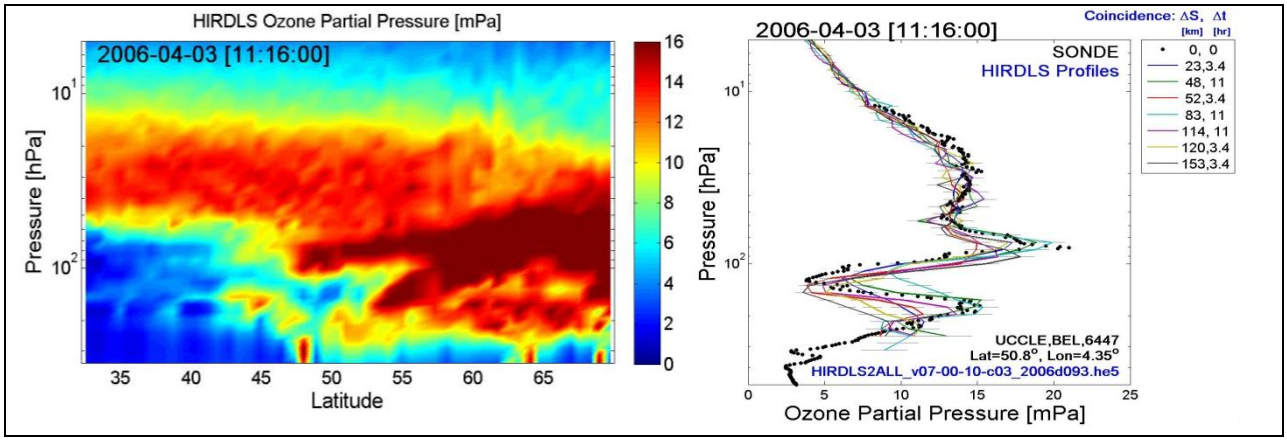

Figure 5.2.2. Shown at left is a HIRDLS observation of a double layered ozone filament in the NH spring UTLS between latitudes 30°N - 60°N, extending to 300 hPa (left). A comparison with a coincident ozonesonde (right, black dots), of the closest seven HIRDLS profiles (colored lines, 23-150 km, 3-11 hours), indicates that the vertical features are well resolved in the HIRDLS measurement as low as 300 hPa.

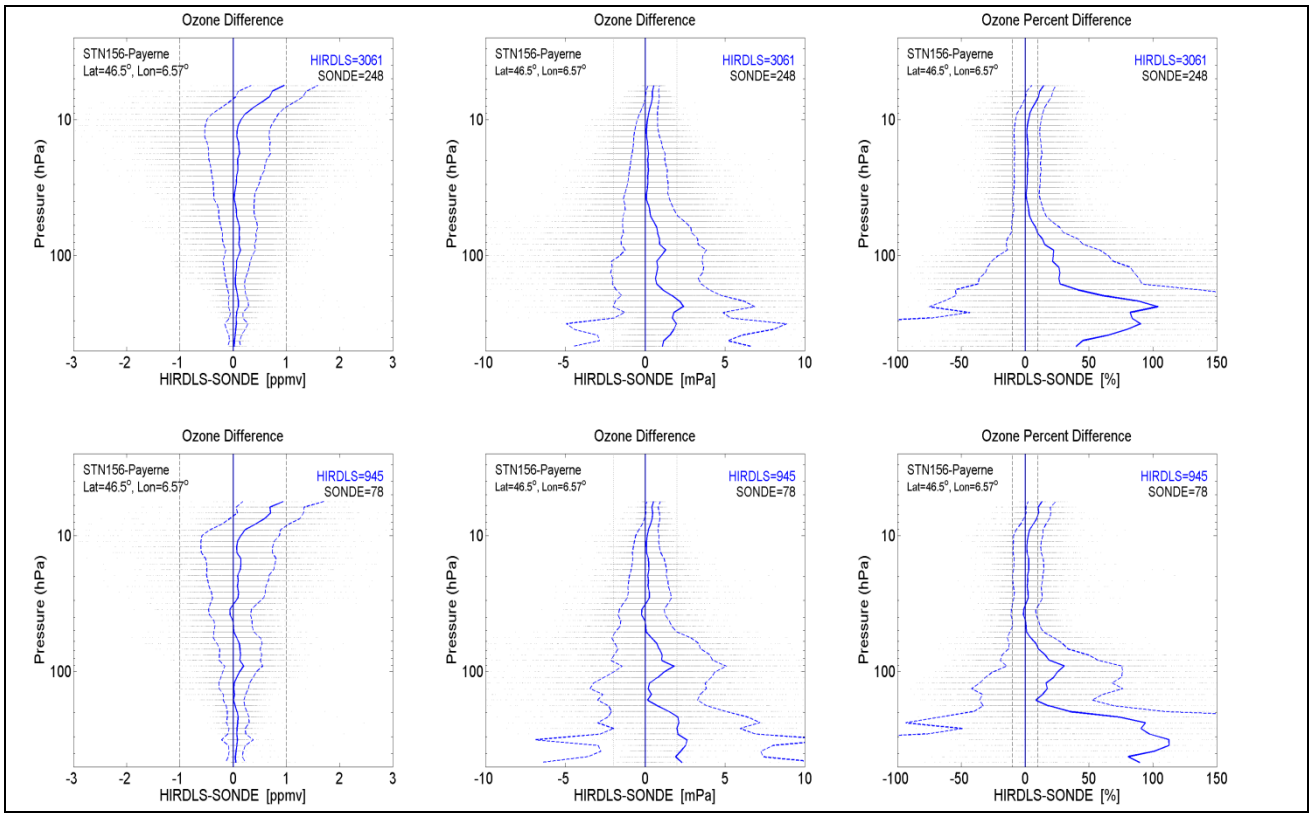

Figure 5.2.3. Above are plots of the HIRDLS ozone bias with respect to coincident ozonesonde profiles at Payerne, Switzerland (46.5N), from the WOUDC site in units of mixing ratio (left), partial pressure (center) and percent-difference (right). The top row of plots includes all coincident profiles from years 2005-2007. The bottom row of plots includes only the coincident profiles during 2005-2007 in which strong lamina were present. The quantity of coincident profiles used are inset on the upper RHS of each plot. The fact that neither the mean difference nor the standard deviation of the differences is significantly higher for the lamina-only case (bottom) indicates that HIRDLS is measuring the thin lamina with close to the same accuracy as profiles with less vertical structure.

Precision

Figure 5.2.4 shows observed precision estimates (blue lines) for latitude bands centered at 70N deg, 10N deg and -50S deg, respectively, compared with predicted ozone precision values (red lines, O3Precision parameter in HIRDLS2 data files). The method used to determine the observed precision is described in Section 5.0, and agrees very well with the predicted precision (red lines).

Observed ozone precision in mixing ratio units is typically 100-300 ppbv or less; it is about 10-100 ppbv in the tropical UTLS. In percentage units, the precision is 2-5% in the region spaceward of 50-100 hPa and earthward of 0.5 hPa, depending on latitude (higher pressure limits corresponding to higher latitudes). At the top of the profiles, between 0.5-0.1 hPa, ozone precision increases spaceward from 5% to 25% for all latitudes. Precision between 100-260 hPa is between 5% and 30% at mid- and high latitudes, increasing earthward. In the

tropics there is a bias which peaks at 100% or more in the region centered near 70-100 hPa. This is probably an effect caused by the presence of aerosols here. The so-called aerosol correction is not implemented in V7 ozone, because collateral ozone degradation arises when such a correction is applied.

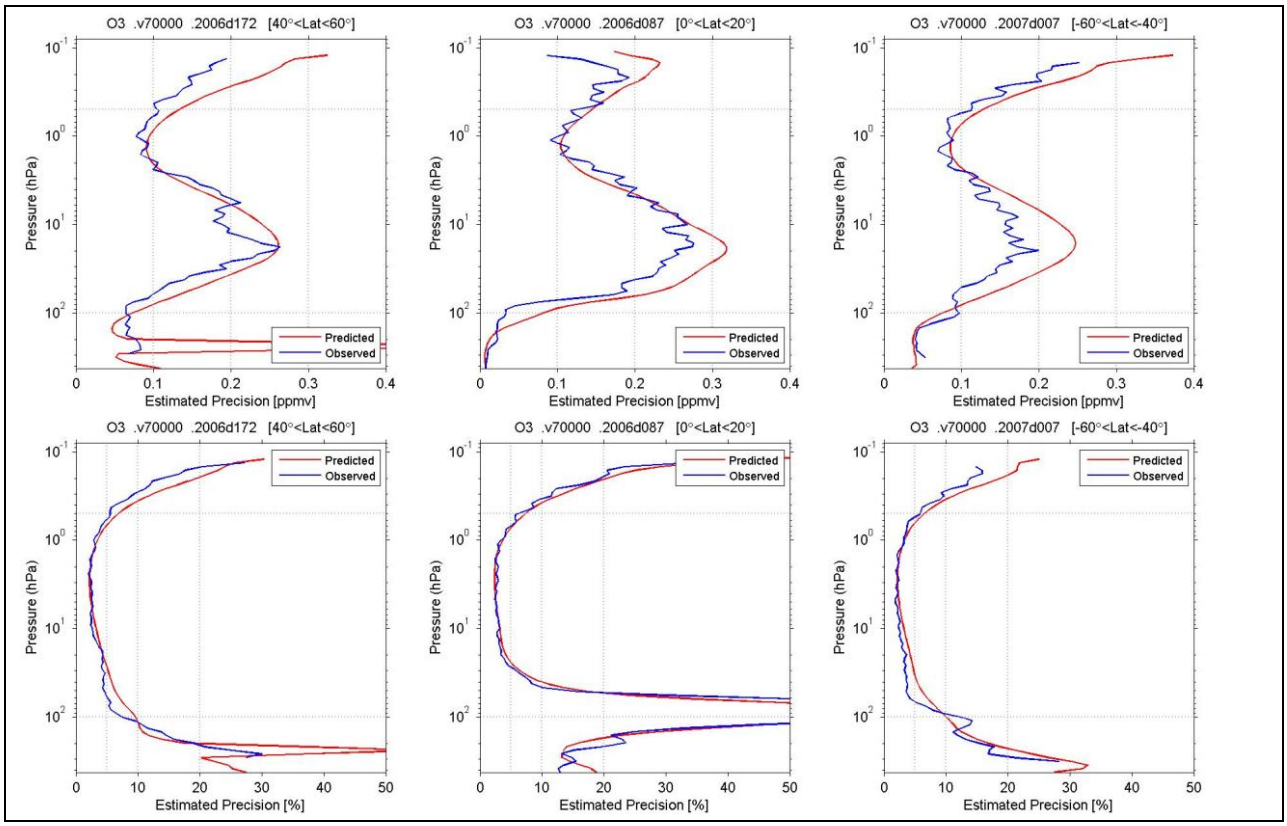

Figure 5.2.4. Shown are the predicted (red) and observed (blue) ozone precision, in units of volume mixing ratio (top row) and percent (bottom row). The 'predicted' precision is computed by the retrieval algorithm, and averaged over all profiles in the indicated latitude band during the 24 hour period. The "observed" precision is computed as the average of the all the detrended sequences of 12 consecutive profiles in that latitude band during the 24 hour period (see Section 5). Three representative latitude bands are shown for relatively undisturbed periods (i.e., NH summer at Northern high latitudes): 40-60 deg N (left), 0-20 deg N (center), -60--40 deg (right).

Accuracy

The HIRDLS V7 ozone bias is determined here via comparisons with ozone-sondes, ozone lidars, and the ACE-FTS and Aura-MLS satellite measurements. The results are presented in terms of volume mixing ratio, percentage difference, and in partial pressure units for the case of ozonesondes.

Comparisons with all coincident measurements indicate that V7 ozone has a low bias centered at about 10 hPa with a magnitude of about 100-600 ppbv, approximately 1-10%. This low bias is latitude dependent, with the largest magnitudes seen in the tropics, and the smallest magnitudes and vertical extent seen at mid latitudes. At high latitudes the low bias magnitude is moderate, but at times has the largest vertical extent (3-30 hPa). This is best illustrated in the MLS comparisons (figures 5.2.7 and 5.2.8), and is confirmed in the lidar comparisons in figure 5.2.6 and the ACE-FTS comparisons in figure 5.2.9.

Between 1-5 hPa, the bias is positive with respect to MLS, with a magnitude of <300ppbv, roughly <5%. Lidars indicate that this upward shift to positive bias happens higher at about 2 hPa. ACE comparisons contradict these, showing a neutral to a negative HIRDLS bias. Known ozonesonde measurement inaccuracies of up to 10% and greater above 10 hPa precludes their use for determining HIRLDS accuracy in this region.

Below the ozone layer peak, at about 20 hPa, the bias is at a minimum. This is seen universally with all comparisons, including ozone sondes (figure 5.2.5), however this bias is latitude dependent. The strongest bias is centered in the tropics at about 70 hPa (about 500 ppmv or more), which can translate to >100% due to the low ozone abundance there. It is not expected that ozone spikes linked to the presence of undetected clouds, a problem cited in earlier HIRDLS releases, contribute significantly to this high bias, but isolated instances of such spikes may be possible at both low and high latitudes. The high bias is probably related to the presence of aerosols here. Although a correction for this has proved useful in some species, (HNO_3, CFCs, NO_2, and others), it was not implemented on ozone as there were negative effects on UTLS ozone in the extra-tropics. This is not well understood, but a modified 'aerosol correction in the future could potentially yield much improved tropical ULTS ozone.

Comparisons at mid-latitudes tend to show the least bias overall, for all comparisons. Ground-based lidar at Table Mountain Facility (39°N) indicates agreement of 3% or better (<300 ppbv) between 2-30 hPa (figure 5.2.5, top).

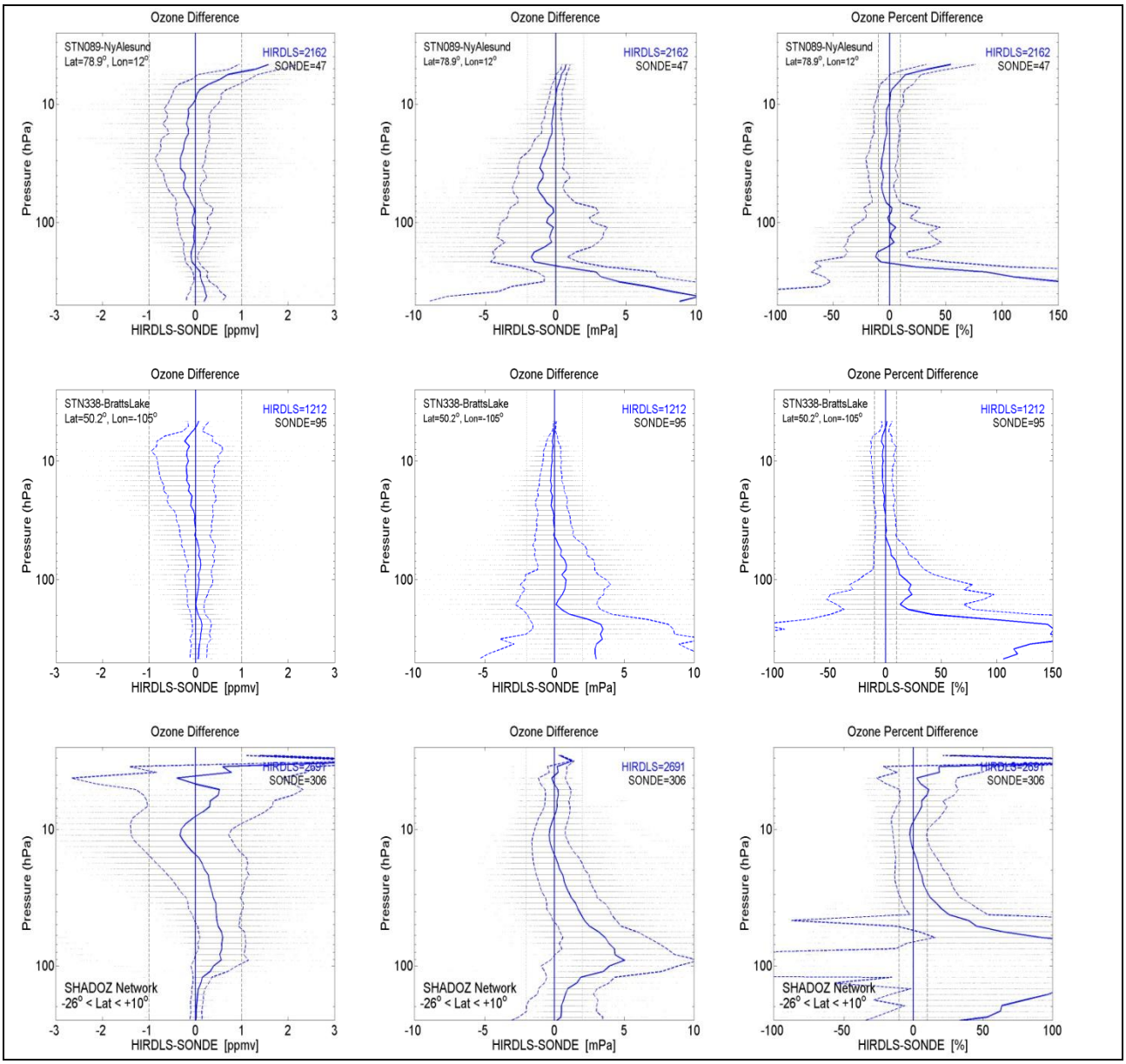

Figure 5.2.5. The mean ozone difference (solid blue lines) from comparisons with ozonesondes are shown for 2006 for the high latitude station at Ny-Alesund, Norway (top), for 2005-2007 for the mid-latitude station at Bratts Lake, Canada (middle) and for the low latitude SHADOZ Network, -26 º < Lat < 10º (bottom). From left to right the plots are in ozone units of volume mixing ratio (ppmv), partial pressure (mPa) and percentage difference. The dashed blue lines are the standard deviation of differences.

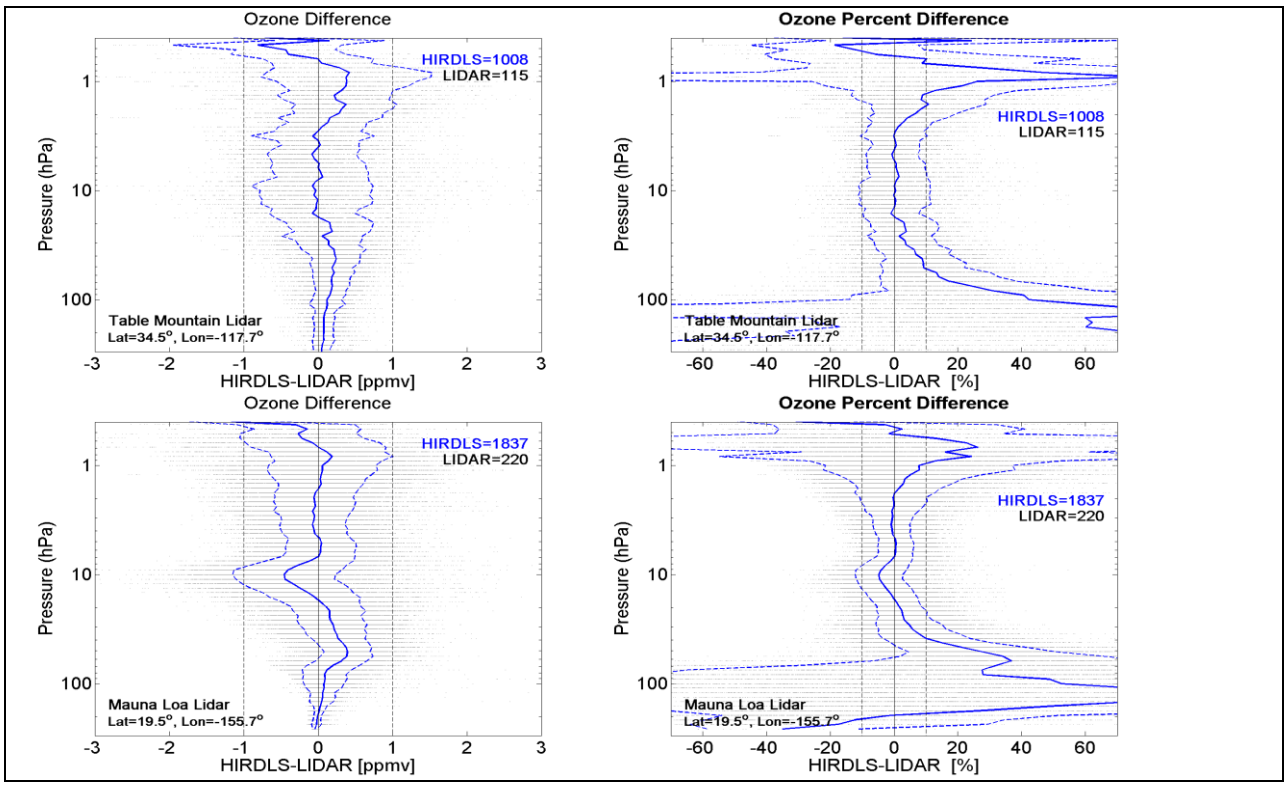

Figure 5.2.6. The mean ozone difference (solid blue lines) from 2005-2007 comparisons with lidars are shown for the mid-latitude station at Table Mountain Facility (39°N, top row) and for the low latitude Mauna Loa Observatory (20°N, bottom row). Left plots are in ozone units of volume mixing ratio (ppmv); right side plots and percentage difference. The dashed blue lines are the standard deviation of differences.

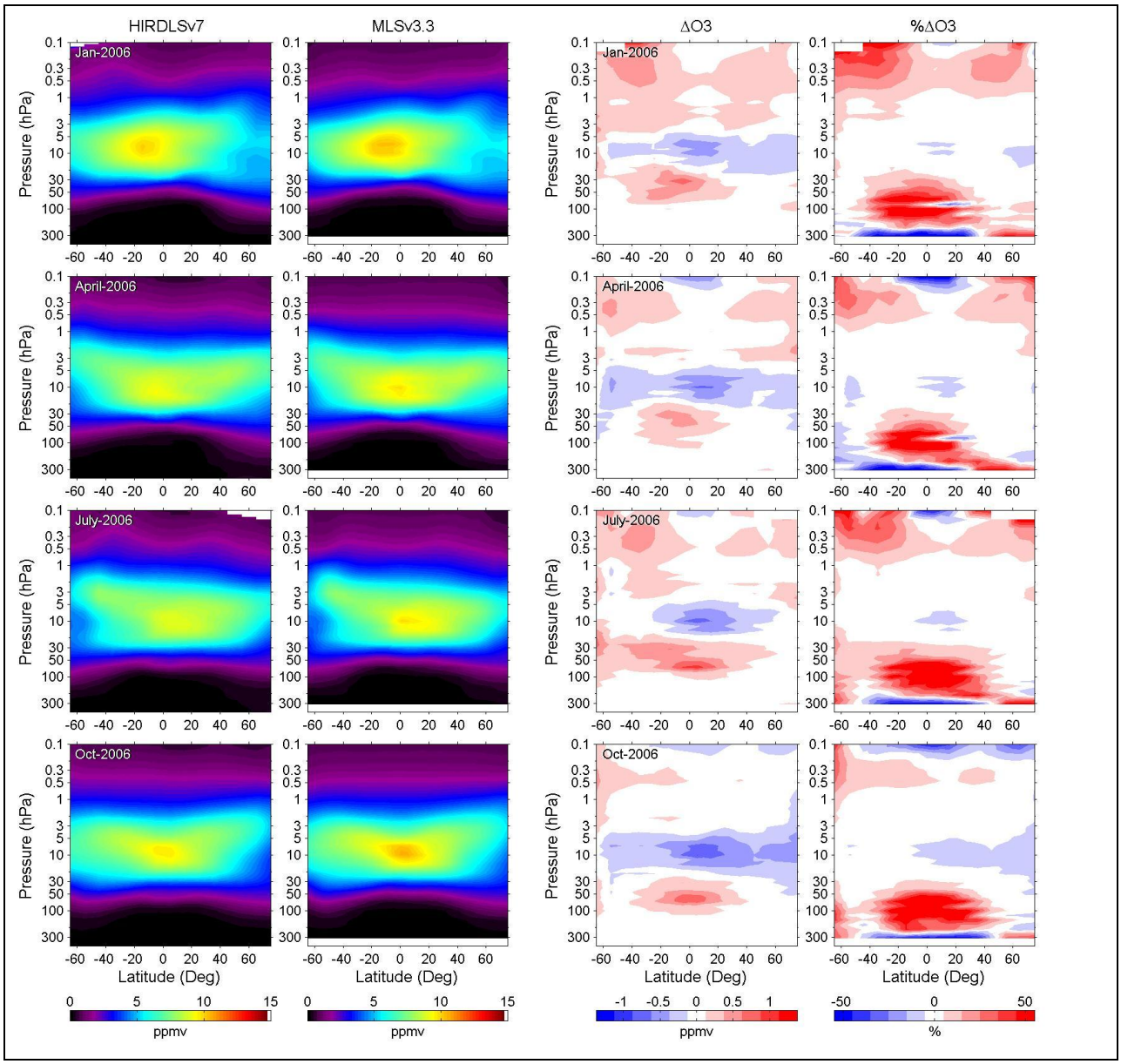

Figure 5.2.7. The two left columns show the monthly zonal mean cross sections for HIRDLS V7 and MLS V3.3 ozone (ppmv), for the months: January, April, July and October of 2006 (as indicated at top left, inset, of each plot in columns 1 and 3). The mixing ratio difference and percentage difference (HIRDLS–MLS)/(MLS) are shown in the 3rd and last columns respectively. The white areas in the difference and percent difference plots correspond to 0 ppbv ±125 ppbv and 0%±5%, respectively; each blue and red color increment in the color band corresponds to a multiple of 250 ppbv and 10%, respectively.

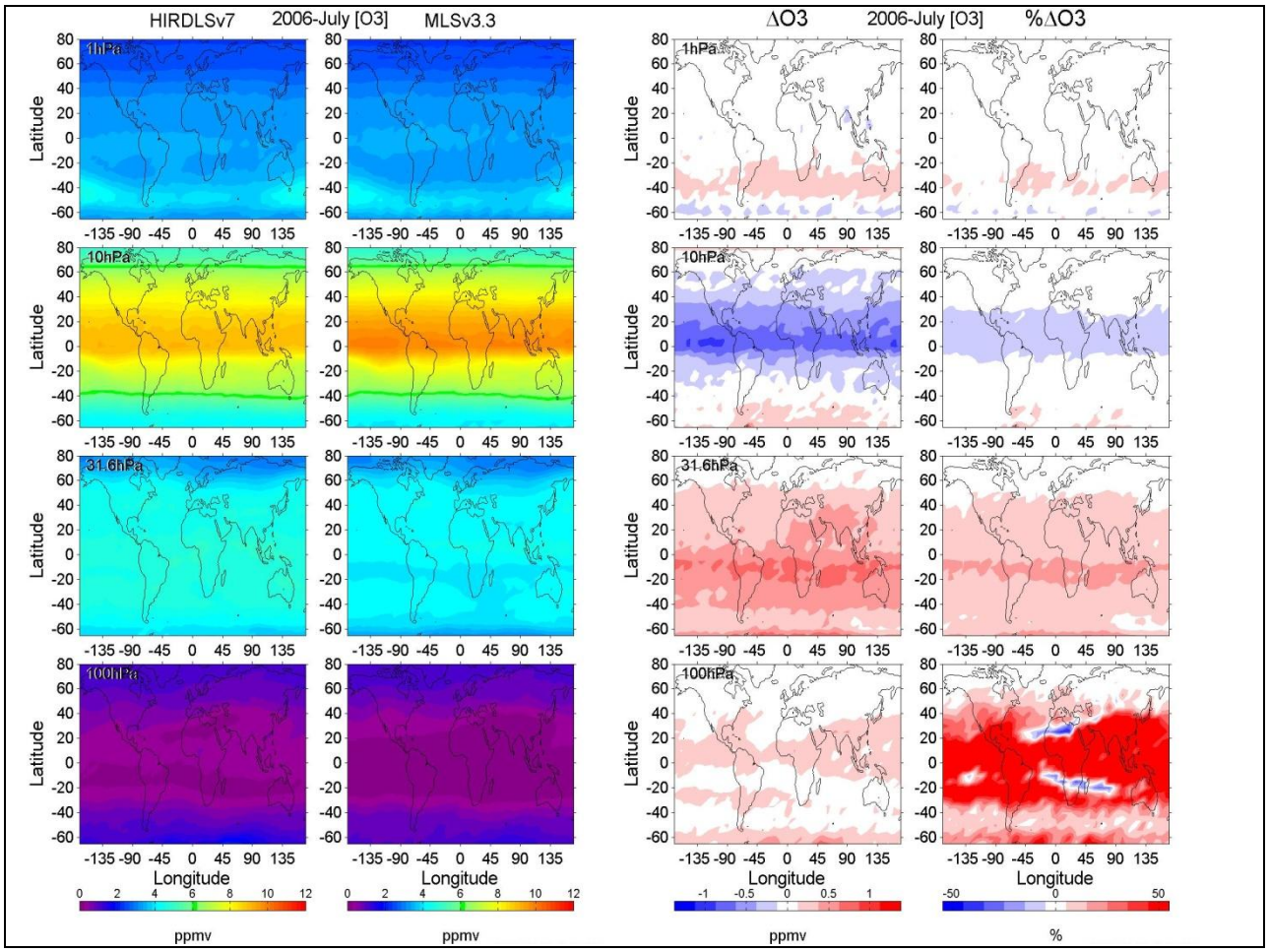

Figure 5.2.8. Shown are July 2006 monthly average Mercator cross sections of HIRDLS and MLS ozone (ppbv) for pressure levels: 1 hPa, 10 hPa , 31 hPa and 100hPa, from the top row to the bottom row. The mixing ratio difference and percentage difference (HIRDLS–MLS)/(MLS) are shown in the 3rd and last columns respectively. The white areas in the difference and percent difference plots correspond to 0 ppbv ±125 ppbv and 0%±5%, respectively; each blue and red color increment corresponds to a multiple of 250 ppbv and 10%, respectively.

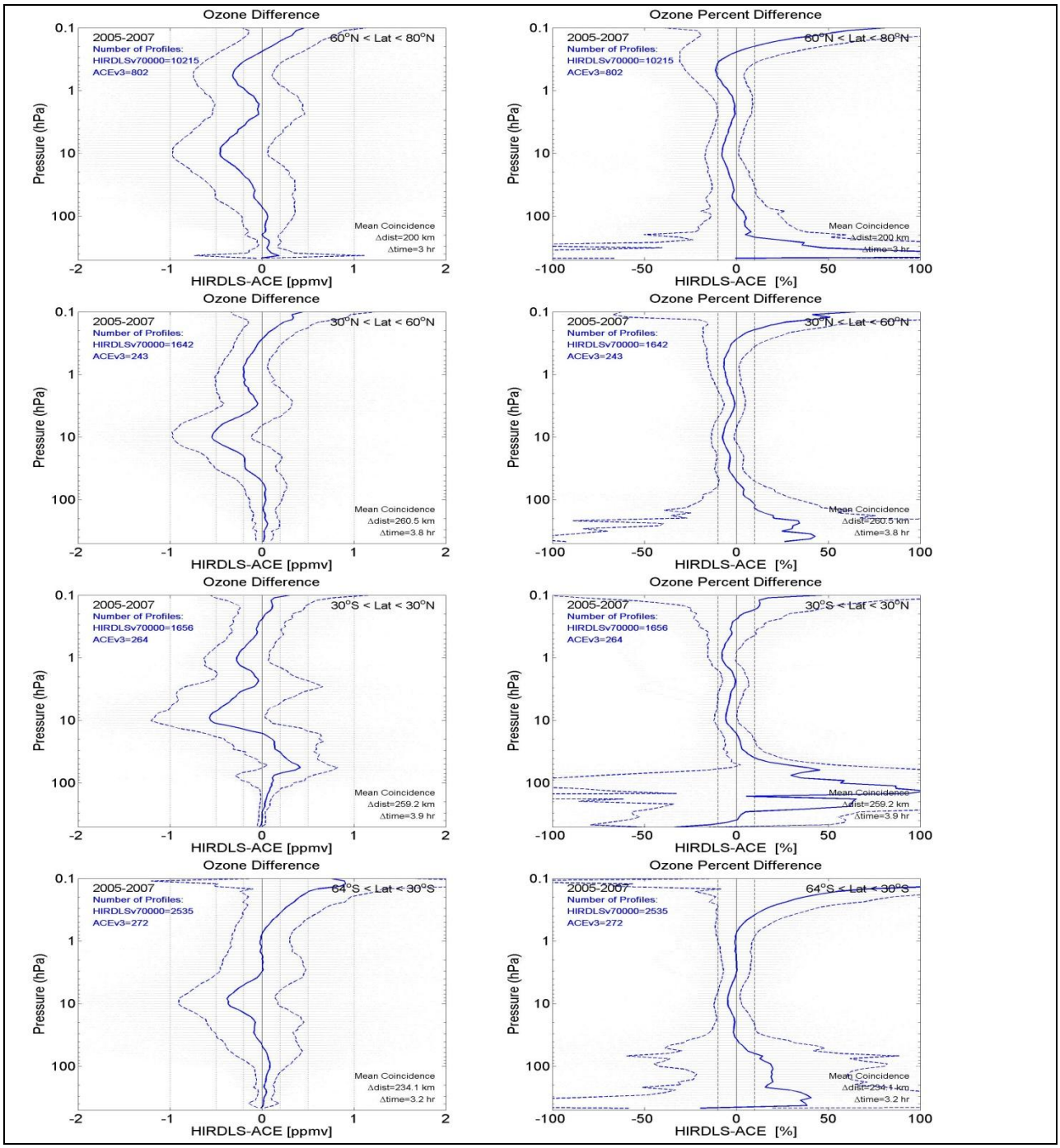

Figure 5.2.9. Shown are mean ozone differences (solid blue lines) from comparisons with coincident ACE-FTS v3 measurements. The plots are in units of volume mixing ratio (left) and percentage difference (right). The dashed blue lines are the standard deviation of the differences. Results are for all coincidences during 2005-2007. Northern high latitudes (60-80N) are shown in the top row, mid-northern latitudes (30-60N) in the 2nd row, low latitudes (30S-30N) in the 3rd row, and mid-southern latitudes (30-64S) on the bottom row. Low latitude coincidences tend to be concentrated in late summer (August); coincidences for all other latitudes are more uniformly distributed temporally.

Data Screening and Artifacts

Negative values of the predicted error ('O3Precision') signify that a large proportion of the ozone information comes from the *a priori*. For example, at pressure levels earthward of a non-zero CloudTopPressure there is a strong *a priori* influence in the retrieved ozone.

The useful range is specified to 420 hPa. The percentage of profiles that extend that low maintaining a positive precision are about 30%, and about 60% of the profiles reach 250 hPa (see Figure 5.2.10).

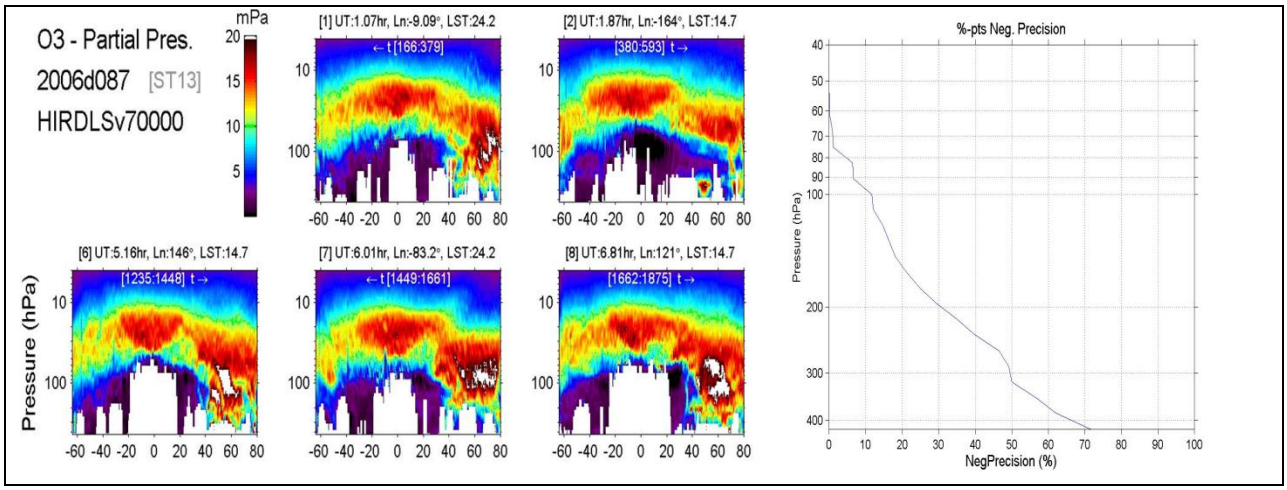

Figure 5.2.10. On the left are shown ozone partial pressure curtain plots for five half-orbits, including descending nodes (panels labeled [1] & [7]) and ascending nodes (panels labeled [2], [6] & [8]), with all negative-precision data points, (that is, points with a high *a-priori* influence) eliminated (white areas). On the right is shown a typical vertical distribution of negative precision values, in percentage units.

Profiles in the tropics often exhibit a bias approaching 100% or more, corresponding roughly to <100 ppbv, at 30-200hPa. This is believed to be an issue related to the presence of aerosols but requires a modification of the aerosol correction currently used in other species (i.e., HNO_3, CFCs).

There is a daytime/nighttime ozone asymmetry, where daytime values are slightly higher than nighttime values, this asymmetry has significantly improved over that seen in V6.

In certain isolated cases, ozone spikes with unrealistically high ozone values may still exist. In such cases one may apply a "gradient filter" by removing points at, and earthward of, the level where the ozone vertical-gradient threshold of >1.9 ppmv/p-level is reached. This filter should be used only in the tropics and not in the NH winter and spring (mostly in Dec-May period) at mid- and high latitudes (roughly 30N-60N), where thin ozone lamina with high vertical gradients are known to be prevalent, especially between 50-200 hPa (see figure 5.2.2).

5.3 Nitric Acid (HNO_3)

Species:	Nitric Acid (HNO_3)
Data Field Name:	HNO_3
Useful Range:	215 hPa – 5.1 hPa
Vertical Resolution:	1 km
Contact:	Bruno Nardi
Email:	nardi@ucar.edu
Validation Paper:	Kinnison, D. E., et al., (> 20 co-authors), Global observations of HNO_3 from the High Resolution Dynamics Limb Sounder (HIRDLS), *J. Geophys. Res.*, 113, D16S44, doi:10.1029/2007JD008814, 2008.

General Comments

HIRDLS HNO_3 data are useable over the full latitude range of 64°S to 80°N and pressure range 100 hPa to 6 hPa, with profiles at extra-tropical latitudes also having useful information between 100 hPa to 215 hPa. The upper and lower altitude limits are determined by the falling signal to noise (S/N) which accompanies the very low mixing ratios at these altitudes. Precision is approximately 200-500 pptv, or 5-20% between 10-200 hPa. Bias is typically ±10% with respect to Aura-MLS and ACE-FTS.

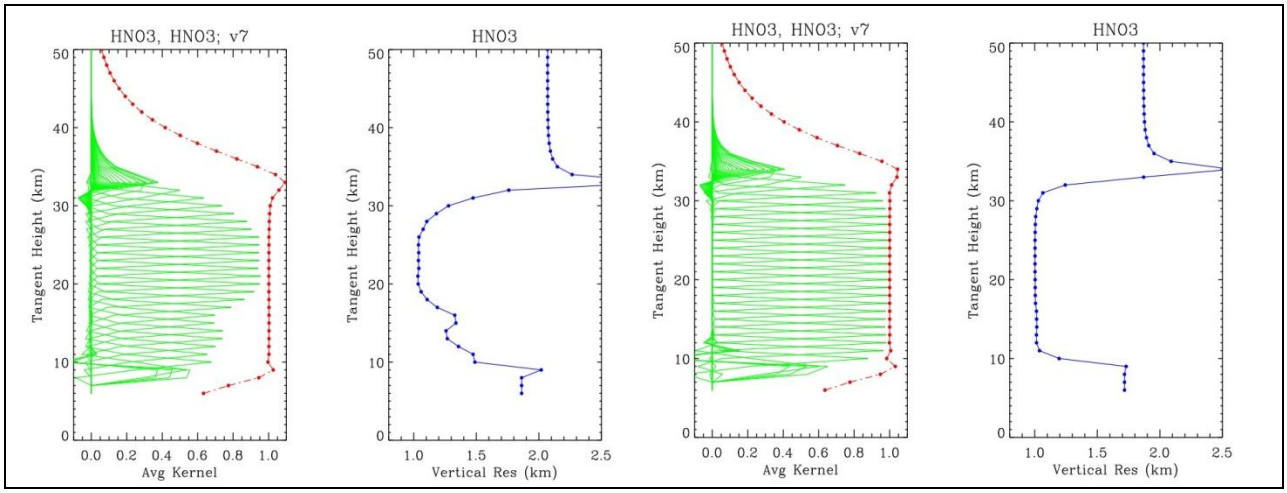

Figure 5.3.1: Shown for low latitudes (first plot) and mid-latitudes (third plot) are the averaging kernels for HIRDLS HNO_3 (green), and the integrated area under each kernel (red). Integrated area values of unity indicate that all information for that vertical step comes fully from measurements and not the *a priori*. The second and fourth plots represent the HNO_3 vertical resolution (blue) as a function of altitude for the respective latitude region, as derived from the FWHM of each kernel.

Vertical Resolution

The HIRDLS HNO_3 vertical resolution is approximately 1 km, but there is some variability with altitude and latitude, as shown in Figure 5.3.1. Due to low HNO_3 mixing ratios in the

tropical stratosphere, the resolution degrades above 35 km. However information content still exists in the measurements as indicated by integrated kernel values (red line), which remain near 1, indicating minimal contributions from *a priori* there.

Precision

The predicted precision is determined by averaging the HIRDLS level-2 HNO_3Precision parameter. The observed precision is obtained by examining HIRDLS variations between adjacent scans in regions when natural variability is at a minimum (i.e., NH high latitudes in summer). The method used to determine the observed precision basically consists of determining the random variability within de-trended sets of 10 consecutive profiles. The linear trend is removed at each altitude, and the variability is averaged over all existing profile sets within a latitude region over a 24 hour period. This is described in Section 5.0. The observed precision is between 100- 600 pptv, or 5-20% (figure 5.3.3, blue lines), better than predicted precision (red lines) by as much as a factor of two.

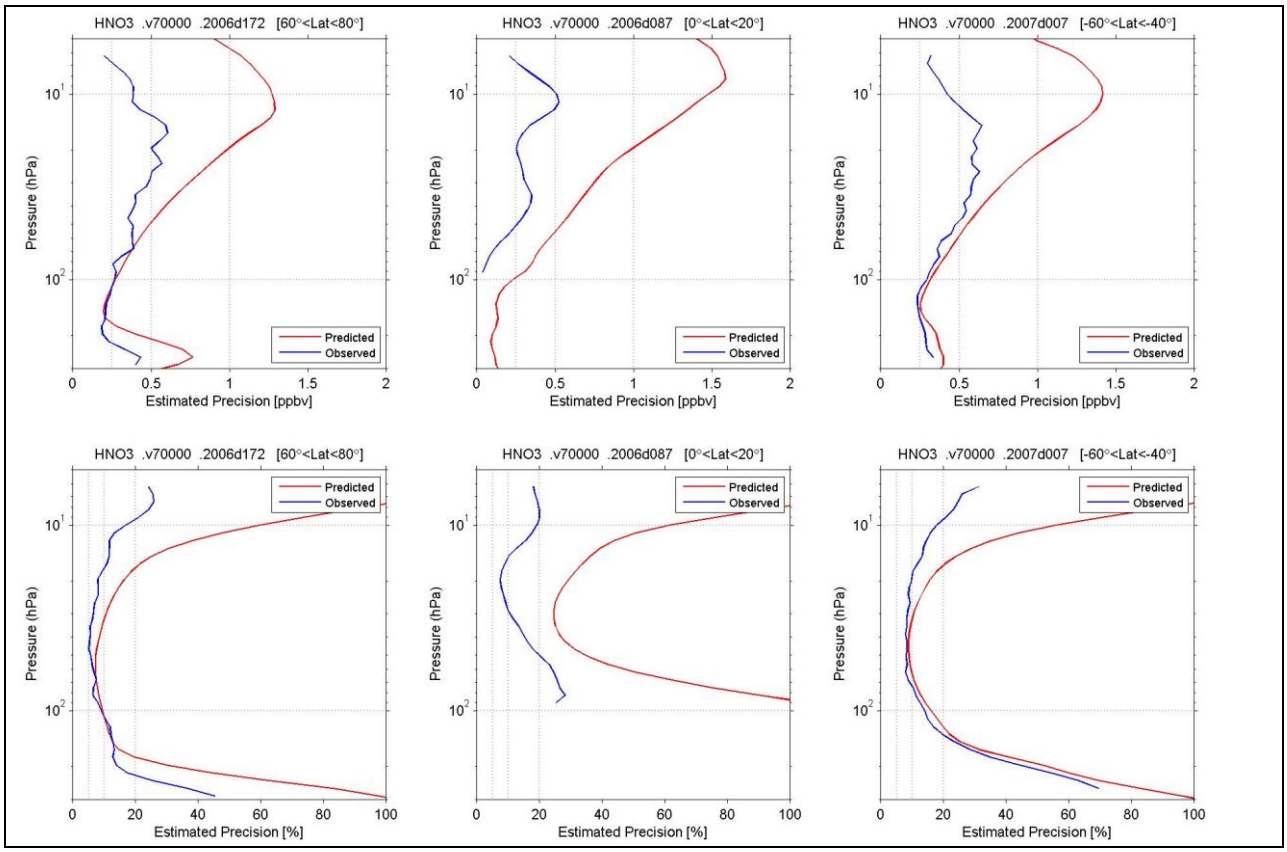

Figure 5.3.3: Shown are the predicted and observed HNO_3 precision for different latitude regions. The 'predicted' precision (red) is that computed by the retrieval program, averaged over the indicated latitude band. Three representative latitude bands are shown: 60-80 deg N (left), 0-20 deg N (center), 40-60 deg S (right). The "observed" precision (blue) is computed as the average of ten de-trended sequences of 12 consecutive profiles in undisturbed regions (see Section 5). Precision is shown in volume mixing ratio (top row) and percent (bottom row).

Accuracy

Accuracy is estimated primarily through comparison with the Aura-MLS and ACE-FTS global satellite data sets.

Aura-MLS Comparisons with MLS Version 3.3 (Figures 5.3.4 and Figures 5.3.5) show very good agreement. Monthly zonal mean comparisons for February, May, August and November of 2006 (figure 5.3.4) show that HIRDLS HNO_3 bias is typically ±<250 pptv relative to MLS between 20-200 hPa, which corresponds to ±<5% where there is the greatest abundance of HNO_3 at mid-to-high latitudes. In the lower stratosphere and troposphere this mixing ratio bias can translate to a low bias of 50% or more.

Anomalously large low biases at high southern latitudes centered at 20hPa and 50hPa can be seen in the zonal mean plots, and are clearly highlighted in the Mercator cross sections at constant pressure levels (figure 5.3.5). These low bias regions are highly localized and may exceed 1 ppbv, but since they occur in the peak of the layer, correspond to about a -10% bias.

ACE-FTS HNO_3 comparisons with ACE-FTS are presented as statistical differences for four latitude bands, 60°-80°N , 30°-60°N ,30°S-30°N and 30°S-63°S (figure 5.3.6). Coincidence criteria are 12-hours and 500 km, and all coincidences within 2005-2007 are counted.

The biases shown with ACE comparisons are fairly consistent with those of MLS with some exceptions. In the tropical and NH-extra-tropical lower stratosphere there tends to be a high bias with respect to ACE, which contradicts what is seen with MLS. It appears that the concentrations measured by HIRDLS fall somewhere between the MLS and ACE measurements in the tropical UTLS. Another difference with MLS is that the large low bias at SH high latitudes is seen only near 10 hPa in the ACE comparison; it is not seen as strongly lower down near 50hPa.

Summary

V7 HNO_3 is significantly improved over V6 in several important ways: (i) the low bias in the stratospheric layer is much smaller in V7; (ii) the high bias in the tropical UTLS is, in V7, a low bias of smaller magnitude; (iii) the high bias at the top of the stratospheric layer (<10 hPa) is much smaller in V7; and finally (iv) there is a significant reduction in the profile noise level, particularly spaceward of 50 hPa, with a corresponding improvement in precision and accuracy there.

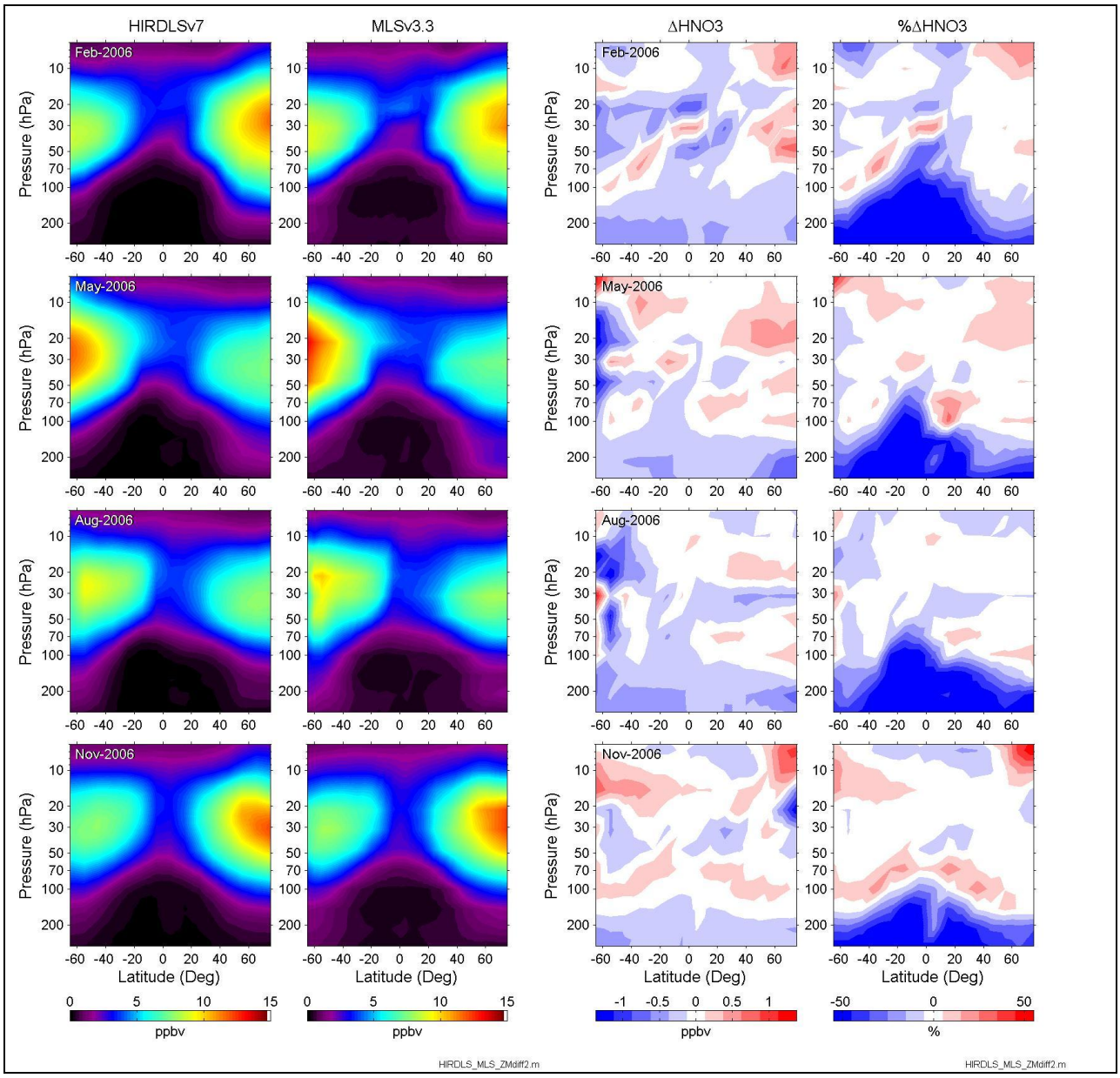

Figure 5.3.4. The two left columns are the monthly zonal mean cross sections for HIRDLS and MLS v3.3 HNO_3, in units of volume mixing ratio (ppmv), for the months in 2006 of February, May, August and November (as indicated at top left, inset, of each row). The mixing ratio difference and percentage difference (HIRDLS–MLS)/(MLS) are shown in the 3rd and last columns respectively. The white areas in the difference and percent difference plots correspond to 0 pptv ±125 pptv and 0%±5%, respectively; each blue and red color increment corresponds to a multiple of 250 pptv and 10%, respectively.

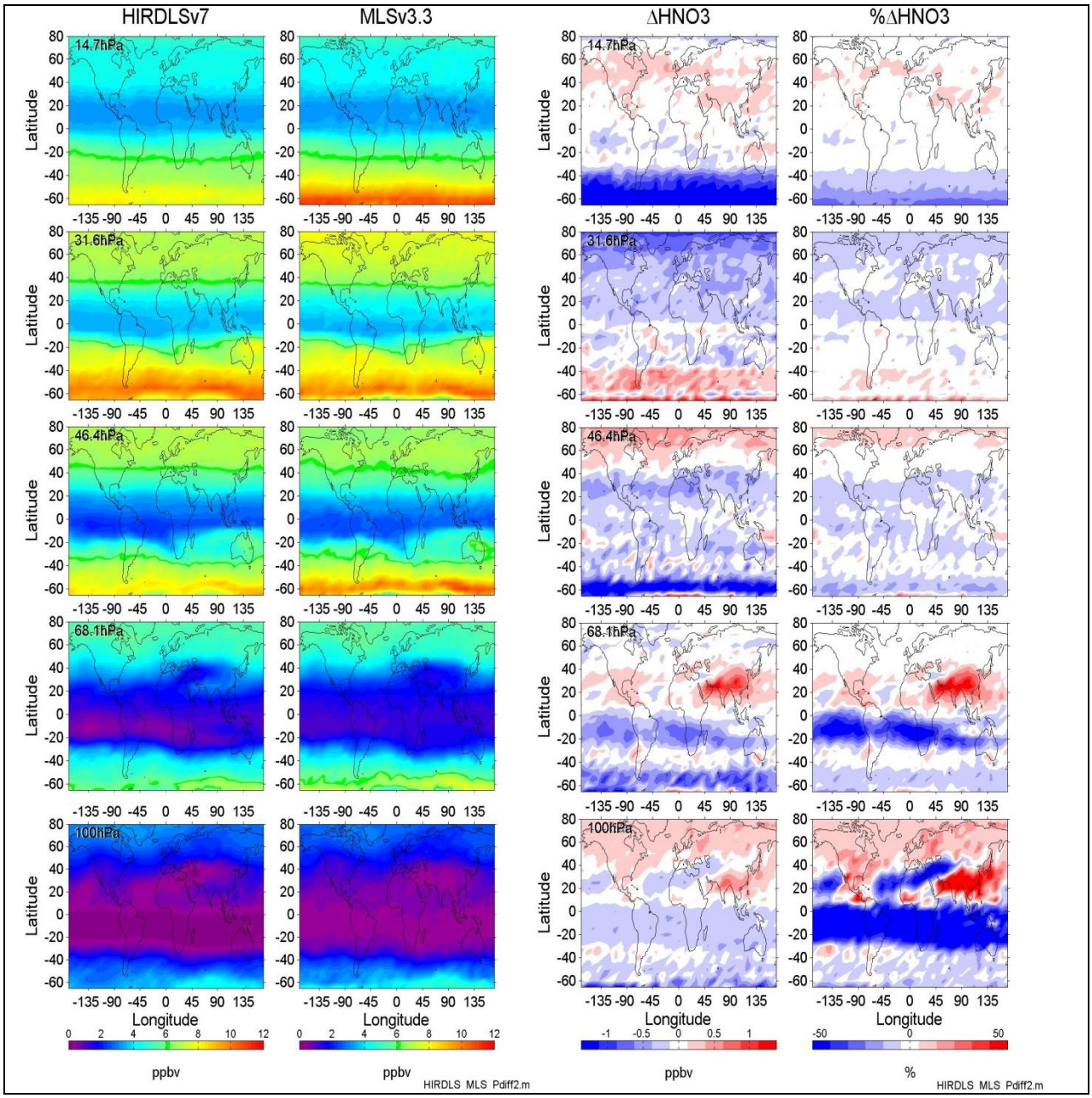

Figure 5.3.5. Shown are the longitude-latitude cross sections of HIRDLS and MLS HNO_3 (ppbv) for July 2006. The rows depict the average for the approximate pressure levels: 15 hPa, 31 hPa , 46 hPa, 68hPa and 100hPa, from top to bottom. The mixing ratio difference and percentage difference (HIRDLS–MLS)/(MLS) are shown in the 3rd and last columns respectively. The white areas in the difference and percent difference plots correspond to 0 pptv ±125 pptv and 0%±5%, respectively; each blue and red color increment corresponds to a multiple of 250 pptv and 10%, respectively.

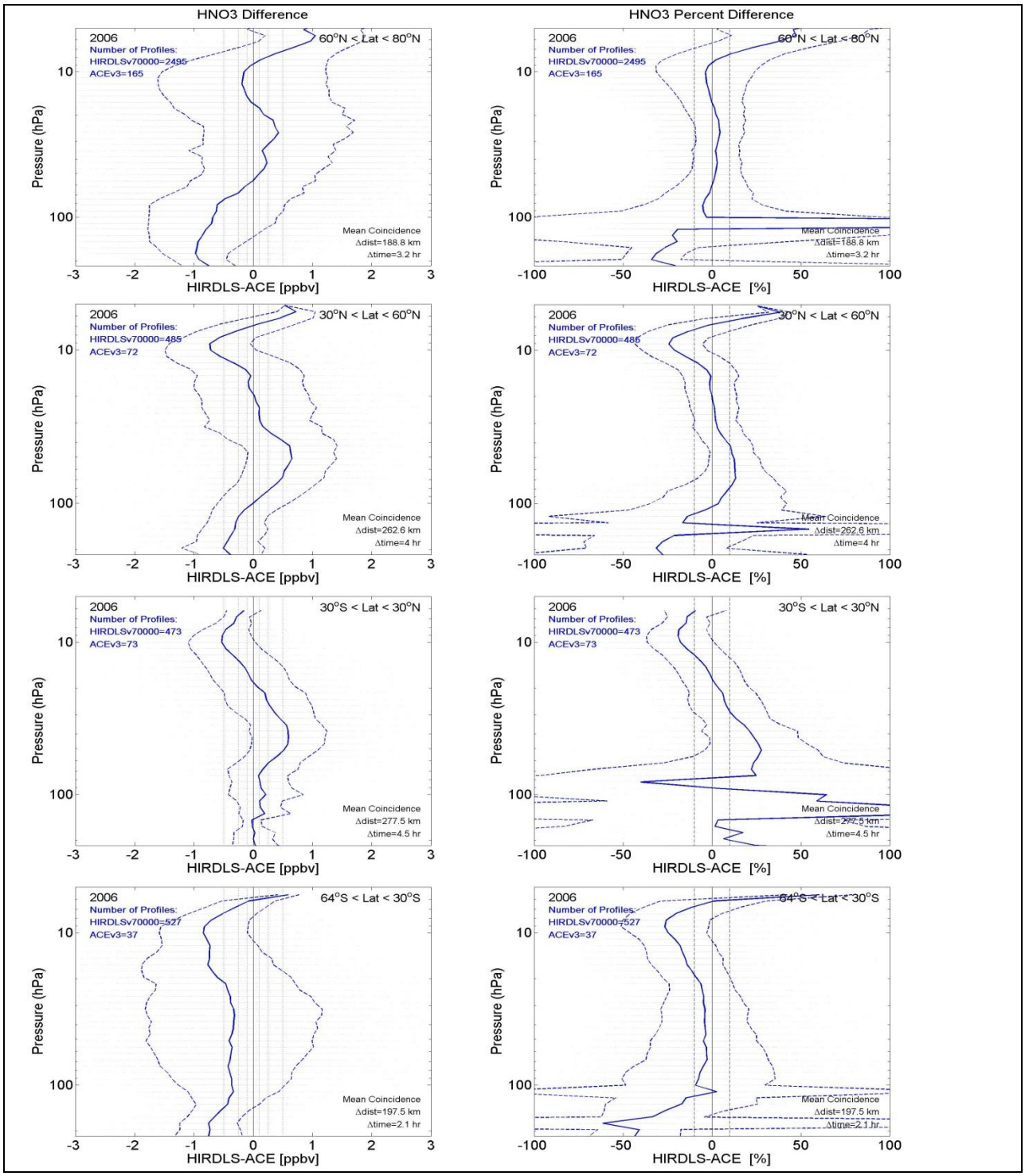

Figure 5.3.6 . Shown are mean HNO_3 differences (solid blue lines) from comparisons with ACE-FTS v3 measurements. Results for all coincidences during 2006 are shown for high latitudes (60-80N, top), for the mid-northern latitudes (30-60N, 2nd row), for low latitudes (30S-30N, 3rd row) and for the mid-southern latitudes (30-64S, bottom). The plots are in units of volume mixing ratio (left) and percentage difference (right). The dashed blue lines are the standard deviation of differences. The number of coincident profles included are shown in the upper left corners.

5.4 CFC11, CFC 12

Species:	CFC11 ($CFCl_3$), CFC12 (CF_2Cl_2)
Data Field Name:	CFC11, CFC12
Useful Range:	CFC11 316 hPa – 17.8 hPa CFC12 316 hPa – 8.3 hPa
Screening Criteria:	Use with caution the following: Data with negative precisions Data with cloud flag $\neq 0$ - data should not be used CFC 11 data above surface value (approx. 250pptv) CFC 12 data above surface value (approx. 540pptv)
Vertical Resolution:	~1 km
Contact:	Bruno Nardi
Email:	nardi@ucar.edu
Validation Paper:	Nardi, B., et al., Validation of V7 HIRDLS CFC11 and CFC12 Observations, *In preparation*.

General Comments

This section will describe HIRDLS observations of CFC11 ($CFCl_3$) and CFC12 (CF_2Cl_2). These human-made gases have common sources, distributions and chemistry in the atmosphere and will be discussed together here. HIRDLS CFC measurements are generally useful between latitudes of 63 S to 80 N and within pressure ranges of 316 hPa –17.8 hPa (about 9 km to 28 km) for CFC11 and 316 hPa –8.3 hPa (about 9 km to 35 km) for CFC12. It should be noted that data outside of the useful range has been eliminated from the publicly released data.

Resolution

Vertical resolution of the CFC observations is described by the vertical averaging kernels as shown in Figure 5.4.1. There is some variation in the vertical resolution with latitude but that variation is small within the useful pressure range. As may be seen in Figure 5.4.1 the vertical resolution for both CFC11 and CFC12, over the useful pressure range, is 1.0-1.2 km. The horizontal resolution of the observations is approximately 100 km along an orbit track with an orbital separation of about 24 degrees of longitude (about 2000 km at 40N), (see section 2.2.2).

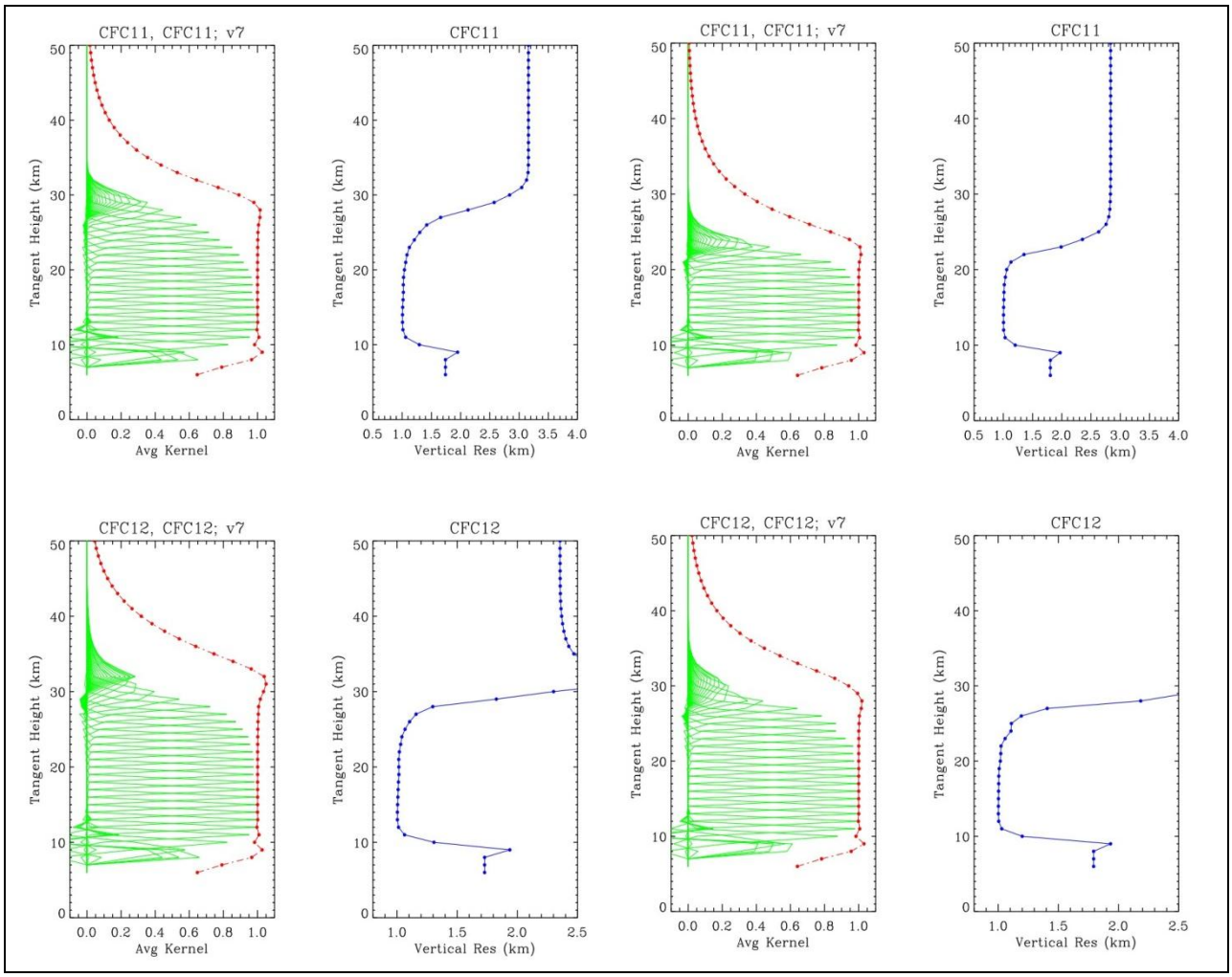

Figure 5.4.1: Shown are the averaging kernels (green) and the integrated area under each kernel (red). for V7 CFC11 (top row) and V7 CFC12 (bottom row), for low latitudes (first column) and mid-latitudes (third column). Integrated area values of unity indicate that all information for that vertical step comes fully from measurements and not the *a priori*. The second (low latitudes) and fourth (mid-latitudes) columns represent the vertical resolution (blue) as a function of altitude, as derived from the FWHM of each kernel.

Precision

The average precision of the zonal mean for CFC11 and CFC12 is shown in Figure 5.4.2. The precision estimated from the average of 10 sets of 12 sequential profiles in undisturbed regions (See Sec. 5.0), shown by the blue line, indicates precisions of 0.005-0.025 ppbv (5%-20%) for CFC11, and 0.02-0.05 ppbv (5%-10%) for CFC12. These are lower than the predicted mean values, CFC11Precision and CFC12Precision (red lines), calculated by the L2 retrieval algorithm.

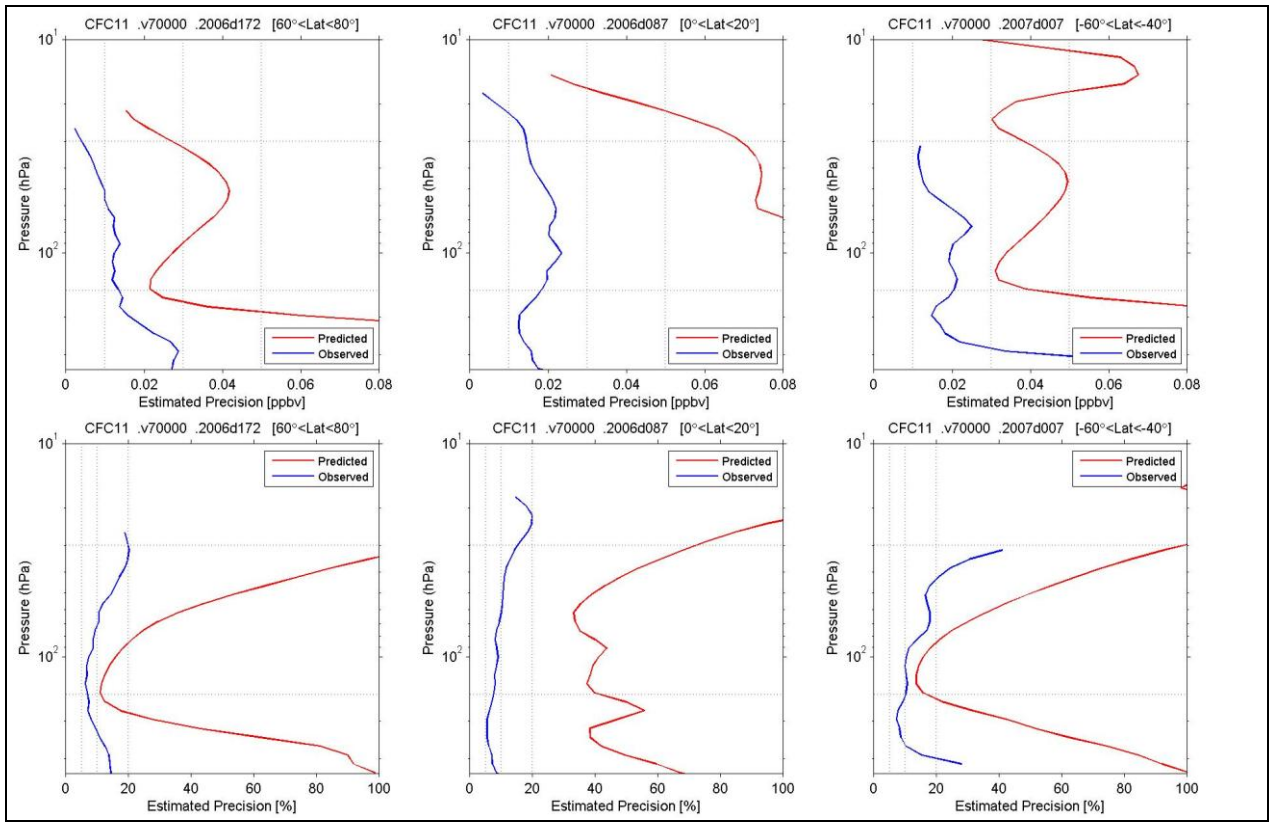

Figure 5.4.2a. Shown are the predicted and observed CFC-11 precision. The "observed" precision (blue) is computed as the average of all de-trended sequences of 12 consecutive profiles in the region indicated (see Section 5). The 'predicted' precision (red) is computed by the retrieval program, and averaged over the indicated latitude band. Three representative latitude bands shown are: 60-80 deg N (left), 0-20 deg N (center), -60--40 deg (right). Precision is shown in volume mixing ratio (top row) and percent (bottom row).

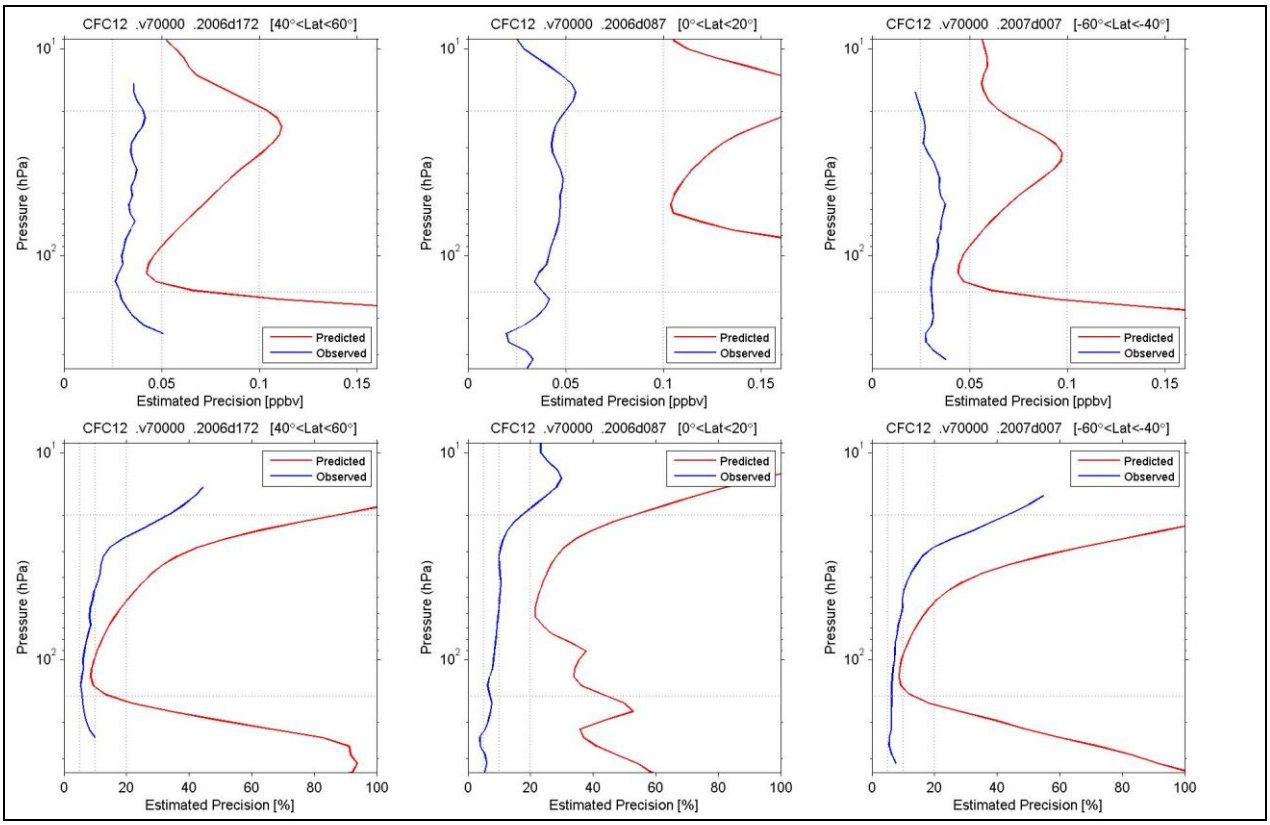

Figure 5.4.2b. Shown are the observed (blue) and predicted (red) CFC-12 precision. The same format is used as for CFC-11 above.

Accuracy

Figure 5.4.3 shows the 2006-May-18 zonal mean cross-sections of CFC11 and CFC12 for V7 (top row) and for V6 (bottom row). The regularly observed excess of CFC11 and CFC12 in the tropical UTLS in V6, which are about 15% and 25% respectively, and whose source was related to the presence of aerosols, is essentially gone in V7.

Regarding the values at the base of the HIRDLS observations: the lifetimes of CFC11 and CFC12 in the atmosphere are relatively long (approximately 50 and 100 years respectively). Thus we may expect CFCs abundances in the troposphere to be fairly uniform and with the same magnitude as the surface value. Surface observations of CFCs have been made by NOAA [Elkins et al., 1994] for many years and show a slowly varying concentration with time. CFC11 surface values, from stations at latitudes from 71N to 90S, in 2006 ranged from 248 to 252 pptv; for CFC12, for the same stations and times, surface amounts were 530-540 pptv. As may be seen in Figure 5.4.3 the tropospheric amounts retrieved by HIRDLS are similar to those measured from the NOAA surface stations.

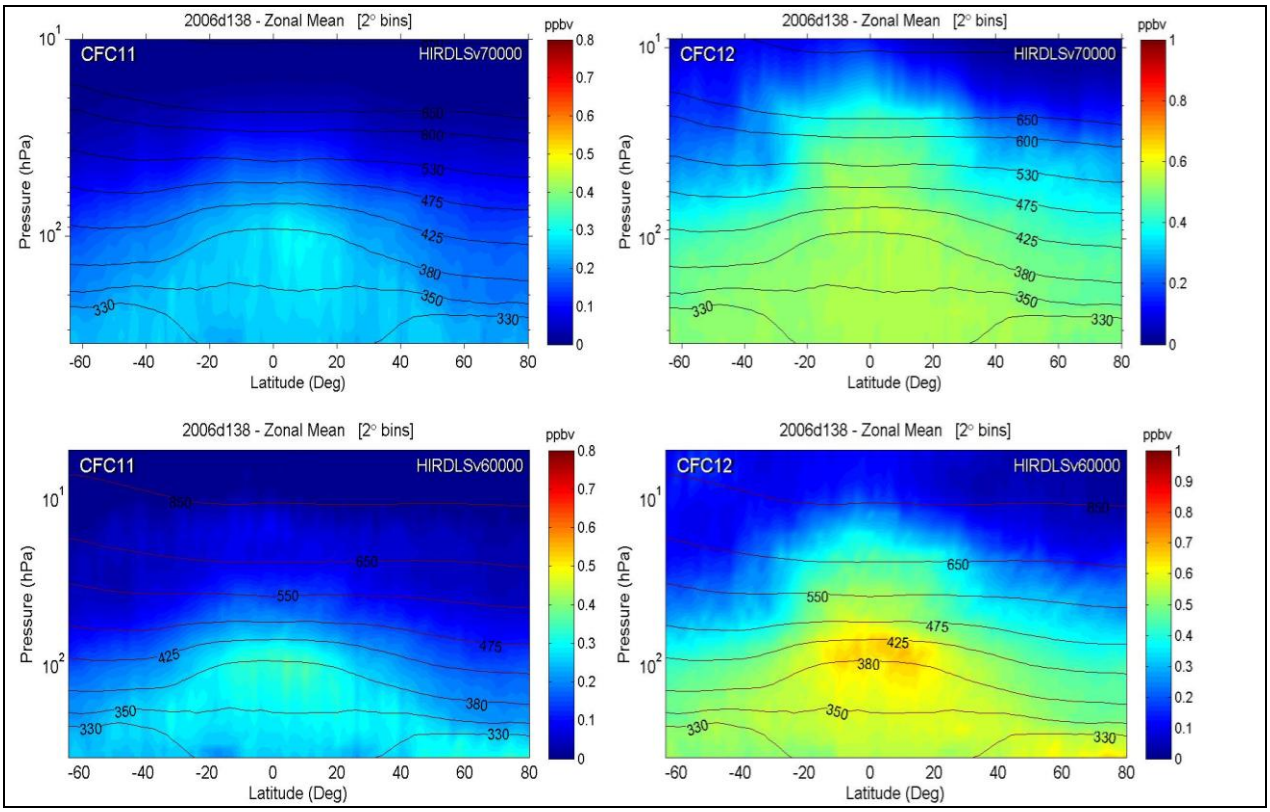

Figure 5.4.3. The top row shows the daily zonal means of CFC11 (left) and CFC12 (right) for 18 May 2006 for V7, and the bottom row shows these zonal means for V6. The black contour lines show the potential temperature surfaces (units: K). The region of high values in the tropical UTLS seen in V6, were an artifact of aerosols on the retrieval process, and have been corrected in V7.

Figure 5.4.4 shows the CFC11 and CFC12 vertical mixing ratio profiles from HIRDLS and results from a number of satellite and balloon-borne instruments. The satellite results are reported in Hoffmann et al, 2008. Care must be taken in comparing the older satellite observations with HIRDLS since both CFC11 and CFC12 show a clear temporal change. CFC11 surface mixing ratio increased steadily until about 1995 and has shown about a 1% per year decrease since then. The CFC12 amount, with a longer lifetime, leveled off around 1995

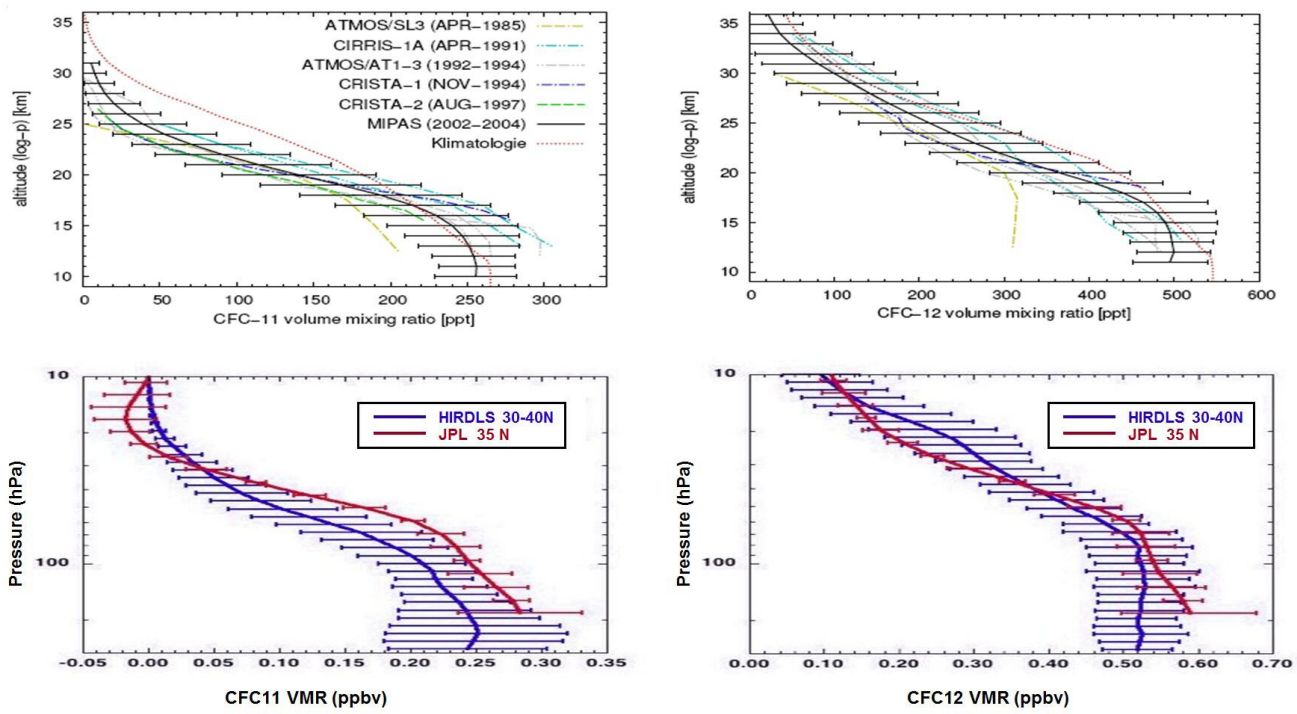

Figure 5.4.4: Vertical profiles of CFC11 and CFC12 from a number of satellite and balloon experiments (ATMOS, CIRRIS, CRISTA, MIPAS, JPL MkIV) and from HIRDLS. Observations are all from northern hemisphere mid-latitudes.

Comparisons are made with other global satellite observations of CFC11 and CFC12. Two satellite-borne experiments that reported measurements of CFC11 and CFC12 for the HIRDLS operational period are the Michelson Interferometer for Passive Atmospheric Sounding (MIPAS) instrument aboard Envisat (launched in March, 2002) and the Atmospheric Chemistry Experiment (ACE) aboard SciSat (launched in August, 2003).

Figure 5.4.5 compares the July 2006 monthly zonal mean of CFC11 and CFC12 for HIRDLS and MIPAS. Good agreement is seen in the CFC11 and CFC12 distributions. CFC11 has about a 10% low bias with respect to MIPAS earthwards of 70 hPa, and it increases to -50% spaceward toward 15-30 hPa. CFC12 has a bias generally within ±5% of the MIPAS values earthwards of 40 hPa. Spaceward toward 10hPa, the CFC12 bias increases to +50% in the tropics and in the southern hemisphere spaceward, and to -50% in the northern extratropics.

Figures 5.4.6 and 5.4.7 show the mean bias of HIRDLS CFC11 and CFC12, respectively, compared with ACE-FTS v3. All coincidences within 400 km and 6 hours are used within the four latitude regions as indicated on the plots.

The CFC11 comparisons with ACE are fairly consistent with those of MIPAS, showing a low bias of typically about <10% earthward of 30hPa. Notable differences in the ACE comparisons

include: (i) a rapidly increasing HIRDLS high bias at northern high latitudes spaceward of 100hPa; (ii) a HIRDLS low bias of 10%-20% in the extra-tropical southern hemisphere; (iii) a spacewardly increasing high bias in the upper regions toward 20 hPa, rather than an increasing low bias seen in MIPAS comparisons.

CFC12 comparisons with ACE have similar commonalities and inconsistencies with MIPAS comparisons as seen with CFC11. The typical HIRDLS CFC12 bias is often 1-2%, similar to the <±5% bias seen with MIPAS comparisons. There is also a greater high bias (~10%) near 50 hPa at northern high latitudes. However, as with CFC11, the bias in the upper regions tends to amplify to an increased high bias (toward 10 hPa) at all latitudes, in contrast with the low bias seen in northern high latitudes in the MIPAS comparisons.

In the V7 of both CFC11 and CFC12, the ubiquitous tropical UTLS high bias seen in V6 is notably absent.

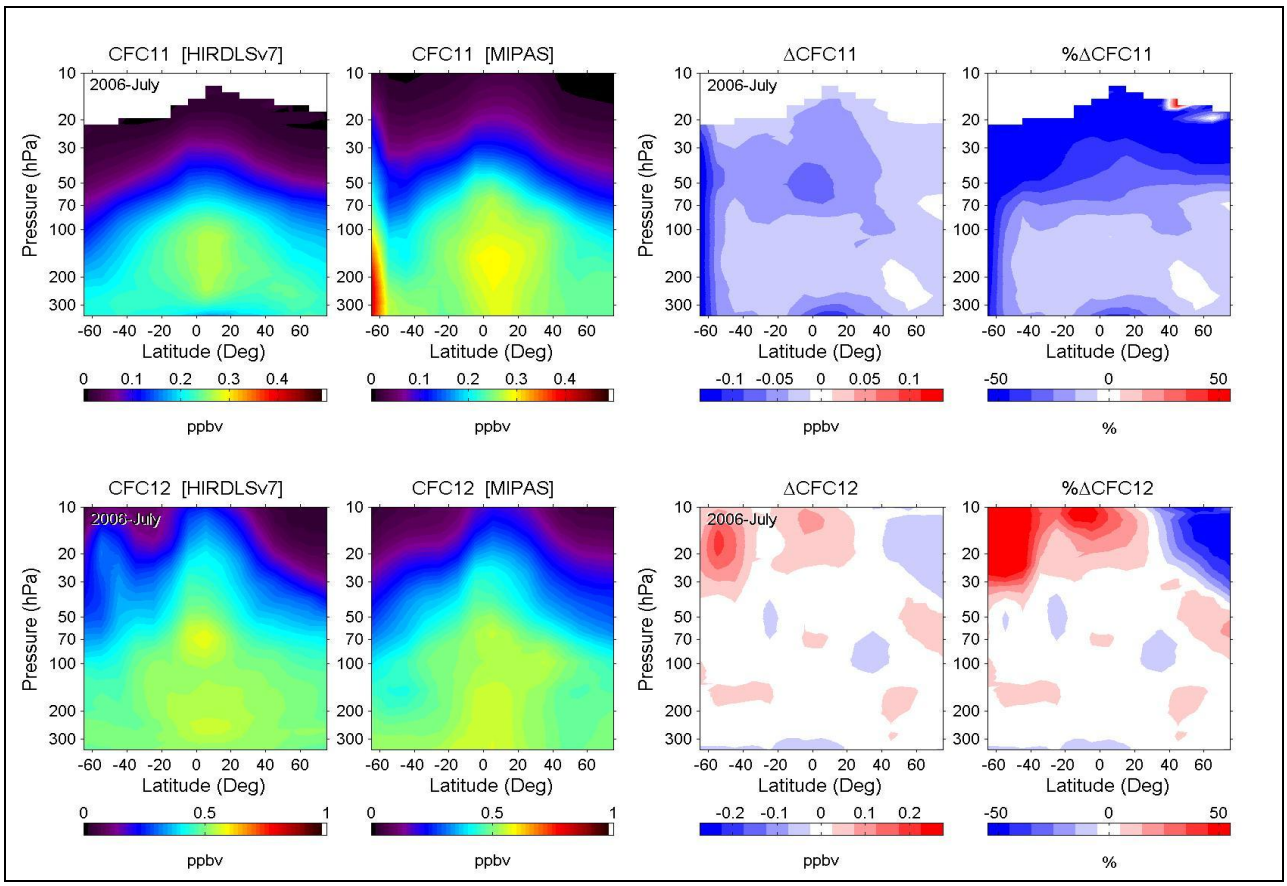

Figure 5.4.5. Shown above are monthly zonal mean cross-sections of CFC11 (top) and CFC12 (bottom) as measured on July 2006 by HIRDLS (1st column) and MIPAS (2nd column). The mixing ratio difference and percentage difference (HIRDLS–MIPAS)/(MIPAS) are shown in the 3rd and 4th columns. The white areas in the difference and %-difference plots correspond to 0±25 pptv and 0%±5%, respectively; each blue and red color increment corresponds to a multiple of 50 pptv and 10%, respectively. The southern high latitude feature in CFC11 is due to a non-geophysical artifact in the MIPAS zonal mean.

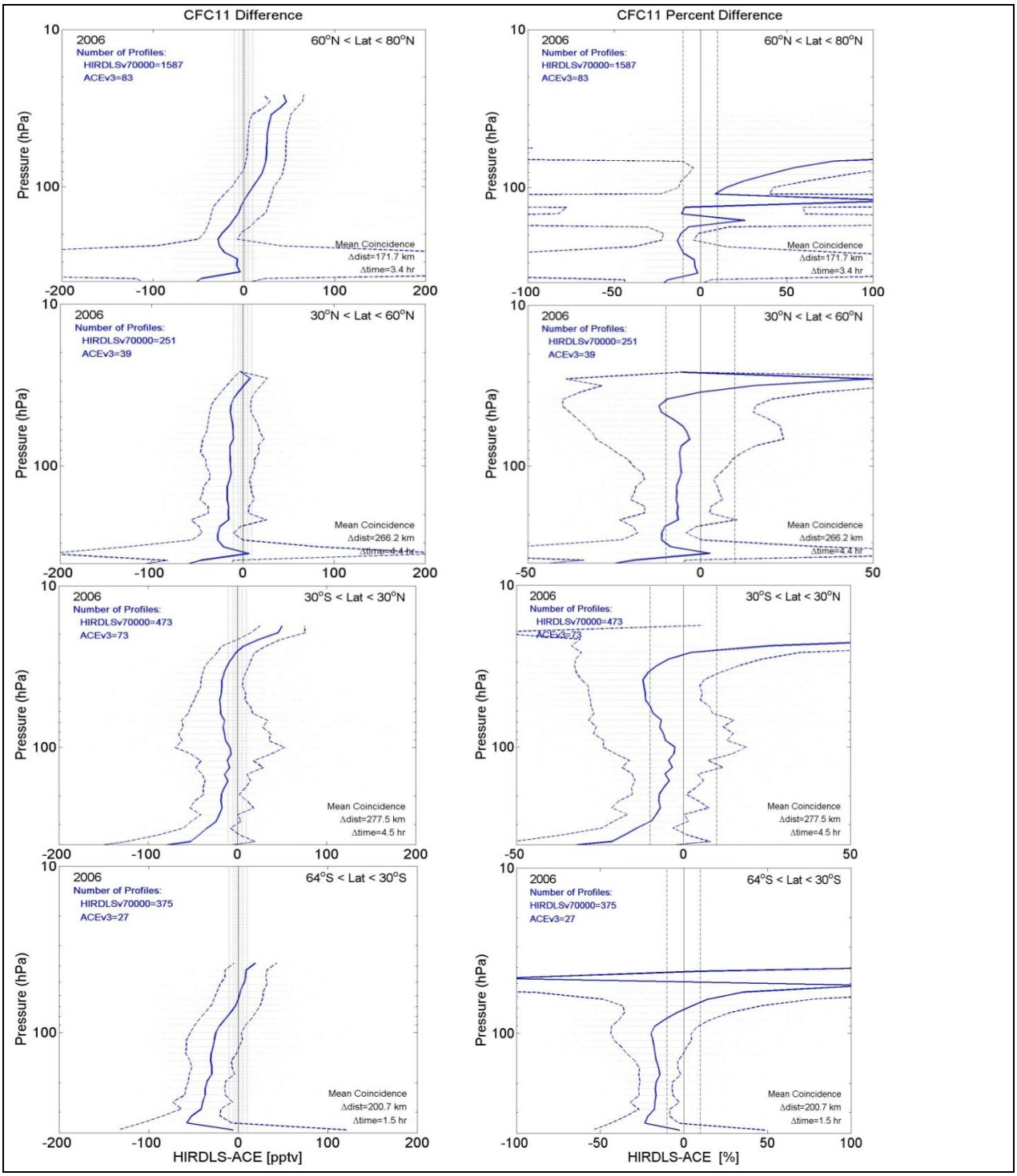

Figure 5.4.6. Shown are mean CFC11 differences (solid blue lines) from comparisons with ACE-FTS v3 measurements. Results for all coincidences during 2006 are shown for high latitudes (60-80N, top), for the mid-northern latitudes (30-60N, 2nd row), for low latitudes (30S-30N, 3rd row) and for the mid-southern latitudes (30-64S, bottom). The plots are in units of volume mixing ratio (left) and percentage difference (right). The dashed blue lines are the standard deviation of differences. The number of coincident profles included are shown in the upper left corners.

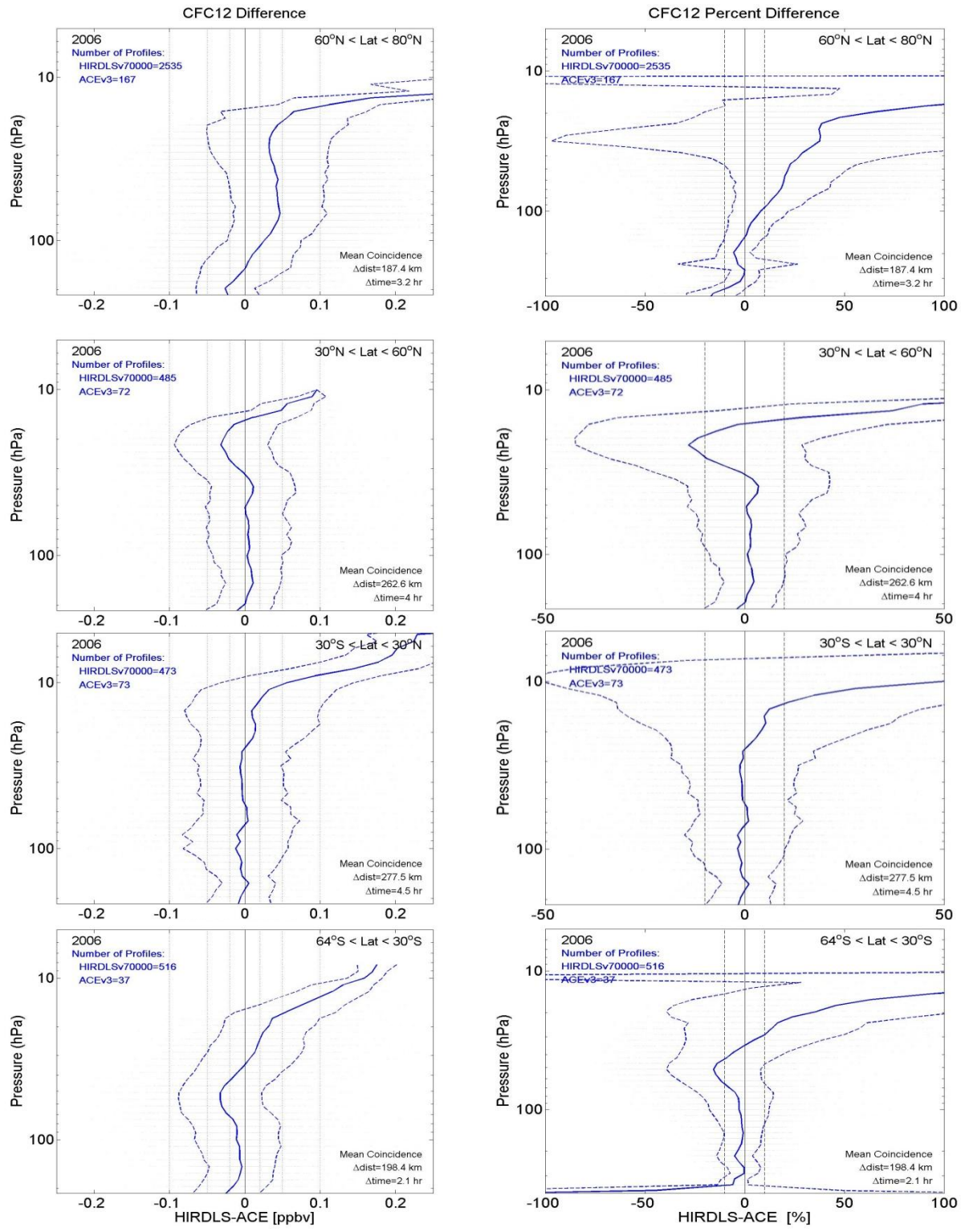

Figure 5.4.7. Shown are mean CFC12 differences (solid blue lines) from comparisons with coincident ACE-FTS v3 measurements. The same format is used as for CFC-11 above.

5.5 Water Vapor (H_2O)

Species: Water Vapor
Data Field Name: Water
Useful Range: 200 – 10 hPa
Vertical Resolution: 1 Km
Contact: John Gille
Email: gille@ucar.edu
Validation paper: TBS

General Comments:

The water vapor distribution is retrieved from radiances measured in channels 18 and 20, in the 6.3 μm band. The radiance in these channels is small, following the black body function, and the criteria for the useful removal of the blockage contribution to the signal is therefore more stringent.

The vertical resolution is determined from the full-width at half maximum of the averaging kernels. These are shown for each altitude level in Figure 5.5.1 for the tropics (left pair of panels) and mid-latitudes (right pair). The green lines show the averaging kernels, while the blue lines show the half-widths explicitly, indicating the vertical resolution is ~1 km from ~ 11 to 55 km.

The red line in the left panel indicates the fraction of the information that comes from the HIRDLS measurements; values of 1 mean that there is negligible influence from the *a priori.*

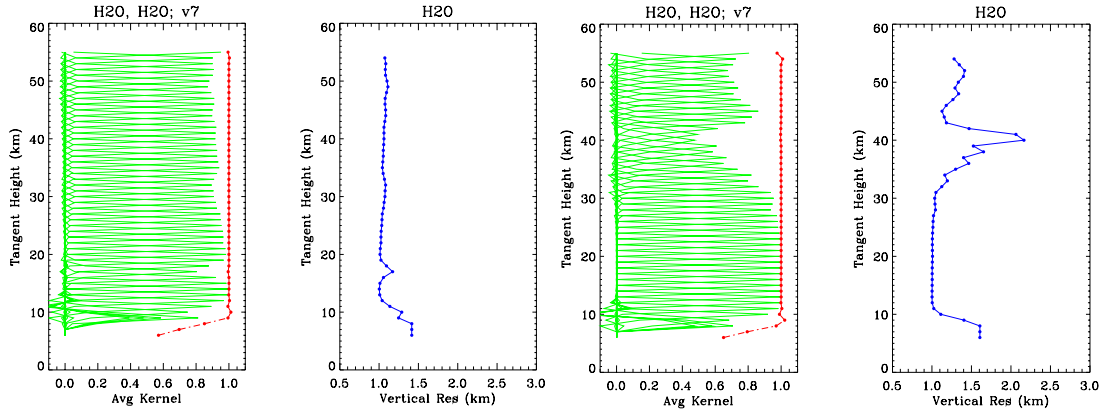

Figure 5.5.1. Averaging kernels (green)and vertical resolution (blue) as a function of altitude for HIRDLS water vapor profiles, calculated for 15 January 2007. Left panels 3°N, right panels 45°N.

The averaging kernels were calculated for 15 January at 3 °N and 45°N with a cloud top altitude of 8 km. The rapid drop of the averaging kernel maxima, increase in the half widths, and increase in the fraction of information from the *a priori* at altitudes below about 12 km results from relaxation to the *a priori*. Under clear conditions HIRDLS profiles extend below 200 hPa, but values at those levels should be carefully evaluated.

The vertical broadening and reduced peaks of the averaging kernels above 30 km are a result of the reduced signal, and thus reduced signal to noise ratio (S/N), at these levels. Use of data above 10 hPa is not recommended.

Precision

The precision of the water data was calculated as described in Section 5.0. The results are displayed in Figure 5.5.2. In the mid-latitudes, at 150 the empirical (observed) and predicted precisions are ~ 0.5 ppmv, or about 10%. From that level up to 10 hPa the empirical uncertainty increases more slowly than the predicted precision, reaching 0.7 ppmv but still about 10%. As noted above, the empirical method of estimating the precision may necessarily include some atmospheric variability, so may overestimate the actual HIRDLS precision. The more rapid increase of the predicted precision with altitude indicates that the noise and uncertainties included in the retrieval may have been too conservative.

In the tropics the observed precision is about 0.6 ppmv at 100 hPa, increasing very slightly to 0.7 ppmv at 10 hPa. This corresponds to ~13% above 50 hPa, but 30 % at 80 hPa, reflecting the low values at the tropical minimum, sometimes referred to as the hygropause. In both tropical and mid-latitudes the precision does not increase rapidly with altitude, making it possible that results may be usable for a few kilometers above the 10 hPa level.

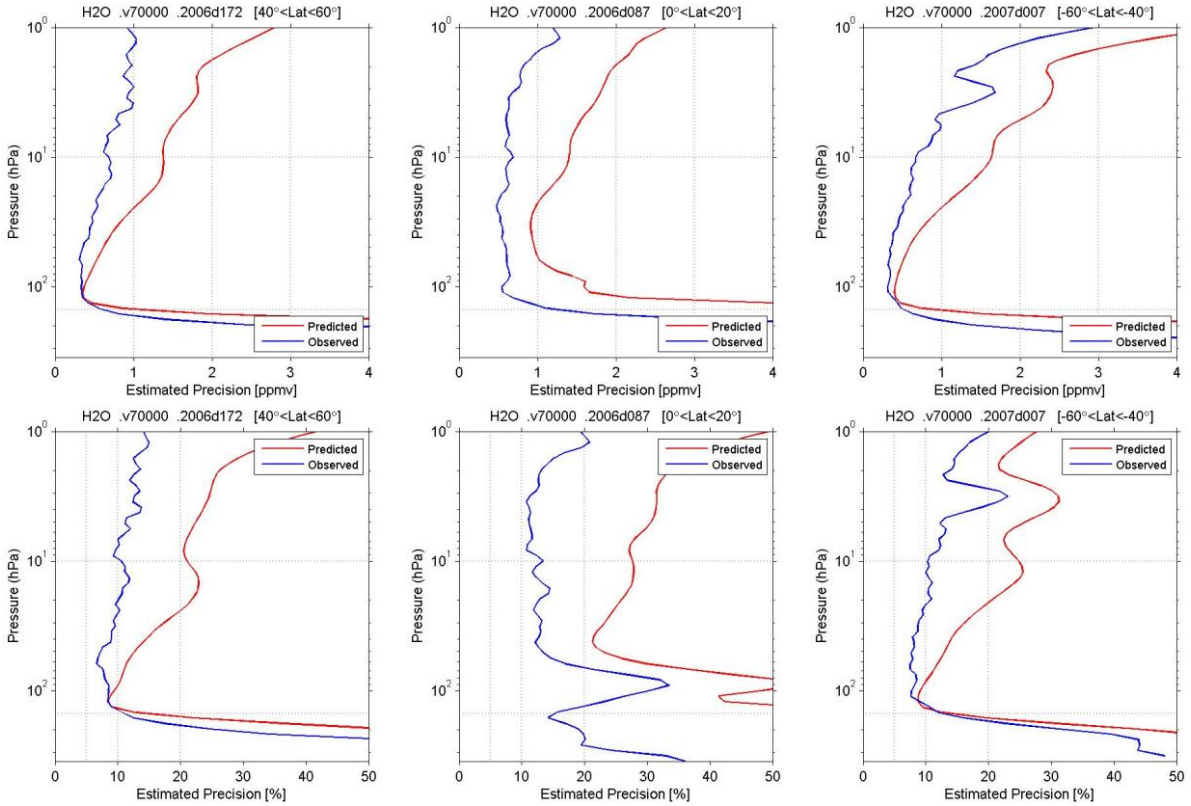

Figure 5.5.2. Estimated observed (empirical) precision of HIRDLS V7 water vapor retrievals (blue lines), compared with precision predicted by the retrieval algorithm (red lines), for mid-southern latitudes (top row), tropics (center) and mid-northern latitudes (bottom), expressed as ppm (left) and percentage (right).

Accuracy (Biases)

HIRDLS water vapor has been compared to several data sets in an effort to determine the extent and magnitude of any biases. An important set of profile comparisons up to about 30 km is between Cryogenic Frost-point Hygrometer (CFH) sondes [Vömel et al., 2007] and nearby HIRDLS temperatures. Figure 5.5.3 shows comparisons between high-resolution CFH sonde profiles and nearby HIRDLS retrievals at Heredia, Costa Rica; Lauder, New Zealand; Boulder, Colorado, U.S.A.; and Sodankyla, Finland. Black dots indicate the sonde measurements, with the closest HIRDLS retrieval shown in blue. Other nearby retrievals are shown by the thin black lines. The differences in space and time are given. Points to note, especially at Heredia in the tropics, is the way the HIRDLS retrievals follow the low mixing ratios in the tropical tropopause region. The agreement extends down to ~200 hPa and even below in some cases.

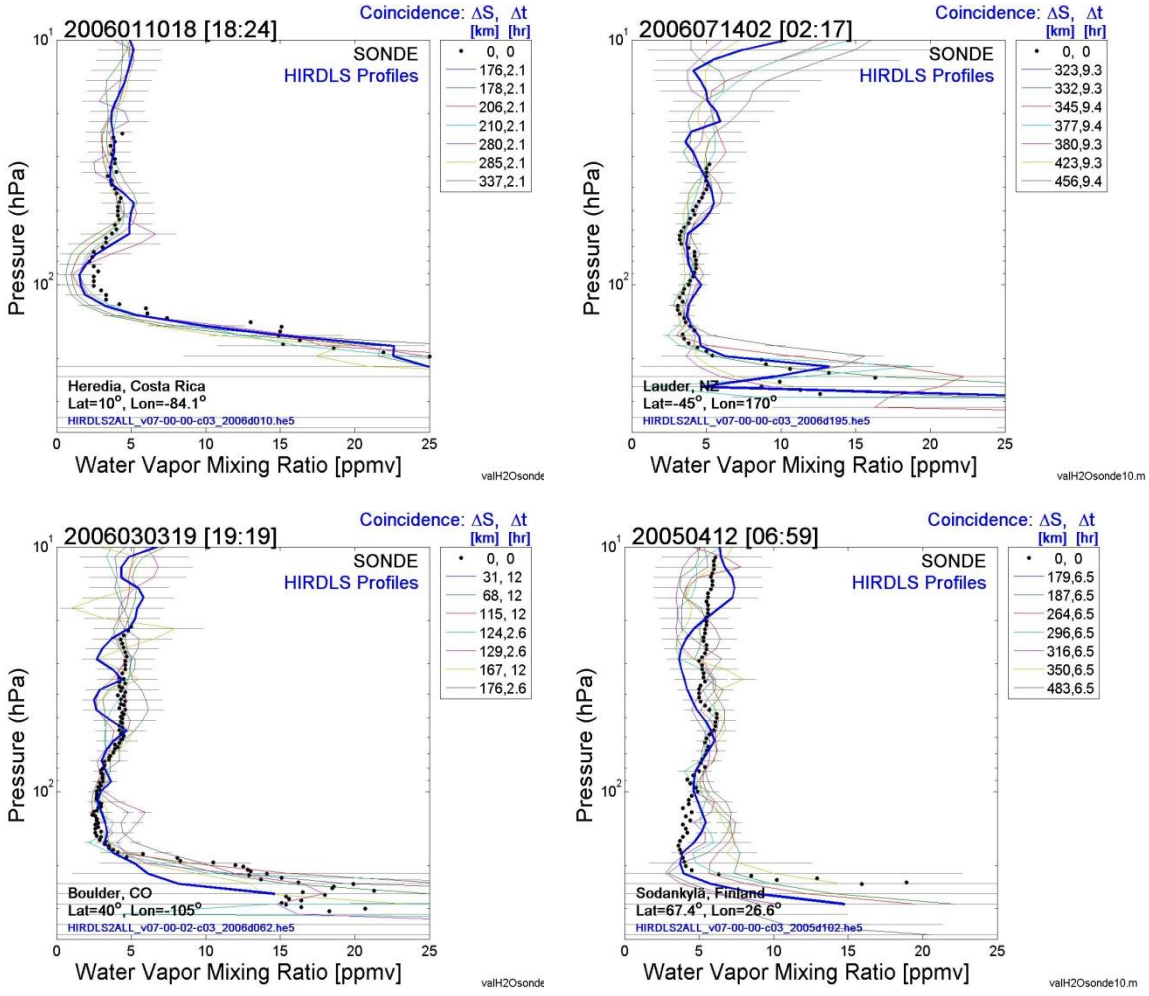

Figure 5.5.3. Water vapor comparisons between sonde profiles at Heredia, Costa Rica (upper left), Lauder, N.Z.(upper right) and Boulder, Colorado (lower left) and Sodankylä, Finland (lower right). Black lines are high-resolution sondes, blue are the closest HIRDLS retrievals, and thin black lines are other nearby HIRDLS retrievals. Differences in distances and times are given.

These results illustrate the good agreement over a range of latitudes. In general, HIRDLS profiles have more high-frequency vertical variations than the sondes, presumably due to the lower signal to noise ratios in the water vapor channels resulting from their low signals, especially in Channel 18, and the incomplete removal of small but rapid variations of the blockage contribution.

Figure 5.5.4 brings together the statistics of 60 such CFH comparisons over the entire mission.

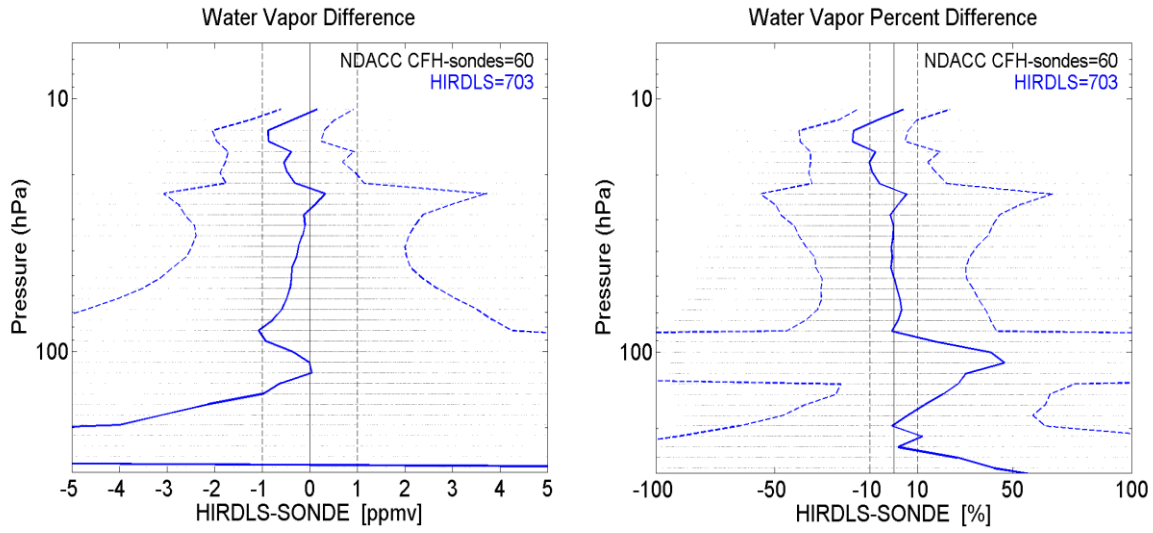

Figure 5.5.4. Comparisons between 60 CFH sonde profiles of water vapor and nearby HIRDLS retrievals. The left panel shows mean differences in mixing ratio, while the right panel shows the mean percentage differences. Solid blue lines indicate the mean differences, and the dashed blue lines are the standard deviations.

The mean mixing ratio differences indicate HIRDLS retrievals are lower than the CFH sondes by less than 1 ppm between about 150-10 hPa, although the standard deviations are large, especially at the lowest levels. The percentage differences are very small from 90-10 hPa, with standard deviations around 30%. Differences and standard deviations are larger around 100 hPa.

HIRDLS profiles are compared with ACE-FTS profiles I Figure 5.5.5, for 1 month in each of 4 different latitude bands. Because of the occultation geometry, the number of coincidences is not uniform with time during the year. These typically show HIRDLS higher in the lower stratosphere, decreasing above ~ 50 hPa. Values in the middle stratosphere are generally within 10% of ACE, but more variable near 100 hPa.

The monthly zonal means of HIRDLS and MLS water vapor are displayed in Fig. 5.5.6 for March 2006 and September 2007. The third panel shows the difference HIRDLS minus MLS, while the fourth presents the percentage differences. Above the 200 hPa level the agreement is relatively good, except for a region at higher latitudes below 100 hPa where HIRDLS appears to have a systematic high bias. Otherwise the differences are rather small, even above 10 hPa.

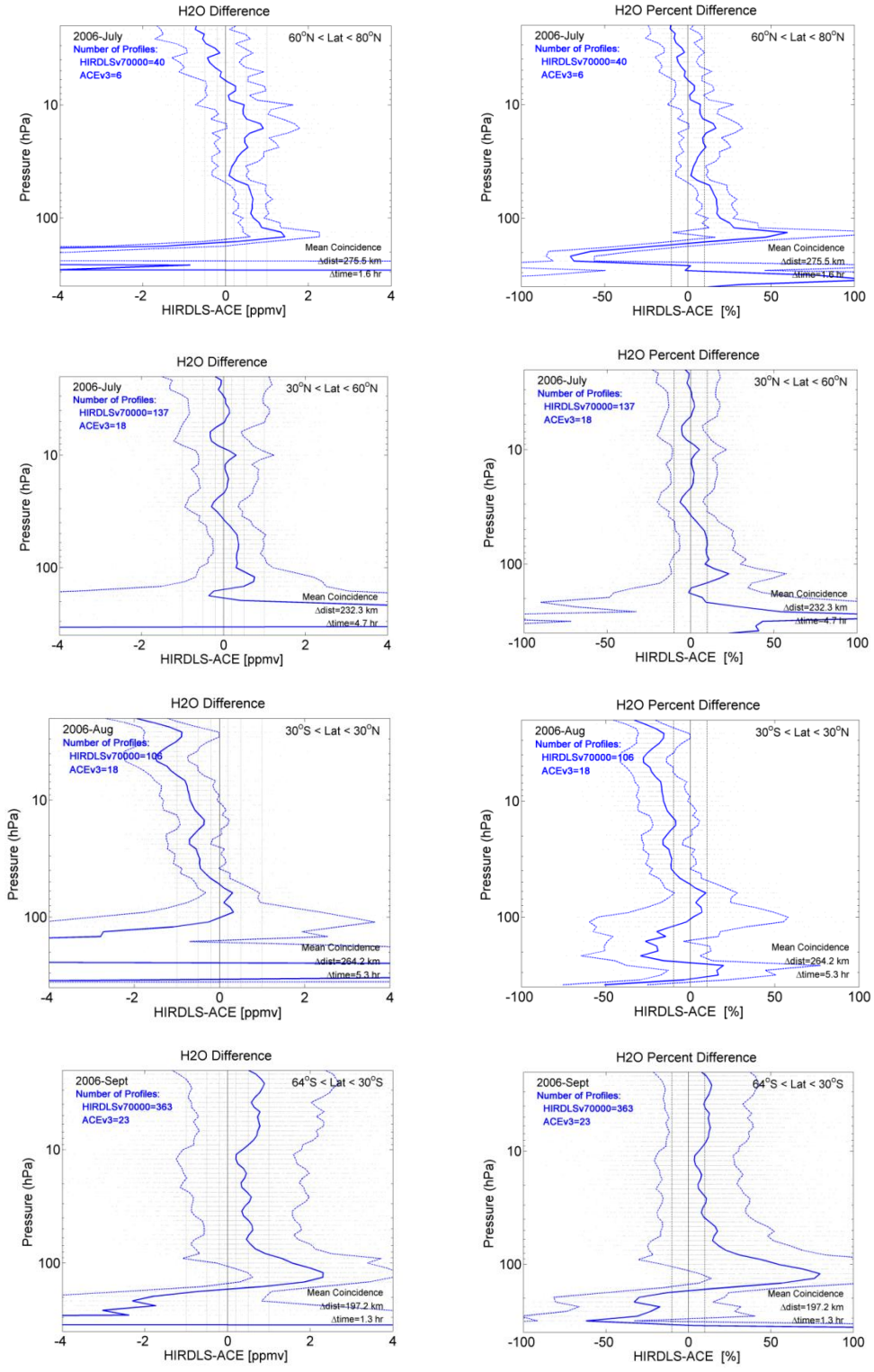

Figure 5.5.5. Statistics of comparisons of HIRDLS water vapor with ACE-FTS for the months indicated. Thick line is mean difference HIRDLS minus ACE-FTS, while thin lines are ± 1 standard deviation. Left column displays differences in ppmv, and right shows percentage differences. Top row- 60-80°N, second row 30-60°N, third row 30°S-30°N, bottom row 30°-64°S. Number of coincidences is shown.

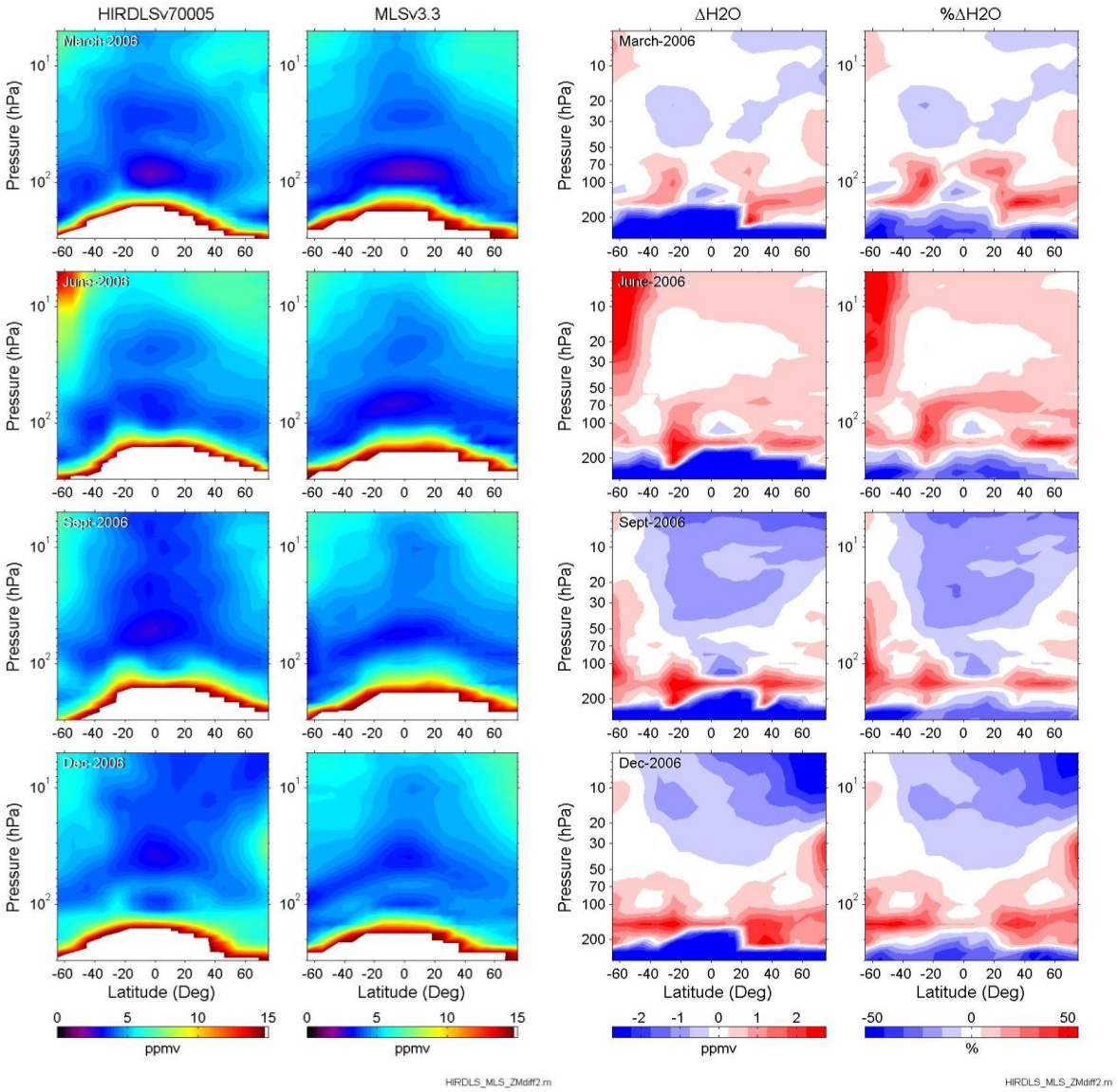
HIRDLSv70005
MLSv3.3
ΔH2O
%ΔH2O
March-2006
June-2006
Sept-2006
Dec-2006
Pressure (hPa)
Latitude (Deg)
ppmv
%
HIRDLS_MLS_ZMdiff2.m

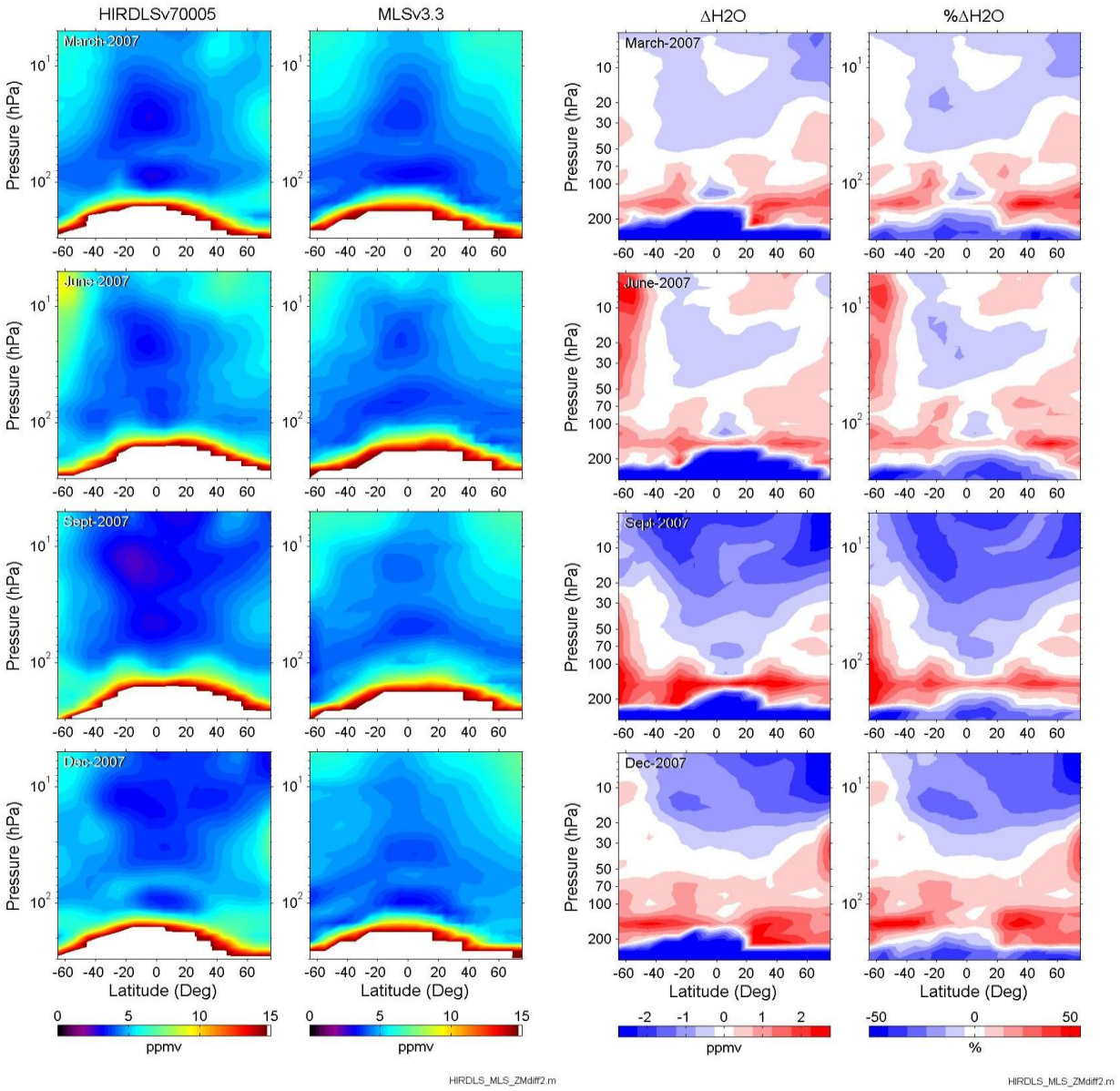

Figure 5.5.6. Monthly mean zonal mean HIRDLS water vapor cross-sections compared to MLS for 4 months each in 2006 and 2007. From top, March, June, September, and December. Left 2 panels show HIRDLS V7 and MLS V3.3; third panel is difference HIRDLS minus MLS in ppmv, and fourth panel is percentage difference.

A final display of the realism of these water data is shown by the tropical "tape recorder", the pattern of alternating higher and lower water vapor amounts that is imprinted on the vertical water vapor distribution in the upwelling air going through the tropical tropopause as a function of time [Mote et al., 1996]. Figure 5.5.7 shows the vertical and temporal variation of the water vapor anomaly as a function of time. The anomaly is the difference between the daily zonal mean water vapor averaged over 12°S-12°N and the time mean of the same quantity.

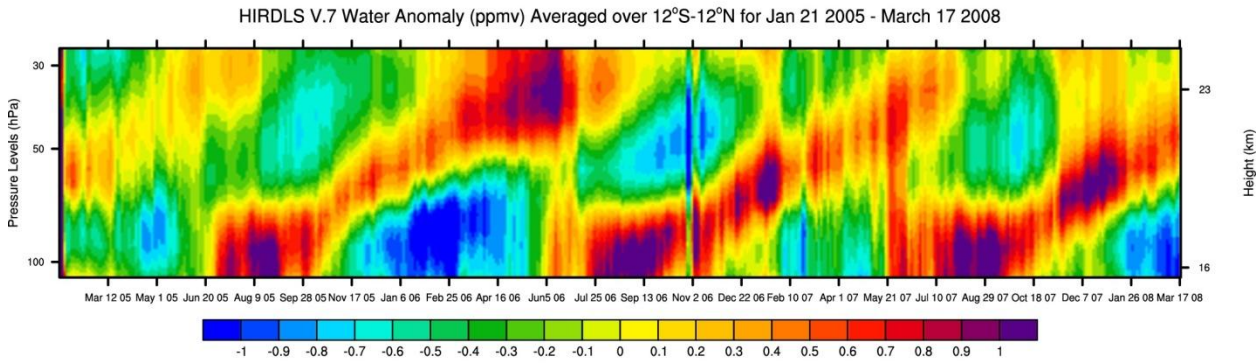

Figure 5.5.7. Time-altitude plot of water vapor anomalies averaged over 12°S to 12°N, showing the "tape recorder" signal, the upward moving pattern of alternating positive and negative values. The anomalies are the daily departures of the zonal mean water vapor from the time means, caused by the annual variation of the tropical tropopause temperature.

5.6 N_2O

Species: Nitrous Oxide (N_2O)
Data Field Name: N_2O
Useful Range: 100-5.1 hPa (approximately 15-35 km); **use zonal mean data***
* See section 5.13.4
Vertical Resolution: 1-1.2km between 12-35 km
Contact: Rashid Khosravi
Email: rashid@ucar.edu

Introduction
Channel 15 of the HIRDLS detector array is the primary channel for measuring N_2O. It is centered at 1270 cm^{-1} over the P branch of the ν_1 transition [Edwards et al., 1995], and contains overlapping spectra from N_2O_5, $ClONO_2$, and CH_4 in channels 14, 16, and 17 respectively. These gases are therefore retrieved simultaneously using channels 14-17. The common contaminants in these channels are CO_2, H_2O, and HNO_3, with O_3 in channel 14 as well. Aerosol extinction is accounted for by simultaneously retrieving it in channel 6, the clearest HIRDLS aerosol channel (at 12.1 μm), and using a spectral model to scale the extinction to the passbands of channels 14-17.

The radiances involved in the N_2O retrieval are affected by the launch-induced aperture blockage in the HIRDLS instrument (section 2), and are processed through the correction algorithms described in section 4 to remove the blockage signal. The corrected radiances are then scaled by the aperture open area fraction (derived as a function of channel and scan elevation angle using instrument data). In the last radiance processing step, the scaled radiances are adjusted by an empirical factor, based on comparison with correlative data, to improve retrieval accuracy.

In the following sections, HIRDLS v7 N_2O retrievals are characterized and their precision and accuracy are assessed. As discussed in section 5.6.4, zonal mean data from 100 to 5 hPa, rather than individual profiles, are recommended for scientific applications.

Resolution
HIRDLS N_2O retrievals are characterized by the averaging kernels shown in Figure 5.6.1. The kernels (green curves) are sharply peaked near 1, which indicates low instrument noise and high vertical resolution of 1-1.2 km between 12-35 km, obtained as the full-width-at-half-max of the green curves. As the signal-to-noise decreases above 35 km, the averaging kernels widen and resolution decreases.

The red line gives the sum of each averaging kernel at its nominal tangent height (red dots), indicating the fraction of the retrieval that comes from the observed radiances; i.e., the closer the value of the sum to unity the less the contribution of the *a priori* to the retrieval. Therefore, with the sum of the kernels being very close to 1 (0.99) between 10-50 km, HIRDLS N_2O retrievals are nearly independent of the *a priori* data (constructed from

specified- dynamics WACCM output). For more details on the retrieval algorithm and characterization, see Khosravi et al., [2009a,b];
http://www.agu.org/journals/jd/jd0920/2009JD011937/

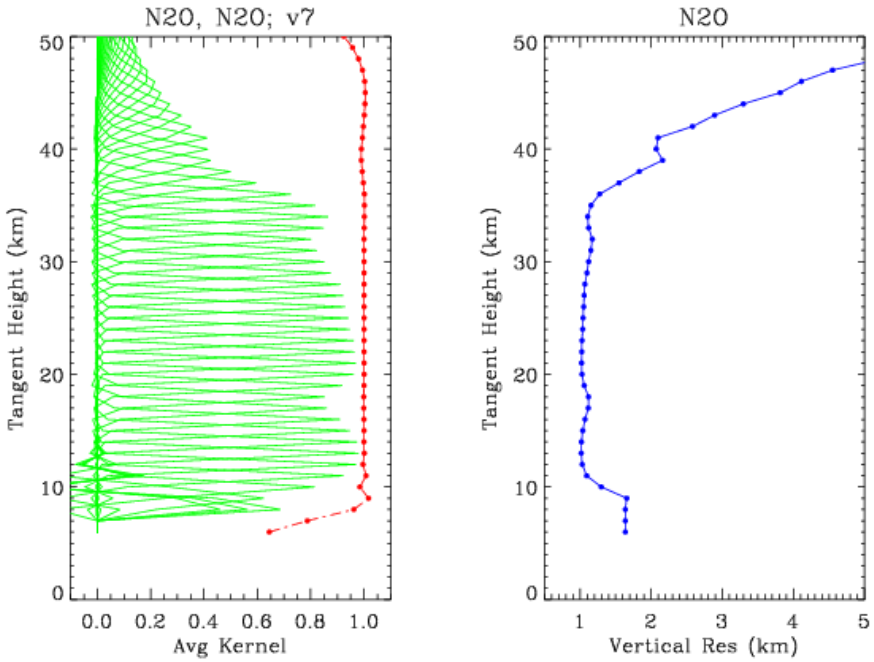

Fig. 5.6.1 Averaging kernels (green curves), sum of rows of the kernels (red line), and the vertical resolution of the HIRDLS N_2O retrievals, calculated for a radiance scan at 3^0 N on 15 Jan., 2007.

Precision

The predicted uncertainty (precision) in HIRDLS N_2O is calculated by the retrieval algorithm as the square root of the diagonal elements of the retrieval error covariance matrix multiplied by the retrieved N_2O volume mixing ratio (see Khosravi et al., [2009a, b] for details). These uncertainties are therefore expressed in terms of volume mixing ratio and are contained in the field 'N_2OPrecision' in the data files. In addition, as customary, when most of the information in the retrieval comes from *a priori* data, precision is flagged as negative to alert the user to decide whether such data are suitable for scientific application.

A representative profile of N_2OPrecision is shown in Fig. 5.6.2 as the standard deviation in the retrieved N_2O; i.e., the ratio of N_2OPrecision to N_2O volume mixing ratio (VMR). In the data range recommended above, the uncertainties vary approximately from 15% at 12 km to 40% at 35 km, increasing to very large values above 35 km, where SNR diminishes rapidly, mainly due to low values of N_2O VMR. The precision also increases rapidly below 10 km, where the *a priori* contribution begins to increase because of the presence of clouds.

When the standard deviation becomes larger than the threshold of 212% (the magenta line), most of the information in the retrieved N_2O is contributed by the *a priori* and the precision at these tangent heights is flagged as negative (the magenta cross). Note that although the precision is positive for the tangent heights just before the magenta line, the *a priori* contribution to the retrieval is still large. For more details on negative precision and calculation of the threshold, see the document "Description of HIRDLS Predicted Precision Data," available from the web page http://www.eos.ucar.edu/hirdls/data.

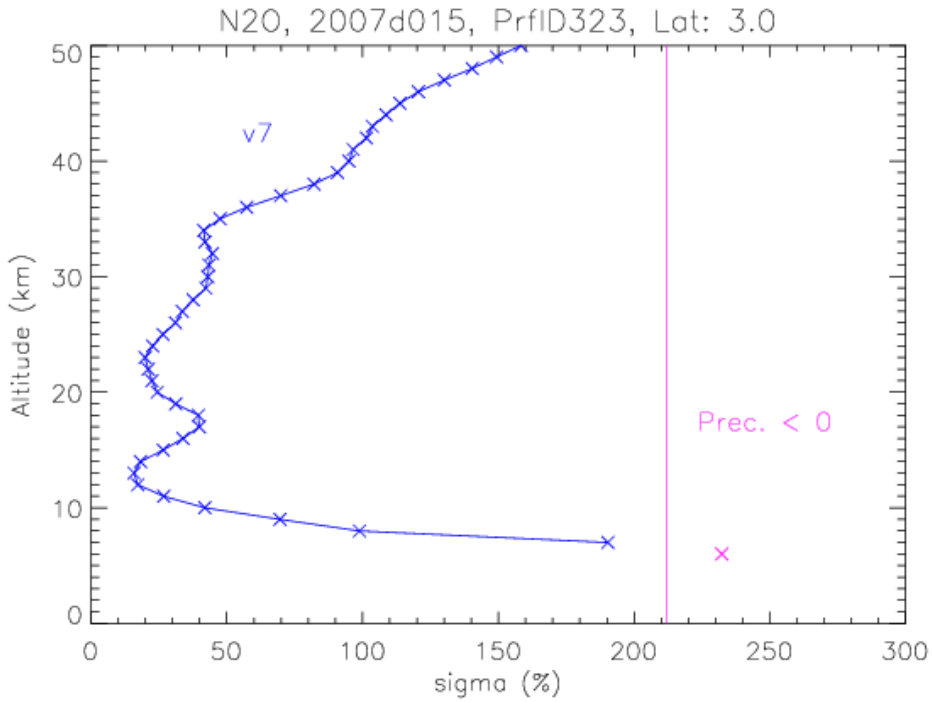

Fig. 5.6.2 Altitude cross section of N_2O Precision for the equatorial retrieval in Fig. 5.13.1 (3° N, Jan. 15, 2007), shown as % standard deviation (sigma); i.e., 100*(square root of the diagonal elements of the retrieval error covariance matrix). The vertical magenta line at 212% demarks the threshold beyond which precision is flagged as negative. Cloud top is at 8 km.

Accuracy

As pointed out in section 5, the aperture obscuration makes it difficult to calculate accuracy based on error propagation. Therefore, HIRDLS N_2O accuracy is assessed by comparing the retrieved data with correlative measurements. Figure 5.6.3 shows comparison of representative HIRDLS v7 N_2O profiles with MLS v3.3 data, collocated to HIRDLS tangent heights for 15 Jan., 2006. It can be seen that while HIRDLS profiles can be considered to be "close" to MLS data, the jagged nature and oscillations in the HIRDLS data result in relative differences of up to 50% or more. These characteristics, which are believed to be due to the contamination of the observed radiances by the obscuration signal, are present in most profiles at most latitudes. In the tropics, however, if cloud tops (CTalt in plot titles) reach high into the troposphere, the *a priori* contribution to the retrieval increases significantly, which could result in somewhat smoother profiles in these regions; e.g., at latitude 1.2 N in Fig. 5.6.3.

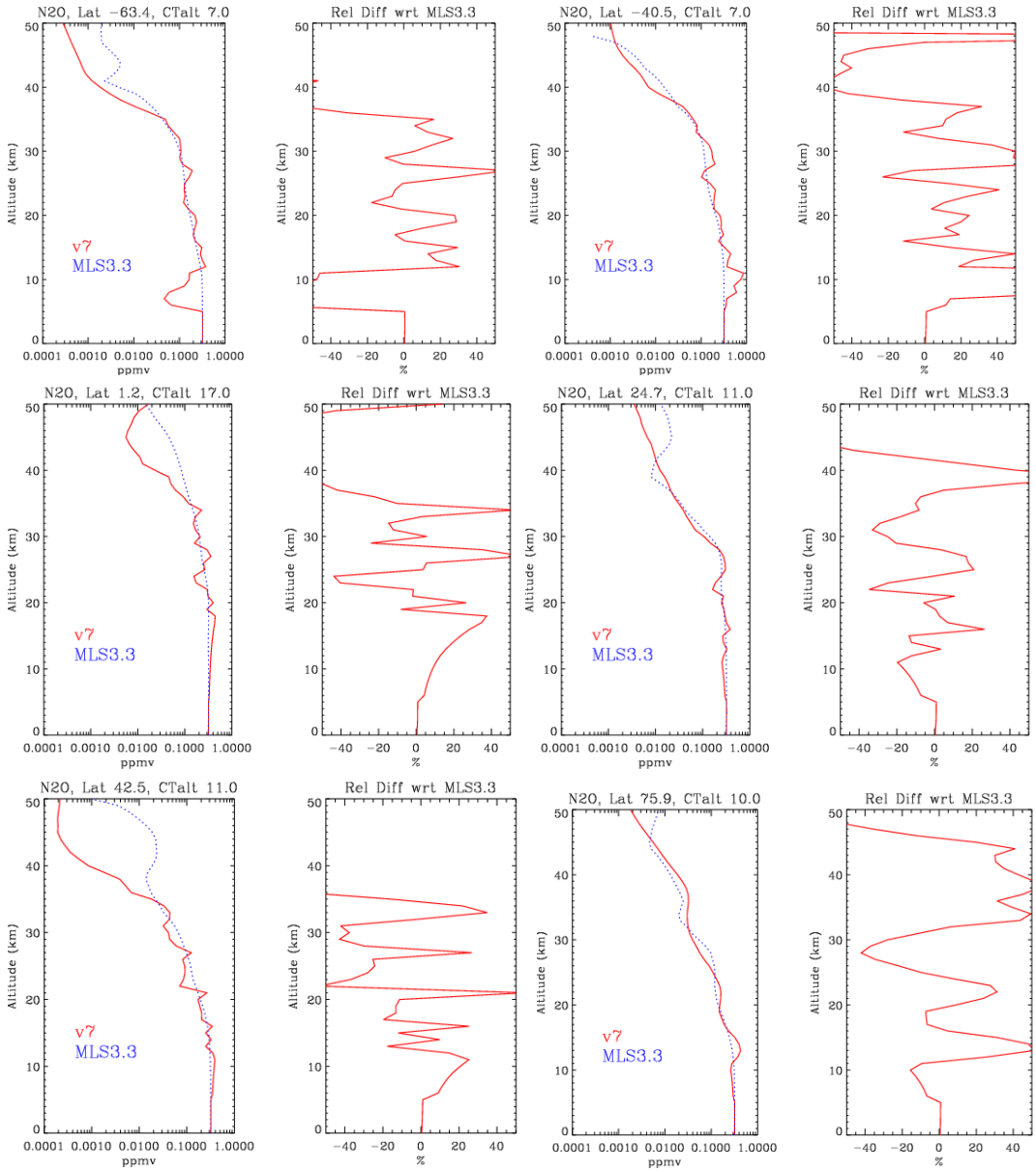

Fig. 5.6.3 Comparison of HIRDLS v7 N_2O profiles with collocated MLS v3.3 data for 15 Jan., 2006. Profiles are shown for high, mid, and low latitudes in both hemispheres. Each pair of plots is for the latitude indicated at the top of the panel on the LHS. The plot on the RHS of each pair shows the percent difference of HIRDLS N_2O VMR with respect to MLS data (100*(HIRDLS/MLS -1)). Cloud top altitude (CTalt) is indicated in the title of the LHS panels.

These characteristics persist to varying degree with respect to time of year. Figure 5.6.4 shows a set of profile comparisons similar to that in Fig. 5.6.3 but for 15 July, 2006. It can be seen, for example, that the high- and mid-latitude southern hemisphere profiles of HIRDLS N_2O exhibit significantly larger errors with respect to MLS data for this date than those for 15 Jan., 2006. However, the high- and mid-latitude northern hemisphere profiles show smaller errors in July than in Jan.

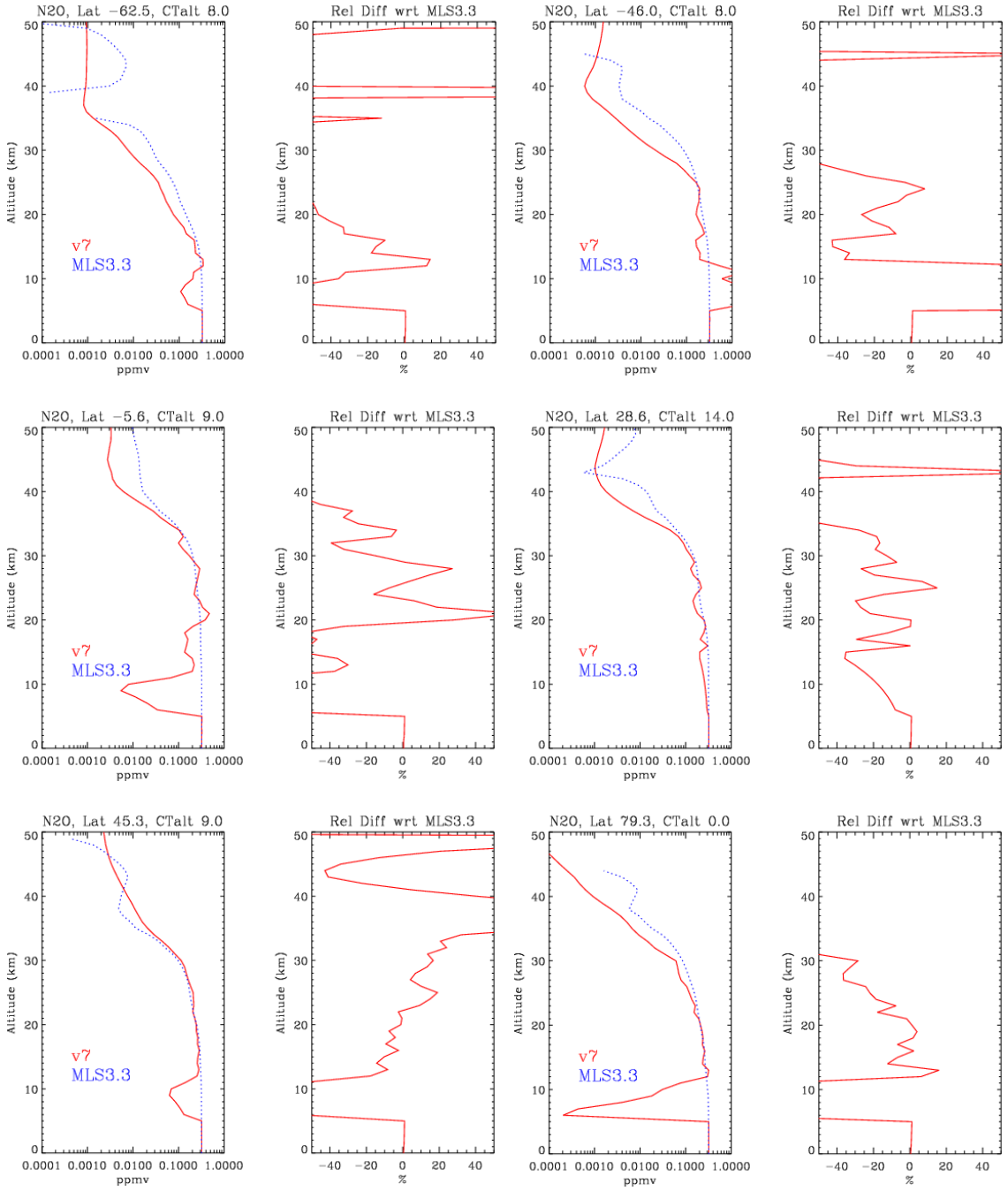

Fig. 5.6.4 As in Fig. 5.6.3 but for 15 July, 2006.

It should also be mentioned that in addition to variation with latitude and time, HIRDLS N_2O accuracy can exhibit significant orbit-to-orbit variations (caused perhaps by the changing Kapton signal during the day and the imperfect correction algorithms to completely remove that signal from the observed radiances). Figures 5.6.5 and 5.6.6 illustrate this orbital variation for three orbits on 18 May, 2006 and 15 Oct., 2006,

respectively, as compared with MLS v3.3 N_2O data. While HIRDLS retrievals capture the basic morphology of N_2O, the variation of the relative difference with respect to MLS data (third panels from left) at many altitude/latitude locations can be large among the three orbits shown for each day.

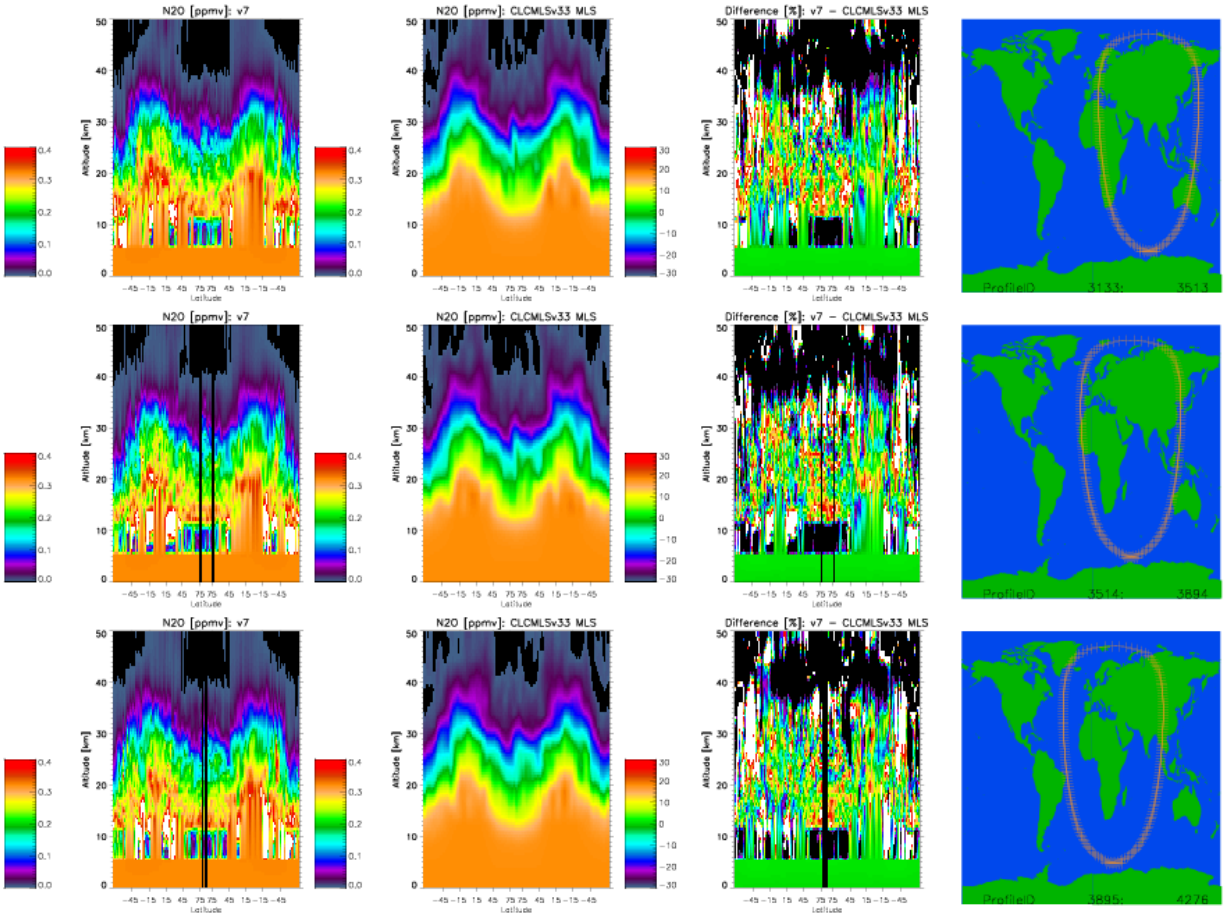

Fig. 5.6.5 Comparison of altitude vs. latitude curtain plots of HIRDLS v7 N_2O profiles (left most panels) with MLS v3.3 data (second panels from left) at tangent points around the orbits shown for 18 May, 2006. The third panels from left show the relative difference, 100*(HIRDLS/MLS – 1). The retrieval bottom level is at 8 km, below which the data are from the WACCM model.

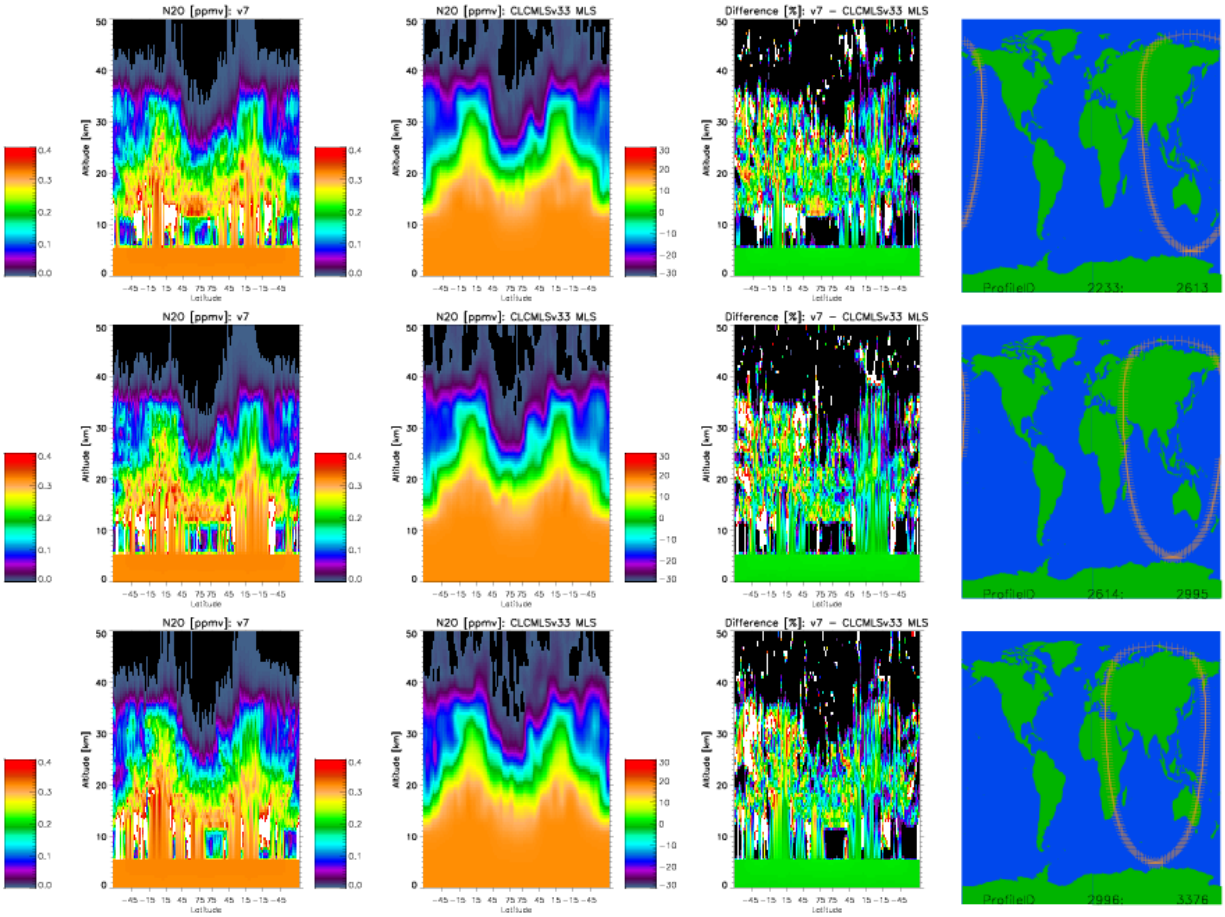

Fig. 5.6.6 As in Fig. 5.13.5 but for 15 Oct., 2006

Because of the characteristics described above, i.e., jaggedness and large variation with latitude, time, and orbit, it is difficult to assign an accuracy estimate to HIRDLS N_2O profile data. However, as shown in Figure 5.6.7, HIRDLS N_2O monthly and zonal mean data are much smoother and show significantly better agreement with MLS data. As seen in the right most panels, the HIRDLS monthly and zonal mean data are within ±10% of MLS data in the 100-5 hPa pressure range for most latitudes, although larger biases can occur at mid- and high latitudes; e.g. in March and Sep. At altitudes above 5 hPa, the zonal mean data show consistent negative bias of 40% or more. However, because of low signal-to-noise ratio at these altitudes, the *a priori* contribution is high and care must be taken to assess the quality and usefulness of the data by screening for negative precision.

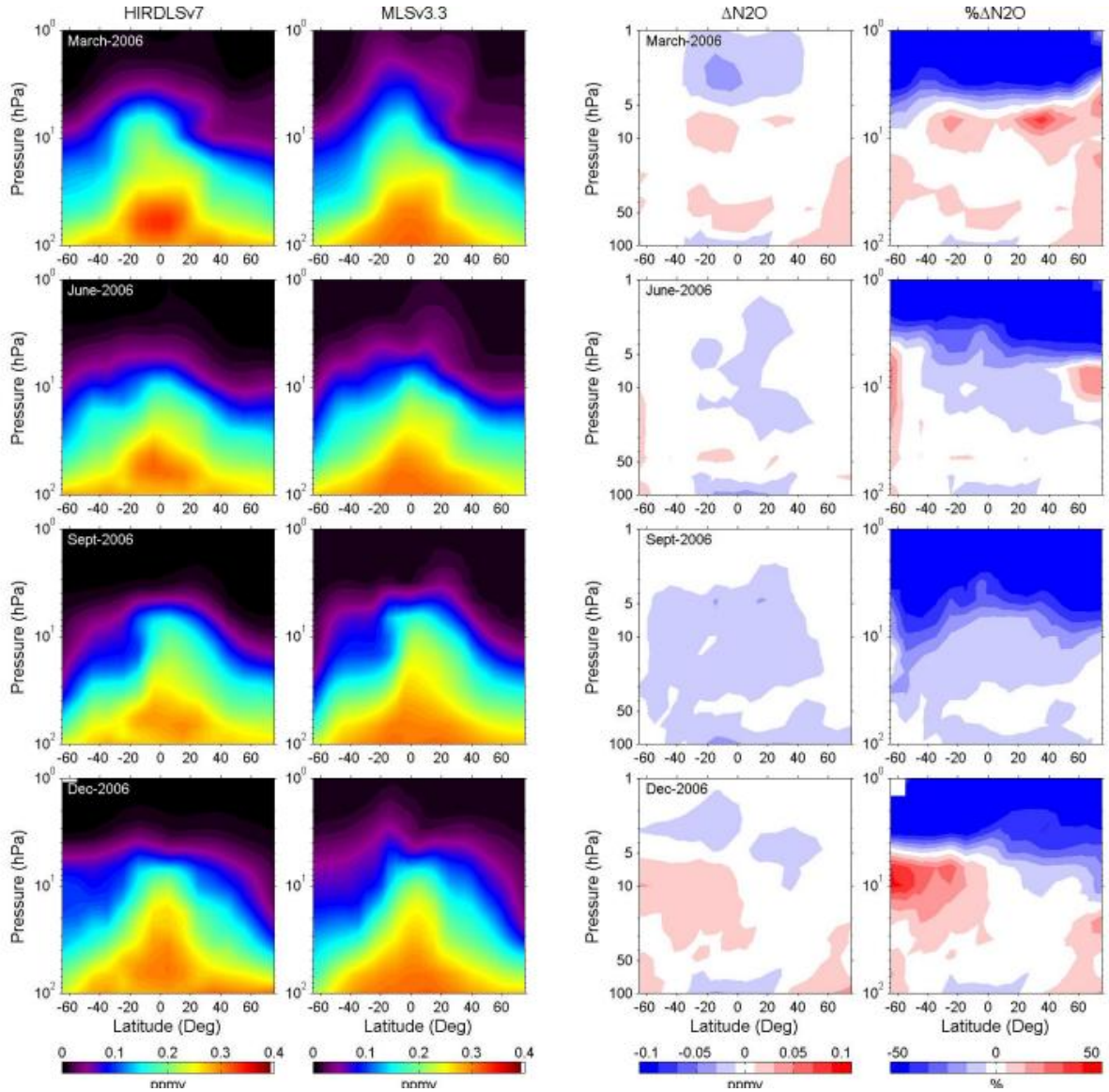

Fig. 5.6.7 Monthly zonal mean HIRDLS v7 N_2O (left most panels) comparison with MLS v3.3 N2O (second panels from left) for March, June, Sept., and Dec. (top to bottom, respectively) 2006. The corresponding differences (HIRDLS-MLS) are shown in the 3rd panels from left in terms of VMR and in the right most panels in terms of percent relative difference.

Summary

Representative version 7 HIRDLS N_2O profile data show vertical resolution of 1-1.2 km and standard deviation of 15-40% (precision/VMR) between 12-35 km altitude range. Profile data also exhibit jaggedness and large biases relative to MLS v3.3 data that vary significantly with altitude, latitude, day of year, and orbit during the day. However, HIRDLS monthly zonal mean v7 N_2O data compare well with MLS data, and may thus be useful for scientific applications in the 100-5 hPa pressure range.

5.7 Methane (CH_4)

Methane retrievals are not included as part of the V7 HIRDLS data product. In assessing these retrievals, the HIRDLS team notes that, at present, they possess excessively high noise and insufficient agreement with climatology and model estimates. This holds for individual limb soundings as well as zonal (or time) means derived from the individual scans. For these reasons the data are not scientifically useful at present. It is possible that a useful methane data product could be developed in future using some of the future ideas listed elsewhere.

5.8 Nitrogen Dioxide (NO_2)

Species: Nitrogen Dioxide (NO_2)
Data Field Name: NO2
Useful Range: 287.3 to 0.1 hPa
Screening criteria: See definition of the validation period
Vertical Resolution: 1.2 km
Prepared by: Maria Belmonte Rivas
Contact: Lesley Smith
Email: lsmith@ucar.edu
Validation paper: In preparation

General Comments

The HIRDLS NO_2 profiles come in two flavors: raw L2 data and Kalman filtered L3 products. In general, we recommend using the latter because of their superior noise properties, although the study of phenomena with time scales shorter than 5 days may warrant the use of the L2 data. Because of the diurnally varying nature of NO_2, the HIRDLS products have been partitioned into ascending (mostly day) and descending (mostly night) orbital segments. The local solar time (LST) of the HIRDLS NO_2 products is a function of latitude, as shown in the left plot on Fig. 5.8.3.

Resolution

The vertical resolution of the HIRDLS NO_2 profiles is approximately 1.2 km at peak VMR levels as determined from the full-width at half maximum of the averaging kernels shown in figure 5.8.1 (daytime on left, nighttime on right) degrading to 2 - 4 km as the NO_2 mixing ratio approaches zero at the upper and lower ends of the gas profile.

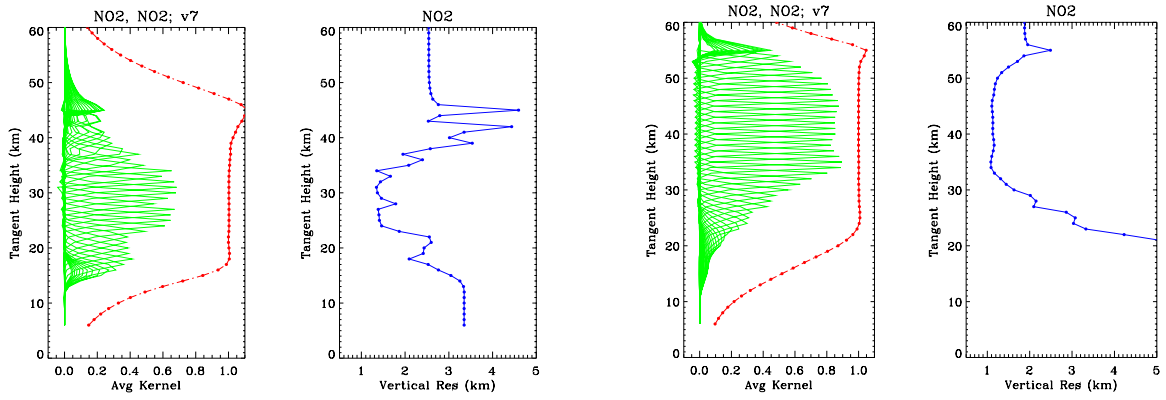

Figure 5.8.1. Averaging kernels (green lines) and vertical resolution (blue curves) as a function of altitude for daytime (left) and nighttime (right) HIRDLS NO_2 zonal means.

Recall that the red line on the left panels indicate the fraction of the information that comes from the HIRDLS measurements; values close to unity indicate that there is negligible influence from the *a priori*. The daytime (nighttime) averaging kernels were calculated for 15 January 2007 at 45°N (3°N) with a cloud top altitude of 8 km: any latitudinal variations should be small over regions with large signal to noise ratio (SNR).

Precision

The precision of the HIRDLS Kalman filtered NO_2 zonal means is displayed in Figure 5.8.2 along with the predicted and observed uncertainties of the L2 raw profile data. The observed uncertainty is derived from the dispersion of L2 data about the Kalman filtered zonal means. The ratio of raw profile to zonal mean precision is commensurate with the squared root of the number of profiles *N* assimilated by the Kalman filter per latitude bin per day (N~17 for 1 degree latitude bins). The precision of the Kalman filtered NO_2 zonal means is < 0.2 (0.4) ppbv for the day (night) products, or about 5-10% at peak VMR levels. The observed precision of the L2 profiles is about 0.7 (1.2) ppbv for the day (night) products, or about 15-30% at peak VMR levels.

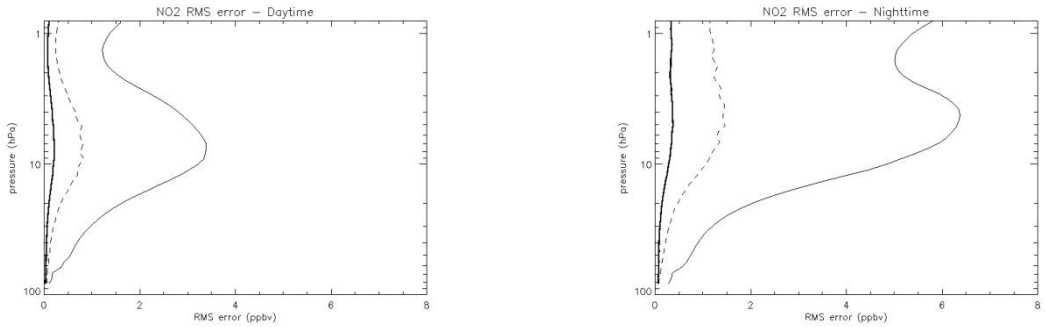

Figure 5.8.2. Estimated precision of the HIRDLS V7 Kalman filtered NO_2 zonal means (thick solid lines) compared with the observed and predicted precision of the original L2 profile data (dashed and thin solid lines).

Accuracy

In order to arrive at an estimate of absolute bias, the daily HIRDLS NO_2 zonal means have been compared to independent MIPAS and ACE-FTS datasets. Because NO_2 exhibits a strong diurnal cycle, a photochemical model has been introduced to correct for differences in local observation times between HIRDLS and the validating instruments.

NO_2 is a short-lived gas in photochemical equilibrium with NO and N_2O_5, featuring a smooth volume mixing ratio (VMR) profile with minimum (maximum) concentrations after sunrise (sunset) and a broad peak between 3 and 10 hPa (30-40 km) as shown in Figs. 5.8.4 and 5.8.5. The photochemical model correction is effected via the ratio of modeled NO_2

profiles evaluated at the appropriate latitude (*lat*) and corresponding observation times (*LST, LST₀*) as:

$$VMR(z,lat,doy,LST) = VMR(z,lat,doy,LST_0) \cdot \frac{VMR_{model}(z,lat,doy,LST)}{VMR_{model}(z,lat,doy,LST_0)}$$

Where *z* refers to altitude and *doy* to day of the year. The photochemical correction to the ACE-FTS profiles is based on the UCI (University of California at Irvine) photochemical box model described in Prather, [1997] and McLinden, [2000], and shown in Figure 5.8.4. The photochemical correction to MIPAS profiles is based on the SD-WACCM model driven by GEOS5 dynamics as described below and shown in Fig. 5.8.5. Uncertainties introduced in the diurnally shifted profiles are expected to be small, generally less than 10% in the middle stratosphere and 20% in the lower/upper stratosphere. Major uncertainties are expected to occur at polar latitudes, particularly around the terminator.

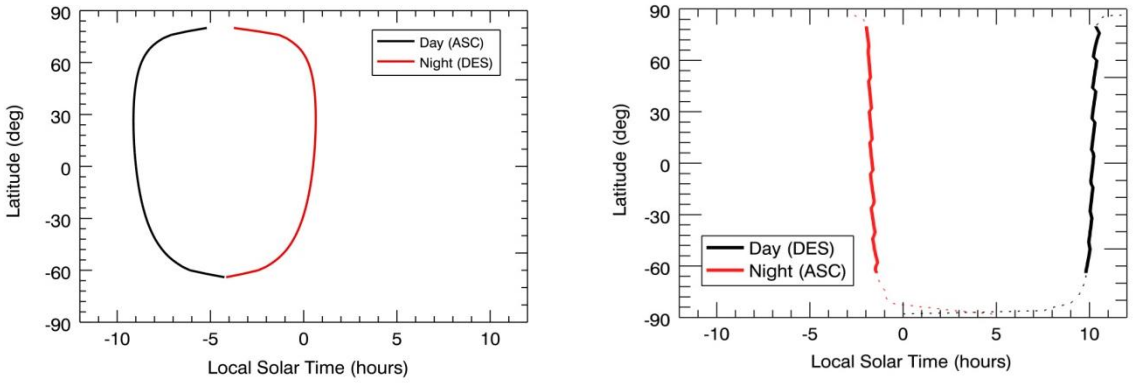

a) HIRDLS b) MIPAS

Figure 5.8.3. Daytime and nighttime local solar times (LST) of the HIRDLS (left) and MIPAS (right) NO_2 zonal means.

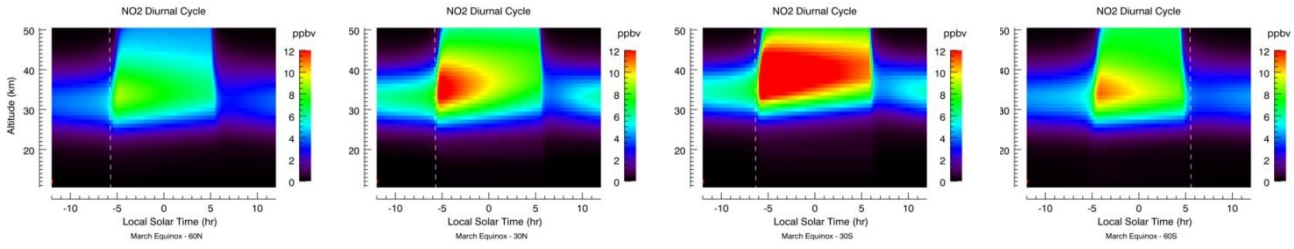

Figure 5.8.4. Diurnal variation of NO_2 (March 21st 2005) from ACE photochemical box model

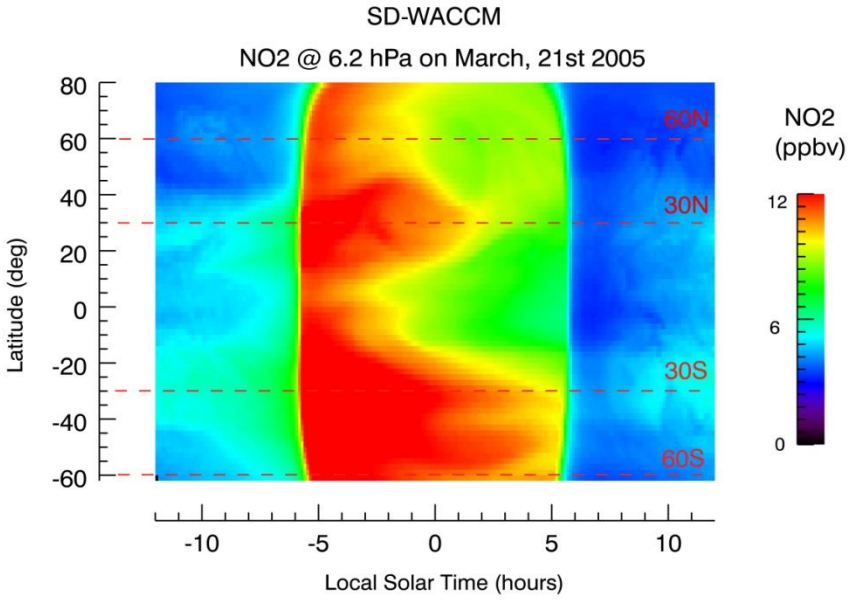

Figure 5.8.5. Diurnal variation of NO_2 (March 21st 2005) from SD-WACCM at peak VMR pressure level

Validation Datasets

MIPAS is a limb-sounding Fourier transform spectrometer that also collects emissions from the atmosphere in the mid-infrared. It measures NO_2 from 6 to 68 km with a vertical resolution of 3.5 to 6.5 km (the latter above 2 hPa). The MIPAS platform flies in a circular orbit at an altitude of 800 km with an inclination of 98.5 deg and descending node at 10.00 (local time), circling the Earth about 14 times a day and collecting profiles every 500 km along the orbit. In this comparison, we use the MIPAS NO_2 zonal means from profiles retrieved using the IMK-IAA processor (Instituut fur Meteorologie und Klimaforschung – Instituto de Astrofisica de Andalucia, version V40) described in von Clarmann, [2003].

A comparison of MIPAS NO2 profiles with correlative measurements (i.e. ground based, HALOE, SAGE II, POAM III and ACE-FTS) indicate that MIPAS provides valuable information from 2 to 30 hPa (25 to 45 km) during day and night with an overall accuracy better than 30% and a precision of 5-15%, with degraded accuracy during perturbed conditions (i.e. strong subsidence of NO_2>100 ppbv in the polar winter mesosphere) as described in Wetzel, [2007].

The **ACE-FTS** instrument records solar occultation spectra in the infrared. The ACE-FTS platform flies in a circular orbit at an altitude of 650 km with an inclination of 74 deg, providing up to 15 sunrise and 15 sunset solar occulations per day over an annually repeating coverage pattern. It measures NO_2 from 13 to 58 km with a vertical resolution of 3-4 km [Boone, 2005]. In this comparison we use the ACE-FTS sunset and sunrise zonal means using the Version 2.2 retrieved profiles.

The retrieved ACE-FTS NO_2 profiles agree with other satellite datasets (ground based, Halogen Occultation Experiment [HALOE], Stratospheric Aerosol and Gas Experiment [SAGE III], Polar Ozone and Aerosol Measurement [POAM III], Scanning Imaging Absorption Spectrometer for Atmospheric Cartography [SCIAMACHY], Optical System for Imaging and Low-intermediate Resolution Integrated Spectroscopy [OSIRIS] and MIPAS) to about 15% from 3 to 30 hPa (25 to 40 km) with a precision of 3% from 20 to 40 km, and inconclusive results for altitudes above 40 km or below 25 km (Kerzenmacher, [2008]). The ACE-FTS validation of NO_2 is overall compelling, with mean absolute differences to correlative measurements within 1 ppbv between 25 and 40 km, with the sole exception of MIPAS, which appears to be biased high (low) by up to 30% relative to ACE-FTS above (below) 10 hPa.

The **SD-WACCM** (Specified Dynamics Whole Atmosphere Community Climate Model, Version 3) is a full global climate model with chemistry based on the Community Atmospheric Model (CAM), featuring 66 vertical levels from the ground to approximately 145 km, and all the physical parameterizations described in Collins, [2004] and Richter, [2008]. The dynamical fields of temperature and wind are specified by Goddard Earth Observing System (GEOS-5) reanalyses, Rieneker, [2008]. The gravity wave drag and vertical diffusion parameterizations are as described in Garcia, [2007]. WACCM3 has a detailed neutral chemistry module for the middle atmosphere, including diurnal cycles for all constituents at all levels in the model domain, as described in Kinnison, [2007]. Vertical resolution is ≤1.5 km between the surface and about 25 km, increasing to 2 km at the stratopause and 3.5 km in the mesosphere. The latitude and longitude grids have spacing of 1.9 and 2.5 degrees, respectively. The SD-WACCM model results will be considered informative, but not conclusive for validation.

Validation period and error statistics

The algorithm for Kapton removal performs independent up and down-scan corrections to the HIRDLS radiances and the retrieval quality may differ substantially between these modes. Also, because of the variable nature of the background emission from the Kapton sheet, the quality of the retrieved gas profiles varies across the duration of the mission. A preliminary comparison between the resulting upscan and downscan modes against the references available (mostly MIPAS and SD-WACCM) provides a qualitative measure of their goodness across the mission and the grounds for a selection of the periods when the data quality appears to be best, which we define as the validation periods. For NO_2, the down-scan mode appears to give the best agreement to reference across the mission. The selected NO_2 zonal mean cross-sections are displayed in Fig. 5.8.6 for day and night products at representative peak VMR pressure levels for the entire duration of the mission. The corresponding MIPAS (photo-corrected to HIRDLS observation times using the WACCM model) and SD-WACCM (using MERRA dynamics) NO_2 zonal mean cross-sections are also displayed for reference.

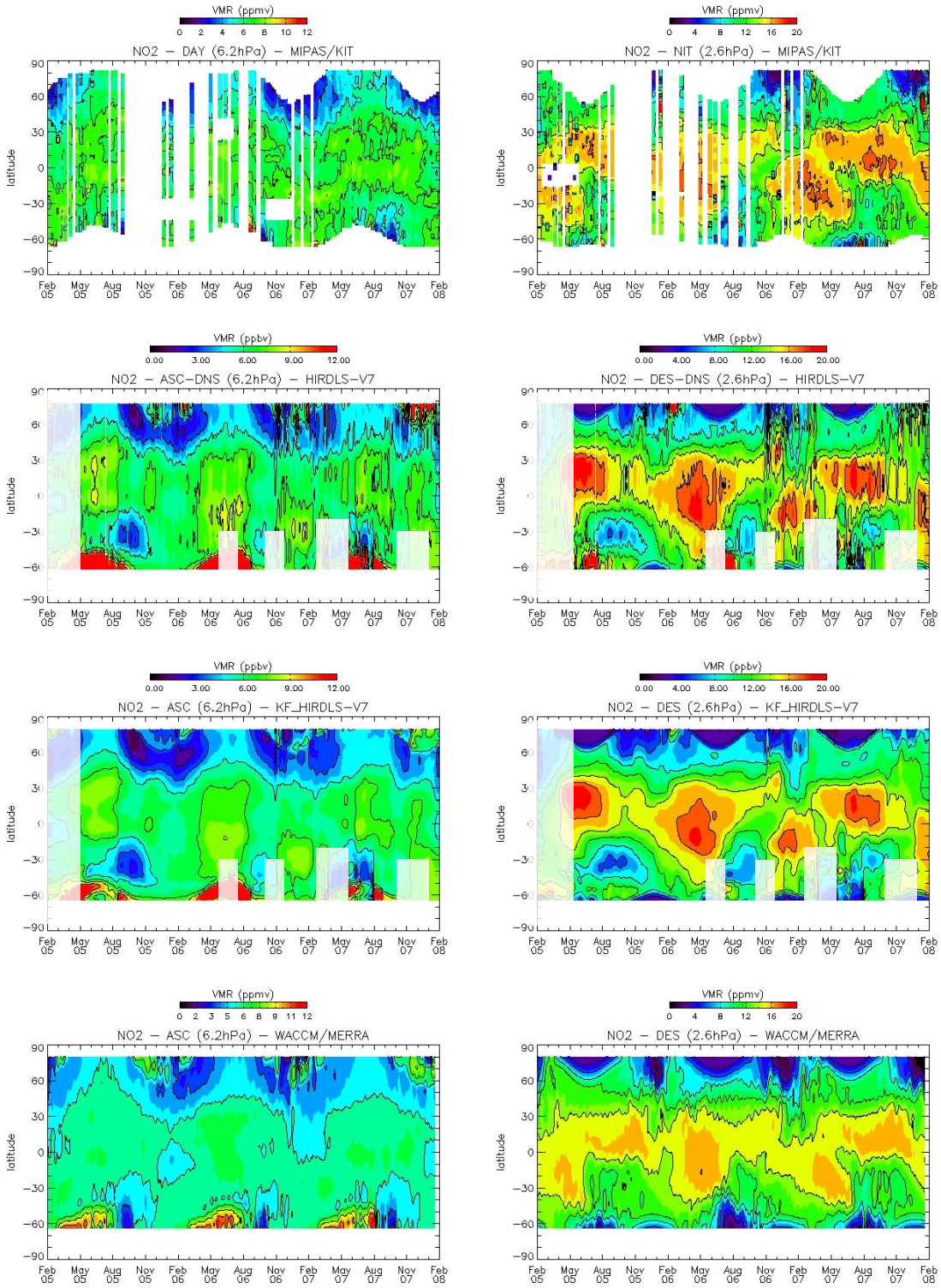

Figure 5.8.6. NO_2 zonal mean cross-section for ascending-day (left column) and descending-night (right column) segments at representative peak VMR levels across the HIRDLS mission. The MIPAS data have been photo-corrected to HIRDLS observation times. The SD-WACCM data use dynamics specified by MERRA. For completeness, the HIRDLS raw (L2) and Kalman filtered (L3) zonal means are displayed (only down-scan selection). On the HIRDLS panels, dates excluded from validation are shaded white.

Based on a preliminary qualitative comparison against our references, we may conclude that the **validation period** for HIRDLS NO_2 spans the entire HIRDLS record excluding:

1) Dates prior to Jun 1st 2005

2) Dates between Jun 15th and Aug 15th 2006 for latitudes < 30S

3) Dates between Nov 6th and Dec 23rd 2006 for latitudes < 30S

4) Dates between Mar 19th and Jun 20th 2007 for latitudes < 20S

5) Dates posterior to Nov 1st 2007 for latitudes < 30S

In addition, there is a persistent artifact in daytime NO_2 concentrations at altitudes between 0.2 and 0.8 hPa and latitudes between 50N and 50S caused by top-of-scan retrieval noise.

A comparison between the NO_2 zonal means from HIRDLS, MIPAS and the SD-WACCM model during the validation period is shown in figures 5.8.7a-b.

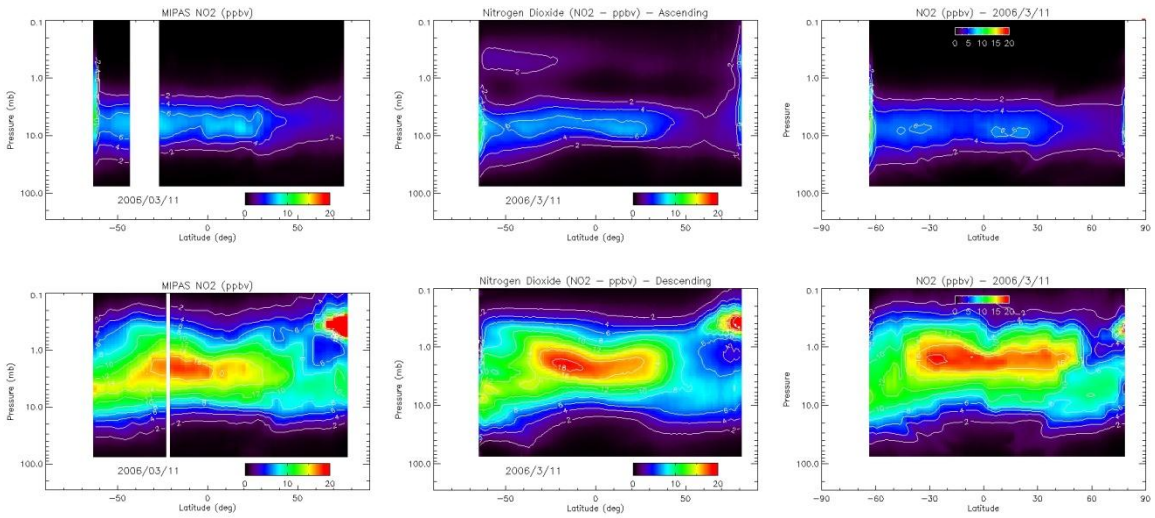

MIPAS HIRDLS SD-WACCM

Figure 5.8.7a. Sample NO2 zonalmeans on Mar 11th 2006 for daytime (top) and nighttime (bottom) from MIPAS (left), HIRDLS (center) and SD-WACCM (right) – time corrected to HIRDLS observation time.

The systematic error analysis that follows is based on the comparison of HIRDLS with MIPAS and ACE-FTS zonal mean observations time-corrected to HIRDLS measurement times and collected over the validation period defined above. The collocation consists of simple latitude matching, with MIPAS and ACE-FTS each having about 14 profiles per latitude bin. The reference profiles have been linearly interpolated to the HIRDLS altitude

grid, without averaging kernel smoothing. The entire collocated set has been split into three latitudinal groups, defined as northern latitudes (30 to 80N), tropics (30S to 30N) and southern latitudes (64S to 30S).

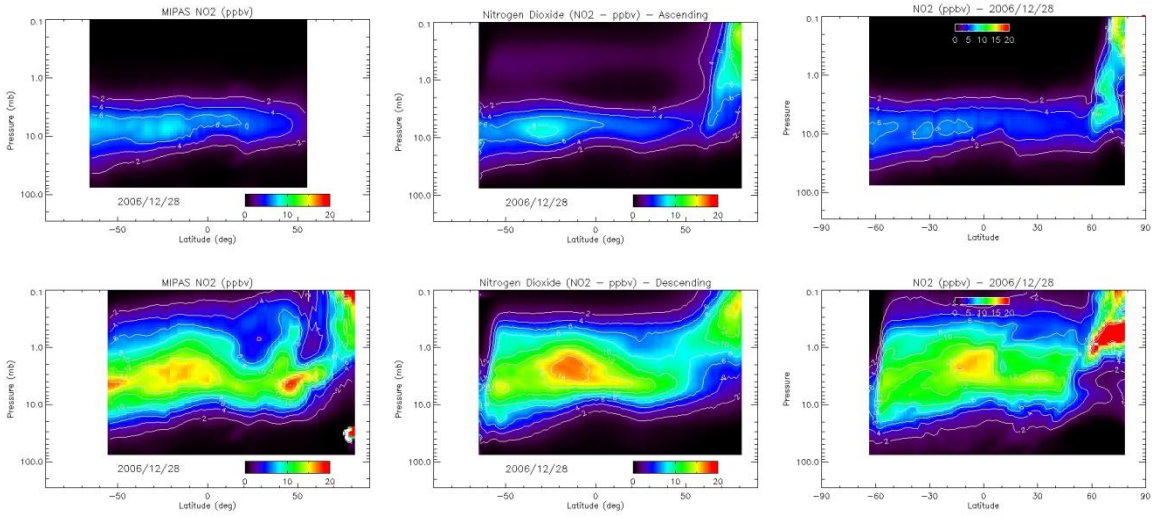

MIPAS HIRDLS SD-WACCM

Figure 5.8.7b. Sample NO2 zonalmeans on Dec 26th 2006 for daytime (top) and nighttime (bottom) from MIPAS (left), HIRDLS (center) and SD-WACCM (right) – time corrected to HIRDLS observation time.

For each latitudinal group, figures 5.8.8-11 contain:

Top panel: The time-averaged VMR profiles of the collocated HIRDLS and validating zonal means, along with their standard deviations and the number of collocated matches.

Middle panel: The time-averaged profile of differences between HIRDLS and the validating instrument, along with the standard deviation.

Bottom panel: The time-averaged profile of relative differences between HIRDLS and the validating instrument, along with the standard deviation.

Table 5.8.1: Bias estimates over validation period: Daytime NO2 mean {min to max} relative differences over the indicated pressure range

	HIRDLS vs MIPAS [3-30 hPa]	HIRDLS vs ACE [3-30 hPa]
Northern latitudes	**3% {-16 to 21%}**	**-6% {-18 to 7%}**
Tropics	**1% {-14 to 19%}**	**-14% {-58 to 24%}**
Southern latitudes	**30% {-5 to 60%}**	**3% {-37 to 13%}**

Table 5.8.2: Bias estimates over validation period: Nighttime NO2 mean {min to max} relative differences over the indicated pressure range

	HIRDLS vs MIPAS [3-30 hPa]	HIRDLS vs ACE [3-30 hPa]
Northern latitudes	**28% {17 to 60%}**	**5% {-2 to 24%}**
Tropics	**22% {5 to 77%}**	**-7% {-30 to 25%}**
Southern latitudes	**48% {12 to 95%}**	**24% {9 to 31%}**

Also, each panel is encased in a dashed square that delineates the pressure range over which the confidence limits of the validating reference are well known, following the validation literature. A summary of the systematic error scores is included in Tables 5.8.1 and 5.8.2. Note that the ACE-FTS dataset only covers the period from Jan 2005 to September 2006, while the MIPAS coverage is denser from September 2006 to February 2008, so that the ACE-FTS and MIPAS references become complementary with regards to time-coverage.

As tables and figures above suggest, the daytime HIRDLS NO_2 zonal means agree with the correlative MIPAS profiles to better than 20% over the 3-30 hPa pressure range and most locations (Fig. 5.8.8). This agreement deteriorates substantially over southern latitudes (<30S) particularly for altitudes below the 5 hPa level. In our preliminary and qualitative comparisons against the references, we observed that changes in the background emission from the Kapton obstruction tended to affect retrievals over southern latitudes the most, often arising as excessively high concentrations. This effect cannot be seen in the ACE-FTS validation scores (Fig. 5.8.9), most likely because the number and time span of the ACE-FTS collocations is much smaller than that of MIPAS. The ACE-FTS validation scores overall support the conclusions drawn from our comparison to MIPAS, namely, that the agreement of the daytime HIRDLS NO_2 to reference is about 20% over most locations. A persistent feature of the daytime HIRDLS NO_2 profiles is that they tend to peak at the same altitude as the references only with a slightly stronger concentration and over a thinner pressure layer.

The nighttime HIRDLS NO_2 zonal means agree with the correlative MIPAS profiles to better than 30% over the 3-30 hPa pressure range and most locations (Fig. 5.8.10), only with concentrations biased high by about 15-20%. As in the daytime case, the agreement with MIPAS deteriorates over the southern latitudes (<30S) at times when the emission from the Kapton obstruction becomes unstable. The ACE-FTS validation scores also support these conclusions, namely, that the agreement of the nighttime HIRDLS NO_2 zonal means to the available references is better than 30% (Fig. 5.8.11).

These figures of quality are overall comparable to those obtained for Version 6, only that they apply over a much more extended span, basically the entire mission excluding the first half of 2005.

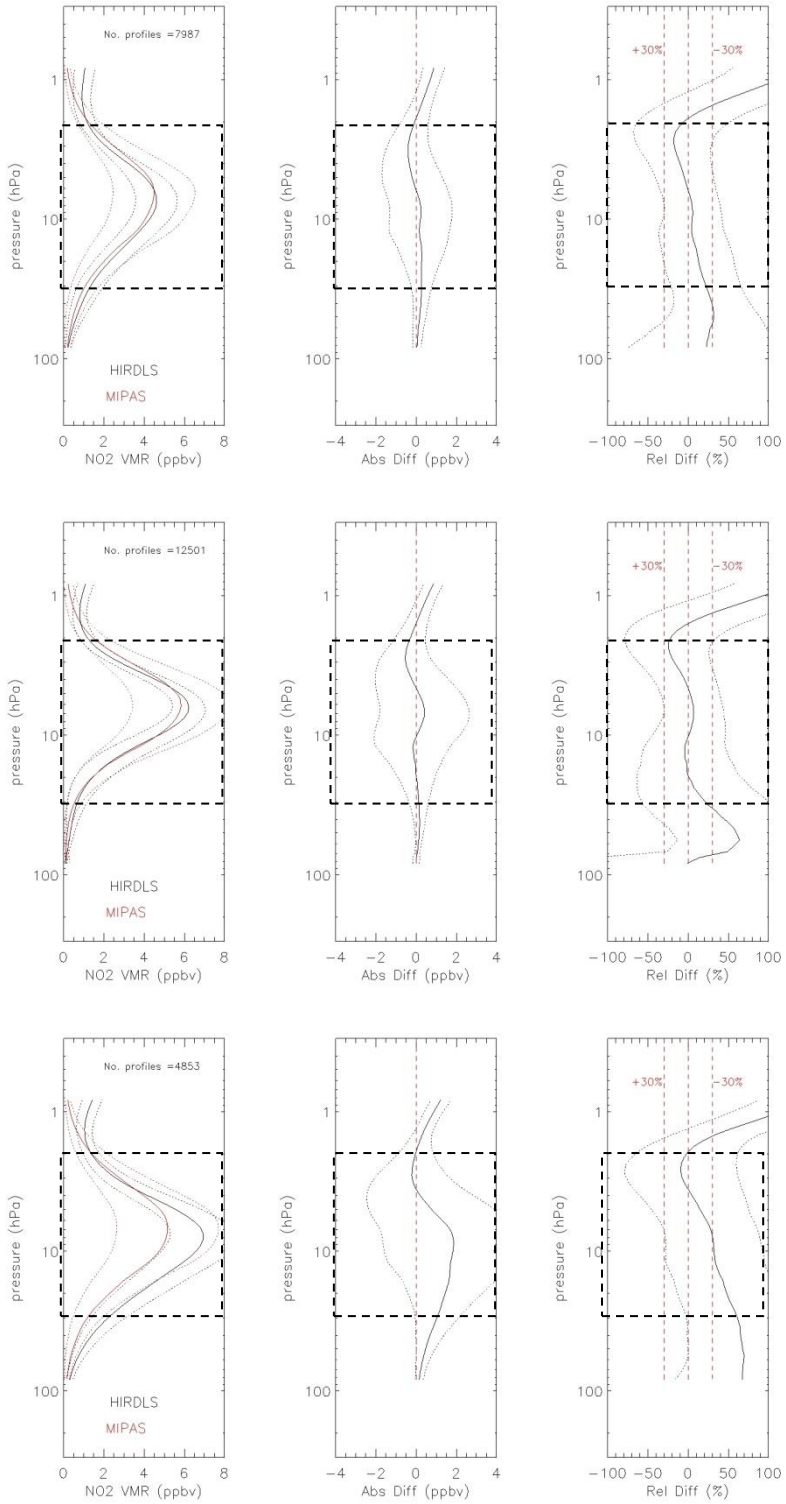

Figure 5.8.8. Systematic errors for daytime HIRDLS vs time corrected MIPAS NO_2 zonal means. Left: mean profiles; Mid: absolute differences; Right: relative differences.

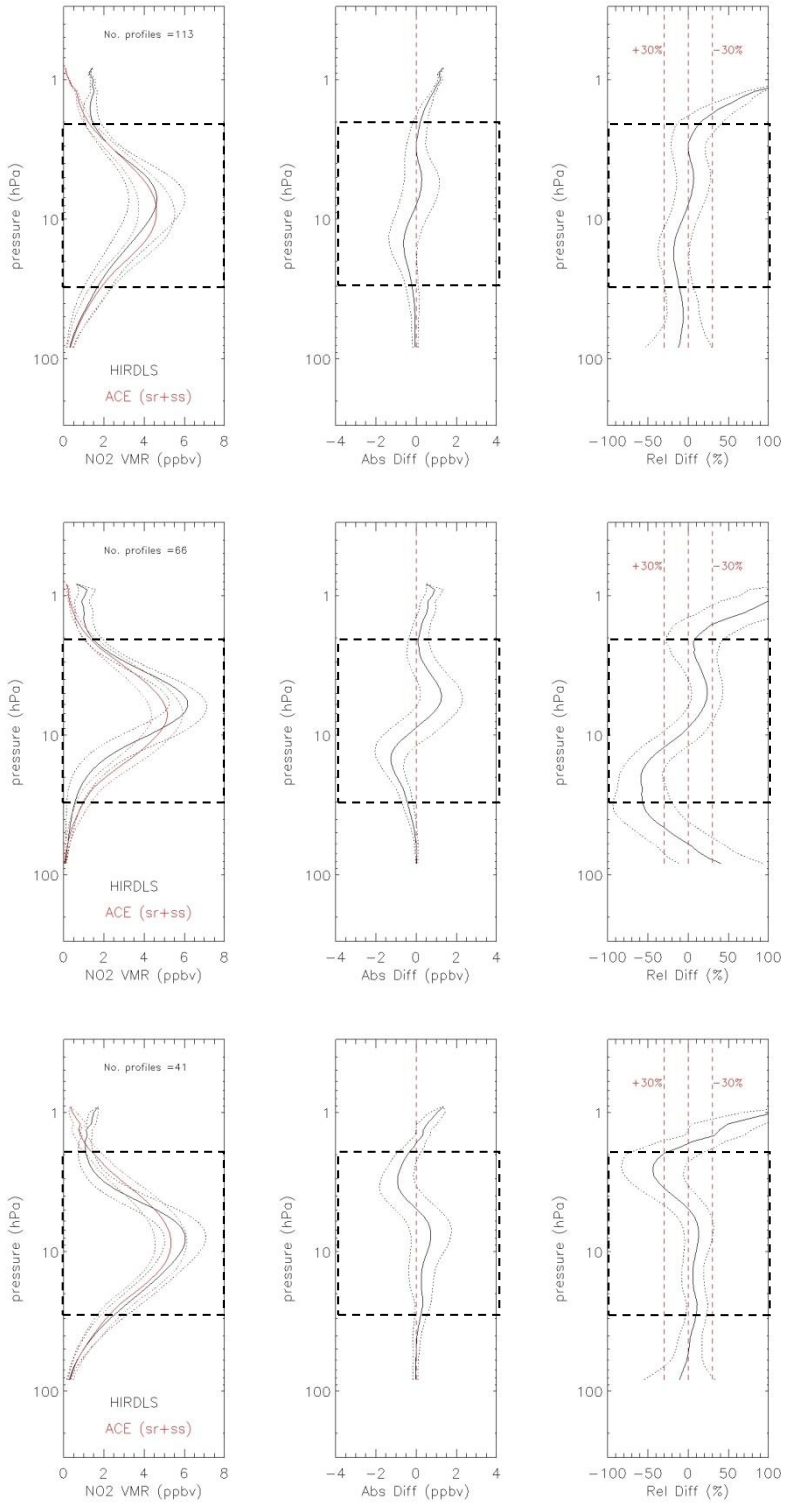

Figure 5.8.9. Systematic errors for daytime HIRDLS vs time corrected ACE-FTS NO_2 zonal means. Left: mean profiles; Mid: absolute differences; Right: relative differences.

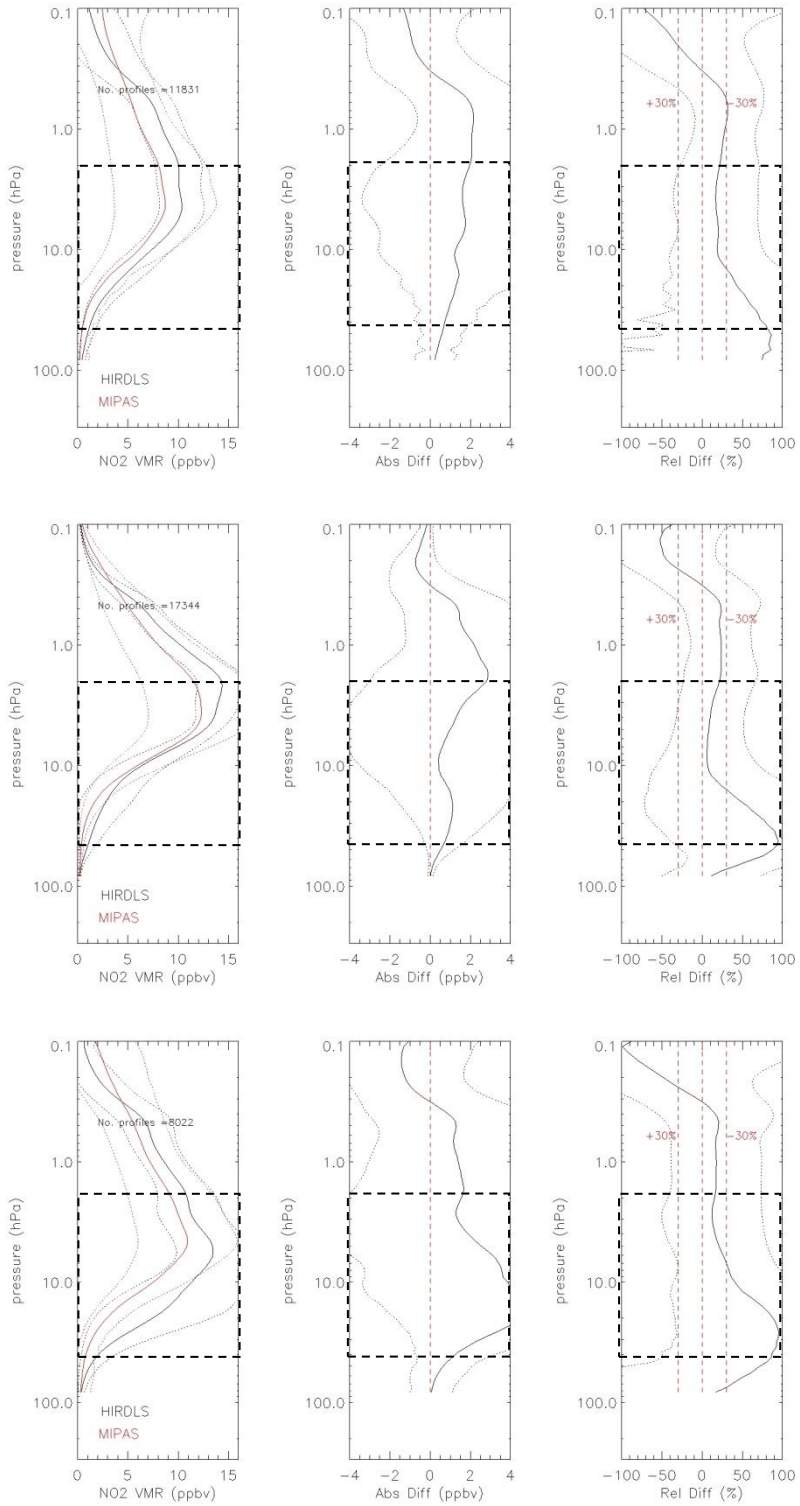

Figure 5.8.10. Systematic errors for nighttime HIRDLS vs time corrected MIPAS NO_2 zonal means. Left: mean profiles; Mid: absolute differences; Right: relative differences.

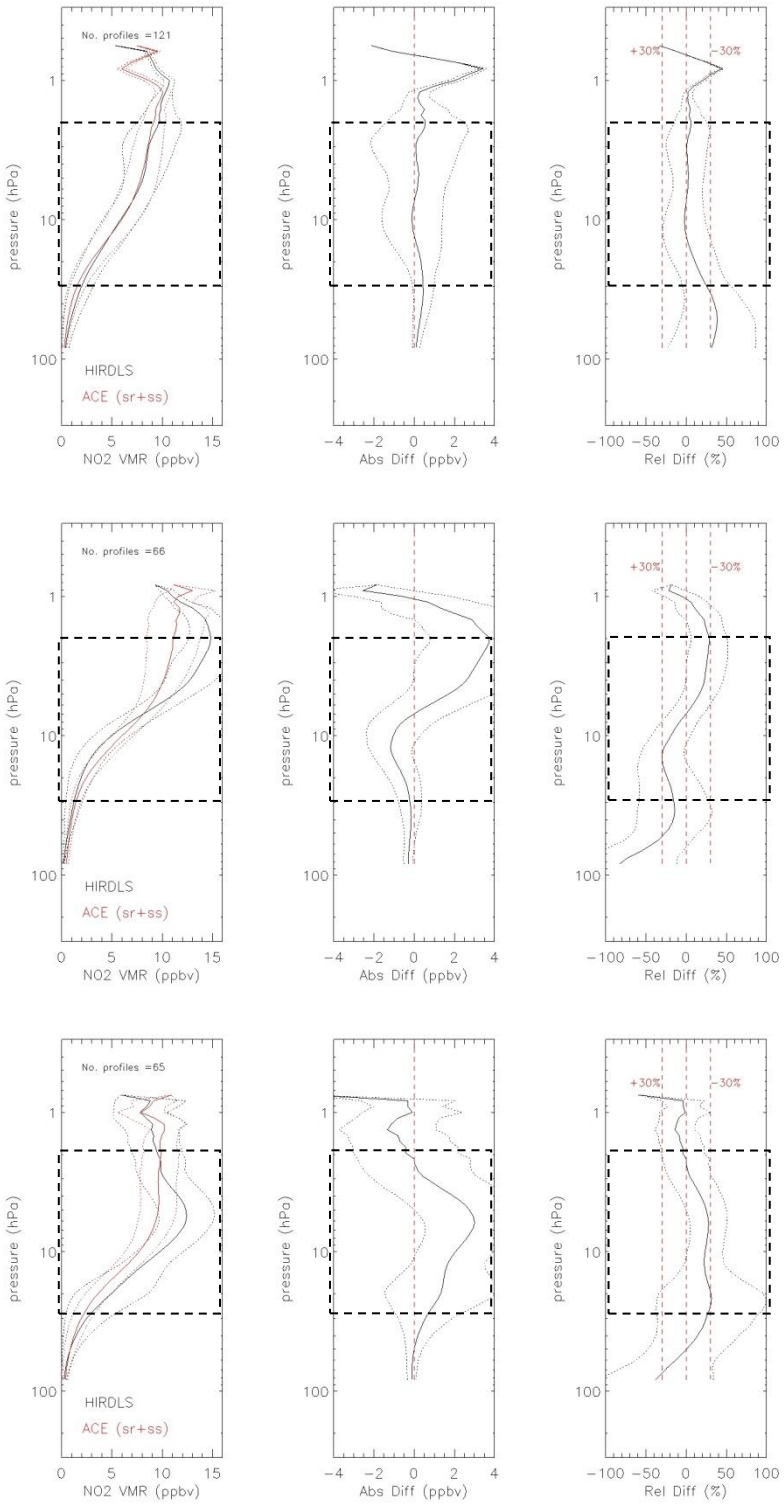

Figure 5.8.11. Systematic errors for nighttime HIRDLS vs time corrected ACE-FTS NO_2 zonal means. Left: mean profiles; Mid: absolute differences; Right: relative differences.

Conclusion

The HIRDLS NO_2 profiles have 1.2 km vertical resolution, a day/night precision of about 15-30% (5-10% for the Kalman filtered products) and agree to better than 20-30% with correlative MIPAS and ACE-FTS datasets over the 3-30 hPa pressure range and most locations. The nighttime NO_2 concentrations appear to be biased high relative to the validating references by about 15-20%, and the southern latitudes (<30S) appear to be more prone to errors caused by instabilities in the background emission from the Kapton obstruction.

5.9 Dinitrogen Pentoxide (N_2O_5)

Species:	Dinitrogen Pentoxide (N_2O_5)
Data Field Name:	N2O5
Useful Range:	82.5 to 1.0 hPa
Screening criteria:	See definition of the validation period
Vertical Resolution:	1.2 km
Prepared by:	Maria Belmonte Rivas
Contact:	Lesley Smith
Email:	lsmith@ucar.edu

General Comments

The HIRDLS N_2O_5 profiles come in two flavors: raw L2 data and Kalman filtered products. In general, we recommend using the latter because of their superior noise properties, although the study of phenomena with time scales shorter than 5 days may warrant the use of the L2 data. Because of the diurnally varying nature of N_2O_5, this HIRDLS product have been partitioned into ascending (mostly day) and descending (mostly night) orbital segments. The local solar time (LST) of the HIRDLS N_2O_5 product is a function of latitude, as already shown Fig. 5.8.3.

Resolution

The vertical resolution of the HIRDLS N_2O_5 profiles is approximately 1.2 km at peak VMR levels, as determined from the full-width at half maximum of the averaging kernels shown in figure 5.9.1 for the daytime (left pair) and nighttime(right pair), gradually decreasing to 2-3 km as the gas mixing ratio approaches zero at the upper and lower ends of the gas profile.

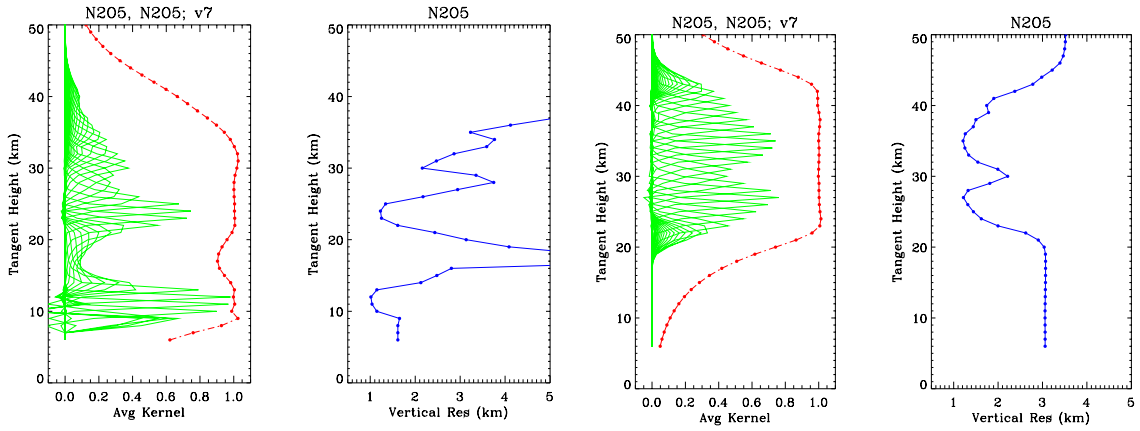

Figure 5.9.1. Averaging kernels (green lines) and vertical resolution (blue curves) as a function of altitude for daytime (left) and nighttime (right) HIRDLS N_2O_5 profiles.

The red line in the left panels of the pair indicates the fraction of information that comes from the HIRDLS measurements; values close to unity mean that there is negligible influence from the *a priori*. The averaging kernels were calculated for 15 January 2007 at 45°N (day) and 3°N (night) with a cloud top altitude of 8 km: any latitudinal variations should be small over regions with large signal to noise ratio.

Precision

The precision of the HIRDLS Kalman filtered L3 N_2O_5 zonal mean is displayed in Figure 5.9.2 along with the predicted and observed (empirical) uncertainties of the L2 raw profile data. The observed uncertainty is derived from the dispersion of L2 data about the Kalman filtered zonal means. The ratio of raw profile to zonal mean precision is commensurate with the square root of the number of profiles *N* assimilated by the Kalman filter per latitude bin per day (N~17 using 1 degree latitude bins). The precision of the Kalman filtered N_2O_5 zonal means is ~0.04 ppbv (5-10%) for the nighttime products. The observed precision of the raw L2 profiles is about 0.15 ppbv, or about 15-30%. For the daytime products, the precision of the Kalman filtered N_2O_5 zonal means is ~0.01 ppbv, and the observed precision of the raw L2 profiles is about 0.04 ppbv.

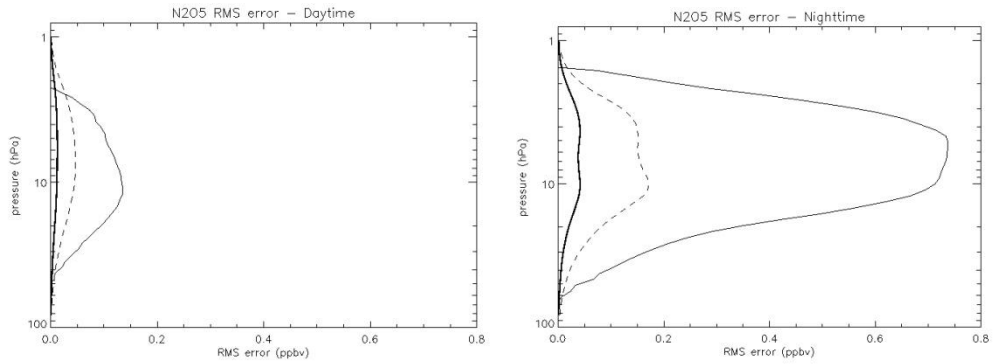

Figure 5.9.2. Estimated precision of the HIRDLS V7 Kalman filtered N_2O_5 zonal means (thick solid lines) compared with the observed and predicted precision of original L2 profile data (dashed lines and thin solid lines).

Accuracy

In order to arrive at an estimate of absolute bias, the HIRDLS Kalman filtered N_2O_5 zonal means have been compared to independent MIPAS and ACE-FTS datasets. To account for the diurnal cycle of N_2O_5 and the different local observation times of HIRDLS and the validating instruments, a photochemical correction is introduced.

N_2O_5 is in photochemical equilibrium with NO and NO_2, featuring a smooth VMR profile with minimum (maximum) concentrations before sunrise (after sunset) and a broad peak at nighttime between 3 and 30 hPa (25 to 40 km) as shown in Figs. 5.9.3 and 5.9.4. The

photochemical model correction is effected through the ratio of modeled N_2O_5 profiles evaluated at the appropriate latitude (*lat*) and corresponding observation times (*LST, LST_0*), as already introduced in section 5.8.

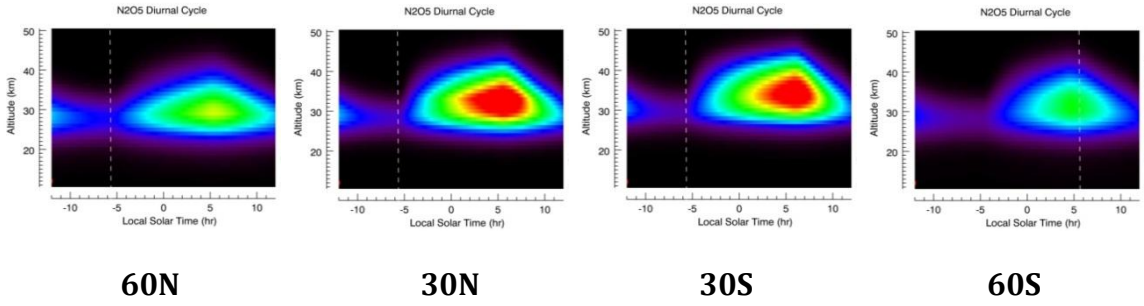

Figure 5.9.3. Diurnal variation of N_2O_5 (Equinox, March 21st 2005) from ACE photochemical box model

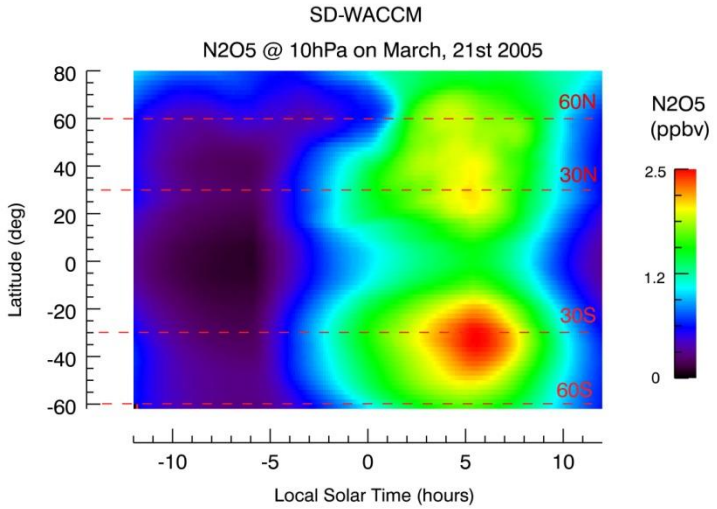

Figure 5.9.4. N2O5 at 10 hPa as a function of local solar time and latitude, showing diurnal variations. Calculated values are from the SD-WACCM model for 10 hPa, the pressure level at the height of peak daytime VMP, 10 hPa.

Validation datasets

For general information on the MIPAS and ACE-FTS instruments, please see section 5.8 in this document. Spectroscopic measurements of N_2O_5 from space are difficult due to the presence of interfering species and aerosol in the bands that are typically used for retrievals. The altitude range of the reference ACE-FTS N_2O_5 profiles (Version 2.2) is 15 to 40 km and their vertical resolution 3-4 km, with a reported single profile precision of 5-15%. The reference MIPAS N_2O_5 profiles have a vertical resolution of about 4-6 km between 30 and 40 km altitude (6-8 km elsewhere) and a reported precision of 5-35% between 20 and 40 km.

Although the agreement between the ACE-FTS and the time-shifted MIPAS N_2O_5 profiles has been evaluated already in Wolff, [2008], our own quality figures using the latest MIPAS N_2O_5 release (Version IMK-IAA Version 4O) reveal that the agreement between MIPAS and sunrise ACE-FTS N_2O_5 zonal means lies within 20% over the northern (>30N) and southern (<30S) latitudes over the 4-60 hPa pressure range (20 to 40 km), and roughly within 30% over the tropical regions for pressures between 3-40 hPa. The sunset (SS) and sunrise (SR) ACE-FTS N_2O_5 profiles are in consistent agreement from 4 to 60 hPa over the northern latitudes, but sunset profiles are biased low by 30-50% relative to MIPAS at all other latitudes.

Validation period and error statistics

The algorithm for Kapton contribution removal performs independent up and down-scan corrections to the HIRDLS radiances and the retrieval quality may differ substantially between these modes. Also, because of the variable nature of the background emission from the Kapton obstruction, the quality of the retrieved gas profiles varies across the duration of the mission. A preliminary comparison between the resulting upscan and downscan modes against the references available (mostly MIPAS and SD-WACCM) provides a qualitative measure of their goodness across the mission and the grounds for a selection of the periods when the data quality appears to be best, which we define as the validation periods. For N_2O_5, the best agreement to reference across the mission appears to arise from a mixture of upscan and downscan modes, as detailed in the Table 5.9.1 below. The selected N_2O_5 zonal mean cross-sections are displayed in Fig. 5.9.5 for day and night products at representative peak VMR pressure levels for the entire duration of the mission. The corresponding MIPAS (photo-corrected to HIRDLS observation times using the WACCM model) and SD-WACCM (using MERRA dynamics) N_2O_5 zonal mean cross-sections are also displayed for reference.

Table 5.9.1: Selection of HIRDLS V7 upscan/downscan mixture that provides best agreement to the available references

DATES	Selected MODE
From BoM to Jun 1st 2005	Downscans
From Jun 1st 2005 to Sep 21st 2005	Upscans
From Sep 21st 2005 to Dec 1st 2006	Downscans
From Dec 1st 2006 to Mar 19th 2007	Upscans
From Mar 19th 2007 to Dec 3rd 2007	Downscans
From Dec 3rd 2007 to EoM	Combined up/down

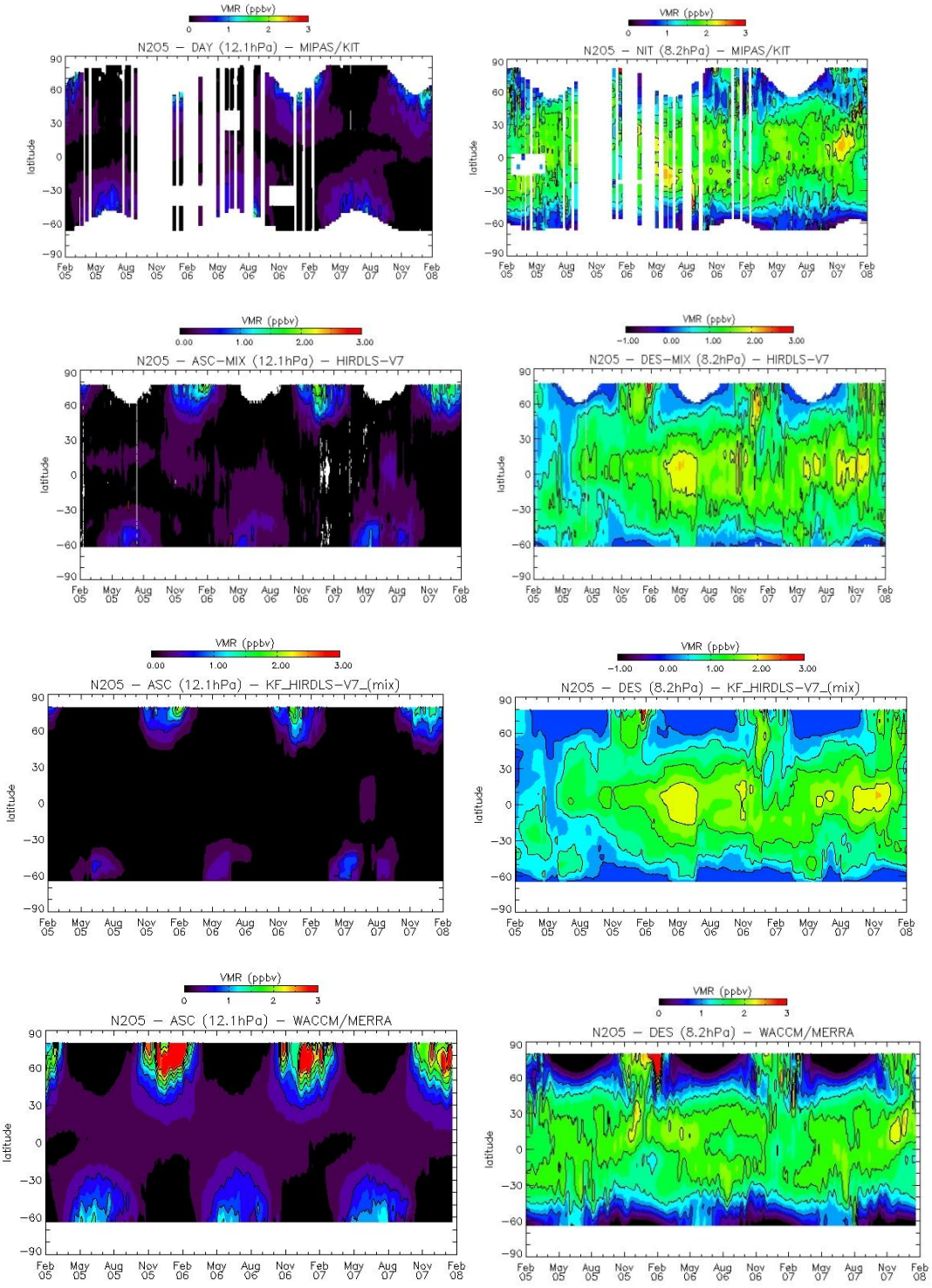

Figure 5.9.5. N_2O_5 zonal mean cross-section for ascending-day (left column) and descending-night (right column) segments at representative peak VMR levels across the HIRDLS mission. The MIPAS data has been photo-corrected to HIRDLS observation times. For completeness, the HIRDLS raw (L2) and Kalman filtered (L3) zonal means are displayed (a mixture of up-scan and down-scan modes). On the HIRDLS panels, dates excluded from validation are shaded white.

Based on a preliminary qualitative comparison against our references, we may conclude that the **validation period** for HIRDLS N_2O_5 spans the entire HIRDLS record excluding:

1) Dates prior to Jun 1st 2005

2) Dates between Jun 1st and Aug 31st 2006

3) Dates between Dec 24th 2006 and Mar 18th 2007

4) Dates between Apr 1st and Aug 31st 2007

In general, the retrieval quality of daytime and nighttime N_2O_5 profiles is not as good as that of NO_2. The HIRDLS N_2O_5 profiles display a morphology that is similar to that given by the references, but HIRDLS magnitudes are persistently lower, particularly in the extra-tropics. On the other hand, the nighttime tropical peaks appear excessively strong.

A sample comparison between the N_2O_5 zonal means from HIRDLS, MIPAS and the SD-WACCM model during the validation period is shown in figures 5.9.6a-c.

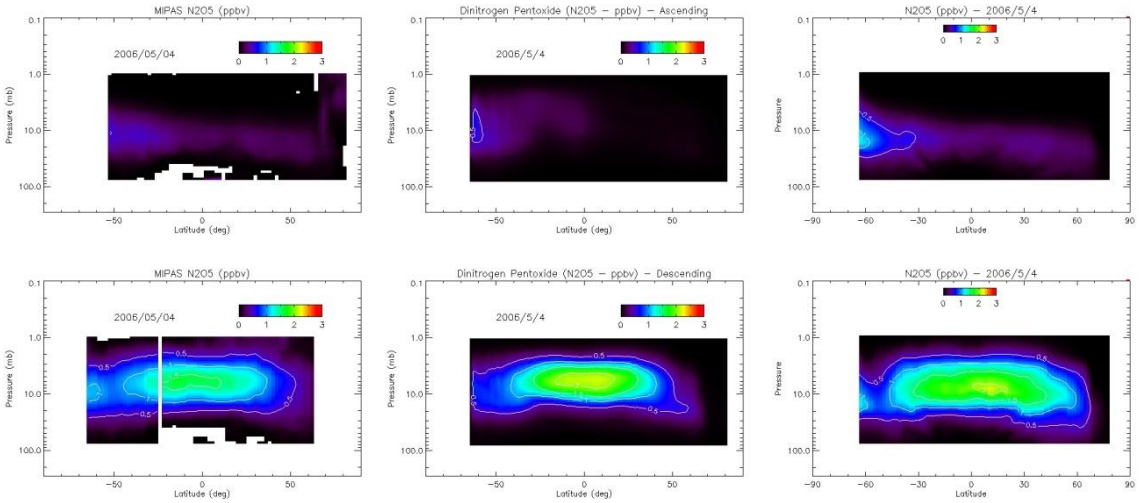

Figure 5.9.6a. Sample N_2O_5 zonal means on May 4th 2006 for daytime (top) and nighttime (bottom) from MIPAS (left), HIRDLS (center) and SD-WACCM (right) – time corrected to HIRDLS observation time.

The systematic error analysis that follows is based on the comparison of HIRDLS with MIPAS and ACE-FTS zonal mean observations time-corrected to HIRDLS measurement times and collected over the validation period defined above The collocation consists of simple latitude matching, with MIPAS and ACE-FTS each having about 14 profiles per latitude bin. The reference profiles have been linearly interpolated to the HIRDLS altitude

grid, without averaging kernel smoothing. The entire collocated set has been split into three latitudinal groups, defined as northern latitudes (30 to 80N), tropics (30S to 30N) and southern latitudes (64S to 30S). For each latitudinal group, Figures 5.9.7-10 contain:

Top panel: The time-averaged VMR profiles of the collocated HIRDLS and validating zonal means, along with their standard deviations and the number of collocated matches.

Middle panel: The time-averaged profile of differences between HIRDLS and the validating instrument, along with the standard deviation.

Bottom panel: The time-averaged profile of relative differences between HIRDLS and the validating instrument, along with the standard deviation.

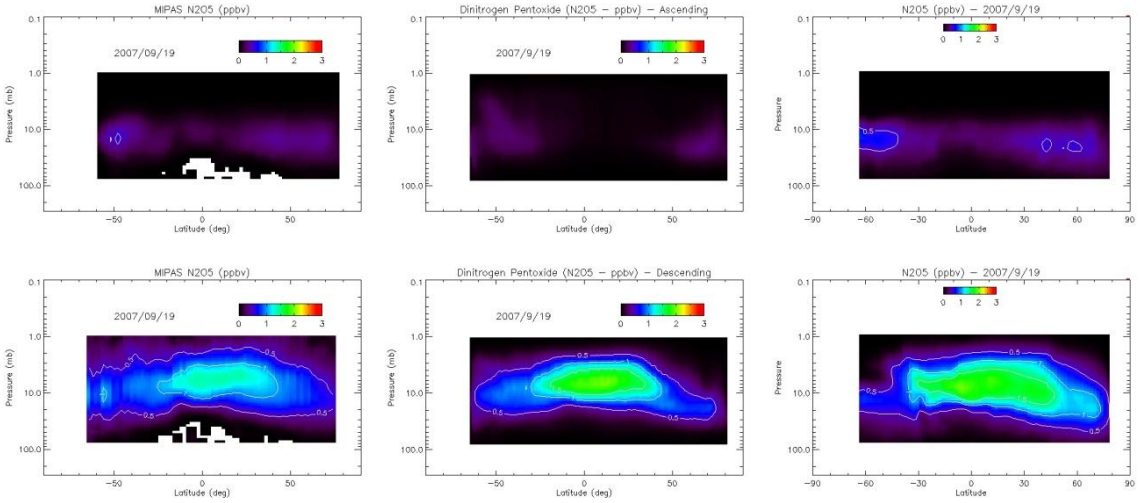

Figure 5.9.6b. Sample N_2O_5 zonal means on Sep 19th 2007 for daytime (top) and nighttime (bottom) from MIPAS (left), HIRDLS (center) and SD-WACCM (right) – time corrected to HIRDLS observation time.

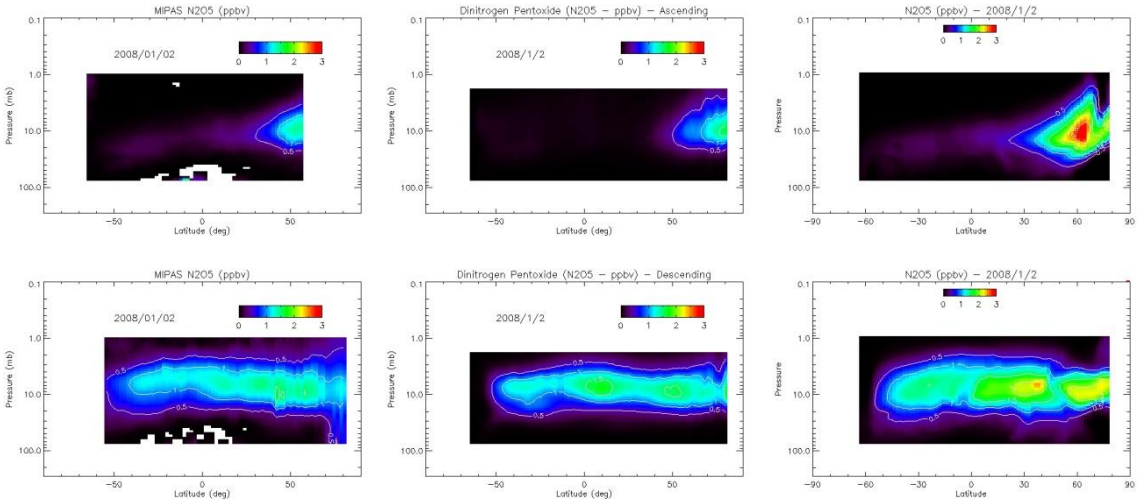

Figure 5.9.6c. Sample N_2O_5 zonal means on Jan 1st 2008 for daytime (top) and nighttime (bottom) from MIPAS (left), HIRDLS (center) and SD-WACCM (right) – time corrected to HIRDLS observation time.

Also, each panel is encased in a dashed square that delineates the pressure range over which the confidence limits of the validation reference are well known, following the validation literature. A summary of the systematic error scores is included in Tables 5.9.2 and 5.9.3.

Table 5.9.2: Systematic error estimates: Daytime N_2O_5 mean {min to max} relative differences over the indicated pressure range ([5.1-60 hPa] over northern and southern latitudes, [5.1-40 hPa] in the tropics)

	HIRDLS vs MIPAS	HIRDLS vs ACE (SR)
Northern latitudes	**-90% {-102 to -72%}**	**-108% {-140 to 4%}**
Tropics	**-56% {-114 to 80%}**	**-88% {-150 to 96%}**
Southern latitudes	**-51% {-77 to 14%}**	**-91% {-114 to 18%}**

Table 5.9.3: Systematic error estimates: Nighttime N_2O_5 mean {min to max} relative differences over the indicated pressure range ([5.1-60 hPa] over northern and southern latitudes, [5.1-40 hPa] in the tropics)

	HIRDLS vs MIPAS	HIRDLS vs ACE (SR)
Northern latitudes	**-31% {-87 to -7%}**	**-53% {-79 to -41%}**
Tropics	**-30% {-40 to 0%}**	**-59% {-90 to -17%}**
Southern latitudes	**-38% {-94 to -14%}**	**-63% {-118 to -37%}**

The quality scores shown in these tables are unambiguous at pointing that HIRDLS N_2O_5 profiles are biased low relative to the references by about 30% according to MIPAS or 50% according to ACE-FTS during nighttime. However, the HIRDLS N_2O_5 zonal mean morphologies in V7 are in much better agreement with the available references than previously in V6, including peak VMR locations, vertical profile shapes, and latitudinal and temporal variability, making this product suitable for continued and improved correction efforts. Because of a much higher SNR, the nighttime HIRDLS N_2O_5 profiles are of much better quality than daytime profiles.

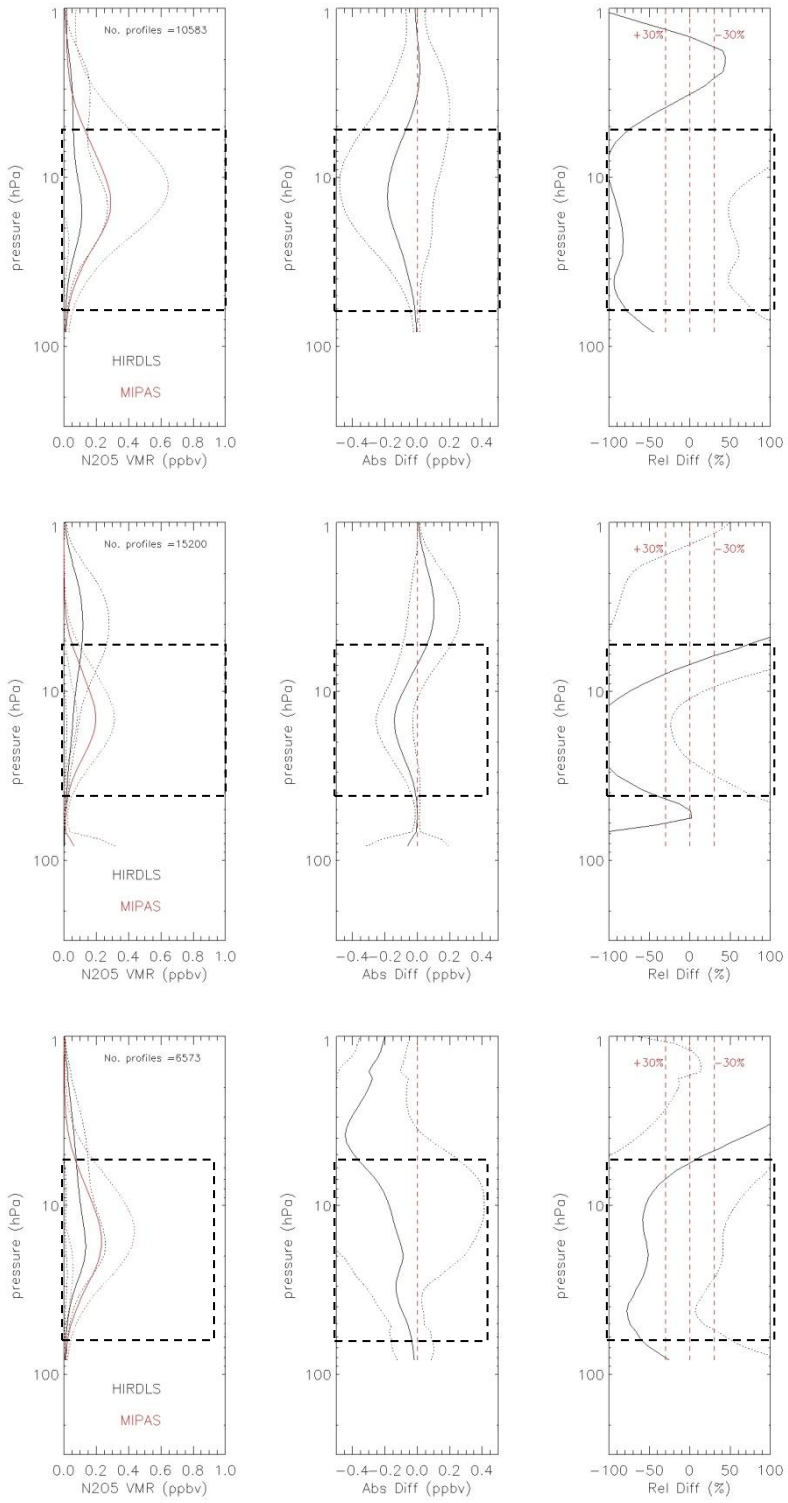

Figure 5.9.7. Systematic errors for daytime HIRDLS vs time corrected MIPAS N_2O_5 zonal means. Left: mean profiles; Mid: absolute differences; Right: relative differences.

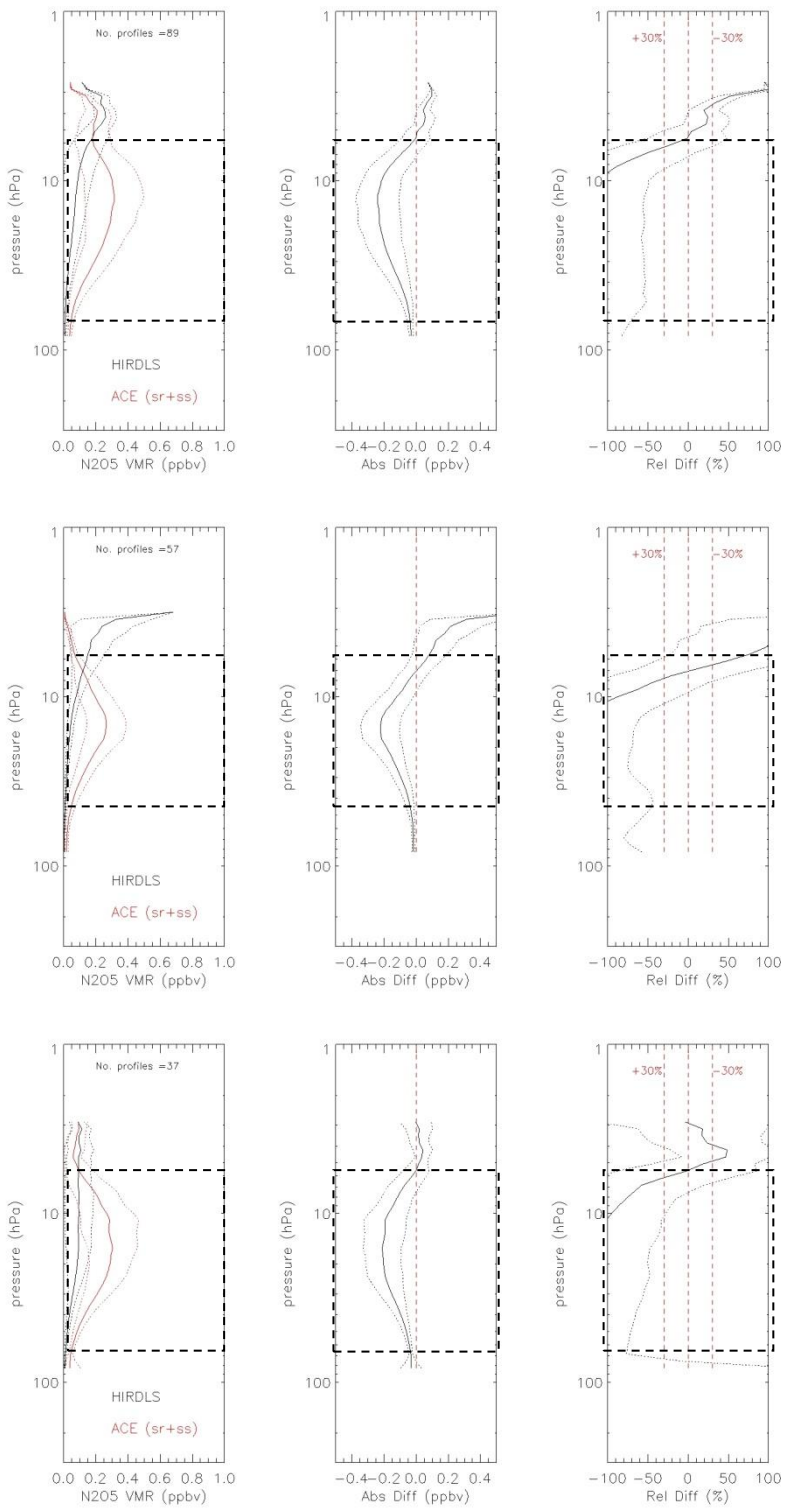

Figure 5.9.8. Systematic errors for daytime HIRDLS vs time correctedACE-FTS N_2O_5 zonal means. Left: mean profiles; Mid: absolute differences; Right: relative differences.

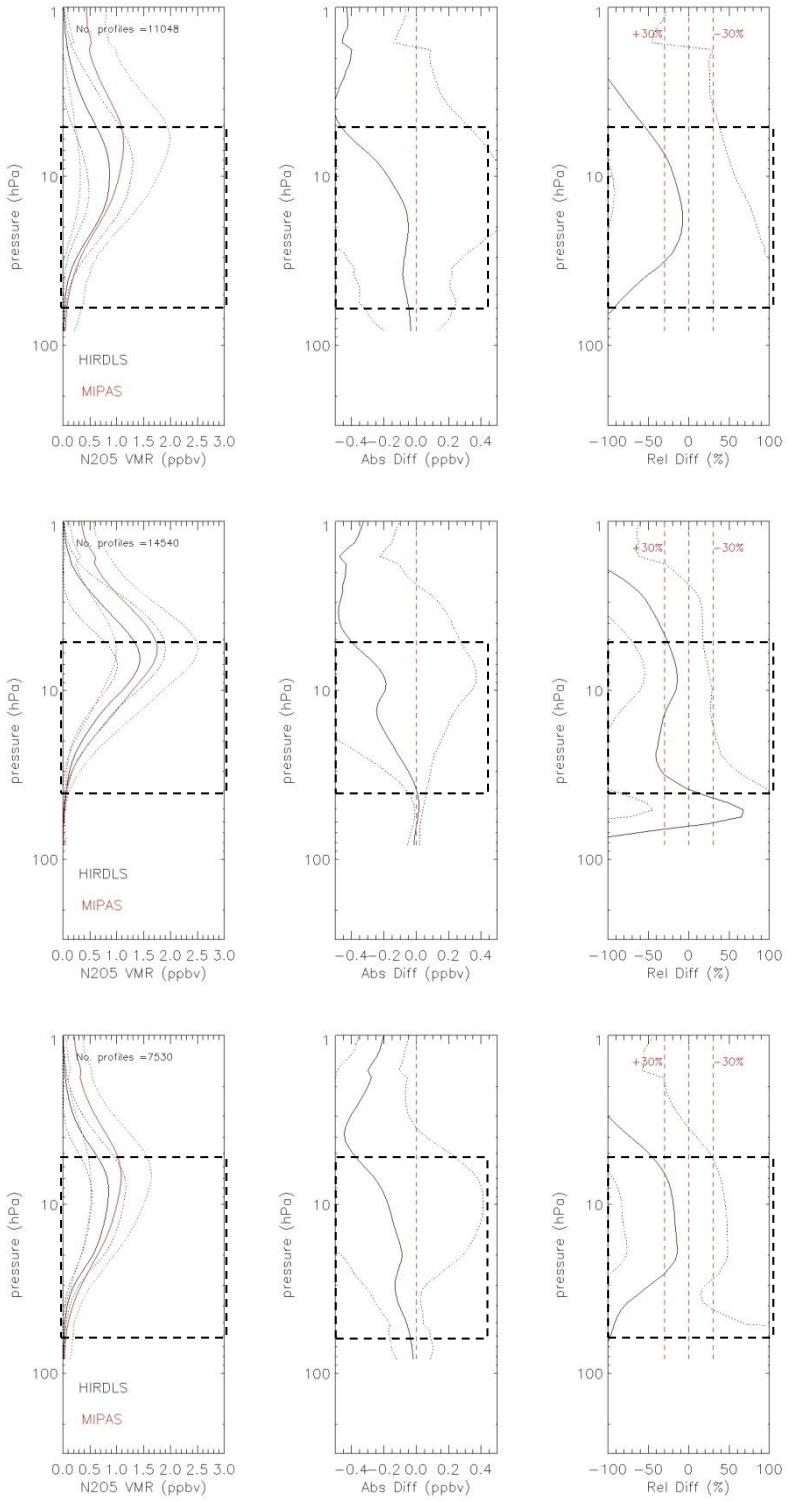

Figure 5.9.9. Systematic errors for nighttime HIRDLS vs time corrected MIPAS N_2O_5 zonal means. Left: mean profiles; Mid: absolute differences; Right: relative differences.

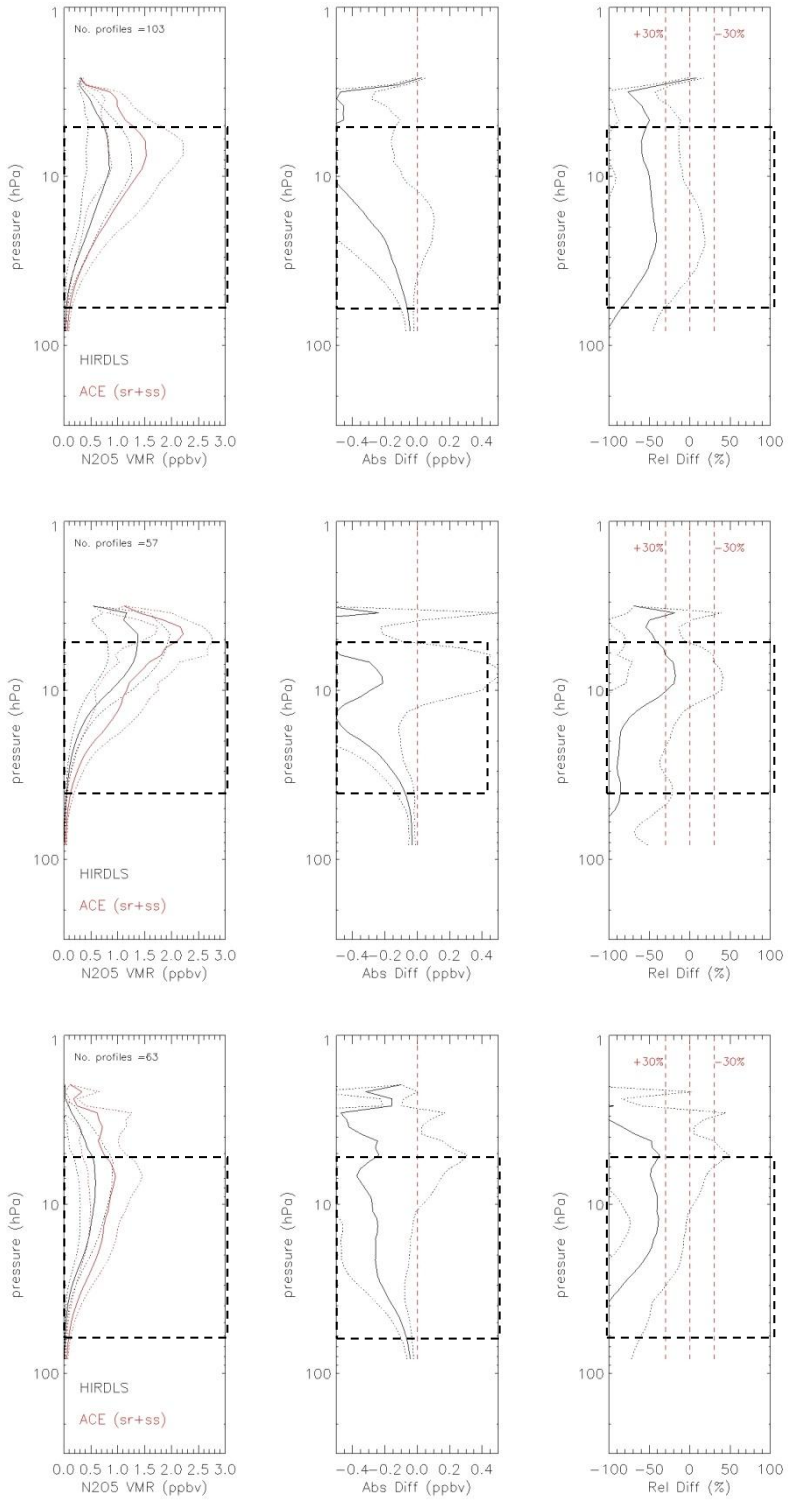

Figure 5.9.10. Systematic errors for nighttime HIRDLS vs time corrected ACE-FTS N_2O_5 zonal means. Left: mean profiles; Mid: absolute differences; Right: relative differences.

Conclusion

The quality scores shown in these tables are unambiguous at pointing that HIRDLS N_2O_5 profiles are biased low relative to the references by about 30% according to MIPAS or 50% according to ACE-FTS during nighttime. However, the HIRDLS N_2O_5 zonal mean morphologies in V7 are in much better agreement with the available references than previously in V6, including peak VMR locations, vertical profile shapes, and latitudinal and temporal variability, making this product suitable for continued and improved correction efforts. Because of a much higher SNR, the nighttime HIRDLS N_2O_5 profiles are of much better quality than daytime profiles.

5.10 $ClONO_2$

Species:	Chlorine Nitrate ($ClONO_2$)
Data Field Name:	ClONO2
Useful Range:	100 to 1.0 hPa
Screening criteria:	See definition of the validation period
Vertical Resolution:	1.5 km
Prepared by:	Maria Belmonte Rivas
Contact:	Lesley Smith
Email:	lsmith@ucar.edu
Validation paper:	N/A

General Comments

The HIRDLS $ClONO_2$ profiles come in two flavors: raw L2 data and Kalman filtered products. In general, we recommend using the latter because of their superior noise properties, although the study of phenomena with time scales shorter than 5 days may warrant the use of the L2 data. Because of the diurnally varying nature of $ClONO_2$, this HIRDLS product has been partitioned into ascending (mostly day) and descending (mostly night) orbital segments. The local solar time (LST) of the HIRDLS $ClONO_2$ product is a function of latitude, as already shown Fig. 5.8.3.

Resolution

The vertical resolution of the HIRDLS $ClONO_2$ profiles is approximately 1.5 km at peak VMR levels, as determined from the full-width at half maximum of the averaging kernels shown in figure 5.10.1, gradually decreasing to 3-4 km as the gas mixing ratio approaches zero at the upper and lower ends of the gas profile.

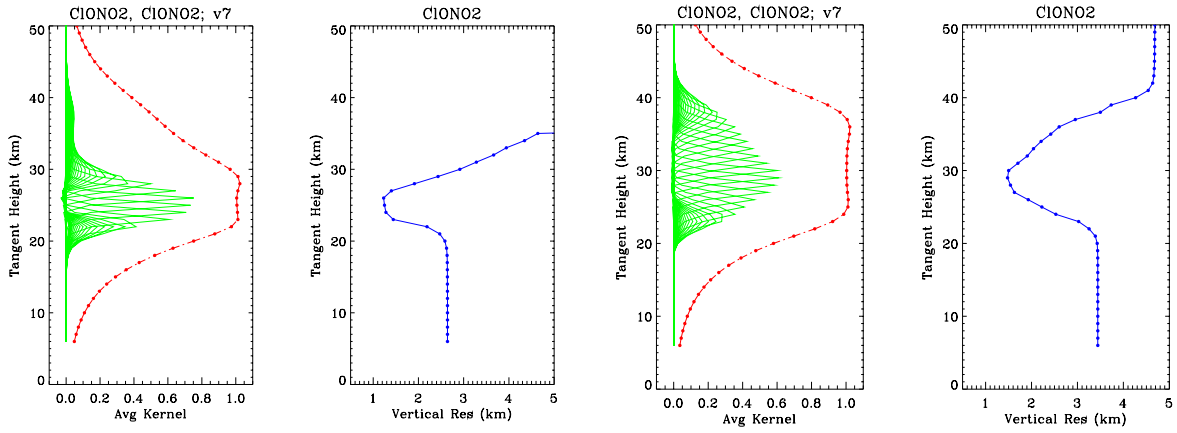

Figure 5.10.1. Averaging kernels (green lines) and vertical resolution (blue curves) as a function of altitude for daytime (left) and nighttime (right) HIRDLS $ClONO_2$ profiles.

The red line in the left panel of each pair indicates the fraction of information that comes from the HIRDLS measurements; values close to unity mean that there is negligible influence from the *a priori*. The daytime (nighttime) averaging kernels were calculated for 15 January 2007 at 45°N (3°N) with a cloud top altitude of 8 km: any latitudinal variations should be small over regions with large signal to noise ratio (SNR).

Precision

The precision of the HIRDLS Kalman filtered $ClONO_2$ zonal mean is displayed in Figure 5.10.2 along with the predicted and observed uncertainties of the L2 raw profile data. The observed uncertainty is derived from the dispersion of L2 data about the Kalman filtered zonal means. The ratio of raw profile to zonal mean precision is commensurate with the square root of the number of profiles *N* assimilated by the Kalman filter per latitude bin per day (N~17 using 1 degree bins). The precision of the Kalman filtered $ClONO_2$ zonal means is ~0.04 ppbv (5-10%) for the daytime and nighttime products. The observed precision of the raw L2 profiles is about 0.15 ppbv, or about 15-30%.

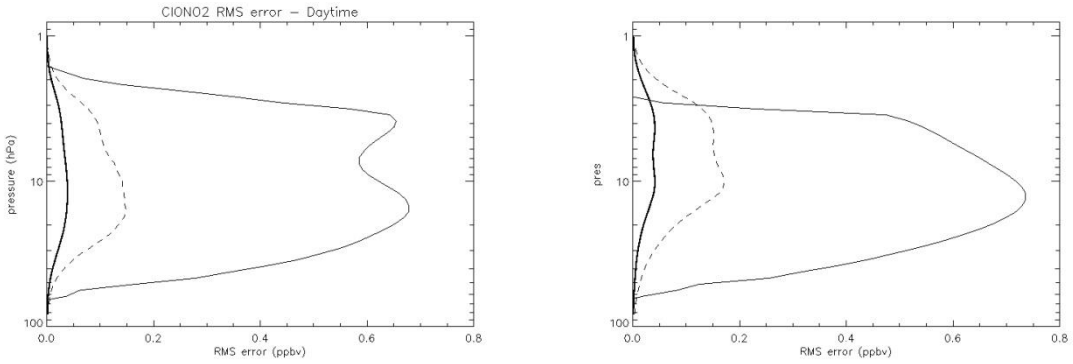

Figure 5.10.2. Estimated precision of the HIRDLS V7 Kalman filtered $ClONO_2$ zonal means (thick solid lines) compared with the observed and predicted precision of original L2 profile data (dashed lines and thin solid lines).

Accuracy

In order to arrive at an estimate of absolute bias, the HIRDLS $ClONO_2$ profiles have been compared to independent MIPAS and ACE-FTS datasets. To account for the diurnal cycle of $ClONO_2$ and the different local observation times of HIRDLS and the validating instruments, a photochemical correction is introduced.

$ClONO_2$ is a major temporary reservoir gas of chlorine in the stratosphere, formed at night from the reaction of ClO with NO_2 and destroyed after sunrise via photolysis and heterogeneous reactions on cold liquid sulfate aerosols, nitric acid trihydrates (NATs) and polar stratospheric clouds (PSCs). It features a smooth VMR profile with maximum concentrations before sunrise and a broad peak at nighttime between 5 and 30 hPa (25 to 35 km) as shown in Figs. 5.10.3 and 5.10.4. The photochemical model correction is effected through the ratio of modeled $ClONO_2$ profiles evaluated at the appropriate latitude (*lat*) and corresponding observation times (*LST, LST$_0$*), as already introduced in section 5.8.

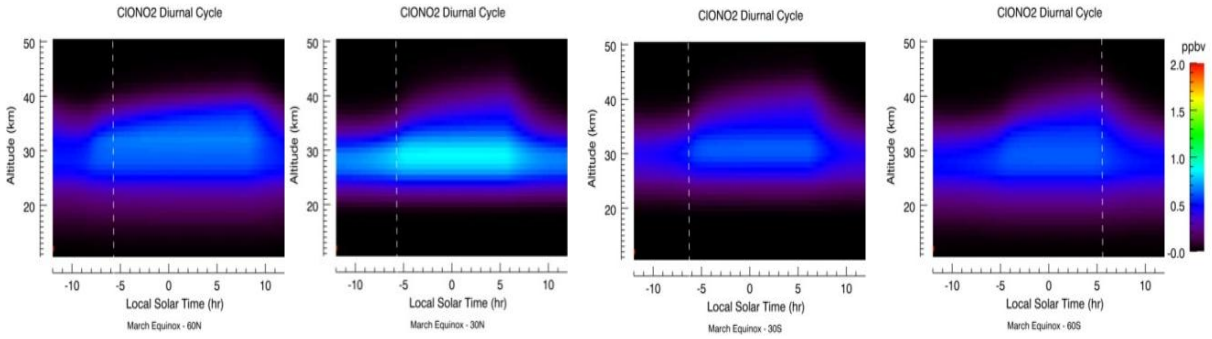

Figure 5.10.3. Diurnal variation of $ClONO_2$ (Equinox, March 21st 2005) from the ACE photochemical box model

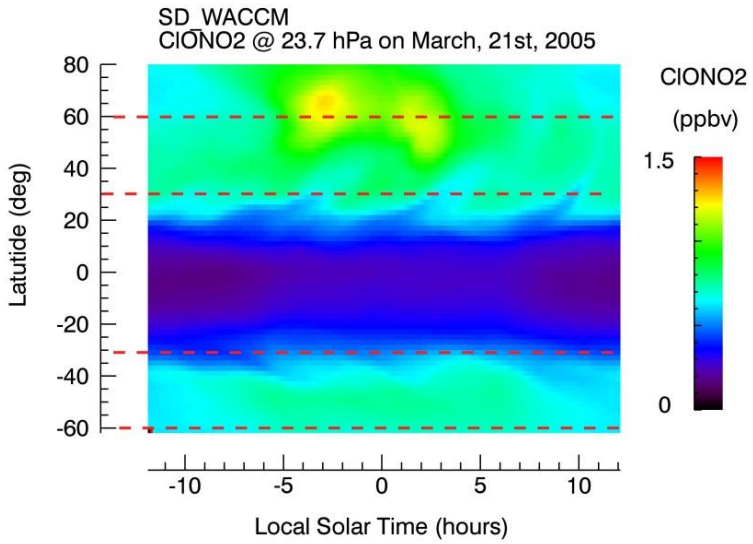

Figure 5.10.4. Diurnal variation of $ClONO_2$ as a function of latitude (Equinox, March 21st 2005) from SD-WACCM (pressure level at peak VMR height for daytime or 23.7 hPa)

Validation datasets

For general information on the MIPAS and ACE-FTS instruments, please see section 5.8 in this document. The altitude range of the reference ACE-FTS $ClONO_2$ profiles (Version 2.2) is 12 to 35 km and their vertical resolution 3-4 km, with a reported single profile precision of 10-20% between 20 and 35 km, and ~40% at 15 km Wolff, [2008]. The reference MIPAS $ClONO_2$ profiles (Version IMK-IAA Version 4O) have a vertical resolution of about 3-8 km between 8 and 40 km altitude and a reported precision of 5-25% between 20 and 40 km Hoepfner, [2007].

The agreement between the ACE-FTS and the time-shifted MIPAS $ClONO_2$ profiles has been evaluated in Wolff, [2008] and Hoepfner, [2007] over the time period from February through March 2004, indicating that mean relative differences lie within 20% over the pressure range from 1 to 100 hPa (15 to 35 km).

Validation period and error statistics

The algorithm for Kapton removal performs independent up and down-scan corrections to the HIRDLS radiances and the retrieval quality may differ substantially between these modes. Also, because of the variable nature of the background emission from the Kapton obstruction, the quality of the retrieved gas profiles varies across the duration of the mission. A preliminary comparison between the resulting upscan and downscan modes against the references available (mostly MIPAS and SD-WACCM) provides a qualitative measure of their goodness across the mission and the grounds for a selection of the periods when the data quality appears to be best, which we define as the validation periods. For $ClONO_2$, the best agreement to reference across the mission appears to arise from a mixture of upscan and downscan modes, as detailed in the Table 5.10.1 below. The selected $ClONO_2$ zonal mean cross-sections are displayed in Fig. 5.10.5 for day and night products at representative peak VMR pressure levels for the entire duration of the mission. The corresponding MIPAS (corrected to HIRDLS observation times using the WACCM model) and SD-WACCM (using MERRA dynamics) $ClONO_2$ zonal mean cross-sections are also displayed for reference.

Table 5.10.1: Selection of HIRDLS V7 upscan/downscan mixture that provides best agreement to the available references for Daytime $ClONO_2$

DATES	Selected Ascending (Day) MODE
From BoM to Nov 5th 2006	Upscans
From Nov 5st 2006 to Dec 25th 2006	Downscans
From Dec 25th 2006 to Aug 24th 2007	Upscans
From Aug 24th 2007 to EoM	Downscans
DATES	**Selected Descending (Night) MODE**
From BoM to Aug 13th 2005	Downscans
From Aug 13th 2005 to Nov 5th 2006	Upscans
From Nov 5th 2006 to Dec 25th 2006	Downscans
From Dec 25th 2007 to Mar 19th 2007	Upscans
From Mar 19th 2007 to May 28th 2007	Downscans
From May 28th 2007 to Sep 5th 2007	Upscans
From Sep 5th 2007 to EoM	Combined up/down

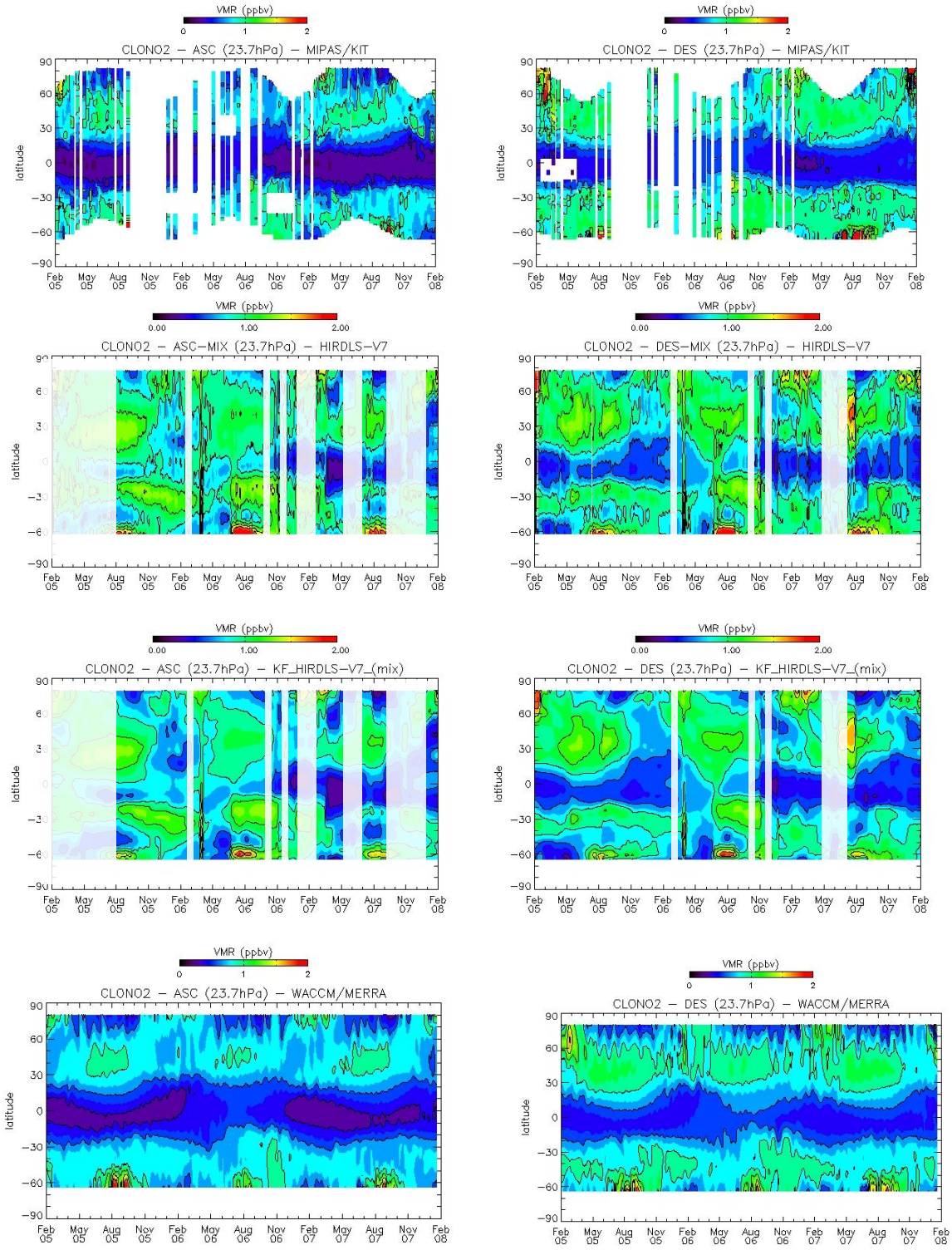

Figure 5.10.5. $ClONO_2$ zonal mean cross-section for ascending-day (left column) and descending-night (right column) segments at representative peak VMR levels across the HIRDLS mission. The MIPAS data has been photo-corrected to HIRDLS observation times. For completeness, the HIRDLS raw (L2) and Kalman filtered (L3) zonal means are displayed (a mixture of up-scan and down-scan modes). On the HIRDLS panels, dates excluded from validation are shaded white.

Based on a preliminary qualitative comparison against our references, we may conclude that the **validation period** for HIRDLS $ClONO_2$ spans the entire HIRDLS record excluding:

1) Dates between Mar 25th and Apr 8th 2006

2) Dates between Nov 1st and Nov 13th 2006

3) Dates between Dec 12th and Dec 28th 2006

4) Dates between Feb 1st and Mar 24th 2007

5) Dates between Jun 8th and Aug 1st 2007

In addition, for daytime $ClONO_2$ the **validation period** should exclude:

6) Dates prior to Aug 13th 2005

7) Dates between Oct 15th 2007 through End of Mission (EoM)

For nighttime $ClONO_2$ the **validation period** should exclude:

8) Dates between Oct 15th and Nov 15th 2007

A sample comparison between the $ClONO_2$ zonal means from HIRDLS, MIPAS and the SD-WACCM model during the validation period is shown in figures 5.10.6a-c.

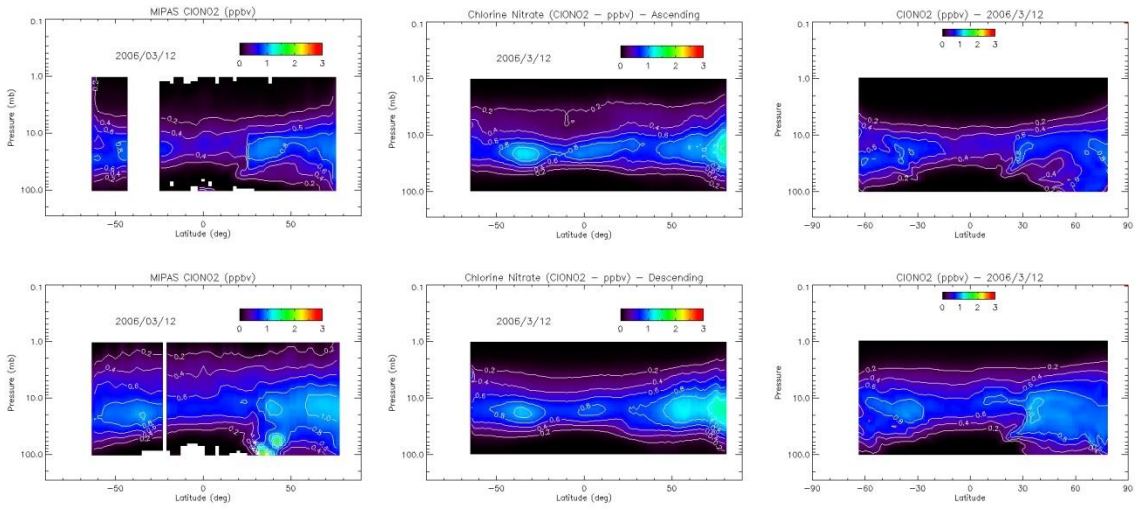

Figure 5.10.6a. Sample $ClONO_2$ zonal means on Mar 12th 2006 for daytime (top) and nighttime (bottom) from MIPAS (left), HIRDLS (center) and SD-WACCM (right) – time corrected to HIRDLS observation time.

The systematic error analysis that follows is based on the comparison of HIRDLS with MIPAS and ACE-FTS zonal mean observations time-corrected to HIRDLS measurement times and collected over the validation period defined above The collocation consists of simple latitude matching, with MIPAS and ACE-FTS each having about 14 profiles per

latitude bin. The reference profiles have been linearly interpolated to the HIRDLS altitudegrid, without averaging kernel smoothing. The entire collocated set has been split into three latitudinal groups, defined as northern latitudes (30 to 80N), tropics (30S to 30N) and southern latitudes (64S to 30S).

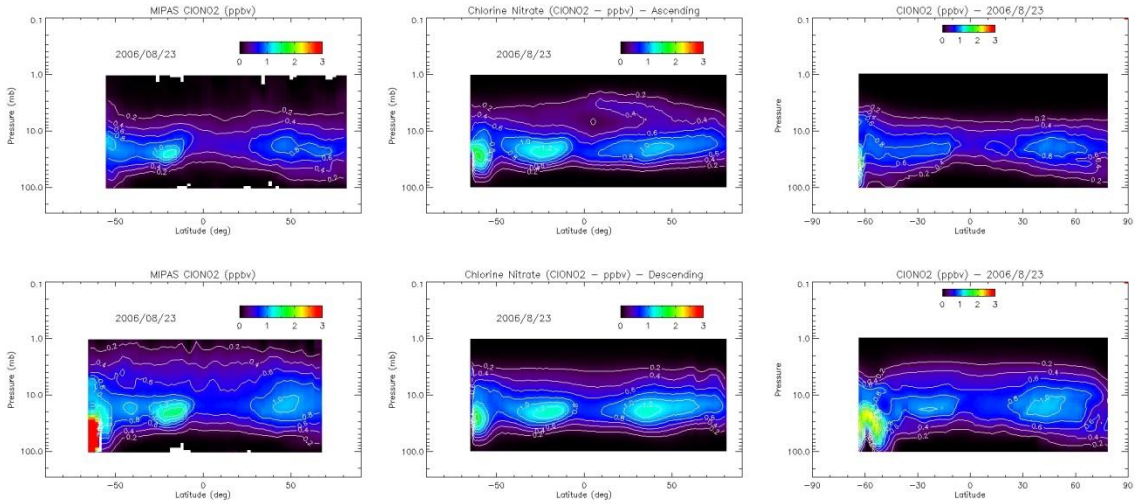

Figure 5.10.6b. Sample $ClONO_2$ zonal means on Aug 23rd 2006 for daytime (top) and nighttime (bottom) from MIPAS (left), HIRDLS (center) and SD-WACCM (right) – time corrected to HIRDLS observation time.

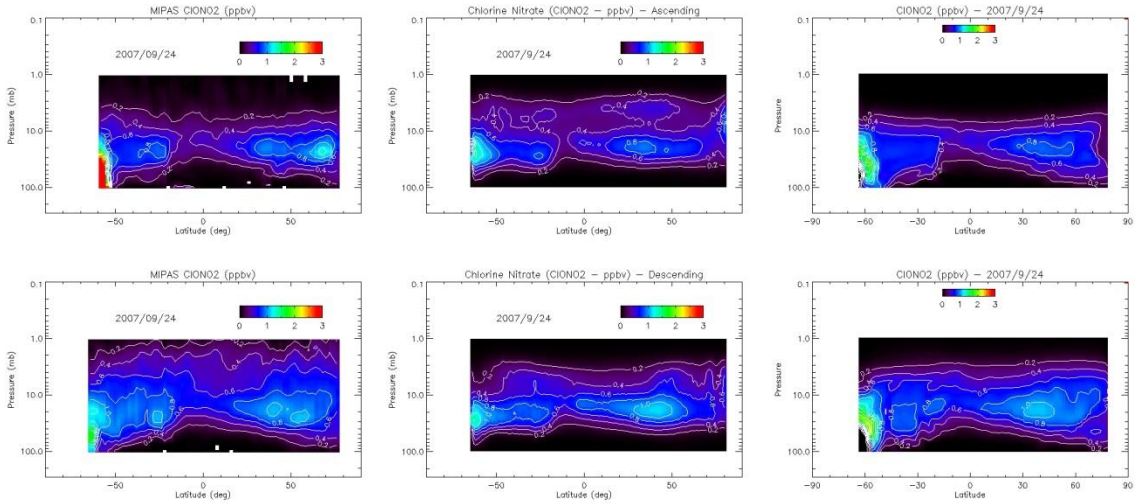

Figure 5.10.6c. Sample $ClONO_2$ zonal means on Sep 24th 2007 for daytime (top) and nighttime (bottom) from MIPAS (left), HIRDLS (center) and SD-WACCM (right) – time corrected to HIRDLS observation time.

For each latitudinal group, Figures 5.10.7-10 contain:

Top panel: The time-averaged VMR profiles of the co-located HIRDLS and validating zonal means, along with their standard deviations and the number of co-located matches.

Middle panel: The time-averaged profile of differences between HIRDLS and the validating instrument, along with the standard deviation.

Bottom panel: The time-averaged profile of relative differences between HIRDLS and the validating instrument, along with the standard deviation.

Also, each panel is encased in a dashed square that delineates the pressure range over which the confidence limits of the validation reference are well known, following the validation literature. A summary of the systematic error scores is included in Tables 5.10.2 and 5.10.3.

Table 5.10.2: Systematic error estimates: Daytime $ClONO_2$ mean {min to max} relative differences over the [5-60 hPa] pressure range

	HIRDLS vs MIPAS	HIRDLS vs ACE (SR)
Northern latitudes	**7% {-68 to 76%}**	**0% {-106 to 92%}**
Tropics	**39% {-35 to 103%}**	**37% {-38 to 72%}**
Southern latitudes	**-8% {-86 to 24%}**	**-12% {-111 to 12%}**

Table 5.10.3: Systematic error estimates: Nighttime $ClONO_2$ mean {min to max} relative differences over the [5-60 hPa] pressure range

	HIRDLS vs MIPAS	HIRDLS vs ACE (SR)
Northern latitudes	**-2% {-39 to 18%}**	**-12% {-69 to 8%}**
Tropics	**3% {-37 to 26%}**	**-2% {-63 to 26%}**
Southern latitudes	**-34% {-107 to 7%}**	**-33% {-105 to -10%}**

The quality scores shown in these tables and figures below indicate that the HIRDLS $ClONO_2$ measurement agree with the MIPAS and ACE-FTS references typically within 30% over the pressure range from 5 to 60 hPa and most locations, an agreement that is particularly satisfying in the extratropics for the daytime products. Daytime $ClONO_2$

measurements across the tropics appear to be too high, an anomaly that can be traced tothe presence of a Kapton artifact that crosses over the $ClONO_2$ peak VMR pressure level at these latitudes, and that is also responsible for excessively high daytime values between 1 and 5 hPa. The HIRDLS nighttime $ClONO_2$ measurements appear to be too low over the southern latitudes, likely caused by instabilities in the emission from the Kapton obstruction. Overall, the quality of the HIRDLS $ClONO_2$ profiles in Version 7 is variable across the mission, with peak VMR locations, vertical profile shapes, and latitudinal and temporal structures that look realistic and appear to be similar to the references.

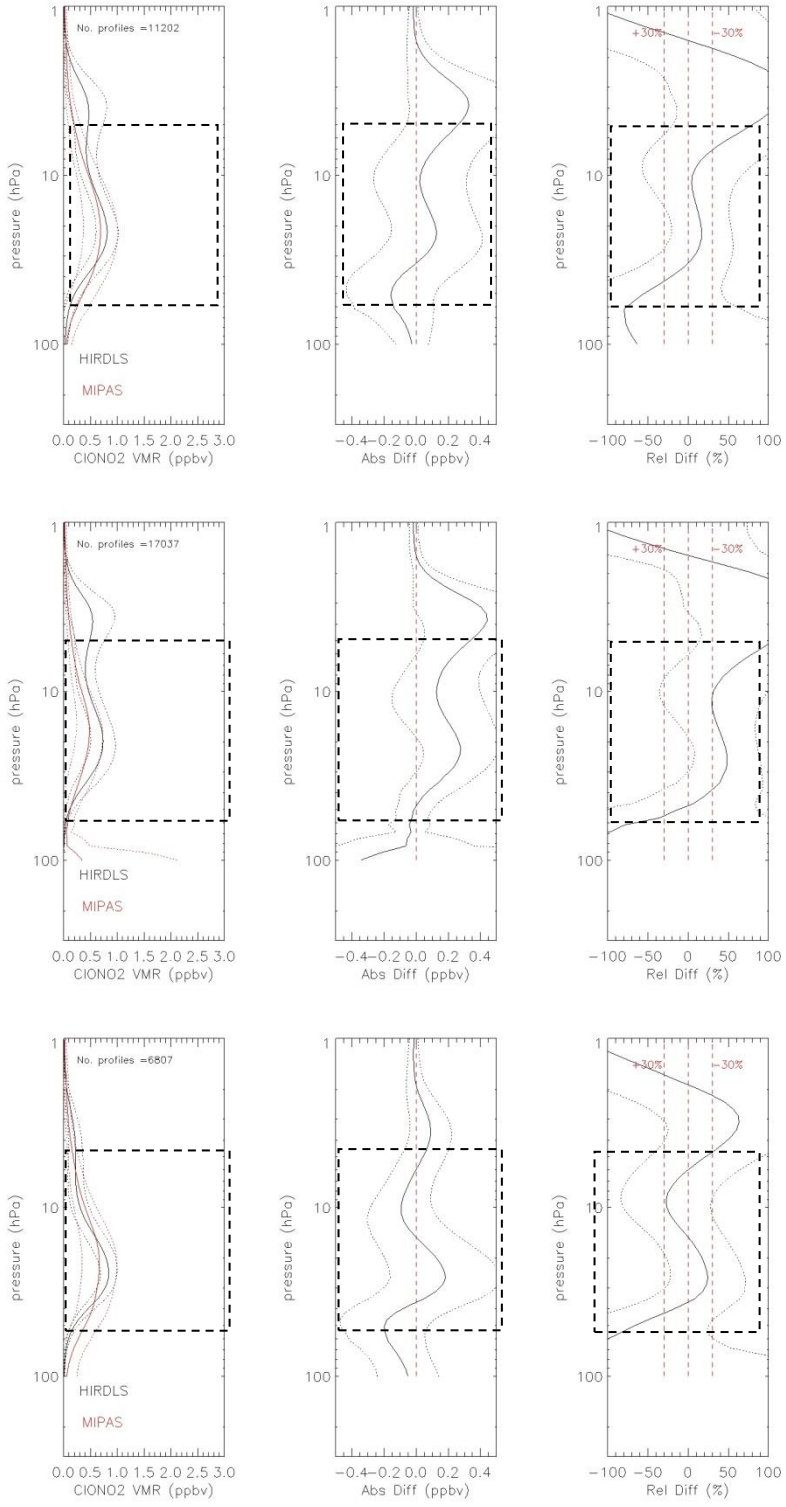

Figure 5.10.7. Systematic errors for daytime HIRDLS vs time corrected MIPAS $ClONO_2$ zonal means. Left: mean profiles; Mid: absolute differences; Right: relative differences.

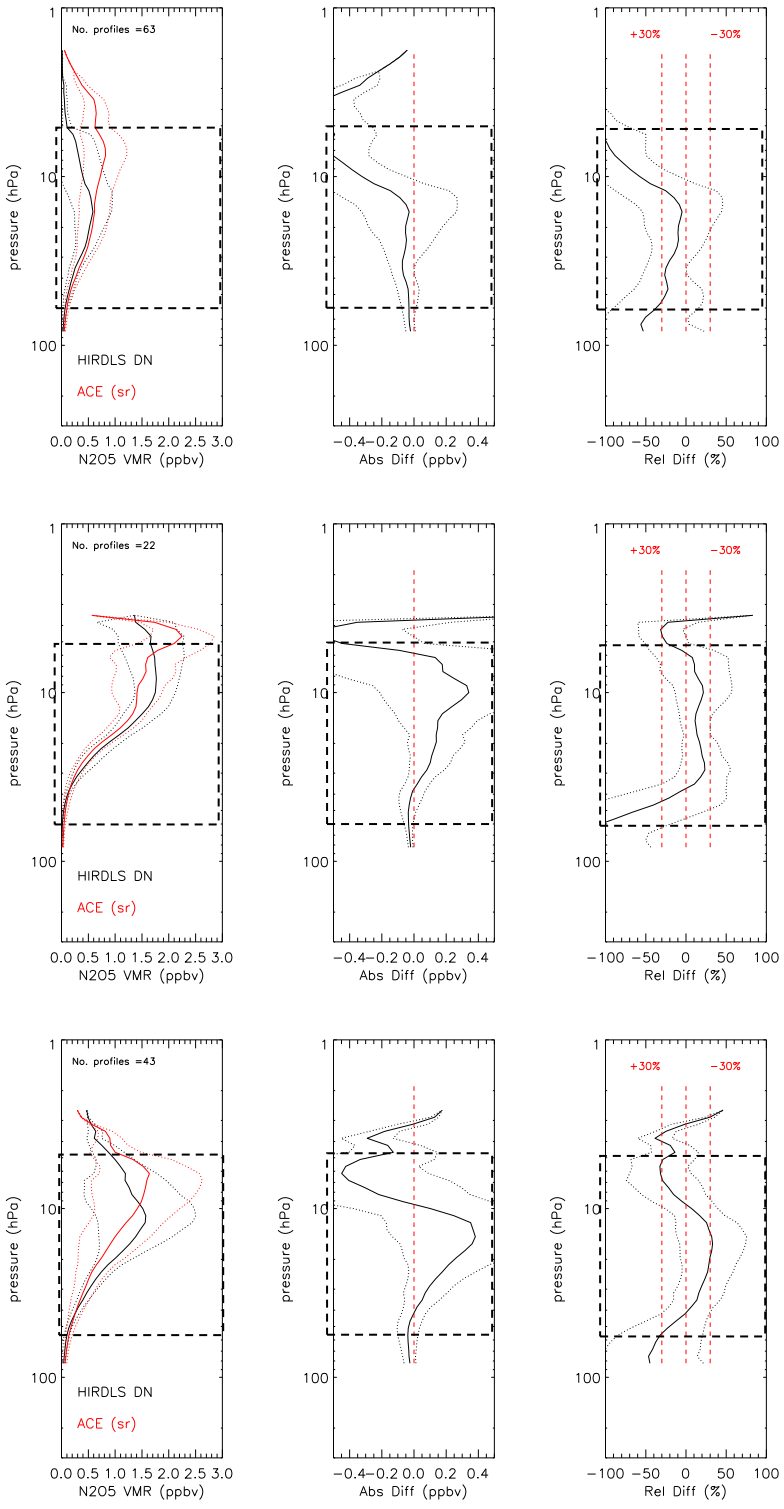

Figure 5.10.8. Systematic errors for daytime HIRDLS vs time corrected ACE-FTS $ClONO_2$ zonal means. Left: mean profiles; Mid: absolute differences; Right: relative differences.

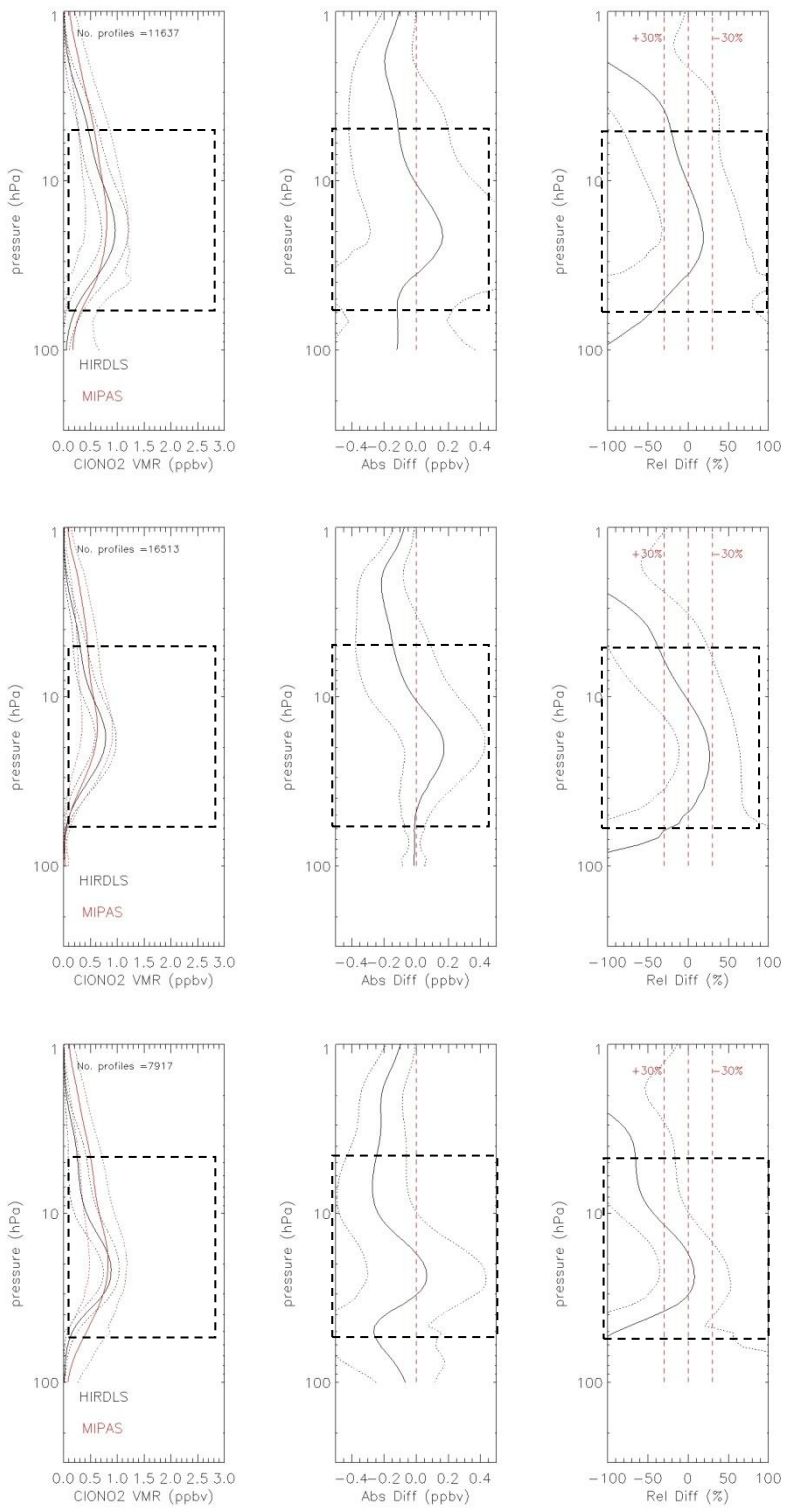

Figure 5.10.9. *Systematic errors for nighttime HIRDLS vs time corrected MIPAS* $ClONO_2$ zonal means. Left: mean profiles; Mid: absolute differences; Right: relative differences.

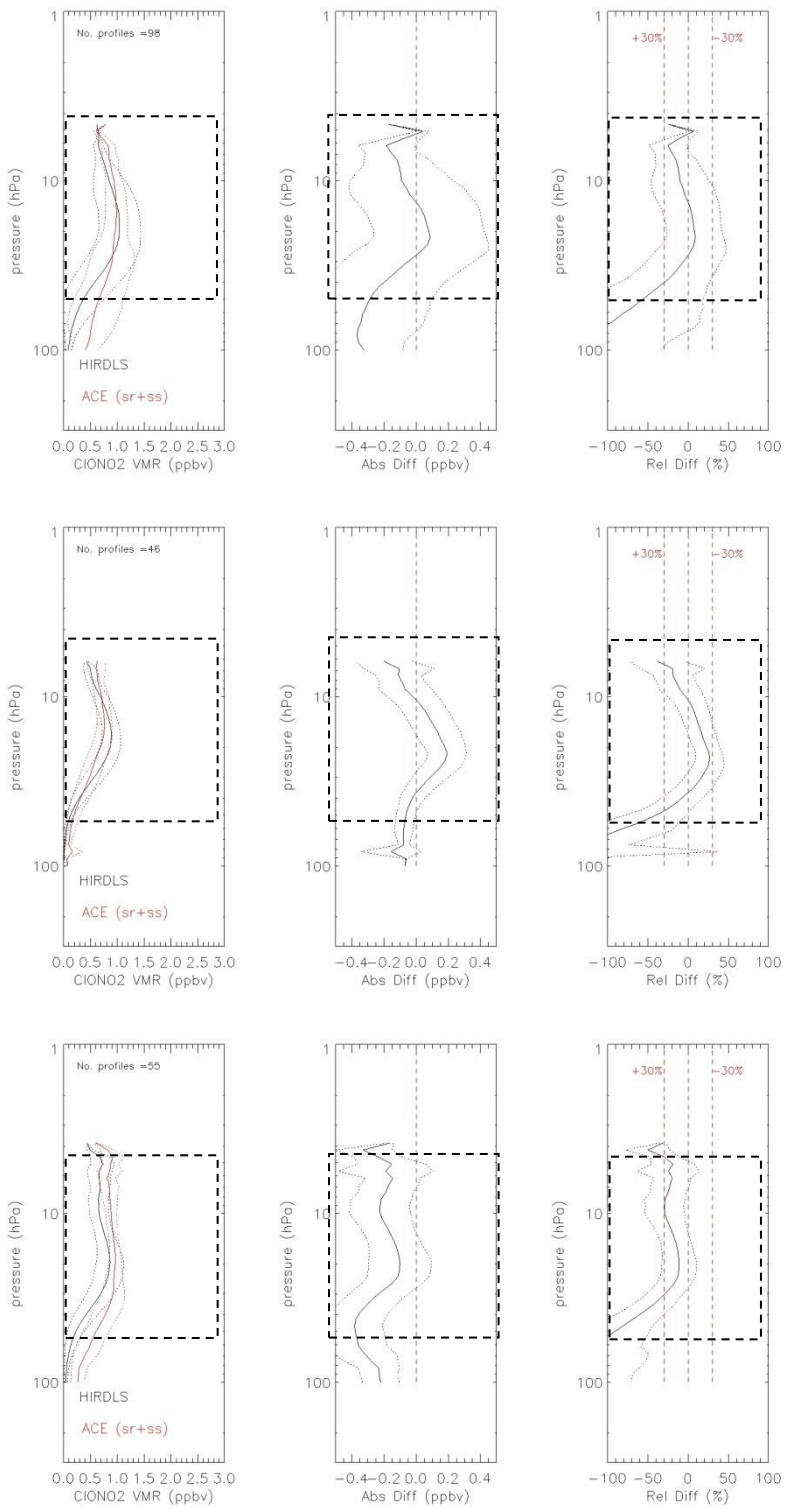

Figure 5.10.10. Systematic errors for nighttime HIRDLS vs time corrected ACE-FTS $ClONO_2$ zonal means. Left: mean profiles; Mid: absolute differences; Right: relative differences.

Conclusion

The HIRDLS $ClONO_2$ profiles have 1.5 km vertical resolution, a precision of about 15-30% (5-10% for the Kalman filtered products) and typically agree with correlative MIPAS and ACE-FTS measurements to better than 30% over a pressure range that goes from 5 to 60 hPa and most locations. The HIRDLS $ClONO_2$ zonal mean morphologies in Version 7 are in reasonable agreement with the references available, displaying correct peak VMR locations, vertical profile shapes, and latitudinal and temporal structures, making this product suitable for continued and improved correction efforts, as well as exploratory scientific studies. Caution should be used with daytime measurements over the tropics and nighttime measurements over the southern latitudes, which may be episodically subject to strong positive (day) and negative (night) biases due to instabilities in the emission of the Kapton obstruction.

5.11 Cloud Products –

Data:	Cloud Top Pressure, Cloud Flags
Data Field Names:	CloudTopPressure, 12.1MicronCloudAerosolFlag, 8.3MicronCloudAerosolFlag
Useful Range:	422-10 hPa
Screening Criteria:	Some false cloud positives are present, z > 20 km
Vertical Resolution:	1 km
Contact:	Steven Massie
Email:	massie@ucar.edu
Validation Paper:	Massie *et al*., High Resolution Dynamics Limb Sounder observations of polar stratospheric clouds and subvisible cirrus, *J. Geophys. Res*., *112*, D24S31, doi:10.1029/2007JD008788, 2007.

General Comments

HIRDLS data files contain cloud flags and cloud top pressures. Details of the determination of cloud top pressures and cloud flags are discussed in Massie et al. (2007).

Cloud flag data is contained in the "12.1MicronCloudAerosolFlag" and "8.3MicronCloudAerosolFlag" data variables. Cloud flags are stated at each pressure level when pressures correspond to altitudes between 5 and 30 km altitude. Cloud flag values are 0 (no clouds), 1 (unknown cloud type), 2 (cirrus layer), 3 (extensive Polar Stratospheric Cloud), and 4 (opaque). If the cloud flag is nonzero, then this indicates that the radiance at that pressure is measurably different from the clear sky radiance profile. Note that the total number of PSCs is equal to the number of cloud flags with values of either 1 or 3.

Comparisons of clear sky and individual radiance profiles of the various cloud types are presented in Figure 5.11.1. Note that radiance perturbations are substantial for several cloud types, since gas opacity in HIRDLS Channel 6, the 12 μm "infrared window" channel, is very low. Any cloud opacity along the HIRDLS limb-view tangent ray path produces a substantial 12 μm radiance signal.

The cloud top pressure (i.e. the 'CloudTopPressure' variable in the archived data file) is determined in the following manner. For a single day's set of radiance profiles, the clear sky radiance profile for HIRDLS channel 6 is calculated by an iterative technique for several latitude bands. For the first iteration, the average profile, its standard deviation, and associated gradients from 5 to 30 km altitude, are calculated summing over all profiles. For the second iteration, profiles are tossed out of the ensemble average (based on the fact that a cloudy radiance profile deviates from the average curve). New standard deviations and associated gradients are recalculated. The iterative process continues for five iterations.

Note that the HIRDLS focal plane has three columns of detectors. The 12 μm detector is in the middle column, while the three ozone detectors 10-12 are in the first column, and the two columns are separated in distance by ~17 km. Situations arise in which the cloud top structure differs along the 17 km horizontal distance, i.e. a cloud top in the first column can be higher than that in the middle column. Subsequent to the methodology and discussions in Massie et al. (2007), the cloud detection routines now also determine cloud tops in the tropics in the transparent ozone channel 12. The cloud top altitude is assigned to be the higher of the channel 12 and channel 6 cloud top altitudes.

Once the clear sky radiance profile is calculated, we determine the altitude level at which cloud radiance perturbations are first noted. The cloud top pressure (in hPa) is the pressure derived by the operational retrieval on an arbitrary altitude grid with 1 km vertical spacing. The cloud top pressure is determined before the temperature, mixing ratio, and extinction profiles are interpolated unto the standard output pressure grid.

There are some instances in which cloud flags falsely indicate the presence of clouds near and above 20 km altitude, especially at polar latitudes, outside of the seasons in which PSCs are expected to occur. These false identifications occur when radiances become very low in the 20 to 30 km altitude range.

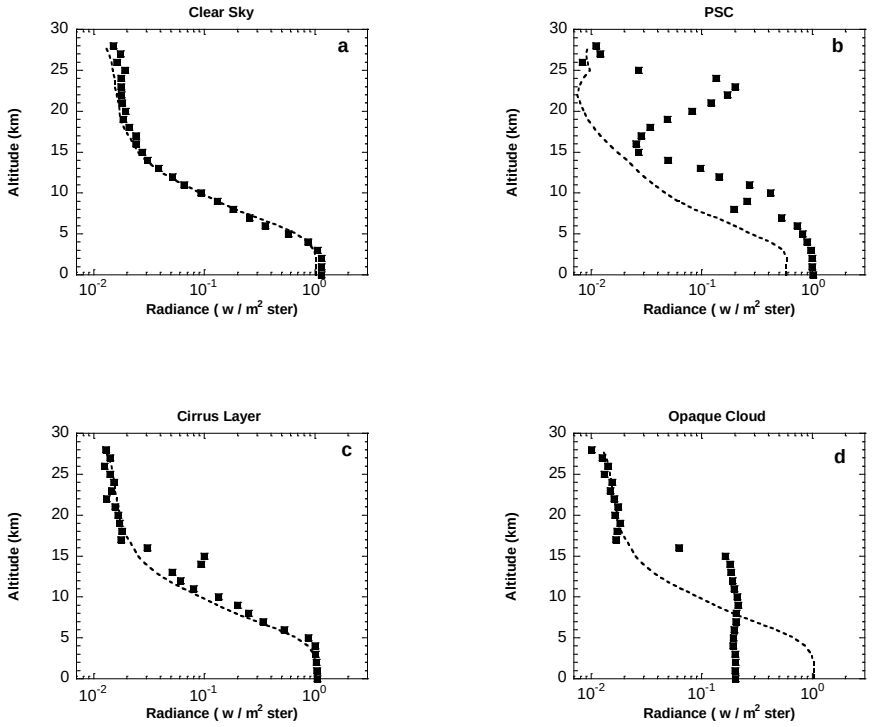

Figure 5.11.1. Four representative Channel 6 (12.1 μm) radiance (single squares) and clear sky average profiles (dotted curves) on January 27 2005, a) clear sky (15.57º N, 216.20º E), b) PSC (68.31º N, 343.41º E), c) tropical cirrus layer (4.32º N, 220.00º E), and d) opaque tropical cloud (16.79º S, 223.72º E) cases. Panels a, b, c, and d correspond to cloud flags equal to 0, 3, 2, and 4, respectively. See Massie et al., 2007.

HALOE and V7 HIRDLS time averaged cloud top statistics are presented in Figure 5.11.2. The normalized distributions of HIRDLS cloud top pressure data in 2007 and HALOE data from 1998 to 2005 in Figure 5.11.2 have correlations of 0.64 and 0.89, respectively. The large differences in the number of observations of the HIRDLS and HALOE experiments are due to the fact that HALOE was an occultation experiment, while HIRDLS made observations every 10 seconds.

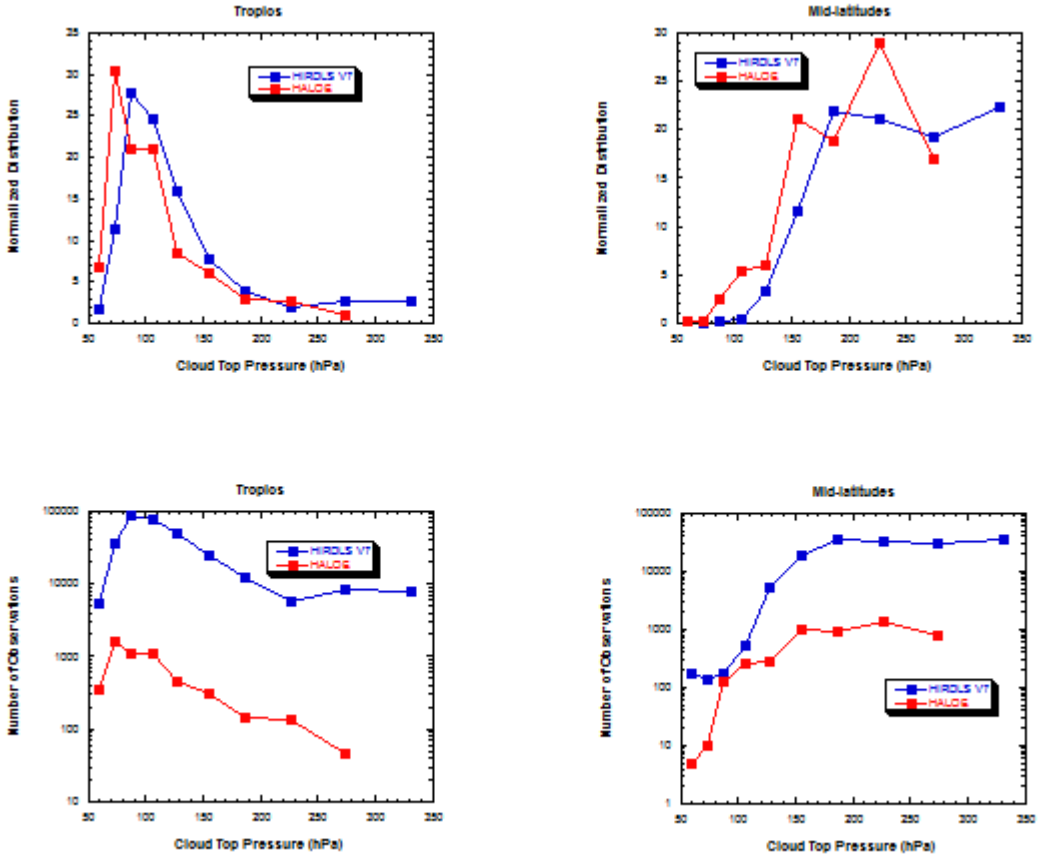

Figure 5.11.2 A comparison of V7 HIRDLS and HALOE cloud top pressure statistics for data in 2007 and HALOE data from 1998 through 2005.

Since the standard gas species retrievals terminate at the cloud top, the frequency of retrieval of gas species will decrease as pressures increase. The fraction of the time for which clouds are absent along HIRDLS limb paths in 2007 is presented in Figure 5.11.3. The latitudinal variation of the cloud free percent frequency is primarily influenced by the location of the tropopause. While the cloud free percent frequency is low at higher pressures, the number of cloud free profiles is still large at higher pressures due to the large number of profiles (~5600 per day) measured by the HIRDLS experiment.

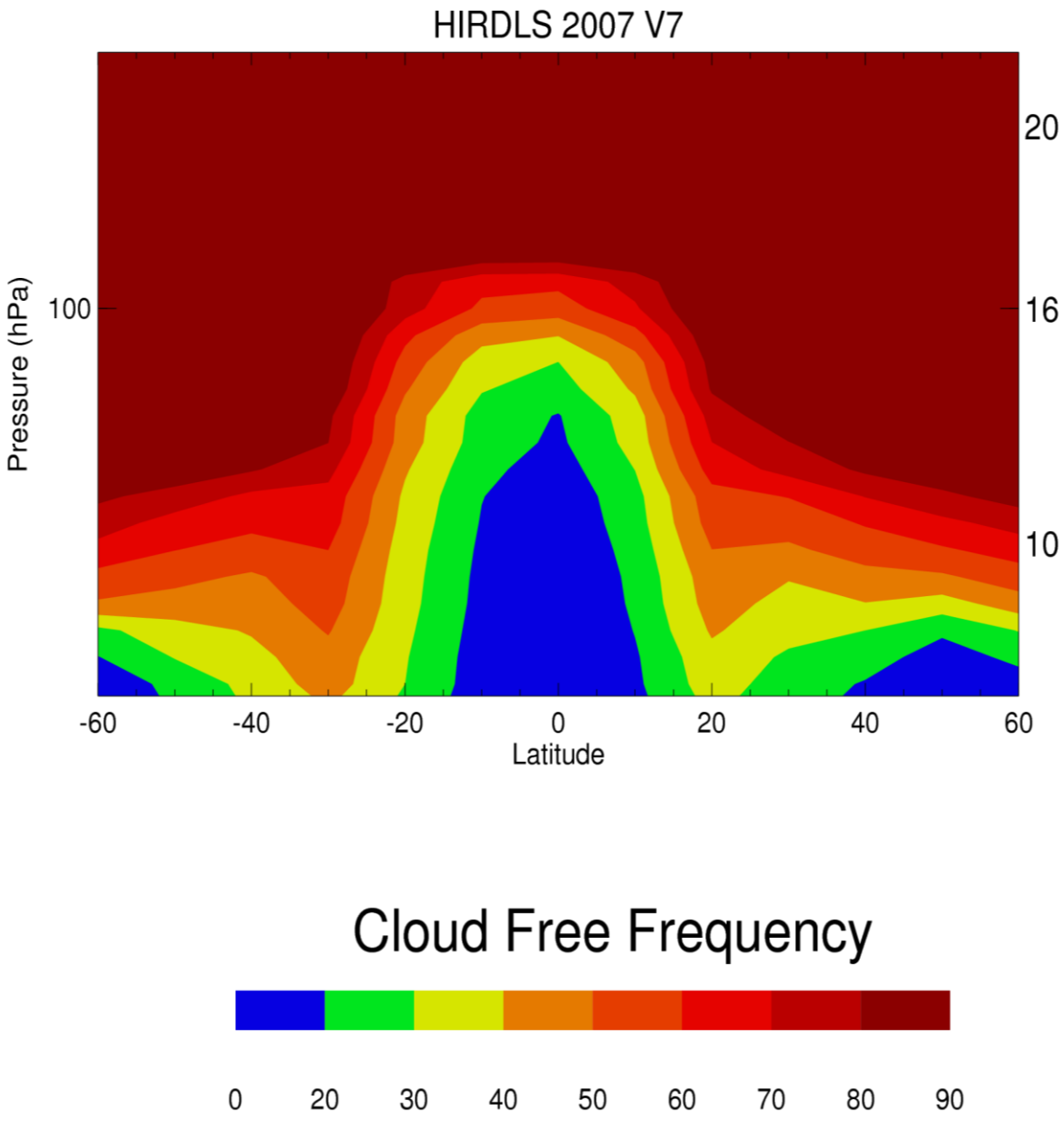

Figure 5.11.3. V7 cloud-free frequency in 2007. All pressures below the cloud top pressure of a single radiance profile are considered to be influenced by clouds. An approximate altitude scale in kilometers is given on the right hand side of the figure.

Figure 5.11.4 presents a comparison of V6 and V7 cloud frequency of occurrence in 2007 at 121 hPa for the four seasons. It is readily apparent that the two frequencies of occurrence are very similar for the two data versions. This figure was created by calculating at each pressure level the fraction of the time that extinction was between 9.0×10^{-4} km^{-1} and 1.0×10^{-2} km^{-1}, the extinction precision was less than 100%, and when the cloud flag was nonzero.

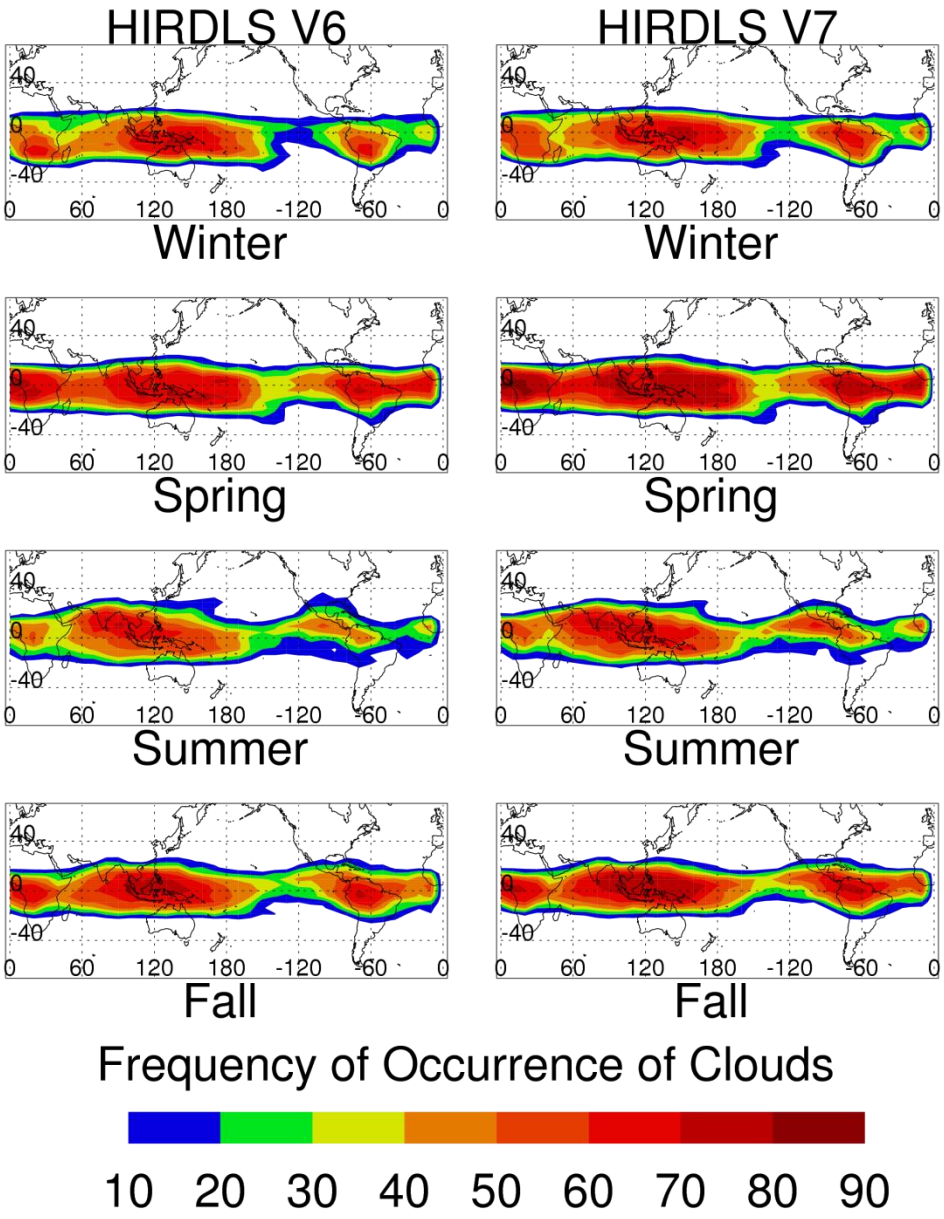

Figure 5.11.4. V6 and V7 cloud frequency of occurrence in 2007 for all cloud types for the four seasons at 121hPa.

5.12 12.1 and 8.3 Micron Extinction

Data:	12.1 and 8.3 Micron Extinction
Data Field Names:	12.1MicronExtinction, 8.3MicronExtinction
Useful Range:	215-20 hPa
Screening Criteria:	Use stratospheric extinction in a qualitative manner Use extinction between 10^{-5} to 10^{-2} km^{-1} Precision/data in 0 to 100% range Clouds are present if the extinction is greater than 9×10^{-4} km^{-1}
Vertical Resolution:	1 km
Contact:	Steven Massie
Email:	massie@ucar.edu

Cloud and aerosol extinction and extinction precisions, in units of km^{-1}, at 12 μm are included in the "12.1MicronExtinction" and "12.1MicronExtinctionPrecision" data fields. Extinction is archived for pressures between 20 to 215 hPa. Data above and below this range of pressure is flagged as -999 in the data files. It is recommended that extinction in the range of 10^{-5} to 10^{-2} km^{-1} be used when the precision is positive from 0 to 100%. Two week (or longer) zonal (hPa versus latitude) averages of extinction above the tropopause are recommended when examining the sulfate aerosol extinction in the stratosphere.

The 20 hPa pressure limit allows for inclusion of PSC observations in the archives and was also determined from comparisons of HIRDLS extinction profiles with correlative profiles. Mid-latitude HIRDLS extinction profiles at pressure levels less than 20 hPa increase in value, which is unrealistic. The higher pressure range of extinction (i.e. 215 hPa) was selected due to the fall off of extinction retrieval frequency (when the precision is less than the extinction) at pressures greater than 215 hPa in the tropics and mid-latitudes. Geospatial patterns of time averaged cloud extinction in latitude-longitude maps are coherent at pressures from 215 hPa up to the tropopause.

Since the 12 μm channel radiances in the absence of clouds are very low (which makes this "infrared window" especially good for detecting clouds), the absolute calibration of the radiances is still problematic. The extinction for the retrieved sulfate aerosol in the stratosphere is larger than correlative measurements (i.e. HALOE extinction zonal averages and University of Denver size distributions, converted to extinction profiles via Mie calculations) by a factor of ~2 for the V4 data, and more so for the V7 data at pressures less than 40 hPa. For this reason the stratospheric (sulfate) data should be used in a qualitative manner, whereby the extinction data is used to indicate sulfate (low) extinction versus cloud extinction in a relative manner. Cloud extinction at 12 μm is present when the

extinction is greater than approximately 9 x 10^{-4} km^{-1} (i.e. the cloud extinction threshold determined previously by John Mergenthaler (Mergenthaler, et al, 1999) based upon analyses of the 12 μm extinctions of the CLAES experiment on the UARS platform). The cloud extinction can be used in a quantitative manner.

Figure 5.12.1 presents seasonal latitude-longitude graphs of V7 and V6 HIRDLS extinction for 2007 at 121 hPa. The extinction averages are similar to those obtained by previous solar occultation experiments, with maxima over the maritime continent, Africa, and South America. Monsoon dynamics influence the distribution of clouds over India during summer, while deep convection during winter produces high cloud frequencies over the maritime continent.

Figure 5.12.2 presents zonal averages of V7 Channel 6 and Channel 13 extinction for January 2007, calculated when the ratio of extinction precision to extinction is between 0 and 100 %. Extinction for pressures between 400 and 20 hPa are displayed in the Figure. The Channel 13 extinction is larger than the Channel 6 extinction. It is expected that the Channel 13 extinction in the stratosphere is larger than that of the Channel 6 extinction since stratospheric sulfate extinction is five times larger at 1220 cm^{-1} that at 830 cm^{-1}. Both extinction graphs display a tropopause contour, as expected. The values of temperature and relative humidity with respect to ice just above the tropopause do not support the existence of ice, so large values of extinction, due to cirrus particles, fall off in frequency of occurrence above the tropopause. The graph also displays the presence of Polar Stratospheric Clouds (PSCs) at northern high latitudes. The presence of PSCs in the southern hemisphere is apparent in graphs of extinction during June – September. Since the HIRDLS experiment only observes to 60° S, however, the full latitudinal range of PSCs in the southern hemisphere is not observed.

In order to validate the absolute values of the extinction, the in-situ stratospheric size distributions of Terry Deshler**, measured from Laramie, Wyoming (41° N, 105° W) between April 2005 and November 2007, were used to calculate Mie extinction profiles of sulfate aerosol at the wavelengths of the Channel 6 and Channel 13 observations. Averages of the ten in-situ extinction profiles were then compared to HIRDLS zonal averages in the 40° - 45° N latitudinal range, averaged over the ten specific days corresponding to the Deshler observations. The standard deviations of the percent differences of the observed and in-situ extinction for Channels 6 and 13 are near 184% and 48%, respectively, for pressures between 20 and 215 hPa. The Channel 6 and 13 standard deviations of the differences in the HIRDLS and Deshler extinctions are 1 x 10^{-5} and 2 x 10^{-5} km^{-1} (the value stated in Table I-1), with mean differences of 2.5 x10^{-5} and 1.4 x 10^{-5} km^{-1} (note that several of the HIRDLS Channel 13 extinctions are less than the Deshler values). Note that cirrus extinction values (with a threshold of 9 x 10^{-4} km^{-1}) are considerably larger than these standard deviations. The Channel 13 to Channel 6 stratospheric sulfate extinction ratio is expected to be near 5. Since the Channel 6 sulfate extinction is considerably larger than the correlative measurements, the observed average ratio is less (~2).

**University of Wyoming stratospheric aerosol size distributions of Terry Deshler are available on the anonymous ftp site: trex.uwyo.edu.

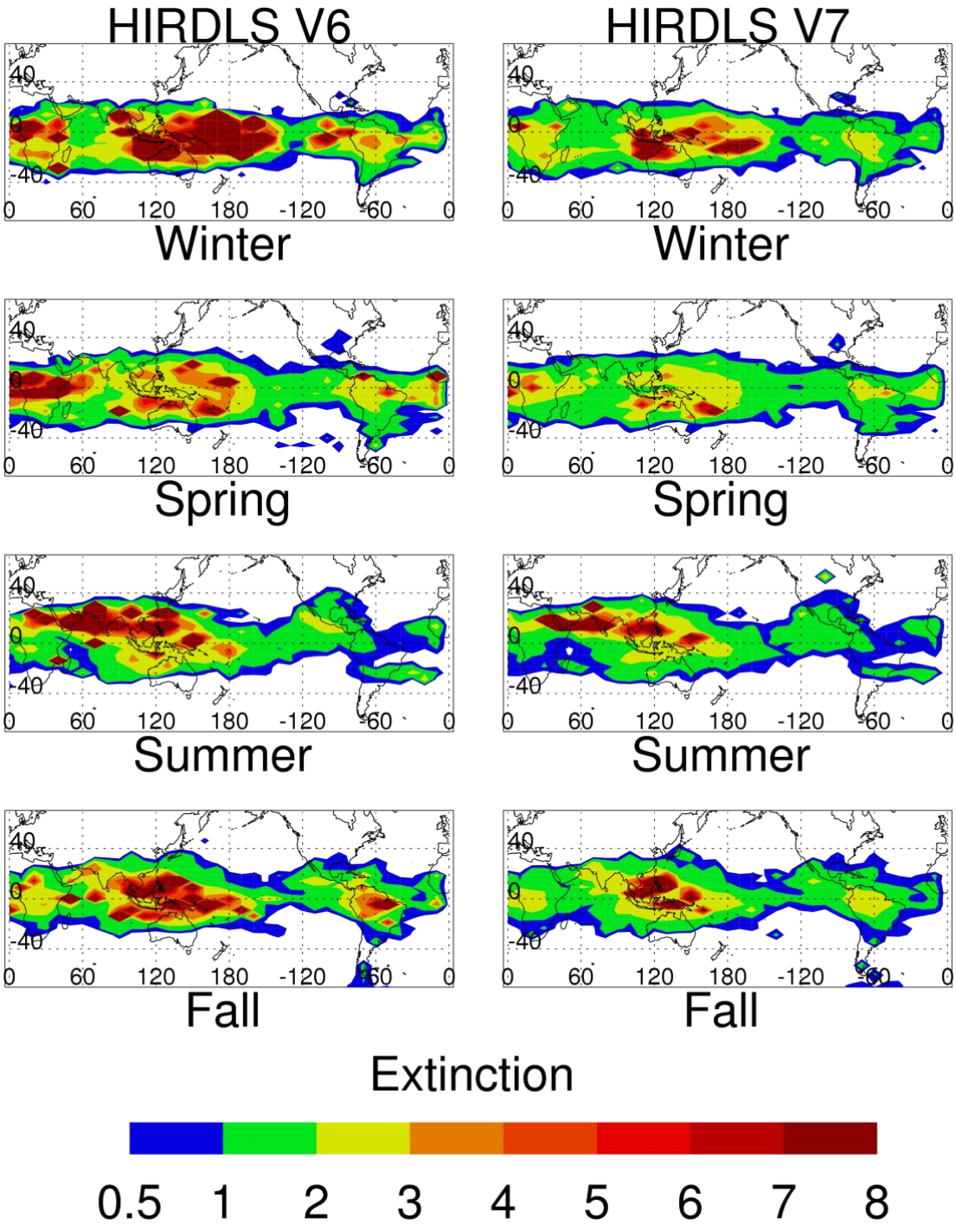

Figure 5.12.1. V7 and V6 HIRDLS seasonal extinction at 121 hPa during 2007. Extinction values are in units of 10^{-3} km^{-1}.

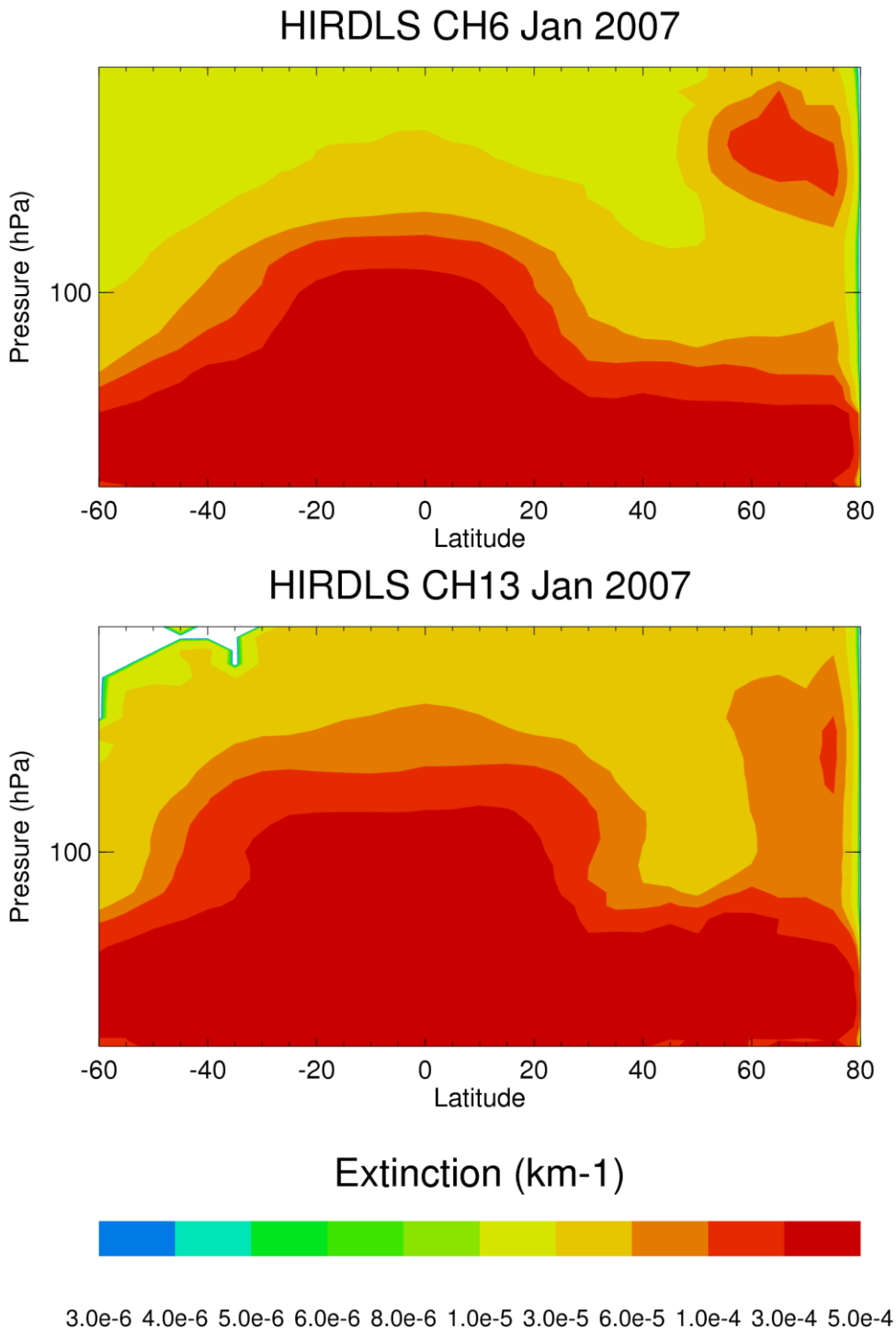

Figure 5.12.2 Zonal averages of V7 Channel 6 and Channel 13 extinction for January 2007.

Reference: Massie, S. T. et al., HIRDLS Observations of PSCs and Subvisible Cirrus, 2007: J. Geophys. Res., doi:10.1029/2007JD008788.

5.13 Geopotential Height (GPH)

Species:	Geopotential Height (GPH).
Data Field Name:	GPH Raw GPH
Useful (vertical) Range:	1000 - 0.01 hPa* * HIRDLS pointing plus *a priori* temperatures for p >383 hPa
Vertical Resolution:	Since GPH involves integrating over HIRDLS Temperatures, GPH is reported every pressure level, so a bit better than 1km. See section 5.1.
Contact:	Lesley Smith
Email:	lsmith@ucar.edu
Validation Paper:	Smith, L., et al., Validation of HIRDLS GPH Observations, *In preparation*.

General Comments:

HIRDLS Geopotential Heights have high (1 km) vertical resolution, based on the high vertical resolution of HIRDLS temperatures and comparisons with MLS, GMAO, NCEP, and ECMWF data. As with the temperatures, in the stratosphere, the Geopotential Height precision is independent of latitude and season, and varies from only slightly in the upper troposphere to about the stratopause, above which it grows slightly, depending on latitude and season. Geopotential Heights are slightly lower than the ECMWF analysis in the tropics especially above 3mb, and slightly higher than the ECMWF analysis at high latitudes.

Precision

The observed precision is estimated in the way described in Section 5.0. GPH values on a pressure level for 12 consecutive profiles are taken at times and locations in which geophysical variation were expected to be low. Data used were in the tropics at equinoxes and solstices for years 2005-2007. The standard deviation of their departures from a linear detrending line was determined, and the average of the 10 smallest values was calculated. These results are presented in Figure 5.13.1, where the solid line indicates this observed precision. The dashed line is the precision predicted by the GPH algorithm incorporating the uncertainties in the input parameters, i.e. the pressures and the temperatures. Notice the uncertainty in the tangent height at nominal altitude has not been accounted for and thus the predicted precision is a lower estimate.

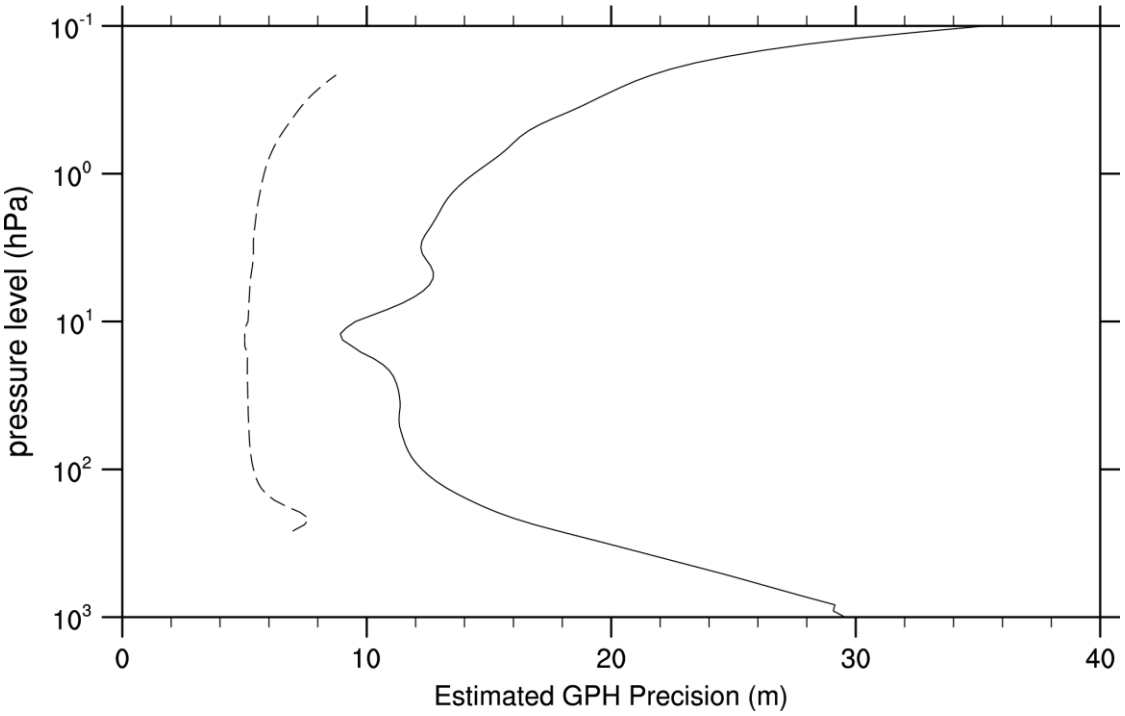

Figure 5.13.1: Estimated precision of HIRDLS V6 GPH (solid line), compared with precision prediction by the GPH algorithm (dashed line).

Accuracy

HIRDLS GPH's have been compared to several data sets in an effort to determine the extent and magnitude of any bias. In Figure 5.13.2 we see HIRDLS GPH binned by latitude, averaged over 2005-2007 minus ERA-Interim, NCEP/NCAR Reanalysis, MLS and GEOS-5 data at sample pressure levels 10hPa and 100hPa. Figure 5.13.2 may indicate a slight low bias in MLS GPH. HIRDLS Version 7 GPH significantly reduced its low bias as compared to Version 6 when we changed to the elevation angle tie-on was implemented instead of an altitude tie-on in the processing stream.

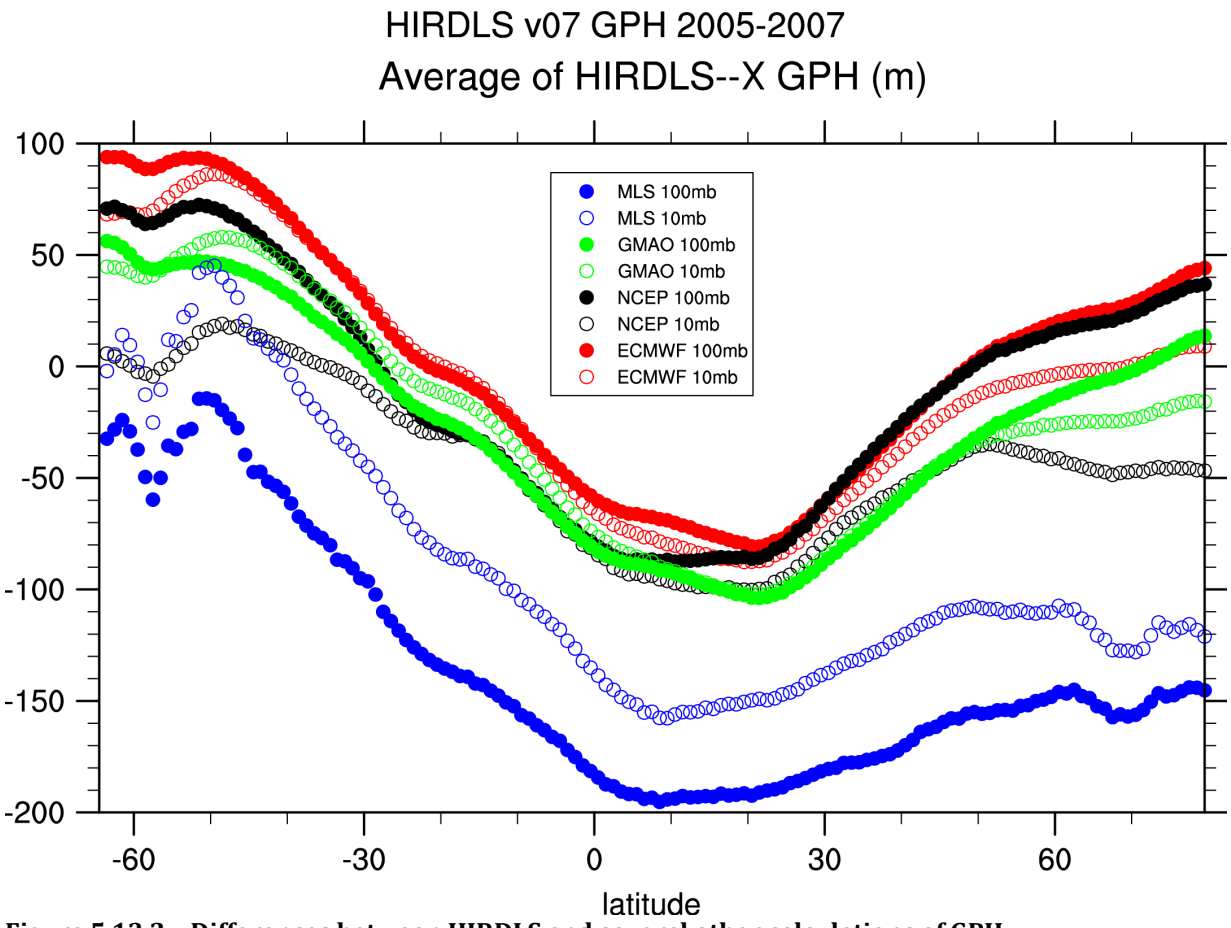

Figure 5.13.2: Differences between HIRDLS and several other calculations of GPH.

In Figure 5.13.3 we see the standard deviation of HIRDLS GPH binned by latitude, averaged over 2005-2007 minus ERA-Interim, NCEP/NCAR Reanalysis, MLS and GEOS-5 data at sample pressure levels 10hPa and 100hPa. Generally, the variations illustrated in Figure 5.13.3 are consistent and reasonable across most latitudes, with the possible exceptions of very high and very low latitudes. Figure 5.13.3 does seem to indicate MLS GPH has a greater variation than the other datasets.

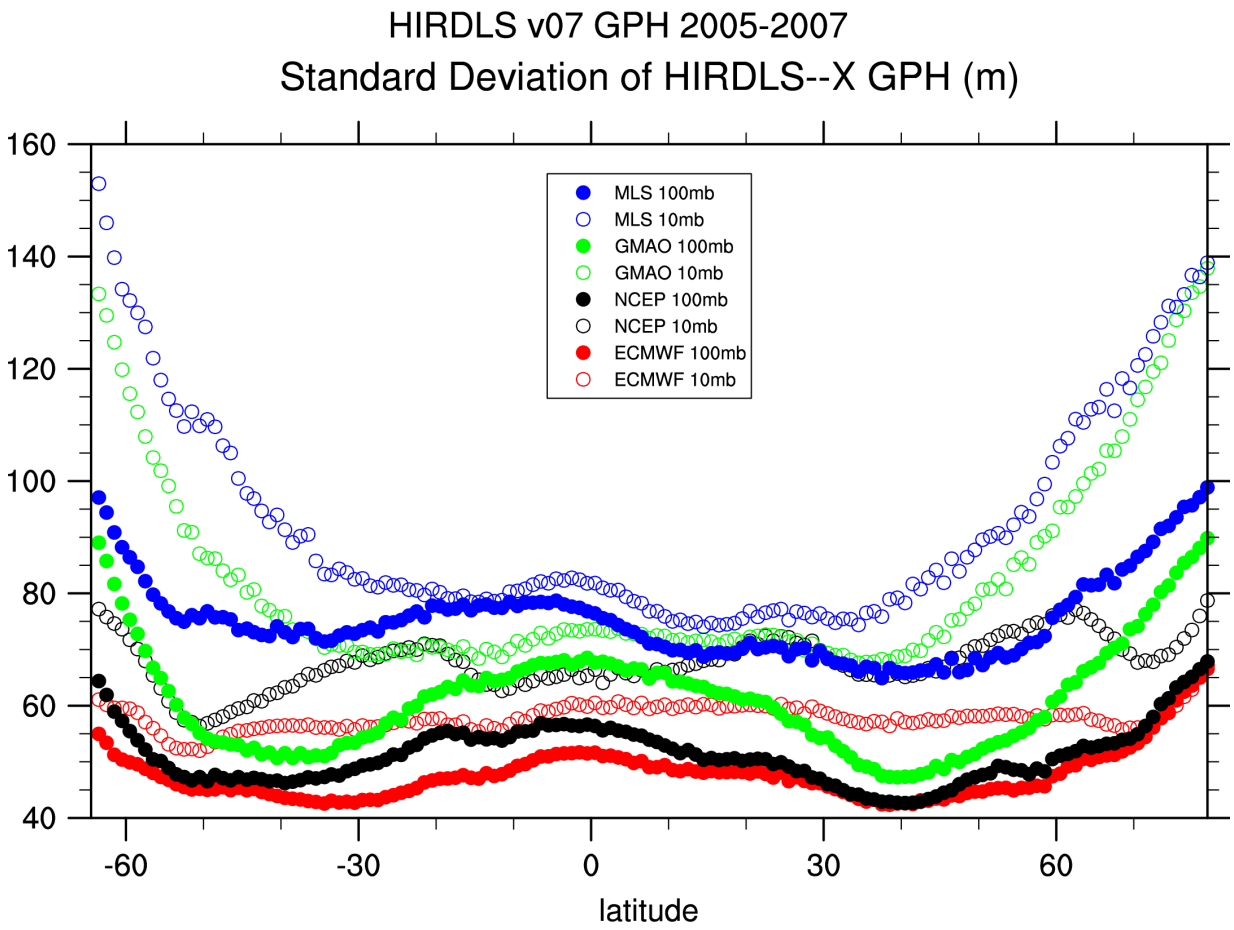

Figure 5.13.3: Standard deviations of differences between HIRDLS and several other calculations of GPH.

Summary

The GPH is based entirely on spacecraft pointing data and HIRDLS temperatures, and it has the corresponding 1 km vertical resolution. From the troposphere to the stratopause the precision is ≤ 15 m, above which it increases to 35 m at 0.1 hPa. The bias in the GPH difference from -63° to the equator is < 90 m at 100 hPa, and <60 m at 10 hPa. The bias in difference from the equator to 80° is < 65 m at 100 hPa, and < 35 m at 10 hPa when compared to conventional analyses based on assimilation of meteorological data. These NH gradients correspond to differences in geostrophic winds at 60° of ≤ 0.5 m/s at 100 hPa, or ≤ 0.3 m/s at 10 hPa. Similarly, winds in the SH would differ from those based on the assimilated data by < 1 m/s at -60°.

6.0 HIRDLS Level 3 Gridded Data Products

Beginning with Version 6, HIRDLS released new level 3 (L3) data products. V7 releases L3 versions of all released L2 products. These were created by applying a Kalman filter mapping algorithm similar to that described by Remsberg *et al.* [1990]. The algorithm inputs L2 retrieval results for each 1° latitude band for the length of the mission, and creates daily estimates of the zonal mean plus amplitudes and phases of the first seven zonal waves using both forward and backward passes through the data. The zonal means plus coefficients for a latitude may then be used to calculate values at any longitude. The algorithm also provides values of precision, which is the root-mean square of the differences between the estimated fields and the input data.

The L3 processor is a Kalman filter used as a sequential estimator that combines weighted data from a single profile with a weighted estimate based on the previous data, as described by Rodgers [1977, 2000], Kohri [1981], and Remsberg *et al.* [1990]. In this process each data point is used to update estimates of the zonal mean and coefficients of the sine and cosine coefficients of the first 7 zonal waves (15 values, equivalent to the mean plus amplitudes and phases of the first 7 zonal waves). This is done for each pressure level and zonal band going both forward and backward in time, and the results are combined, thus ensuring smooth time evolution. Values are output at one time of day, resulting in daily values of the estimated quantities every 1° in latitude. This produces an optimal estimate of the state of the system in this representation. In general the final estimated field will not go through the input points, but will have an rms difference from them, termed the precision, approximately equal to the precision of the single profile observations. The output data includes this rms value, as well as the values from each of the diagonal elements of the covariance matrix that give the predicted variance of each of the estimated quantities. The output data also includes the number of points that went into producing the estimate for that day. Since the Kalman estimator produces estimates even in the absence of data, a negative number of points indicates the number of days without data since (or until) a day with data.

Level 3 Zonal Fourier Coefficient Files

The HIRDLS L3 Zonal Fourier Coefficient product is written using the HDF-EOS Grid library. This is a single file per species containing daily zonal Fourier Coefficients for the Combined, Ascending and Descending cases, where available. For the Combined cases, we used 7 waves. For the Ascending and Descending cases, we used 4 waves.

Level 3 Zonal Average Files

Released in V6 are now included in the Zonal Fourier Coefficient Files.

Level 3 Partial Column Files

The HIRDLS L3 partial column product is written using the HDF-EOS Grid library. This is a single file containing daily 1^o x 1^o latitude/longitude grids of the partial column products. Only the daytime NO2 product is being released.

Review of gridding procedure

This iterative Kalman filter is based on the method of Khori [1981] and Remsberg *et. al.* [1990] generalized to data ungridded in latitude. It is initialized by examining a day of data and setting (at each pressure and latitude) the estimate coeffficients equal to the zonal mean and no longitudinal waves. The diagonal values of the covariance matrix are set larger than 2 times the data variance. The initial ds/dt is set to the average sigma of the input points. Then the filter is run forwards and backwards over the data. The forward and reverse estimates and covariance are combined. As Remsburg, *et. al*. [1990] suggested, ds/dt can be approximated by the variance of the ith wave amplitude divided by the relaxation time. Since the Kalman filter is relatively insensitive to the value of ds/dt, we use a relaxation time of 1 day for all heights and components. In practice, two to four iterative applications of the mapper to the data converges quickly to a stable solution.

With more than 14 measurements per day at each latitude, we nominally expect 7 fourier waves (a zonal mean plus 7 pairs of wave coefficients or 15 variables) to be defined by the data. Mapping runs were examined for the power in each longitudinal wave and that was compared to the noise. For strong signals such as temperature, power in all 7 waves exceeded background noise.

Validation of the Kalman mapper was achieved in three ways. First, a simple binning process can be used to derive zonal means on a given day. These values were compared to the zonal means from the Kalman filter and good agreement was found. Second, a one-month subset of the temperature data was analyzed with a Salby filter technique. Good agreement with the Kalman filter was again found. Finally, model output from WACCM for the HIRDLS period was used to generate a simulated dataset with a known field. Good agreement was found between the Kalman result and the original field. [refer to paper to be published?]

6.1 Temperature

Four criteria are applied to assess the L3 temperature data. The first is to require that the L3 fields match, within their measurement precision, the individual L2 data points they are created to represent. A standard output of the mapping routine is the rms difference between the reconstructed field and the input data. Plots of this (not shown) verify that this is the case.

A second criterion is that a gridded field, such as the zonal mean, represents the zonal mean of the L2 data. The left panel of Figure 6.1.1 compares zonally averaged L2 data for day 172 (the northern summer solstice) of 2007 with the L3 zonal mean. There is good agreement up to 0.1 hPa, except at high

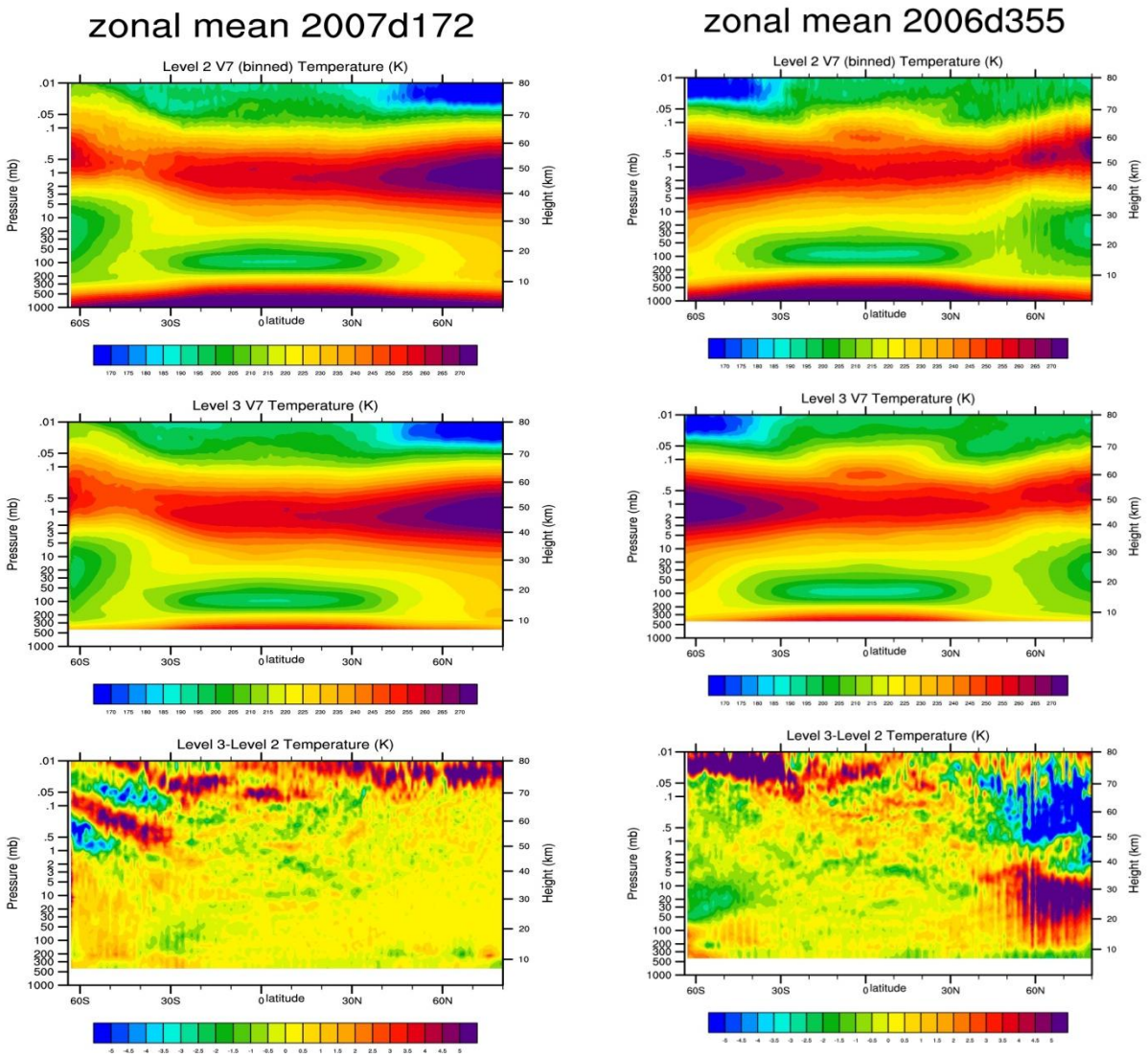

Figure 6.1.1. The upper panel displays the results of zonally averaging the individual L2 profiles; the middle panel presents the zonal mean temperatures resulting from the L3 gridding; and the bottom shows the differences for a (left) 2006 day 172 and b (right) 2006day 355.

southern latitudes. A different example, during northern winter, is shown in the right panel of Fig. 6.1.1, for a day in northern winter. Here there are significant differences in high northern latitudes, where the atmosphere may be changing rapidly. The Kalman filter would be expected to provide a better representation at any given time than a simple average of individual orbits. This effect would be exacerbated by any missing orbits of data, although this is relatively rare.

A third criterion is the extent to which these reconstructed maps agree with other maps of the temperature fields from trusted sources. Typical examples are shown in Figure 6.1.2 where polar stereographic maps of temperature at 10 and 82 hPa for HIRDLS V7 are compared with GEOS5 maps.

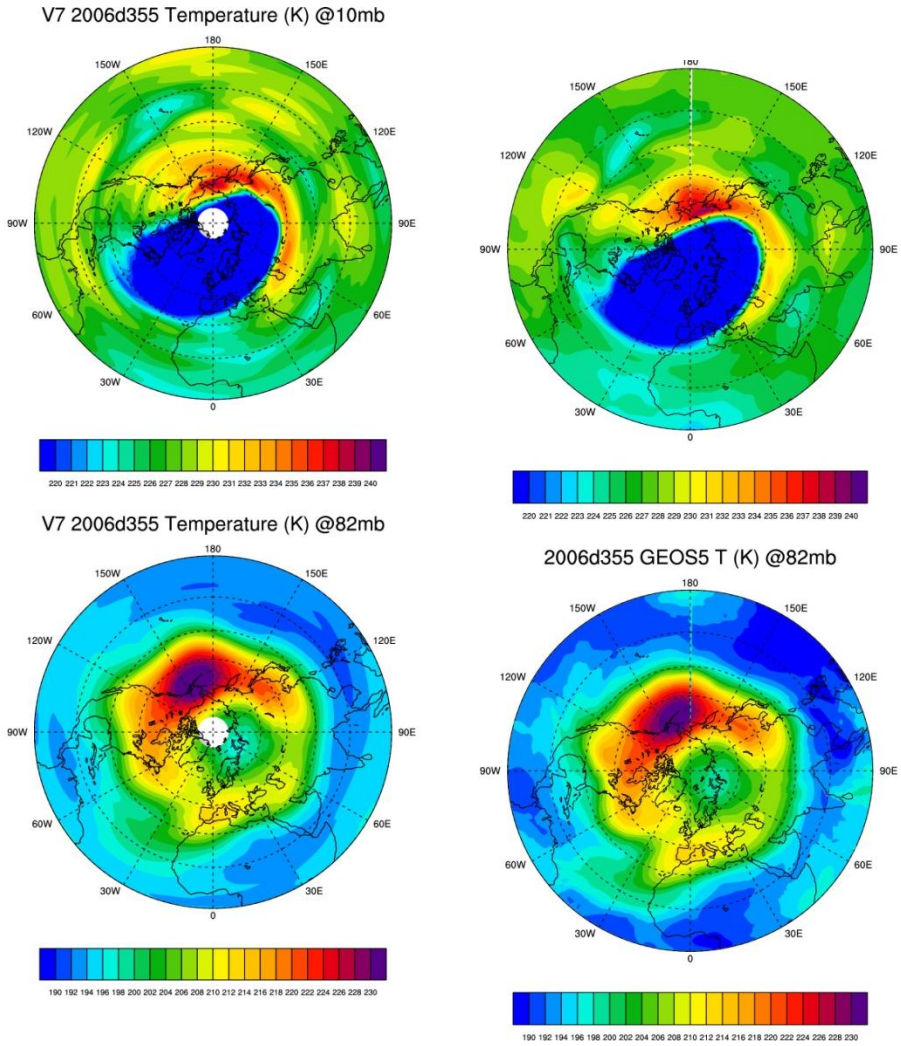

Figure 6.1.2. Polar stereographic maps of HIRDLS (left) and GEOS5 (right) temperatures on the 10 and 82 hPa surfaces for 2006 day 355.

The HIRDLS maps show all the major features seen in the GEOS5 data, although of course features smaller than WN 7 are not represented.

The final criterion is that there be time continuity, and the temporal variations show expected phenomena, with no periods of unexpected behavior. Two examples are shown in Fig. 6.1.3. In the left panel, the differences between the individual days measurements and the temporal mean, termed the anomalies, for the 5°S-5°N latitude band over the observing period are plotted. The effects of the semi-annual oscillation in the upper and middle stratosphere, and the quasi-biennial oscillation (QBO) in the lower stratosphere, can clearly be seen.

The right panel in Figure 6.1.3 displays the zonal mean temperatures at 70°N. Notable features are the annual variation of stratopause temperatures, as well as the mid-winter sudden stratospheric warming in 2006.

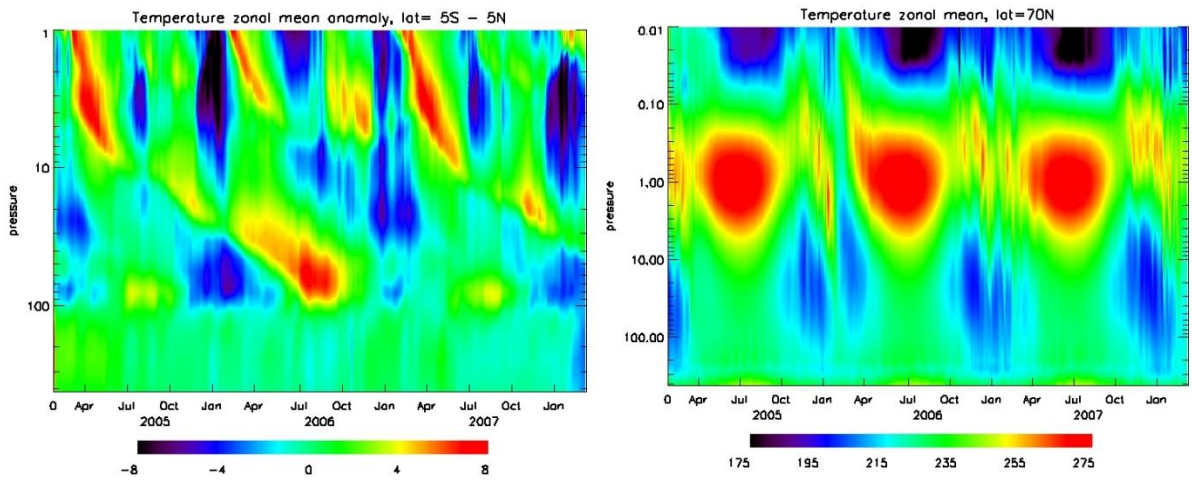

Figure 6.1.3. Left- zonal mean departures from the time mean temperatures (anomalies) averaged over the 5°S-5°N latitude band. Right- zonal mean temperatures at 70°N, showing variations in stratopause temperatures, and warm mid-winter temperatures in the stratosphere (sudden stratospheric warming) in 2006.

Based on these results, the L3 V7 temperatures are a good representation of the L2 data, in good agreement with GEOS5 data, and show the expected temporal variability.

6.2 L3 Ozone (O_3)

The Combined Ozone Zonal Fourier Coefficients were created using 7 waves. Figure 6.2.1 gives pressure level versus day of mission zonal mean contour plots for Combined Ozone for a tropical latitude, 5^o N, and for a high latitude 55^o N.

The Ascending and Descending Ozone Zonal Fourier Coefficients were created using 4 waves. Pressure level versus day of mission zonal mean contour plots for the Ascending and Descending modes (not shown) are similar to those for the combined case.

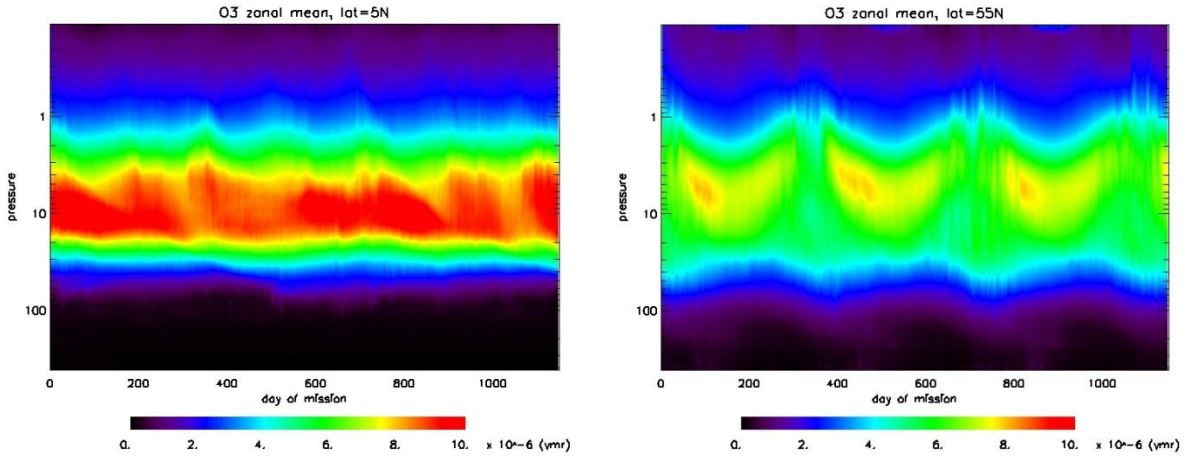

Figure 6.2.1: Time series of gridded L3 ozone for the entire HIRDLS mission of the zonal means at 5°N (left) and 55°N (right), all in volume mixing ratio.

In the tropics between 30S – 23N, earthward of 67 hPa, ozone is known to be consistently high, on the order of 50-100+% when compared with most correlative data sources. Therefore in this specific region ozone is not considered to be of good scientific quality and is not included in the released L3 product.

Ozone data with negative precision are filtered out. They occur predominantly at the bottoms of the profiles (and to a lesser extent at the tops of profiles). If they were to be included in computed zonal averages they would have the tendency to reduce ozone values in the tropical UTLS, as more realistic a priori information for that region dilutes the high-biased measurement.

Figure 6.2.2 shows that the L3 gridded zonal mean ozone field is a good representation of the zonal mean of the L2 data. The left panels compare the zonal averages for 2006 day 172 (the northern summer solstice) and the right panels compare the zonal averages for 2005 day 355 (the northern winter solstice). The largest discrepancies are at high latitude of the winter solstice hemisphere, and above 0.5 hPa.

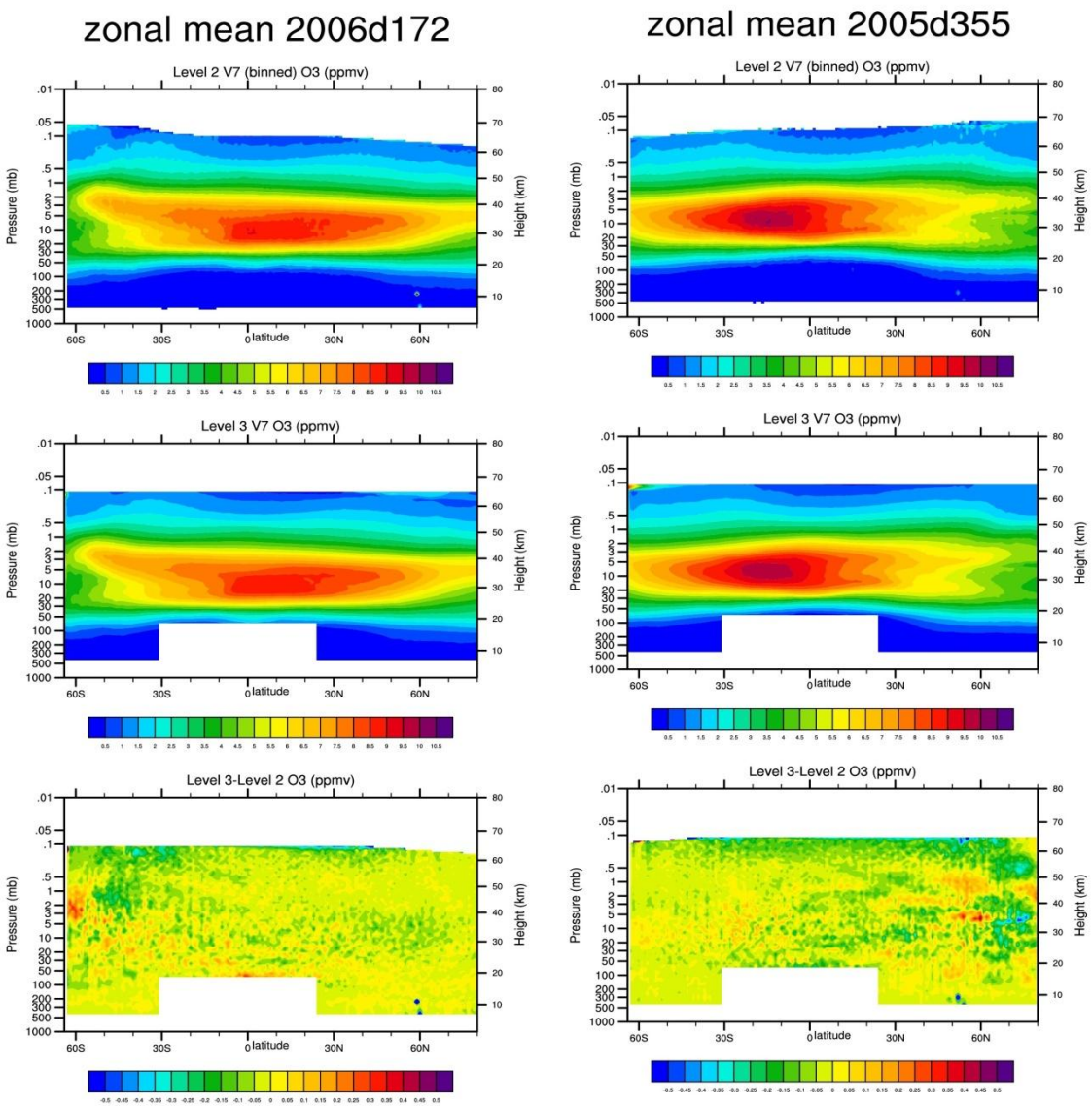

Figure 6.2.2: The upper panel shows the zonal average of individual L2 ozone profiles; the middle panel shows the gridded-L3 zonal mean ozone; and the bottom shows the differences, for (left) 2006 day 172 and (right) 2005 day 355.

Figure 6.2.3 shows a standard output of the mapping routine, the RMS difference between the reconstructed field and the input data. These indicate that statistically the L3 gridded data are within the error as given earlier in the L2 section of this document (Figure 5.2.4).

Figure 6.2.4 shows a typical example for sample day, 2006d172, of Mercator maps of gridded-L3 V7 HIRDLS ozone at 10 hPa.

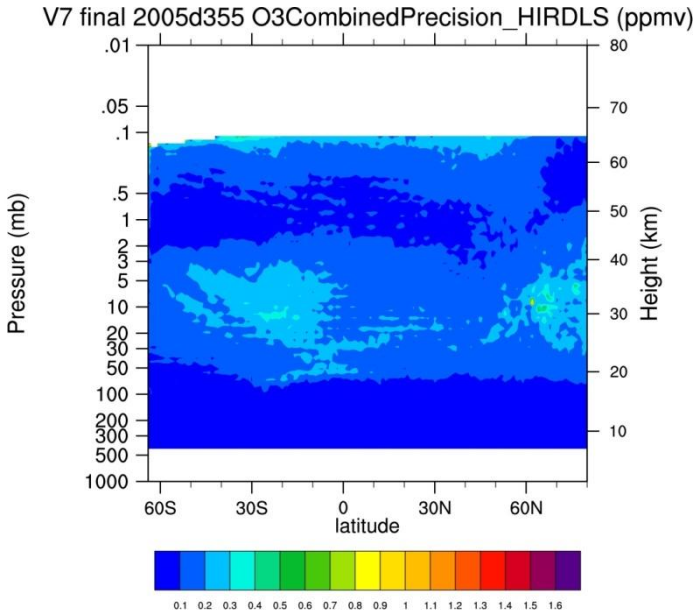

Figure 6.2.3: HIRDLS Version 7 Level 3 ozone precision (ppmv) for sample day 2005d355.

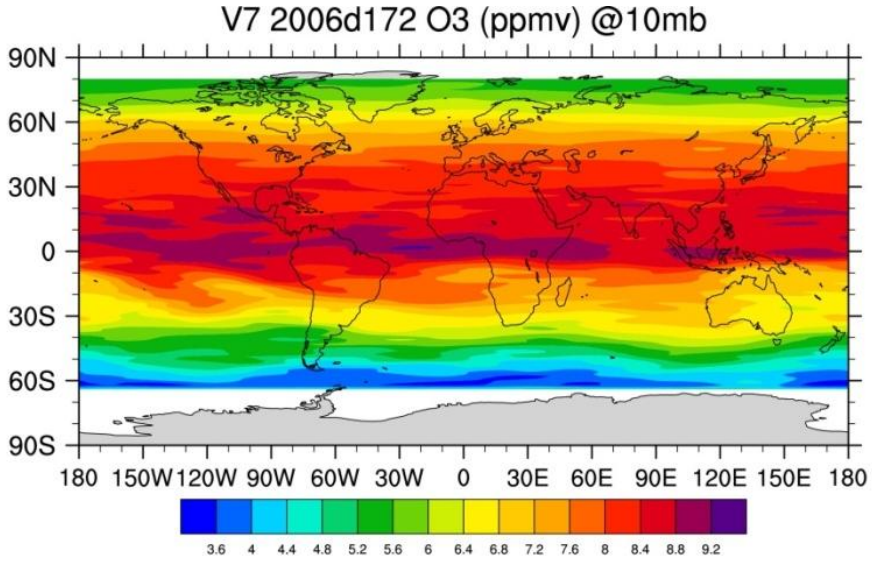

Figure 6.2.4: Mercator maps of HIRDLS Version 7 ozone.

6.3 Nitric Acid (HNO_3)

The Combined HNO_3 Zonal Fourier Coefficients were created using 7 waves. Figure 6.3.1 gives pressure level versus day of mission zonal mean contour plots for Combined HNO_3 for a tropical latitude, 5^o N, and for a high latitude 55^o N.

The Ascending and Descending HNO_3 Zonal Fourier Coefficients were created using 4 waves. Pressure level versus day of mission zonal mean contour plots for the Ascending and Descending modes (not shown) are similar to those for the combined case.

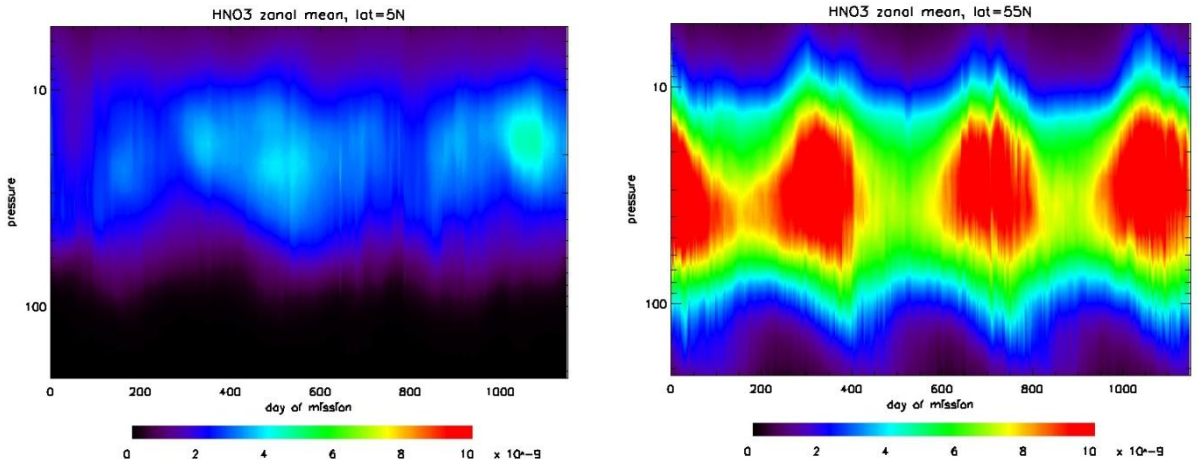

Figure 6.3.1: Time series of gridded L3 HNO_3 for the entire HIRDLS mission of the zonal means at 5°N (left) and 55°N (right), all in volume mixing ratio.

Figure 6.3.2 shows that the L3 gridded zonal mean HNO_3 field is a good representation of the zonal mean of the L2 data. The left panels compare the zonal averages for 2006 day 172 (the northern summer solstice) and the right panels compare the zonal averages for 2005 day 355 (the northern winter solstice). Again, the largest discrepancies are at high latitude of the winter solstice hemisphere.

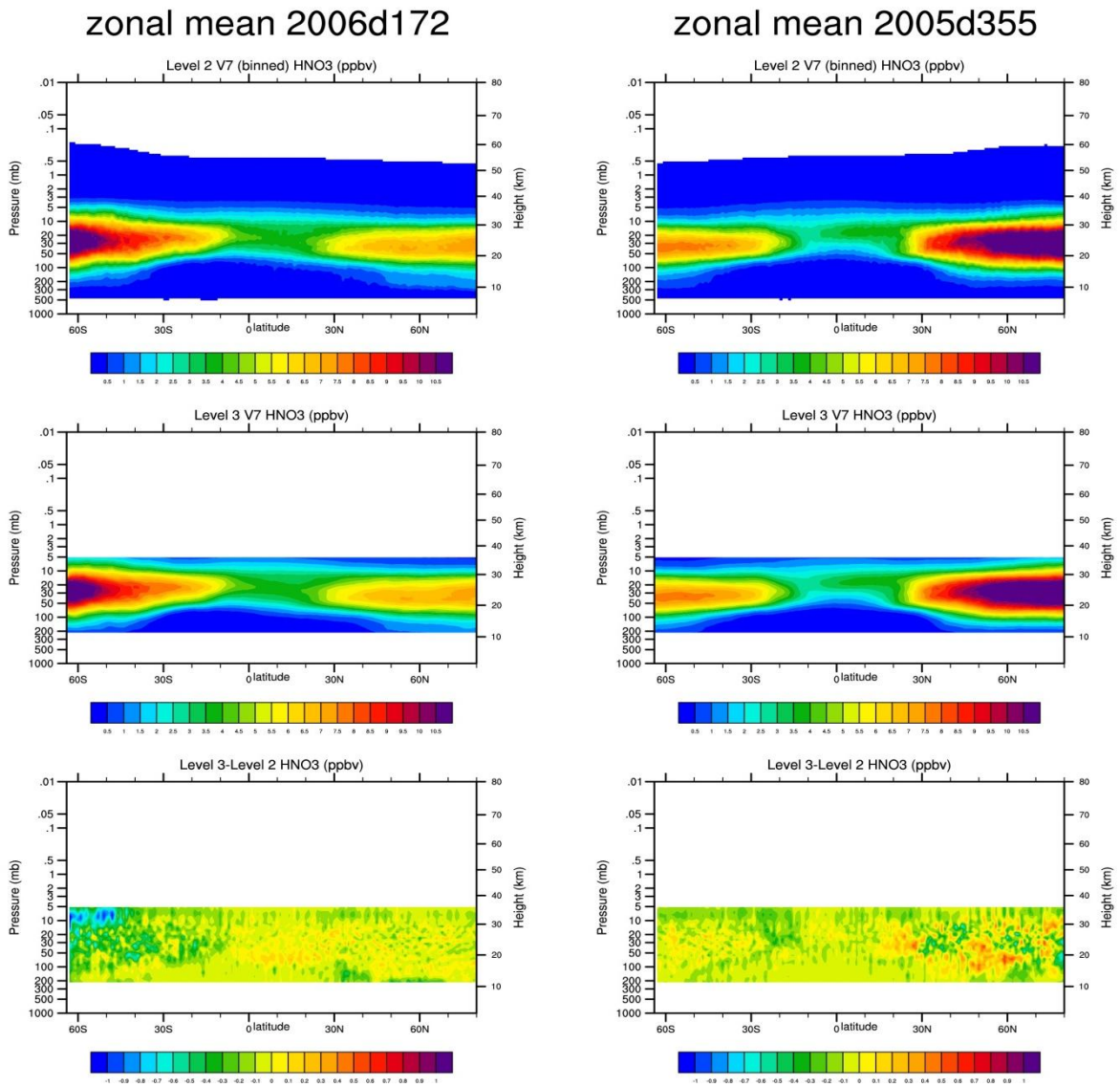

Figure 6.3.2: The upper panel shows the zonal average of individual L2 HNO_3 profiles; the middle panel shows the gridded-L3 zonal mean HNO_3; and the bottom shows the differences, for (left) 2006 day 172 and (right) 2005 day 355.

Figure 6.3.3 shows a standard output of the mapping routine, the RMS difference between the reconstructed field and the input data. These indicate that statistically the L3 gridded data are within the error as given earlier in the L2 section of this document (Figure 5.3.3).

Figure 6.3.4 shows a typical example for sample day 2006d172, of a Mercator map of gridded-L3 V7 HIRDLS HNO_3 at the randomly chosen pressure level, 82 hPa.

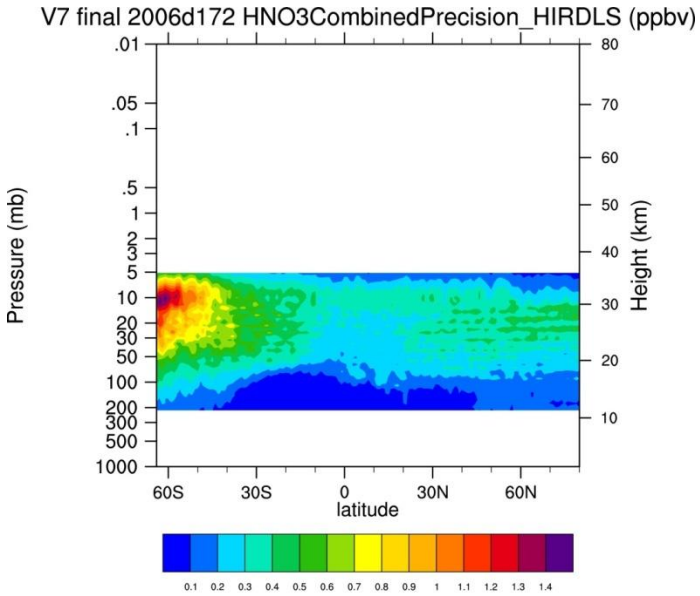

Figure 6.3.3: HIRDLS Version 7 Level 3 HNO_3 precision (ppbv) for sample day 2006d172.

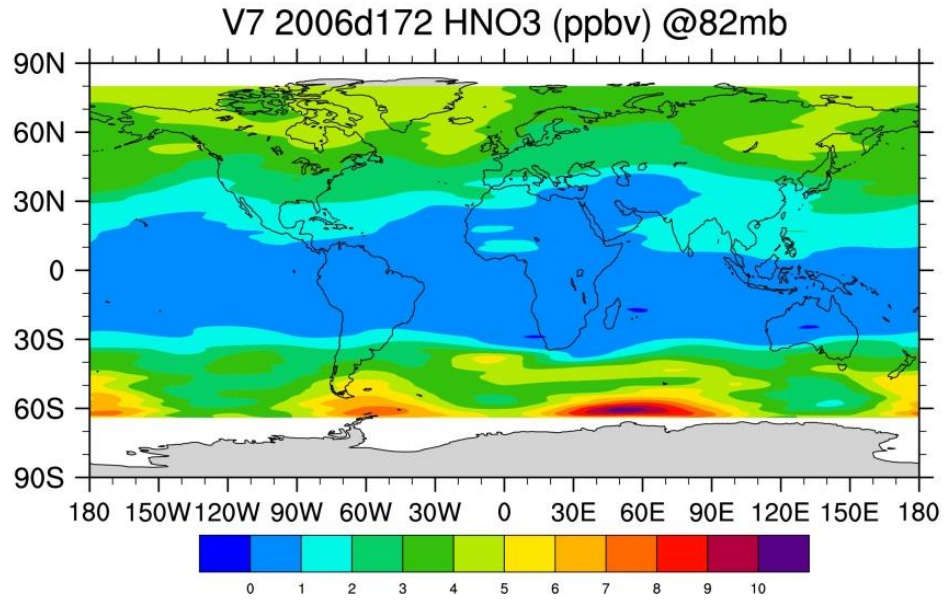

Figure 6.3.4: Mercator maps of HIRDLS Version 7 HNO_3.

6.4 $CFCl_3$ (CFC11)

The Combined CFC11 Zonal Fourier Coefficients were created using 7 waves. Figure 6.4.1 gives pressure level versus day of mission zonal mean contour plots for Combined CFC11 for a tropical latitude, 5^o N, and for a high latitude 55^o N.

The Ascending and Descending CFC11 Zonal Fourier Coefficients were created using 4 waves. Pressure level versus day of mission zonal mean contour plots for the Ascending and Descending modes (not shown) are similar to those for the combined case.

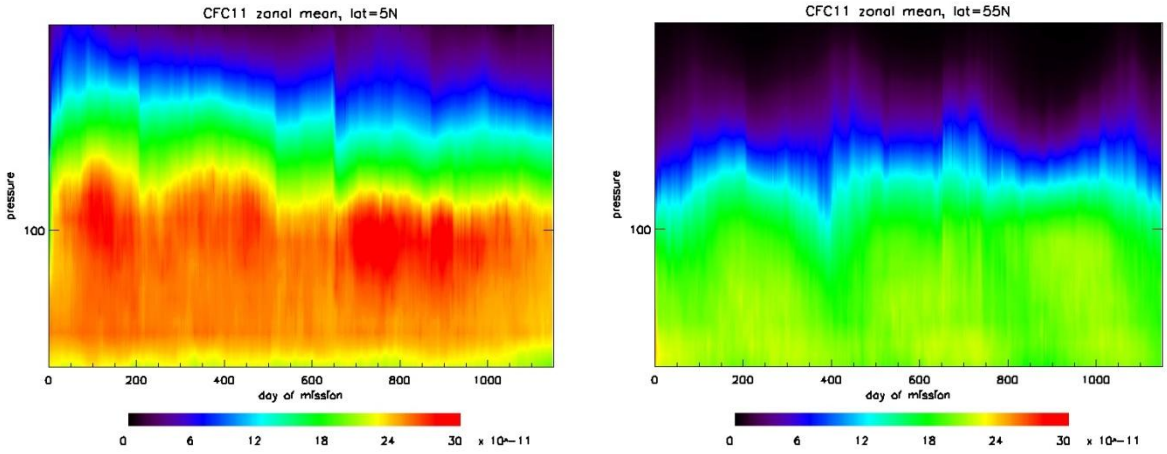

Figure 6.4.1: Time series of gridded L3 CFC11 for the entire HIRDLS mission of the zonal means at 5°N (left) and 55°N (right), all in volume mixing ratio.

Figure 6.4.2 shows that the L3 gridded zonal mean CFC11 field is a good representation of the zonal mean of the L2 data. The left panels compare the zonal averages for 2006 day 172 (the northern summer solstice) and the right panels compare the zonal averages for 2005 day 355 (the northern winter solstice). Again, the largest discrepancies are below 200 hPa. The larger vertical range shown in the level 2 plots are due to the fact that they are not filtered. Above about 18 hPa the data are associated with large variability (Figure 5.4.2a of L2 Data Quality Document), are likely to have negative precisions indicating strong a-priori influence, and are not recommended for use.

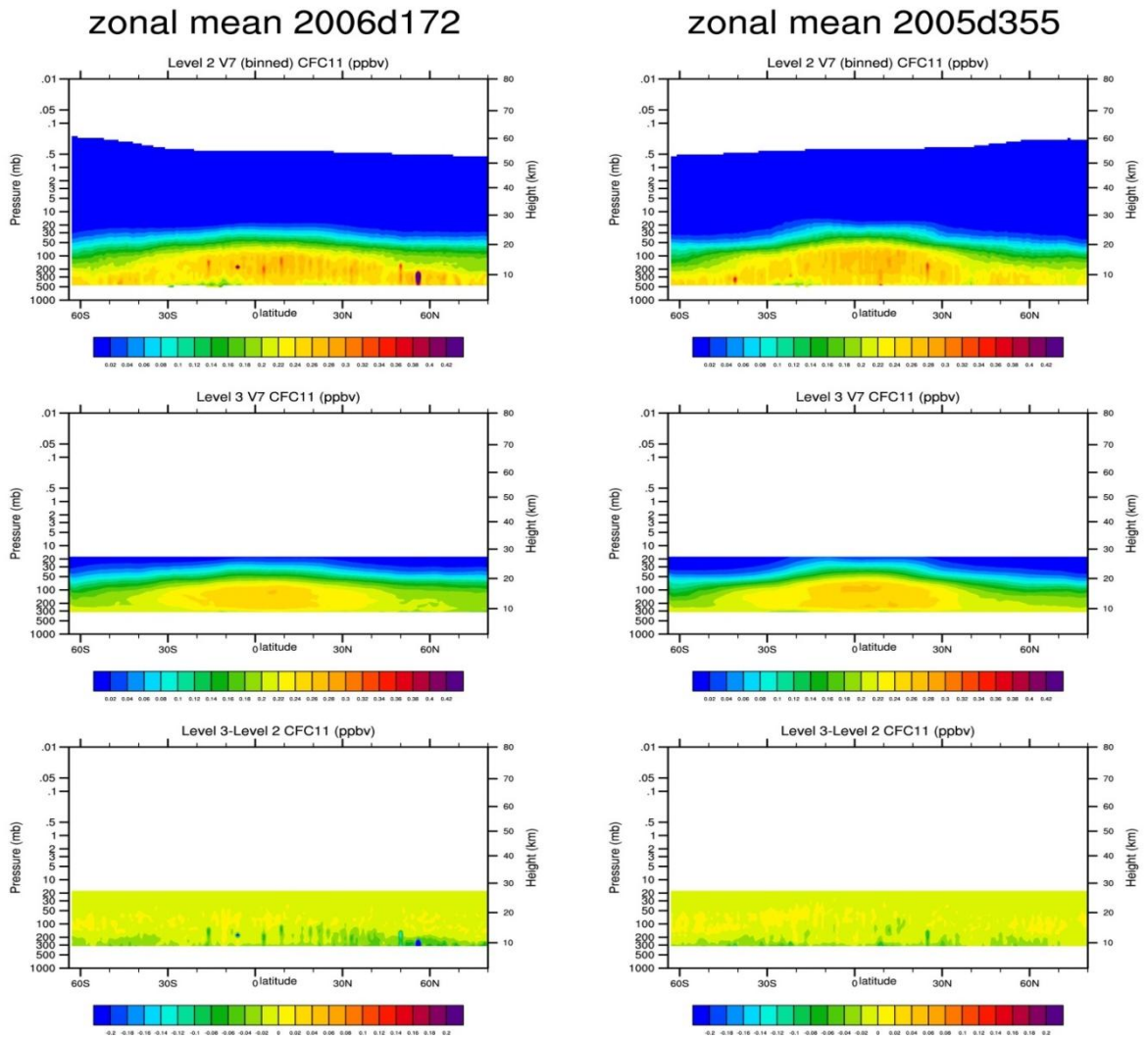

Figure 6.4.2: The upper panel shows the zonal average of individual L2 CFC11 profiles; the middle panel shows the gridded-L3 zonal mean CFC11; and the bottom shows the differences, for (left) 2006 day 172 and (right) 2005 day 355.

Figure 6.4.3 shows a standard output of the mapping routine, the RMS difference between the reconstructed field and the input data. These indicate that statistically the L3 gridded data are within the error as given earlier in the L2 section of this document (Figure 5.4.2a).

Figure 6.4.4 shows a typical example for sample day 2006d172, of a Mercator map of gridded-L3 V7 HIRDLS CFC11 at the randomly chosen pressure level, 82 hPa.

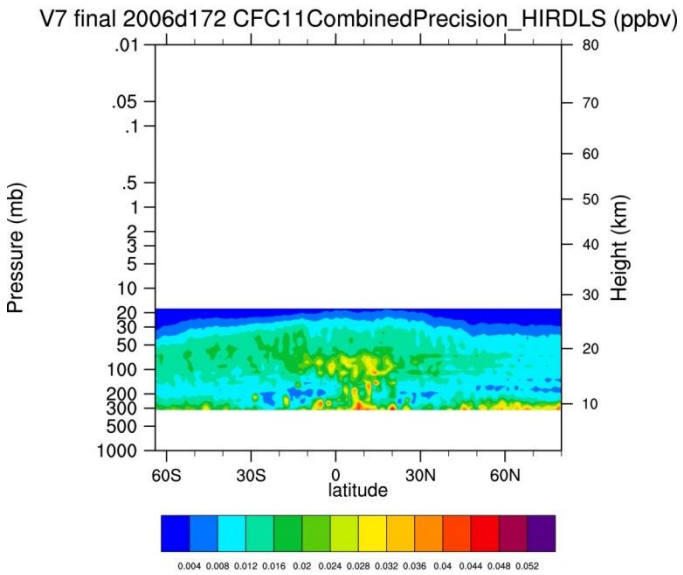

Figure 6.4.3: HIRDLS Version 7 Level 3 CFC11 precision (ppbv) for sample day 2006d172.

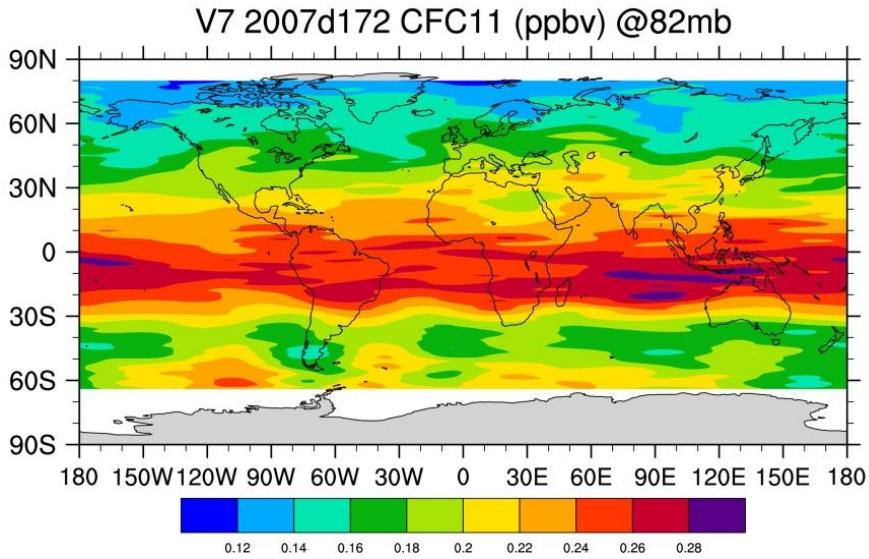

Figure 6.4.4: Mercator maps of HIRDLS Version 7 CFC11.

6.5 CF_2Cl_2 (CFC12)

The Combined CFC12 Zonal Fourier Coefficients were created using 7 waves. Figure 6.5.1 gives pressure level versus day of mission zonal mean contour plots for Combined CFC12 for a tropical latitude, 5^o N, and for a high latitude 55^o N.

The Ascending and Descending CFC12 Zonal Fourier Coefficients were created using 4 waves. Pressure level versus day of mission zonal mean contour plots for the Ascending and Descending modes (not shown) are similar to those for the combined case.

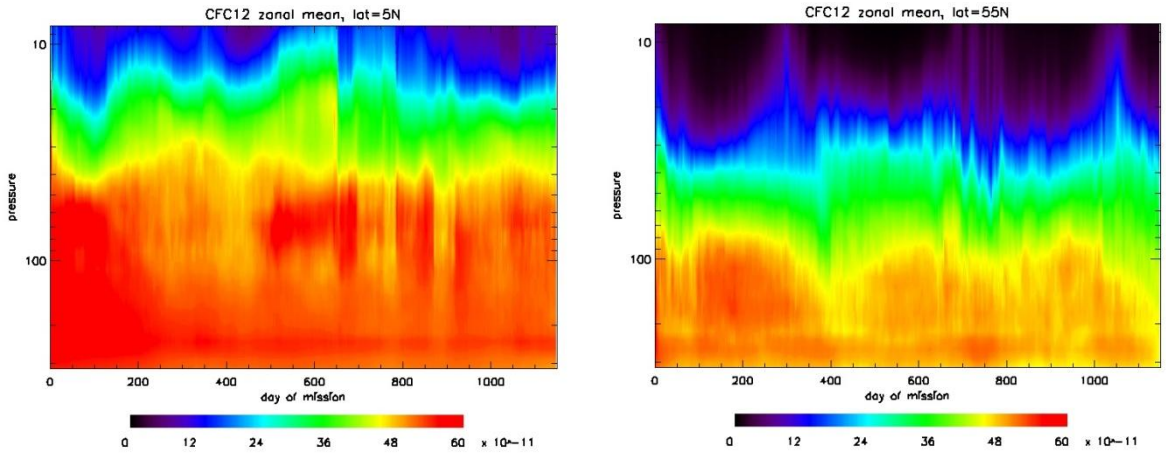

Figure 6.5.1: Time series of gridded L3 CFC12 for the entire HIRDLS mission of the zonal means at 5°N (left) and 55°N (right), all in volume mixing ratio.

Figure 6.5.2 shows that the L3 gridded zonal mean CFC12 field is a good representation of the zonal mean of the L2 data. The left panels compare the zonal averages for 2006 day 172 (the northern summer solstice) and the right panels compare the zonal averages for 2005 day 355 (the northern winter solstice). Again, the largest discrepancies are above 30 hPa. The larger vertical range shown in the level 2 plots are due to the fact that they are not filtered. Above about 8 hPa the data are associated with large variability (Figure 5.4.2b of L2 Data Quality Document), are likely to have negative precisions indicating strong a-priori influence, and are not recommended for use.

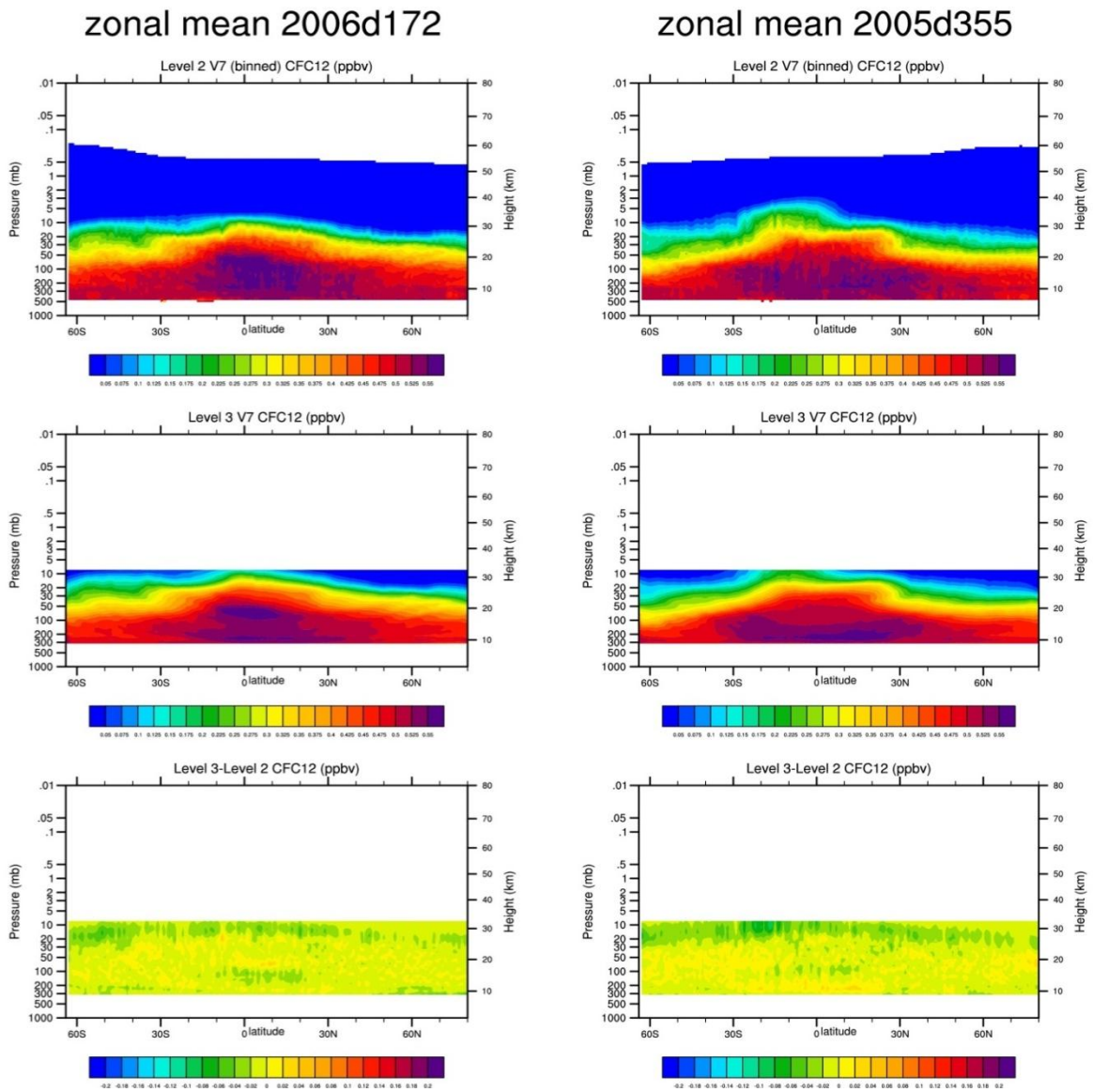

Figure 6.5.2: The upper panel shows the zonal average of individual L2 CFC12 profiles; the middle panel shows the gridded-L3 zonal mean CFC12; and the bottom shows the differences, for (left) 2006 day 172 and (right) 2005 day 355.

Figure 6.5.3 shows a standard output of the mapping routine, the RMS difference between the reconstructed field and the input data. These indicate that statistically the L3 gridded data are within the error as given earlier in the L2 section of this document (Figure 5.4.2b).

Figure 6.5.4 shows a typical example for sample day 2006d172, of a Mercator map of gridded-L3 V7 HIRDLS CFC12 at the randomly chosen pressure level, 82 hPa.

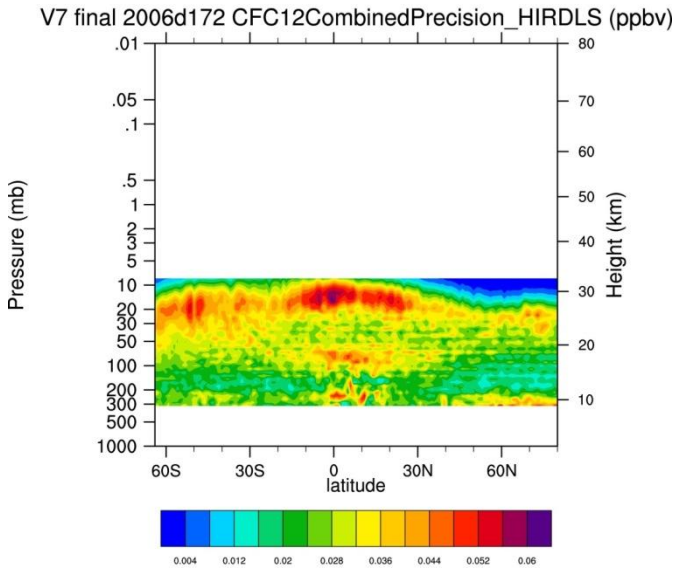

Figure 6.5.3: HIRDLS Version 7 Level 3 CFC12 precision (ppbv) for sample day 2006d172.

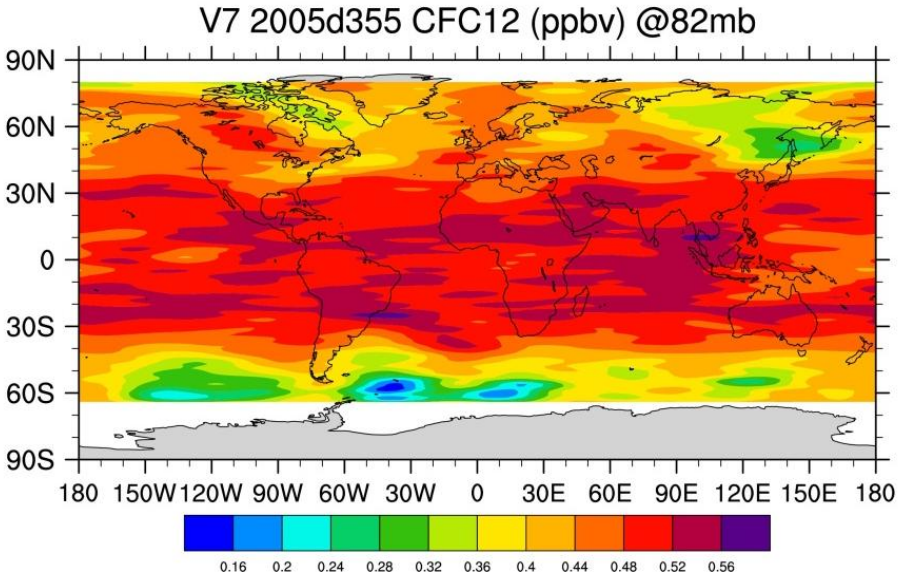

Figure 6.5.4: Mercator maps of HIRDLS Version 7 CFC12.

6.6 Water Vapor (H_2O)

Four criteria are again applied to assess the L3 water vapor data. The first is to require that the L3 fields match, within their measurement precision, the individual L2 data points they are created to represent. A standard output of the mapping routine is the rms difference between the reconstructed field and the input data. Plots of this (not shown) verify that this is the case.

A second criterion is that a gridded field, such as the zonal mean, represents the zonal mean of the L2 data. The left side of Figure 6.6.1 compares zonally averaged L2 data for day 172 (the northern summer solstice) of 2006 with the L3 zonal mean. The L2 data extend up to 0.5 hPa, but they are only recommended for use up to 10 hPa, the top level of the L3 data. There is good agreement except in the upper tropical troposphere.

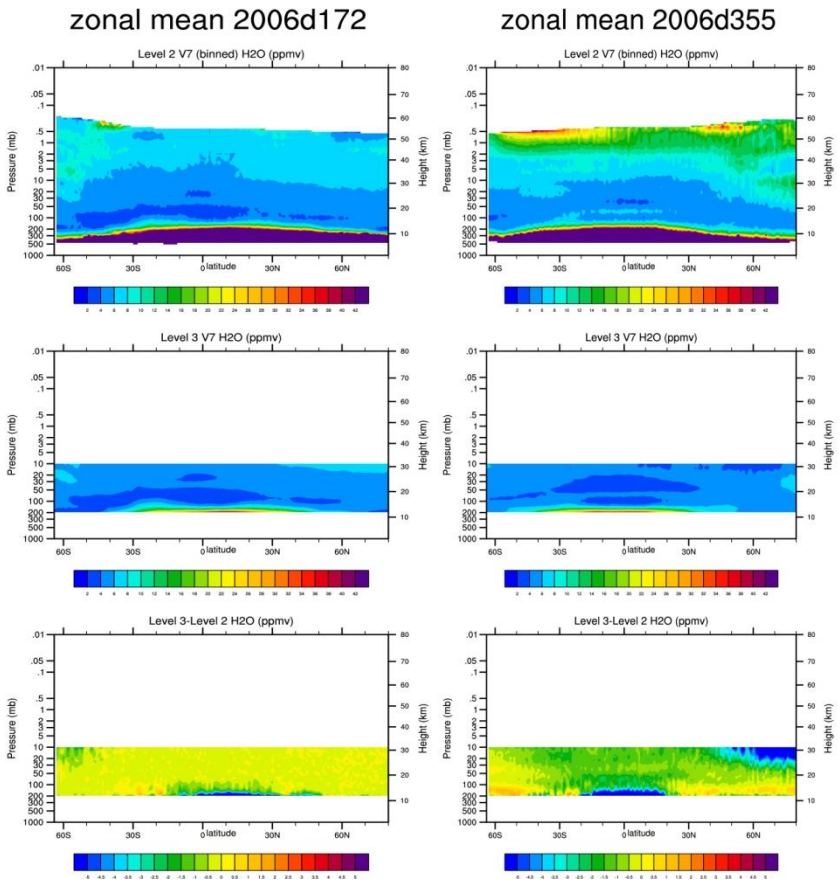

Figure 6.6.1. The upper panel presents the zonal mean water vapor mixing ratios resulting from zonally averaging the individual L2 profiles, the middle panel displays the results of the L3 gridding;, and the bottom shows the differences for a (left) 2006 day 172 and b (right) 2006day 355.

In that region differences could be due to inclusion of data with negative precision in the L2 data, while those were screened out in L3.

A different example, at the northern winter solstice, is shown in the right panel of Fig. 6.6.1. Here there are larger differences in low and mid-latitudes, as well as a region at high latitudes where the L3 data are significantly lower than the L2 mean. These again may be due to the differences in handling negative precisions, due to rapid changes which are not captured by the simple means, or due to missing L2 data. The Kalman filter would be expected to provide a better representation at any given time than a simple average of individual orbits.

A third criterion is the extent to which these reconstructed maps agree with what might be expected on physical grounds. Some examples are shown in Figure 6.6.2 where map of water vapor on the 82 hPa surface are shown. The end of the northern summer (2005 day 265) is shown on the left, where high water vapor is seen over the Tibetan plateau and at a similar latitude in the southern hemisphere, as would be expected for the effects of the Asian monsoon. The map on the right shows the figure at the end of the winter, where very low water is seen in the tropics, showing the effects of strong equatorial upwelling.

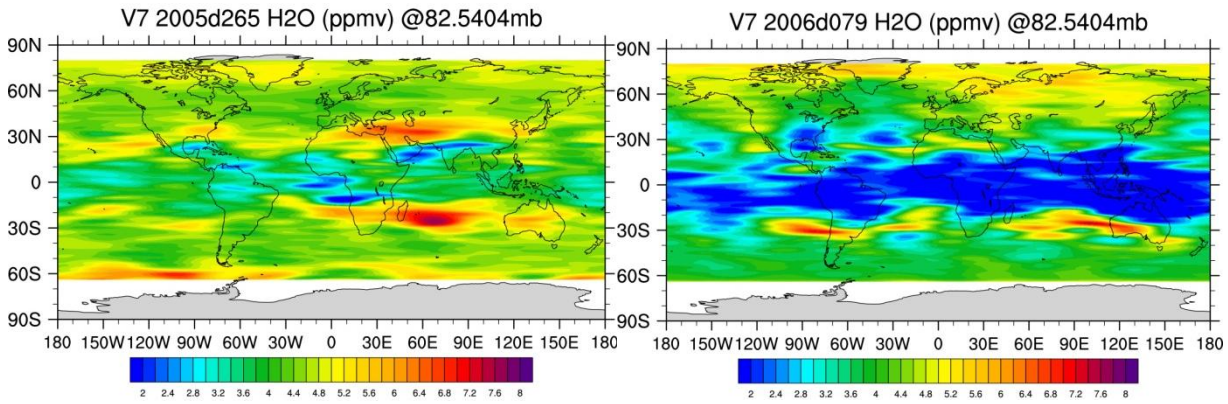

Figure 6.6.2. Maps of HIRDLS water vapor on the 82.5 hPa surface on (left) 2005 day 265 and (right) 2006 day 079.

A criterion is the extent to which these reconstructed maps agree with other maps of the water fields from trusted sources. Typical examples are shown in Figure 6.6.3 where maps of water at 82 hPa for HIRDLS V7 are compared with MLS maps, for two different dates.

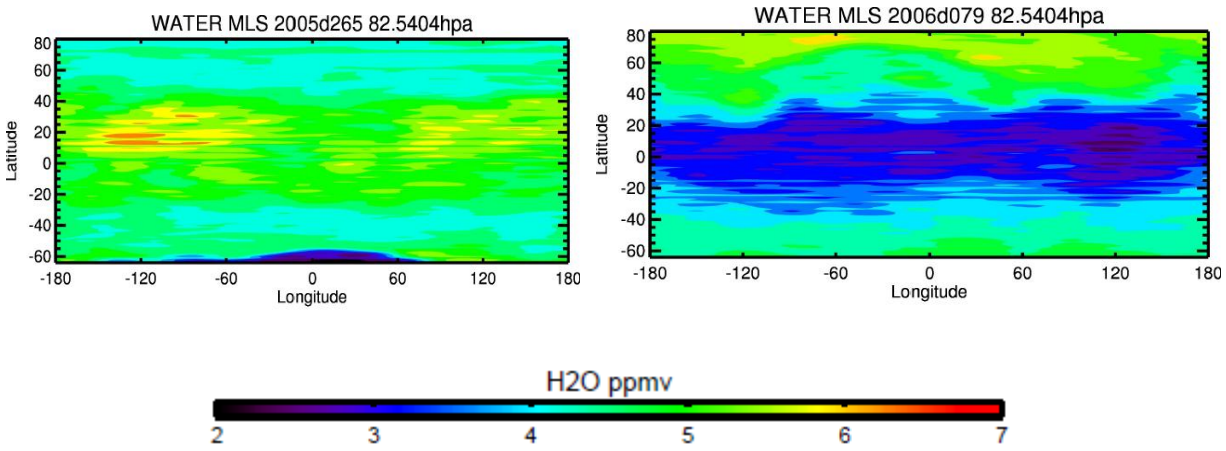

Figure 6.6.3. Maps of MLS water vapor on the 82 hPa surface on (left) 2005 day 265 and (right) 2006 day 079.

Figure 6.6.4 shows water vapor on the 34.8 hPa surface at the June and December solstices. The effects of stronger upwelling in the winter, and evidence of strong descent at high latitudes can be seen in December, and stronger descent in the southern hemisphere in June.

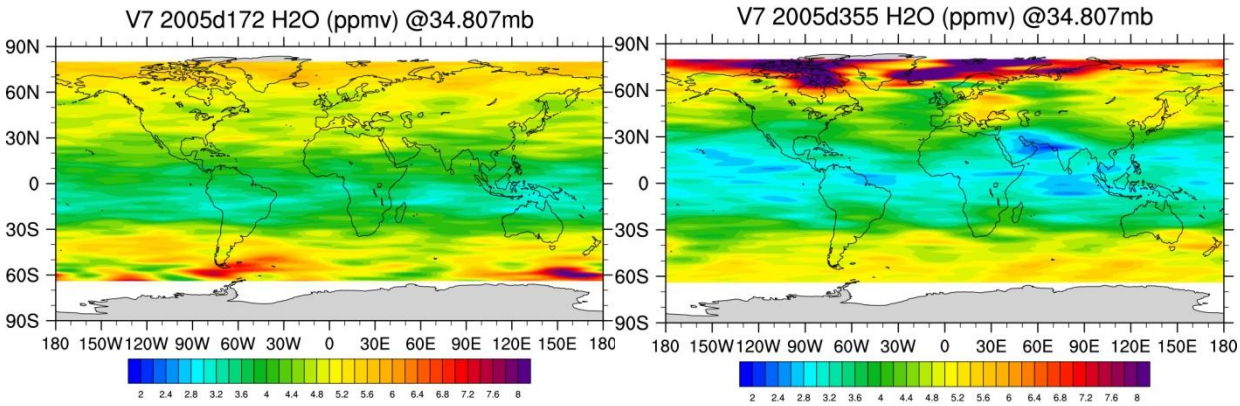

Figure 6.6.4. Maps of HIRDLS water vapor on the 34.8 hPa surface on (left) 2005 day 172 and (right) 2005 day 355.

Thus the HIRDLS maps show very reasonable horizontal distributions.

The final criterion is that there be time continuity, and the temporal variations show expected phenomena, with no periods of unexpected behavior. An example is shown in Fig. 6.6.5. In the panel, the differences between the individual day's measurements and the temporal mean, termed the anomalies, for the 5°S-5°N latitude band over the observing period are plotted. The water vapor "tape recorder" can be seen in the alternating high and low water vapor anomalies, caused by the annual variation of the tropopause temperatures, and being advected to higher altitudes with time.

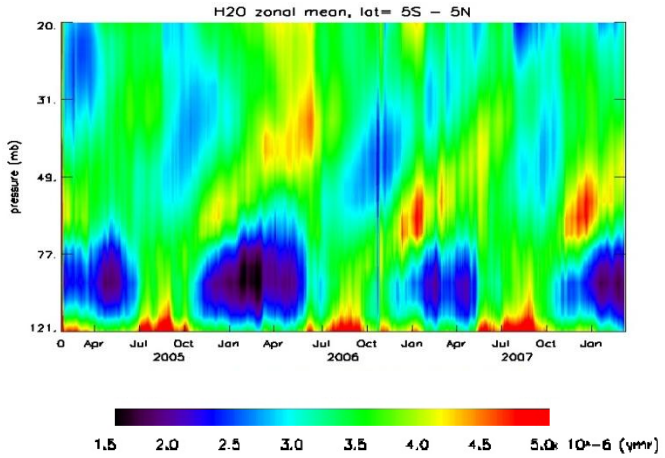

Figure 6.6.5. Zonal mean departures from the time mean water vapor (anomalies) averaged over the 5°S-5°N latitude band, showing the water vapor "tape recorder".

Another example is shown in Fig. 6.6.6 The left panel in Figure 6.6.6 displays the latitudinal and temporal variations of zonal mean HIRDLS water vapor on the 100 hPa surface, showing the low values at the equator during late northern autumn and winter. A notable feature is the indication of the transport of low water vapor to higher latitudes at this level. The right panel in Figure 6.6.6 displays the latitudinal and temporal variations of zonal mean MLS water vapor on the 100 hPa surface, also showing the low values at the equator during late northern autumn and winter. Notice the similarities between the HIRDLS and MLS data.

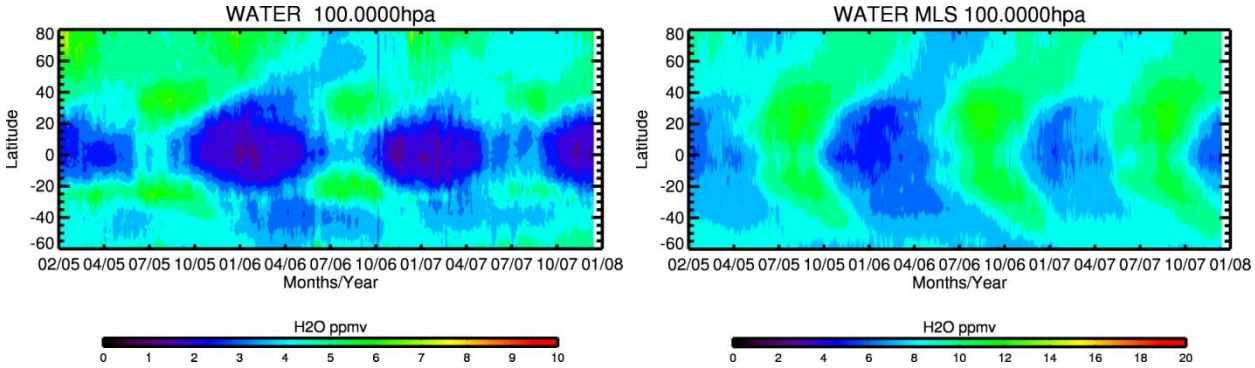

Figure 6.6.6. Zonal mean water vapor on the 100 hPa surface, for HIRDLS and MLS, all in ppmv, illustrating tropical variations driven by tropopause temperatures, and transports to mid-latitudes.

Based on these results, the L3 V7 water vapor grids are a good representation of the L2 data, show a reasonable horizontal morphology, and show the expected temporal variability.

6.7 Nitrous Oxide (N_2O)

The Combined N_2O Zonal Fourier Coefficients were created using 7 waves. Figure 6.7.1 gives pressure level versus day of mission zonal mean contour plots for Combined N_2O for a tropical latitude, 5^o N, and for a high latitude 55^o N.

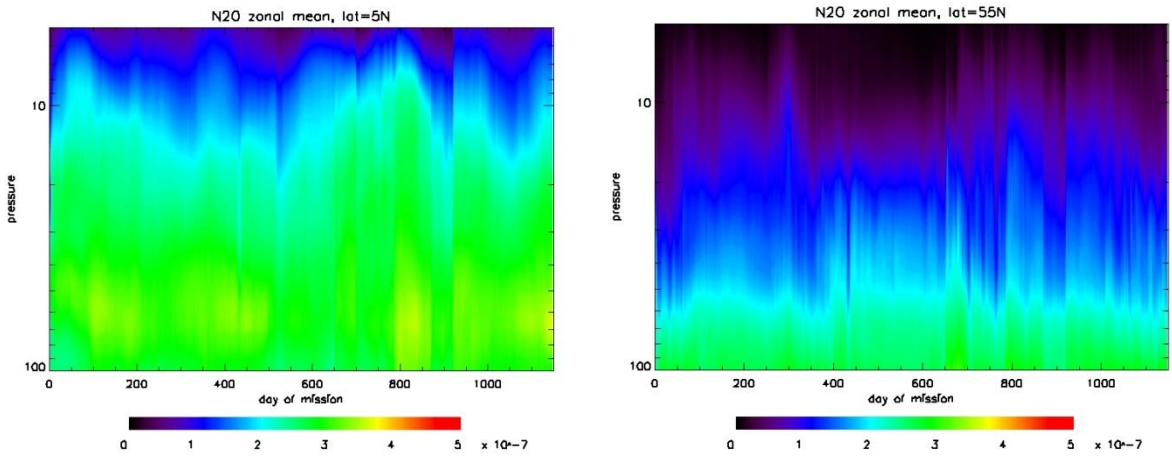

Figure 6.7.1

The Ascending and Descending N_2O Zonal Fourier Coefficients were created using 4 waves. Pressure level versus day of mission zonal mean contour plots for the Ascending and Descending modes (not shown) are similar to those for the combined case.

6.8 Nitrogen Dioxide (NO_2)

The Ascending and Descending NO_2 Zonal Fourier Coefficients were created using 4 waves.

To assess the L3 NO_2 data we first examine whether the L3 fields match, within their measurement precision, the individual L2 data points they are created to represent. A standard output of the mapping routine is the rms difference between the reconstructed field and the input data. As shown in Figure 6.8.1 a.) for the ascending case, and b.) for the descending case, for a random sample day 2006d265 , these indicate statistically the gridded L3 data are within the error of the L2 data as given earlier in this document.

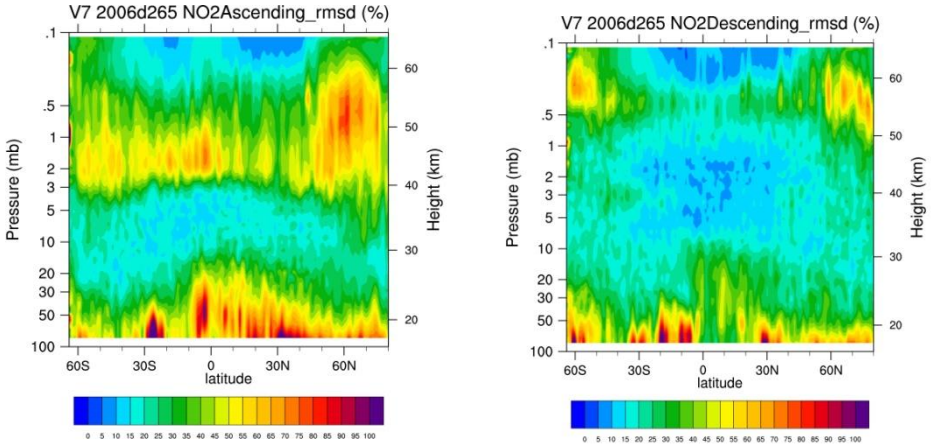

Figure 6.8.1: HIRDLS Version 7 Level 3 NO_2 a.) ascending and b.)descending precision (%) for sample day 2006d265.

The L3 gridded field zonal means also represents the zonal means of the L2 data fairly well. Figure 6.8.2 shows this for sample day 2006d265, with the L2 data not corrected for precisions. Thus, this figure illustrates an upper limit on the differences.

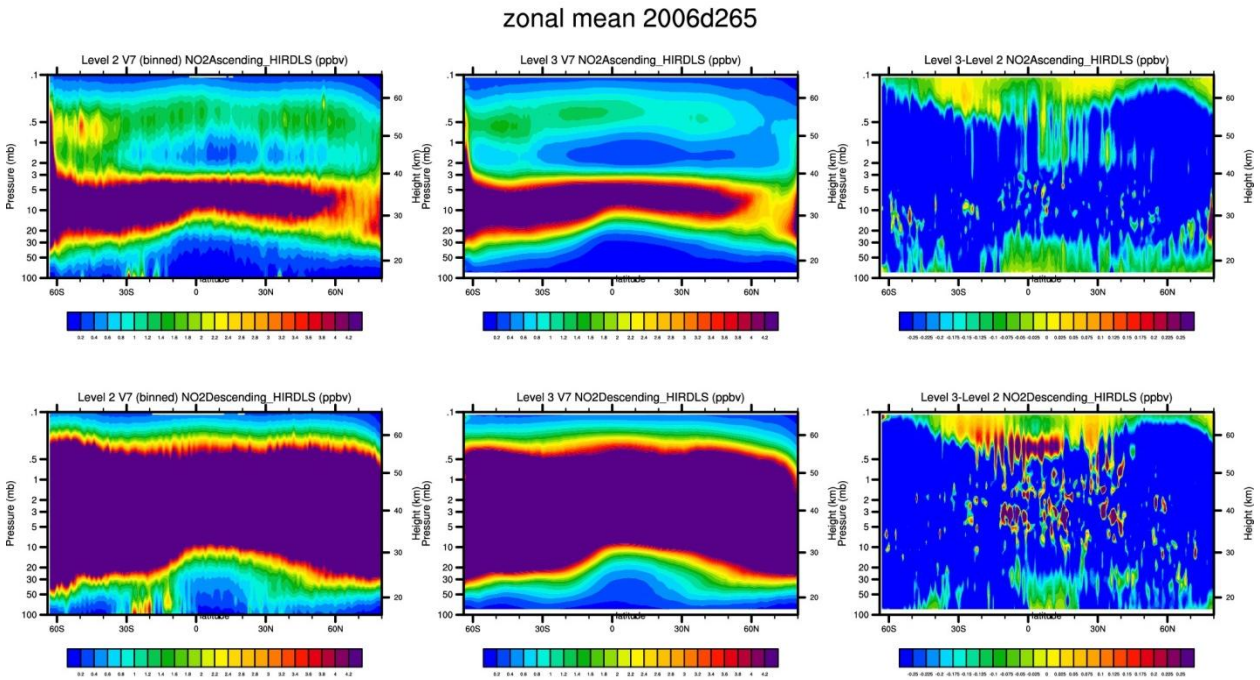

Figure 6.8.2: The top row is for the NO_2 ascending case (mostly daytime) and the bottom row is for the descending case (mostly nighttime). In all cases, the left panel displays the results of zonally averaging the individual L2 profiles, the middle panel displays the zonal mean NO_2 resulting from the L3 gridding; and the right panel shows the differences for sample day 2006d265, all in ppbv.

Another criterion is the extent to which the HIRDLS data agrees with that from trusted sources. Please see section 5.8 of this document for comparisons of HIRDLS data with MIPAS, ACE-FTS, and SD_WACCM.

The final criterion is that there be time continuity, and the temporal variations show expected phenomena, with no periods of unexpected behavior. Figure 6.8.3 gives pressure level versus day of mission zonal mean contour plots for Descending $NO_2$for a tropical latitude, 5^o N, and for a high latitude 75^o N. The 75^oN plot, in particular, shows the diurnal variation.

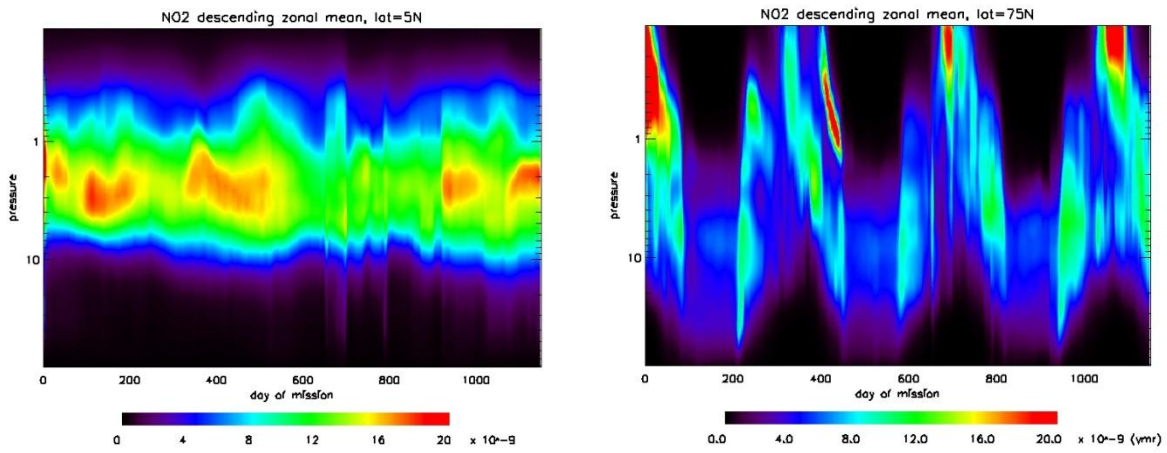

Figure 6.8.3: Descending NO_2, pressure versus day of mission, for 5°N and 75°N, in vmr.

Figure 6.8.4 gives pressure level versus day of mission zonal mean contour plots for Ascending NO_2 for a tropical latitude, 5° N, and for a high latitude 75° N. The 75°N plot shows the diurnal variation.

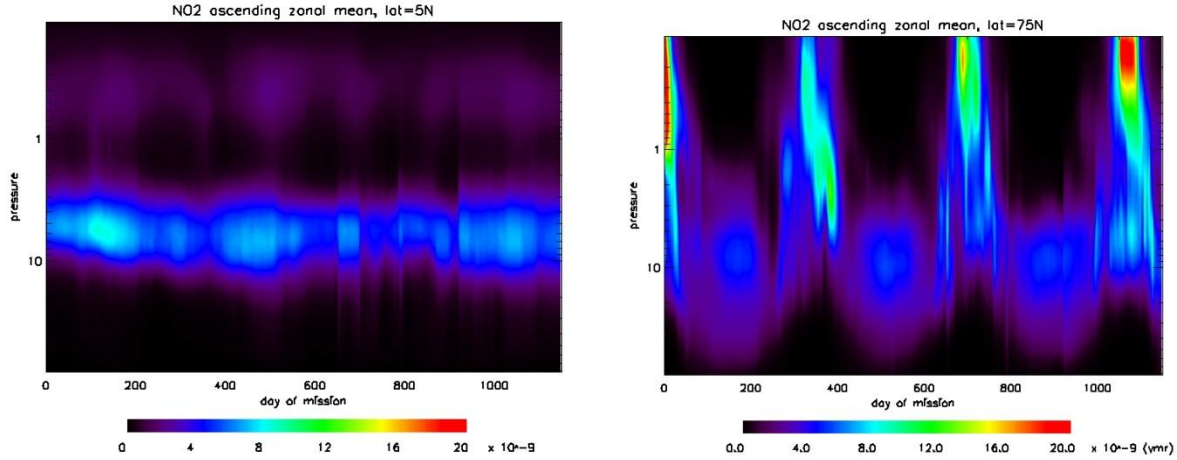

Figure 6.8.4: Ascending NO_2, pressure versus day of mission, for 5°N and 75°N, in vmr.

Based on these results, the L3 V7 NO_2 are a good representation of the L2 data, and show the expected temporal variability.

6.9 Dinitrogen Pentoxide (N_2O_5)

The Ascending and Descending N_2O_5 Zonal Fourier Coefficients were created using 4 waves.

To assess the L3 N_2O_5 data we first examine whether the L3 fields match, within their measurement precision, the individual L2 data points they are created to represent. A standard output of the mapping routine is the rms difference between the reconstructed field and the input data. As shown in Figure 6.9.1 a.) for the ascending case, and b.) for the descending case, for a random sample day 2006d265, these indicate statistically the gridded L3 data are within the error of the L2 data as given earlier in this document.

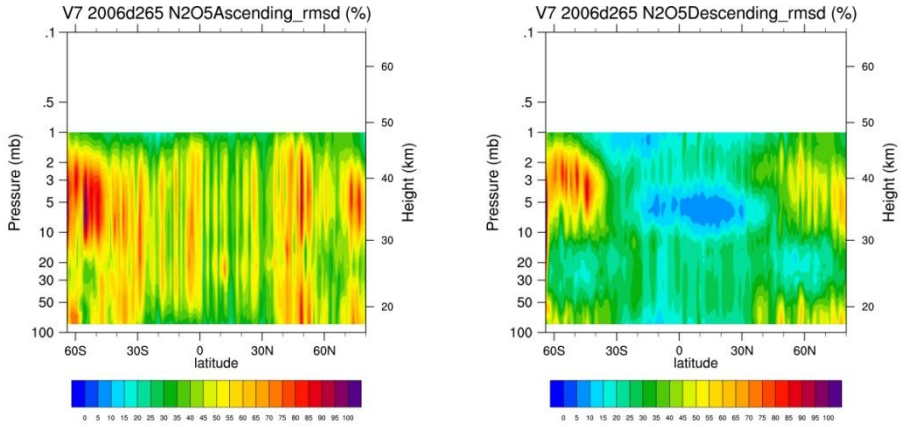

Figure 6.9.1: HIRDLS Version 7 Level 3 N_2O_5 a.) ascending and b.) descending precision (%) for sample day 2006d265.

The L3 gridded field zonal means also represents the zonal means of the L2 data fairly well. Figure 6.9.2 shows this for sample day 2006d265, with the L2 data not corrected for precisions. Furthermore, the N_2O_5 Level 3 data has been corrected according to Table 5.9.1 of this document. Thus, this figure illustrates an upper limit on the differences.

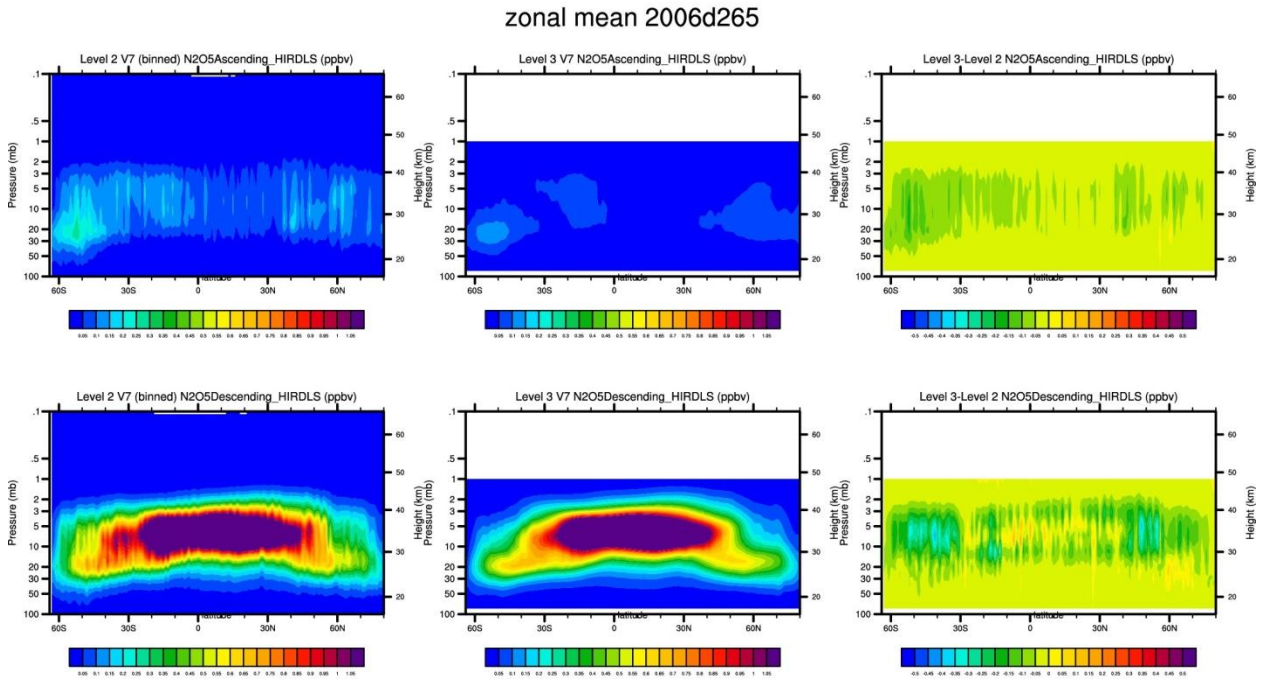

Figure 6.9.2: The top row is for the N_2O_5 ascending case and the bottom row is for the descending case. In all cases, the left panel displays the results of zonally averaging the individual L2 profiles, the middle panel displays the zonal mean N_2O_5 resulting from the L3 gridding; and the right panel shows the differences for sample day 2006d265, all in ppbv.

Another criterion is the extent to which the HIRDLS data agrees with that from trusted sources. Please see section 5.9 of this document for comparisons of HIRDLS data with MIPAS, ACE-FTS, and SD_WACCM.

The final criterion is that there be time continuity, and the temporal variations show expected phenomena, with no periods of unexpected behavior. Figure 6.9.3 gives pressure level versus day of mission zonal mean contour plots for Descending N_2O_5 for a tropical latitude, 5^o N, and for a high latitude 75^o N. The 75^oN plot shows the diurnal variation.

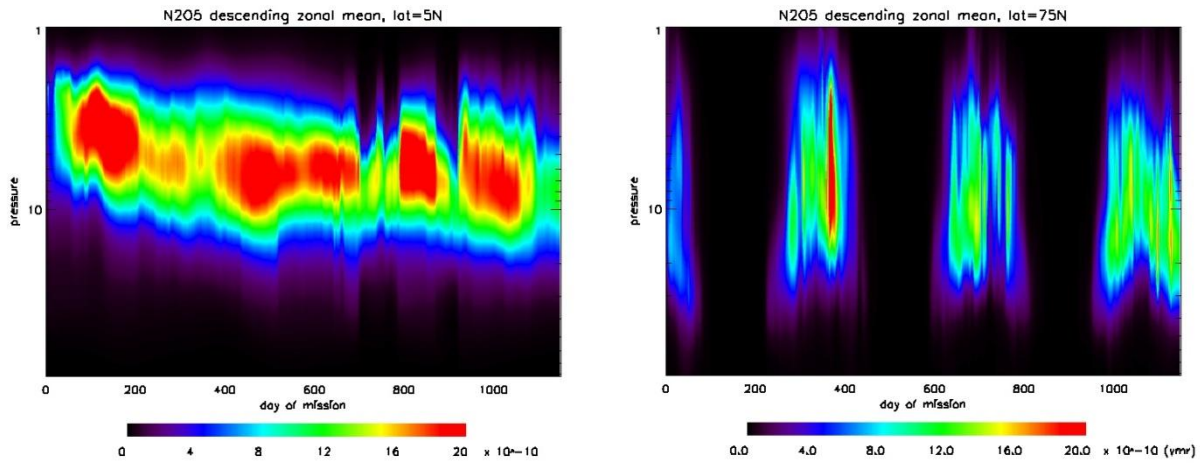

Figure 6.9.3: Descending N_2O_5, pressure versus day of mission, for 5°N and 75°N, in vmr.

Figure 6.9.4 gives pressure level versus day of mission zonal mean contour plots for Ascending N_2O_5 for a tropical latitude, 5^o N, and for a high latitude 75^o N. The 75°N plot shows the diurnal variation.

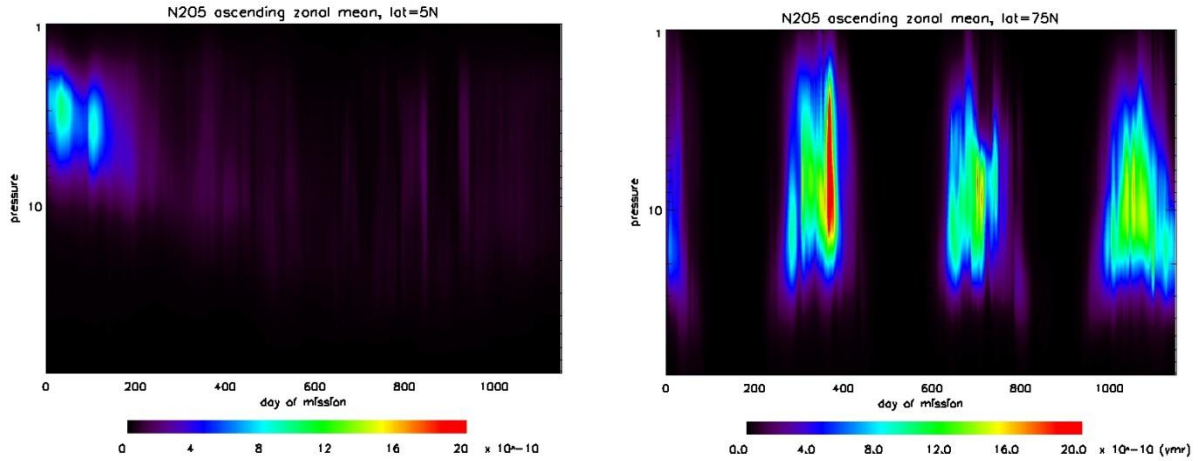

Figure 6.9.4: Ascending N_2O_5, pressure versus day of mission, for 5°N and 75°N, in vmr.

Based on these results, the L3 V7 N_2O_5 are a good representation of the L2 data, and show the expected temporal variability.

6.10 Chlorine Nitrate ($ClONO_2$)

The Ascending and Descending $ClONO_2$ Zonal Fourier Coefficients were created using 4 waves.

To assess the L3 $ClONO_2$ data we first examine whether the L3 fields match, within their measurement precision, the individual L2 data points they are created to represent. A standard output of the mapping routine is the rms difference between the reconstructed field and the input data. As shown in Figure 6.10.1 a.) for the ascending case, and b.) for the descending case, for a random sample day 2006d265, these indicate statistically the gridded L3 data are within the error of the L2 data as given earlier in this document.

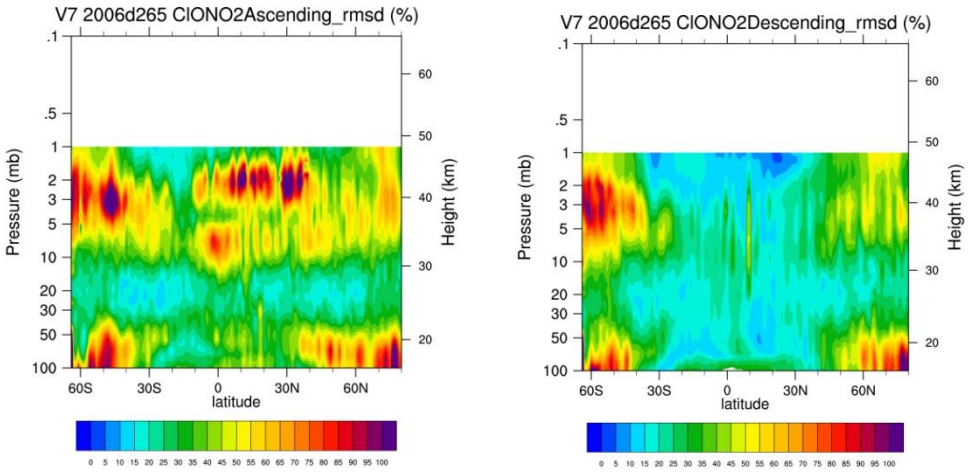

Figure 6.10.1: HIRDLS Version 7 Level 3 $ClONO_2$ a.) ascending and b.) descending precision (%) for sample day 2006d265.

The L3 gridded field zonal means also represents the zonal means of the L2 data fairly well. Figure 6.10.2 shows this for sample day 2006d265, with the L2 data not corrected for precisions. Furthermore, the $ClONO_2$ Level 3 data has been corrected according to Table 5.10.1 of this document. Thus, this figure illustrates an upper limit on the differences.

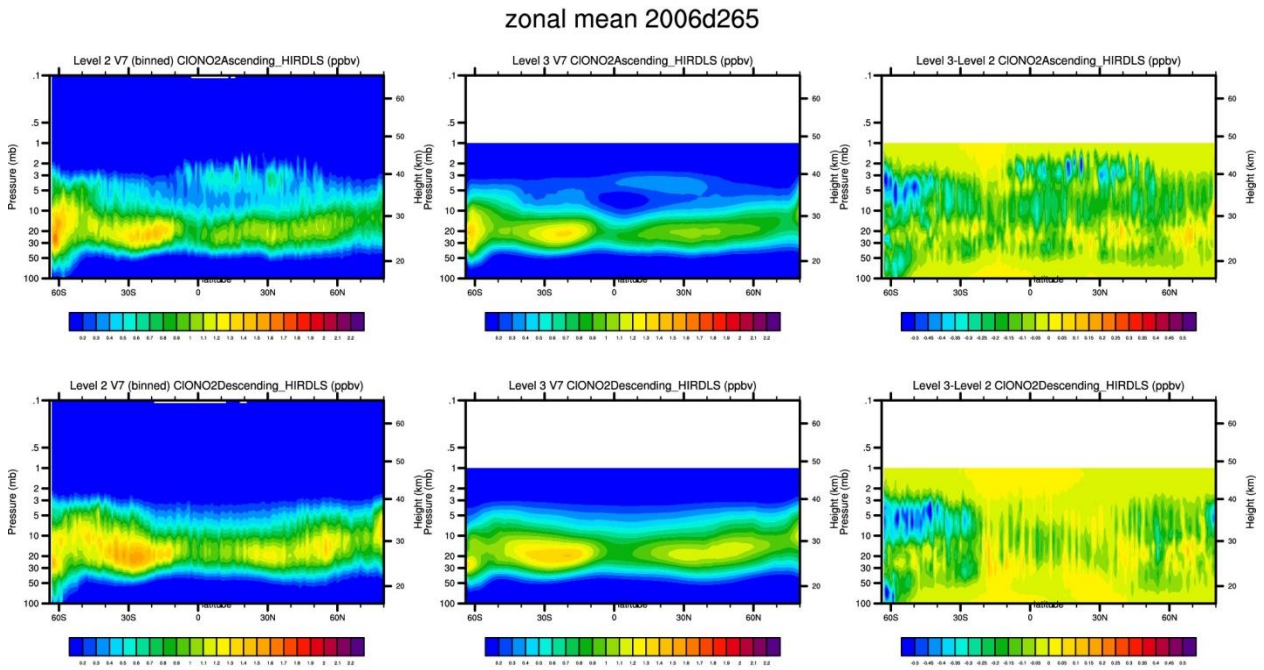

Figure 6.10.2: The top row is for the $ClONO_2$ ascending case and the bottom row is for the descending case. In all cases, the left panel displays the results of zonally averaging the individual L2 profiles, the middle panel displays the zonal mean $ClONO_2$ resulting from the L3 gridding; and the right panel shows the differences for sample day 2006d265, all in ppbv.

Another criterion is the extent to which the HIRDLS data agrees with that from trusted sources. Please see section 5.10 of this document for comparisons of HIRDLS data with MIPAS, ACE-FTS, and SD_WACCM.

The final criterion is that there be time continuity, and the temporal variations show expected phenomena, with no periods of unexpected behavior. Figure 6.10.3 gives pressure level versus day of mission zonal mean contour plots for descending $ClONO_2$ for a tropical latitude, 5^o N, and for a high latitude 75^o N.

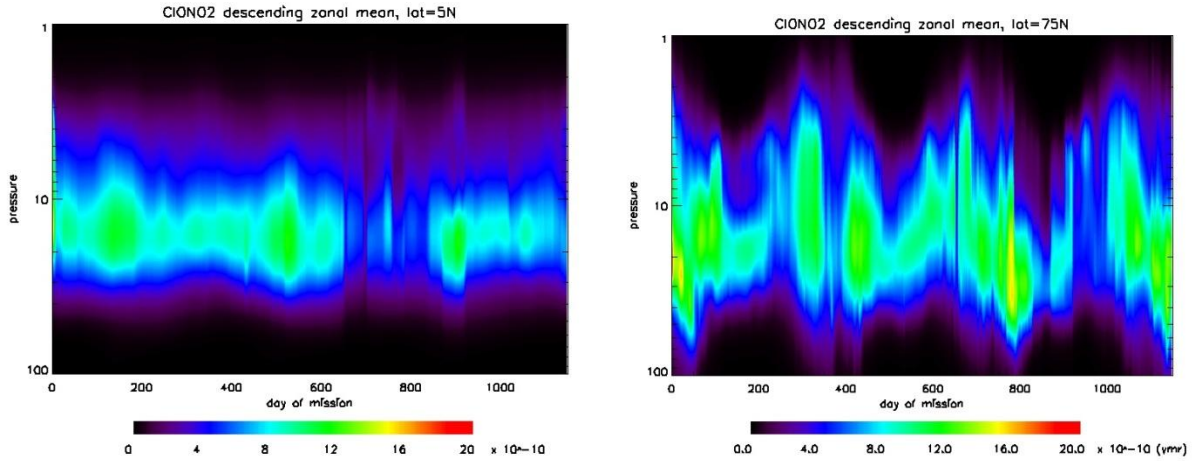

Figure 6.10.3: Descending $ClONO_2$, pressure versus day of mission, for 5^oN and 75^oN, in vmr.

Figure 6.10.4 gives pressure level versus day of mission zonal mean contour plots for Ascending $ClONO_2$ for a tropical latitude, 5^o N, and for a high latitude 75^o N.

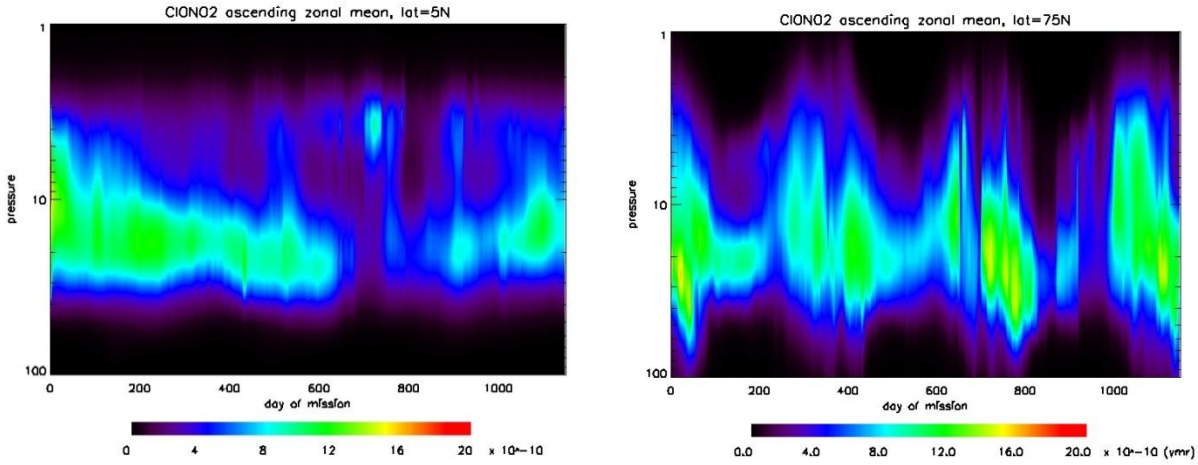

Figure 6.10.4: Ascending $ClONO_2$, pressure versus day of mission, for 5^oN and 75^oN, in vmr.

Based on these results, the L3 V7 $ClONO_2$ are a good representation of the L2 data, and show the expected temporal variability.

6.11 L3 Geopotential Height (GPH)

The L3 GPH products match the L2 data they are created to represent fairly well. A standard output of the mapping routine is the rms difference between the reconstructed field and the input data. As shown in Figure 6.11.1 for a random sample day 2006d265 , these indicate statistically the gridded L3 data are within the error of the L2 data as given earlier in this document.

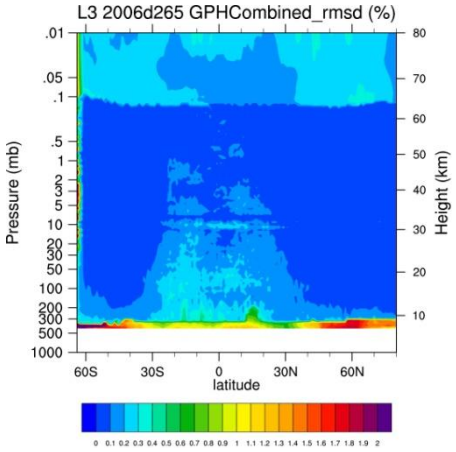

Figure 6.11.1: HIRDLS Version 7 Level 3 GPH precision (%) for sample day 2006d265.

The L3 gridded field zonal means also represents the zonal means of the L2 data fairly well. Figure 6.11.2 shows this for sample day 2006d265, with the L2 data not corrected for precisions; thus this is an upper limit on the differences. There is good agreement up to 0.1 hPa, except possibly at high southern latitudes.

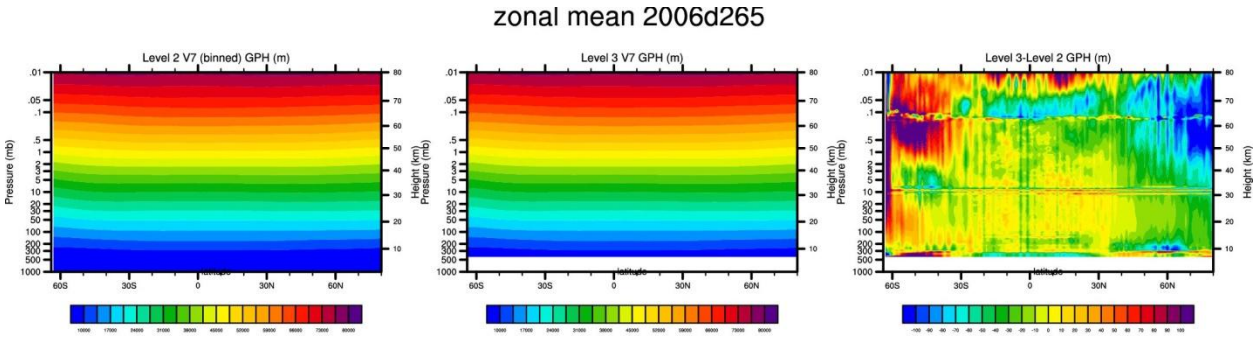

Figure 6.11.2: The left panel displays the results of zonally averaging the individual L2 profiles, the middle panel displays the zonal mean temperatures resulting from the L3 gridding; and the right panel shows the differences for sample day 2006d265, all in meters.

The HIRDLS Level 3 GPH maps agree well with other maps of the GPH. A typical example is shown for our sample day, 2006d265, in Figure 6.11.3 for Mercator maps of GPH at a randomly chosen level, 100 hPa, for HIRDLS V7 and GEOS5.

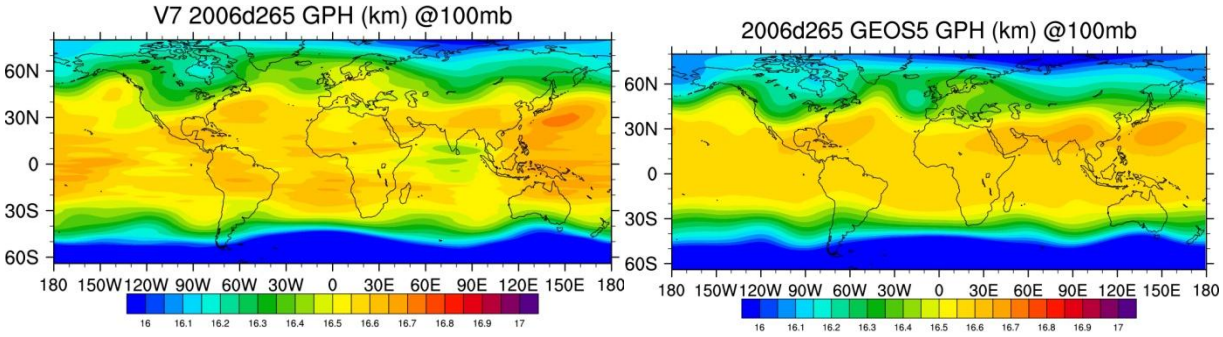

Figure 6.11.3: Mercator maps of HIRDLS (left) and GEOS5 (right) GPHs on the 100 hPa surfaces for 2006 day 265, in kilometers.

The HIRDLS maps show all the major features seen in the GEOS5 data, although of course features smaller than WN 7 are not represented.

To examine the time continuity and look for any periods of anomalous behavior, the time series for the entire HIRLDS mission of the zonal means at 5°N (left) and 55°N (right) are shown in Figure 6.11.4. Both of these plots indicate GPH shows good time continuity and no anomalous behavior.

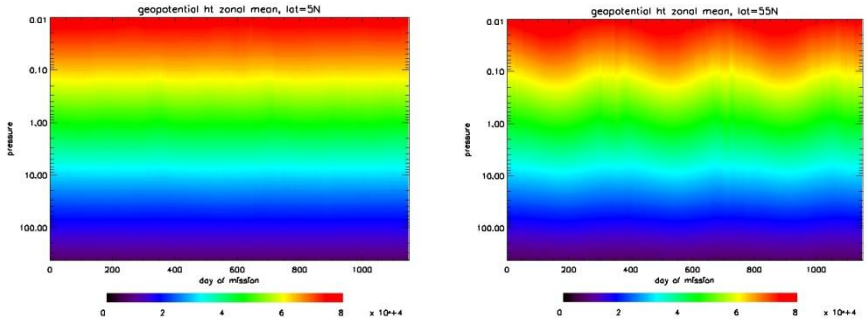

Figure 6.11.4: Time series of GPH for the entire HIRDLS mission of the zonal means at 5°N (left) and 55°N (right), all in 10^4 meters.

Based on these results, the Level 3 Version 7 GPHs are a good representation of the Level 2 data, and in good agreement with GEOS5 data.

6.12 - 12.1 and 8.3 Micron Extinction

The Combined 12.1micron extinction Zonal Fourier Coefficients were created using 7 waves. Figure 6.12.1 displays 12.1 micron extinction for March 20, 2006. One sees both stratospheric aerosol and cirrus extinction in this zonal average. Of the two extinction products (12.1 and 8.3 micron data), the 12.1 micron data is most informative since gaseous absorption is very low (compared to the aerosol and cirrus contributions to the optical depths along the observation ray paths) in the 12.1 micron data.

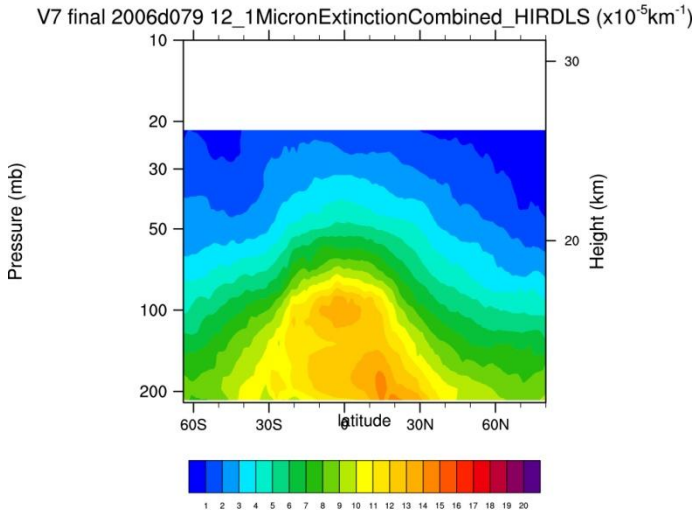

Figure 6.12.1 Micron Extinction for March 20, 2006

Figure 6.12.2 gives pressure level versus day of mission zonal mean contour plots for Combined 12.1 micron extinction for a tropical latitude, 5^{o} N, and for a high latitude 55^{o} N.

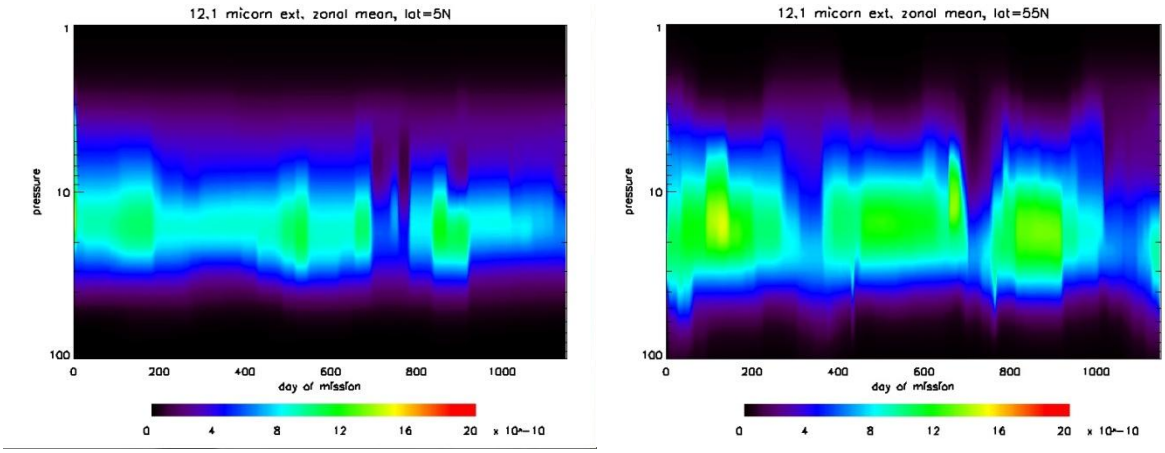

Figure 6.12.2 Pressure level versus day of mission zonal mean 12.1 micron extinction

The Ascending and Descending 12.1 micron extinction Zonal Fourier Coefficients were created using 4 waves. Pressure level versus day of mission zonal mean contour plots for the Ascending and Descending modes (not shown nor included in the L3 data) are similar to those for the combined case.

8.3 Micron Extinction The Combined 8.3micron extinction Zonal Fourier Coefficients were created using 7 waves. Figure 6.12.3 displays 8.3 micron extinction values for March 20, 2006. One sees both stratospheric aerosol and cirrus extinction in this zonal average. As remarked above, the 8.3 micron extinction data is not as informative as that of the 12.1 extinction data.

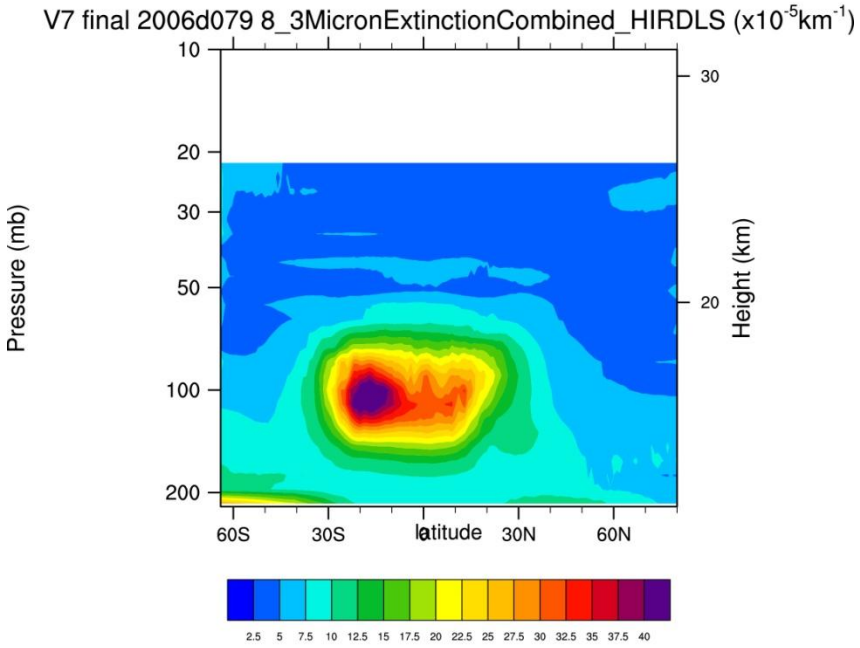

Figure 6.12.3 8.3 micron extinction values for March 20, 2006

Figure 6.12.4 gives pressure level versus day of mission zonal mean contour plots for Combined 8.3 micron extinction for a tropical latitude, 5^{o} N, and for a high latitude 55^{o} N.

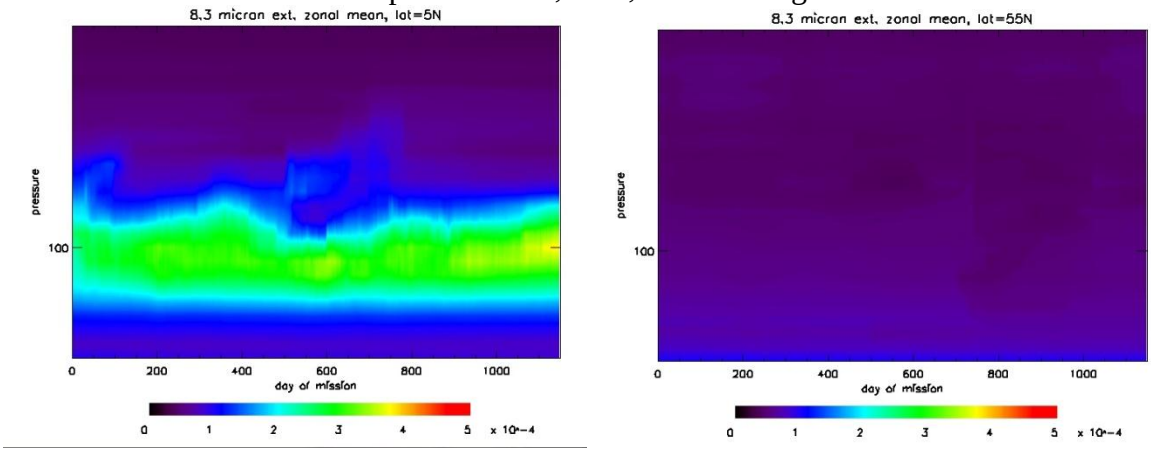

Figure 6.12.4 Pressure level versus day of mission zonal mean 8.3 micron extinction

The Ascending and Descending 8.3 micron extinction Zonal Fourier Coefficients were created using 4 waves. Pressure level versus day of mission zonal mean contour plots for the Ascending and Descending modes (not shown) are similar to those for the combined case.

7.0 Data File Structure and Content

Contact: Vince Dean
Email: vdean@ucar.edu

HIRDLS Level 2 and Level 3 data are stored in the HDF-EOS5 format and the fields are as described in the HDF-EOS Aura File Format Guidelines document[2]. These data files can be read via C/C++ or Fortran using either the HDF-EOS5 or HDF5 library. HIRDLS has developed both an IDL routine "get_aura" and a set of Fortran90 routines to access the HIRDLS Level 2 data. Both of these routines are available for download via the HIRDLS web site, http://www.eos.ucar.edu/hirdls/data/access.shtml. The routines can also be supplied via email upon request.

Users should obtain the pre-compiled HDF5 library for their operating system, if possible, otherwise source code is also available from the HDF Group (see http://www.hdfgroup.org). These are prerequisite in order to compile the HDF-EOS5 library (see http://www.hdfeos.org/). Both libraries are needed to fully access the Aura HIRDLS data files. For additional help contact the GES DISC at help-disc@listserv.gsfc.nasa.gov or telephone 301-614-5224.

Level 2 Files

Each HIRDLS Level 2 file contains one day's worth of data and contains all species that HIRDLS measures. For users who require only a subset of the HIRDLS species, the GES DISC has the ability to subset data before distributing it to users. Contact the DISC directly for more information on this service.

Individual HIRDLS data values for a product are stored in fields labeled with the species name (see the appropriate section above for the exact Data Field Name). The estimated precision of each data point is a corresponding field named *Species*Precision (for instance, Temperature and TemperaturePrecision). Two additional fields for each species, *Species*NormChiSq and *Species*Quality, are filled with “missing values” for V7. CloudTopPressure does not have Precision, NormChiSq or Quality fields.

There are two time fields in the HIRDLS data files, Time and SecondsInDay. Time is stored in TAI time (seconds since the epoch of 00.00 UTC 1-1-1993). The conversion between TAI time and UTC time requires correcting for leap seconds, and is not entirely straightforward. For this reason, HIRDLS also stores SecondsInDay, or seconds since midnight of the data day. Leap seconds do not pose a problem when using this field. Note that the SecondsInDay for the first data point of a day may be negative, indicating a time stamp before midnight. This is normal when the first profile of day spans a day boundary.

Level 3 Data Products

HIRDLS V7 will include two level 3 data products. One, which is new with V7, will contain zonal Fourier coefficients. The other contains a gridded column of daytime stratospheric NO_2 first released with V6. Both are produced using the Kalman mapping procedure.

The file structure for these products will be documented in the updated Data Quality document for HIRDLS V7 that includes Level 3 products.

http://earthdata.nasa.gov/library/esds-rfc-009

8.0 Version History

The HIRDLS version number appears in the file name. The GEOS-DISC identifies the versions by "collection number", 001 through 006.

HIRDLS Version	GES-DISC Collection Number	Changes
2.00	001	[Baseline]
2.01		Modified to process Scan Table 22
2.02.07	002	Modified to process Scan Tables 30, 13, 22 and 23
2.04.09	003	Modified to include more precise geo-location, updated cloud detection, updated calibration constants, and bug fixes.
2.04.19	004	Added new products: CFC11, CFC12, 12.1 micron aerosol extinction. Implemented updated open area fractions, improved cloud detection and out-of-field correction. Added correction for instrument-spacecraft alignment (equivalent to 2 km shift).
5.00.00	005	Includes packet checksum check; decreases tangent pt. altitude by 250 m; changes radiance scale factors and adds offsets; uses NoiseFac3 for radiance error spectrum, consistent with the latest Open Area Fraction (OAF) values (12/19/2008); incorporates 4/30/08 deoscillation Empirical Orthogonal Function (EOF) values; has +4-2 interpolation for el. angle tie-on; corrects C++ de-oscillator, adjusts alt. range that the boresight must cover to allow processing of ST30; corrects descaling/scaling of rad. errors; uses GEOS-5.1.0 for T radiance adjustment (v24), LOS gradient correction, and T *a priori*; corrects OrbAscFlag; adds capability to selectively adjust radiances

HIRDLS Version	GES DISC Collection Number	Changes
5.00.00 (con't)	005	by channels; adds OrbitNumber and SpacecraftDayFlag fields to HIRRADNC file; radiance adj. done on all channels except 7, 8, 9 (i.e., HNO3 and CFCs not adjusted); looks for clouds at lower altitude if too many negative radiances; uses toolkit 5.2.15; upgrades to Fortran compiler 10.1.015; releases GPH as new product; reduced output pressure levels from .001 to .01; includes option for using GEOS O_3 and H_2O for *a priori*; adds OrbitNumber as a field in the output files; can now retrieve H_2O using channels 18 and 20 separately; capability to use 72-level GEOS data; applies geoid correction for GPH calculations; adds new Raw and Smoothed GPH calculations; includes capability to adjust input *a priori* errors at/below cloud tops or 10 km, whichever is higher; reduces T and O_3 *a priori* errors at these levels to 2k and 75%, respectively; radiance and retrieval ranges are now specified in altitude instead of pressure; T is retrieved to 120 km; number of diverged retrievals (dropouts) is substantially reduced, especially for T; improves lower mesospheric T retrievals;
V6.00.00	006	Updated radiance error value; removes radiance error bandpass reduction; uses WAACM93 / MLS v3.33/Mozart for contaminants; corrected gamma_evalue; incorporated the latest GPH algorithm; incorporated up-scan 2x2 (no substitution) kapton correction scheme; incorporated the new deoscillation 25-fcn EOF files and algorithm (single window fitting for atmospheric EOFs and ST23 EOF set selection); uses radiance adjustment file v26 cycle 6

HIRDLS Version	GES DISC Collection Number	Changes
6.00.00 (con't)	006	(lower top level in radiance adjustments, and no adjustments for channels 15, 16, 17, 18, 20); incorporated changes in L2 algorithm and new L3 algorithm to output daily zonal means of day/night NO_2 and N_2O_5 as well as NO_2 stratospheric columns; producing monthly means of Ice Water Content (IWC).
7.00.00	**V7**	L1X - opened up chopper frequency screening criterion to 7.5Hz, to allow more days to be processed L1C - deleted some unused fields; updated bad date/time exclusions; handles 25EOF deoscillation scheme; added 13 point triangular filtered spaceview radiances before calculating mean profile tie-on; kapton correction tie-on in elevation angle space; kapton correction EOF coefficient generation uses smoothed scan radiances; uses >1 Pitch Up day to calculate means to handle temporal variations thru-out mission; remove negative radiances, SV=0; handles Scan Tables 13 & 30 L2PP - added logic to smooth tangent height altitude; incorporates radiance adjustment file v27c19 L2 - updated GPH routine; extended NO2 retrieval top to 65km; implemented aerosol/instrument correction (retrieves ch 6 aero extinction in each block & uses aero spectral model to obtain approx. aero extinction for channels involved); retrieves all products w/ Forward Model 1 in stage 1 and Forward Model 2 in stage 2; uses MLSColloc 2.5 (WACCM daily instead of

HIRDLS Version	GES DISC Collection Number	Changes
		MOZART monthly mean) for contaminants L3 - added code to produce additional zonal fourier coefficient products and gridded maps (45 products in all)

9.0 References

Barnett, et al., [2008]; Cross-validation of HIRDLS and COSMIC radio-occultation retrievals, particularly in relation to fine vertical structure, Proceedings of the SPIE, 7082, 16-7, doi:10.1117/12.800702,2008. 739, 745,747.

Boone, C, et al, [2005]; Retrievals for the atmospheric chemistry experiment Fourier Tranform Spectrometer, Applied Optics, 44(33), 7218-7231.

Collins, W. D., et al., [2004]; Description of the NCAR Community Atmosphere Model (CAM3), NCAR Technical Note, NCAR/TN-464+STR, 226 pp.

Dee, D.P., S.M. Uppala and A.J. Simmons, et al., [2011]; The ERA-Interim reanalysis: configuration and performance of the data assimilation system , Q. J. Roy. Met. Soc. 137, 553-597.

Edwards, D.P., J. C. Gille, P. L. Bailey, and J. J. Barnett, "Selection of sounding channels for the High Resolution Dynamics Limb Sounder," App. Opt., vol. 34, no. 30, pp.7006-70018, 20 October, 1995.

Elkins J.W., Thompson T.M., Swanson T.H., Butler J.H., Hall B.D., Cummings S.O., Fisher D.A. and Raffo A.G., [1993]; Decrease in the growth rates of atmospheric chlorofluorocarbons 11 and 12. *Nature* **364**, 780-783.

Garcia, R. R., et al., [2007]; Simulations of secular trends in the middle atmosphere, J. Geophys. Res., 112, D09301, doi:10.1029/2006JD007485.

Gille et al. [2008]; The High Resolution Dynamics Limb Sounder (HIRDLS): Experiment Overview, Results and Validation of Initial Temperature Data, *Journal of Geophysical Research*; doi:10.1029/2007JD008824.

Gille et al. [2010]; Advances in Modeling the Obstruction I the HIRDLS Optical Train, and Resulting Data, Proc. of SPIE Vol. 7808, 780813, doi: 10.1117/12.860907.

Hoepfner at al. [2007]; "Validation of MIPAS ClONO2 measurements", Atmospheric Chemistry and Physics, 7, pp.257-281.

Hoffman, et al. [2008]; Envisat MIPAS measurements of CFC-11: retrieval, validation, and climatology, Chemistry and Physics Discussions 8, 2, 4561-4602.

Kerzenmacher, T., et al., [2008]; "Validation of NO2 and NO from the Atmospheric Chemistry Experiment (ACE)", ACP, 8, 5801-5841.

Khosravi, R., et al., [2009a]; Overview and characterization of retrievals of temperature, pressure, and atmospheric constituents from the High Resolution Dynamics Limb Sounder (HIRDLS) measurements, J. Geophys. Res., 114, D20304, doi:10.1029/2009JD011937.

Khosravi, R., et al., [2009b]; Correction to ‘‘Overview and characterizati7/17/2011on of retrievals of temperature, pressure, and atmospheric constituents from High Resolution Dynamics Limb Sounder (HIRDLS) measurements,’’ J. Geophys. Res., 114, D23399, doi:10.1029/2009JD013507.

Kinnison, D. E., et al., [2007]; Sensitivity of chemical tracers to meteorological parameters in the MOZART-3 chemical transport model, J. Geophys. Res., 112, D20302, doi:10.1029/2006JD007879.

Kinnison et al., [2008]; Global Observations of HNO3 from the High Resolution Dynamics Limb Sounder (HIRDLS) – First Results, *Journal of Geophysical Research*; doi:10.1029/2007JD008814.

Kohri, W.J., [1981]; LRIR Observations of the Structure and Propagation of the Stationary Planetary Waves in the Northern Hemisphere during December, 1975; Cooperative Thesis No. 63, Drexel University and National Center for Atmospheric Research.

Massie et al., [2007]; High Resolution Dynamics Limb Sounder observations of polar stratospheric clouds and subvisible cirrus, *J. Geophys. Res.*, *112*, D24S31, doi:10.1029/2007JD008788.

McLinden, C.A., Haley, C.S., Sioris, C.E.,[2000]; “Diurnal effects in limb scatter observations”, J. Geophys. Res., 111(D14), pp 302.

Mergenthaler, J.L, et al., [1999]; Cryogenic Limb Array Etalon Spectrometer observations of tropical cirrus, Journal of Geophysical Research, Vol. 104, No. D18, pps. 22,183 – 22194.

Mote, P., K. Rosenlof, M. McIntyre, E. Carr, J. Gille, J. Holton, J. Kinnersley, H. Pumphrey, J. Russell III and J. Waters (1996), An atmospheric tape recorder: The imprint of tropical tropopause temperatures on stratospheric water vapor. *J. Geophys. Res. 101*, 3989-4006.

Nardi et al., [2008]; Validation of HIRDLS Ozone Measurements, *Journal of Geophysical Research*; doi:10.1029/2007JD008837.

Prather, M.J.,[1997]; “Catastrophic loss of stratospheric ozone in dense volcanic clouds”, J. Geophys. Res., 97, 10.187-10.191.

Remsberg E.E., et. al, [1990]; Estimation of Synopic Fields of Middle Atmosphere Parameters from Nimbus-7 LIMS Profile Data; Journal Atmos. And Oceanic Tec., Oct, 1990, p. 689.

Remsberg, E. E., et al., [2008]; Assessment of the quality of the Version 1.07 temperature-versus-pressure profiles of the middle atmosphere from TIMED/SABER, *J. Geophys. Res., 113*, D17101, doi:10.1029/2008JD010013.

Richter, J.H., et al., [2008] Dynamics of the middle atmosphere as simulated by the Whole Atmosphere Community Climate Model, version 3 (WACCM3), J. Geophys. Res., 113, D08101, doi:10.1029/2007JD009269, 2008.

Rieneker, M.M., et al., [2008]; "The GEOS-5 Data Assimilation System – Documentation of Versions 5.01, 5.10 and %.20", NASA/TM–2008–104606, Vol. 27.

Rodgers, C.D., [1977]; "Statistical Principles of Inversion Theory"; Inversion methods in Atmospheric Remote Sounding. A. Deepak (ed.). Academic Press, N.Y., pp. 117-138.

Rodgers, C.D., [2000]; "Inverse Methods for Atmospheric Sounding; Theory and Practice", World Scientific Publishing Co. Pte. Ltd. ISBN 981-02-2740-X

Schwartz, M.J., et al., [2008]; Validation of the Aura microwave limb sounder temperature and geopotential height measurements, *J. Geophys. Res. 113*, D15S11, doi:10.1029/2007JD008783.

Vömel, H., D. David, and K. Smith [2007], Accuracy of tropospheric and stratospheric water vapor measurements by the Cryogenic Frost point Hygrometer (CFH): Instrumental details and observations, J. Geophys. Res., 112, D08305, doi:10.1029/2006JD007224.

Von Clarmann, T., et al., [2003]; "Remote sensing of the middle atmosphere with MIPAS", Remote Sensing of Clouds and the Atmosphere VII, SPIE Vol., 4882, pgs. 172-183

Wetzel, G., et al., [2007]; "Validation of MIPAS-ENVISAT NO2 operational data", ACP, 7, 3261-3284.

Wolff, M.A., et al., [2008]; "Validation of HNO3, ClONO2 and N_2O_5 from the Atmospheric Chemistry Experiment Fourier Transform Spectrometer (ACE-FTS)", ACP, 8, pp 3529-3562.

Wright, C.J., Belmonte Rivas, M., and Gille, J.C.: [2011]; Intercomparisons of HIRDLS, COSMIC and SABER for the detection of stratospheric gravity waves, Atmos. Meas. Tech. Discuss., 4, 737-764, doi:10.5194/amtd-4-737-2011.